

**PHYSICOCHEMICAL AND BIOLOGICAL
PROPERTIES OF MODIFIED BACTERIAL
CELLULOSE**

By

SOUMA TAHIR



A thesis submitted to the University of Birmingham for the degree of

DOCTOR OF PHILOSOPHY

Biomaterials Research

Metallurgy and Materials

University of Birmingham

December 2015

UNIVERSITY OF
BIRMINGHAM

University of Birmingham Research Archive

e-theses repository

This unpublished thesis/dissertation is copyright of the author and/or third parties. The intellectual property rights of the author or third parties in respect of this work are as defined by The Copyright Designs and Patents Act 1988 or as modified by any successor legislation.

Any use made of information contained in this thesis/dissertation must be in accordance with that legislation and must be properly acknowledged. Further distribution or reproduction in any format is prohibited without the permission of the copyright holder.

Abstract

Bacterial cellulose (BC) was biosynthesised by *Gluconacetobacter xylinus*. The aim of this work was to study the effect of surface treatment with 5, 7 and 9 wt.% NaOH on the properties and structure of BC. The effect of BC (2, 4, 6 8 and 10 wt.%) as a filler on the mechanical properties and biocompatibility of reinforced polycaprolactone (PCL) composites processed by electrospinning and twin extrusion followed by injection moulding was also studied.

FTIR showed an increase in crystallinity and cellulose II/I ratio with increasing NaOH concentration and treatment time. Thermogravimetric analysis (TGA) showed improved thermal stability of BC with increasing NaOH solution concentration and time. There was a significant difference between the viability of bone marrow cells on days 6 and 10 for the samples treated with higher NaOH concentration, leading to the conclusion that mercerisation did have a significant effect on the biocompatibility, studied by MTT assay. Cryogenic SEM studies showed that the morphology of BC changed with NaOH treatments from a dense fibre network to randomly distributed fibres with increased porosity.

PCL-BC composites did not show significant improvement in the thermal stability studied by DSC with increasing BC content. An increase in the melting temperature of PCL-BC composites with increasing BC content was observed. A decrease in the ultimate tensile strength was observed with increasing BC content, whereas the yield strength did not show much change. The Young's modulus increased significantly with increasing BC content.

The electrospun PCL-BC composites showed a decrease in the degree of crystallinity studied by DSC as the BC content increased. Cell studies showed successful cell proliferation and viability.

Acknowledgements

I would like to say a special thanks **Dr Artemis Stamboulis**, for helping and supporting me throughout my PhD study. She has been an excellent supervisor and mentor but more importantly a supportive friend. She has been my role model from the moment she joined the Metallurgy and Materials department, she is an inspiration. I admire her ability to balance all aspects of life, her role as a strong career woman, a wife and a mother to her beautiful son. Without her guidance, support, experience and novel ideas, this project would never reach completion.

I would also like to thank my family who shared my stress and, who advised and supported me throughout my times of difficulty.

Contents

Abstract.....	1
Acknowledgements.....	2
Contents	3
List of Figures	7
List of Tables	11
List of Abbreviations	13
CHAPTER 1	15
Introduction and Literature Review	15
1.1 Biomaterials and tissue engineering.....	15
1.2 Bio-composites	18
1.3 Cellulose	20
1.3.1 Sources of Cellulose	21
1.3.1.1 Cellulose derived from plants	22
1.3.1.2 Bacterial Cellulose	27
1.3.1.2.1 History of bacterial cellulose.....	27
1.3.1.2.2 Mechanisms of bacterial cellulose production.....	30
1.3.1.2.3 Bacterial cellulose purification.....	35
1.3.1.2.4 Synthesis of bacterial cellulose.....	37
1.3.2 Crystalline structure of cellulose	41
1.3.3 Converting cellulose I to cellulose II.....	46
1.3.4 Surface modification of Bacterial Cellulose.....	48
1.3.5 Applications of Bacterial Cellulose	51
1.3.6 Bacterial Cellulose composites.....	53
1.3.7 Bacterial cellulose based scaffolds for tissue engineering.	60
1.3.8 Cellular interactions with bacterial cellulose.....	65
1.4 Aims and Objectives	66

CHAPTER 2	68
Materials and Methods	68
2.1 Culturing Bacteria	68
2.1.1 Preservation of the <i>Gluconacetobacter xylinus</i>	68
2.1.2 Gram staining.....	72
2.2 Culture medium.....	73
2.2.1 Preparing the seed broth	73
2.2.2 Pellicle of BC.....	74
2.3 Purification Treatment of Bacterial Cellulose.....	74
2.4 Preparation of BC Sheet.....	74
2.5 Morphological analysis	75
2.6 Tensile testing.....	75
2.7 Thermogravimetric analysis (TGA).....	75
2.8 X-ray diffraction analysis.....	76
2.9 FT-IR analysis	76
2.10 Surface modification treatment of Bacterial Cellulose	76
2.11 Cell Culture	77
2.11.1 Cell culture medium	78
2.11.2 Cell seeding	78
2.12 Phase-contrast imaging.....	79
2.12.1 Preparation of cells for Phase contrast imaging	79
2.13 MTT Assay.....	79
2.14 Cell count	80
2.15 Differential scanning calorimetry for composites.....	81
2.16 Extraction of bacterial cellulose whiskers.....	82
2.17 TEM of BC whiskers.....	82
2.18 Electrospinning nanocomposites.....	82
2.19 Composite samples for mechanical testing	84

CHAPTER 3	86
Results and Discussion.....	86
3.1 Bacterial cellulose	86
3.1.1 Formation of BC pellicles.....	86
3.2 Characterisation of Bacterial Cellulose	87
3.2.1 Purification of BC	87
3.3 Surface modification of BC by mercerisation	89
3.3.1 FT-IR analysis	89
3.3.2 Lattice Type (Cellulose I and Cellulose II)	95
3.3.3 Thermal Analysis.....	103
3.3.4 Cryo-SEM characterisation	107
3.3.5 Cell Culture.....	116
3.3.5.1 MTT Assay & Phase-contrast Imaging of Dermal Fibroblasts.....	116
3.3.5.2 MTT Assay & Phase-contrast Imaging of Bone Marrow Fibroblasts	125
3.4 Polycaprolactone-Bacterial Cellulose nanocomposites.....	133
3.4.1 Acid hydrolysis of BC	133
3.4.2 Electrospinning PCL-BC fibres.....	136
3.4.3 White light interferometry	143
3.4.4 DSC of PCL nanocomposites	145
3.4.5 MTT Assay & Phase-contrast Imaging	148
3.4.6 PCL-BC composites	152
3.4.7 Tensile testing PCL-BC composites	154
3.4.8 Thermogravimetric analysis PCL-BC composites	157
GENERAL DISCUSSION.....	163
CHAPTER 4	170
Conclusions	170

CHAPTER 5	175
Future work	175
References.....	177
Appendices	210
Appendix I.....	210
FTIR- Full List of Band Assignments	210
Appendix II.....	211
Appendix III.....	214
MTT results of day 3	214
Statistical analysis for MTT for surface modified bacterial cellulose	214
Appendix IV	216
T-Test values for PCL-BC composites cell culture	216
TGA curves for PCL and PCL-BC composites.....	217
Statistical analysis for PCL-BC mechanical testing	219

List of Figures

Figure 1.1: General process of tissue engineering.....	17
Figure 1.2: Classification of composite materials.....	19
Figure 1.3: The cellulose polymer chain structure.....	21
Figure 1.3.1: Structure of cellulose.....	23
Figure 1.3.2: Chemical structure of hemicellulose.....	24
Figure 1.3.3: Schematic of cell wall.....	25
Figure 1.3.4: Assembly of plant cellulose chains into microfibrils that build up the plant cell wall.....	26
Figure 1.3.5: Optically transparent bacterial cellulose based composite.....	29
Figure 1.3.6: Assembly of microfibrils by <i>Gluconacetobacter xylinus</i>	32
Figure 1.3.8: Cellulose unit cell.....	43
Figure 1.3.9: Crystal structure models of celluloses.....	44
Figure 1.3.10: Suggested arrangement of molecules in crystal of (a) cellulose I and (b) cellulose II.....	45
Figure 1.3.11: Inter-conversion of the polymorphs of cellulose.....	46
Figure 1.3.12: Nata de coco.....	52
Figure 1.3.13: Potential applications of electrospun polymer nanofibres.....	63
Figure 1.3.14: Fused deposition modelling schematic.....	64
Figure 2.1: Transfer process of the bacteria onto the surface of solid agar media by an inoculating - hand loop under sterilized condition.....	70

Figure 2.2: Bacteria kept in tilted test tubes to provide a larger surface area of solid agar media.....	70
Figure 2.3: <i>Gluconacetobacter xylinus</i> bacteria colony growing and observed by eye.....	70
Figure 2.4: SEM micrograph of <i>Gluconacetobacter xylinus</i> bacteria.....	70
Figure 2.5: Gram stain of individual cells from after gram staining the colony of bacteria.....	72
Figure 2.6: The pellicle of bacterial cellulose placed between stainless steel plates and wire mesh	74
Figure 2.8: Calculation of cell density.....	80
Figure 2.9: Schematic diagram of electrospinning method.....	83
Figure 2.10: Electrospinning setup for study.....	84
Figure 3.1: The white layer appeared on medium B after four days of inoculation.....	85
Figure 3.2: Cryo-field emission SEM micrograph of untreated BC.....	87
Figure 3.3: Cryo-field emission SEM micrograph Images of (a) NaOH-treated and (b) NaOH+NaOCl-treated bacterial cellulose.....	89
Figure 3.4: FT-IR spectra of NaOH treated and untreated BC 3500-1600cm ⁻¹	91
Figure 3.5: FT-IR spectra of NaOH treated and untreated BC 1500-870cm ⁻¹	92
Figure 3.6: Effect of sodium hydroxide concentration on the crystallinity on the scaffolds treated for 5, 10 and 12 hours.....	94
Figure 3.7: Effect of sodium hydroxide treatment period on the crystallinity of scaffolds treated with 5, 7 and 9% NaOH.....	95

Figure 3.8: Effect of sodium hydroxide concentration on the proportion of cellulose I after 5, 10 and 12 hours	98
Figure 3.9: Effect of sodium hydroxide treatment period on proportion of cellulose I with 5, 7 and 9% NaOH.....	99
Figure 3.10: Comparison of FTIR spectra - samples B and J in 1500-879 cm^{-1}	99
Figure 3.11: Comparison of FTIR spectra - samples E and J in 1500-879 cm^{-1}	99
Figure 3.12: Comparison of FTIR spectra - samples H and J in 1500-879 cm^{-1}	100
Figure 3.13: TGA curve of bacterial cellulose.....	104
Figure 3.14: TG curves for untreated and treated BC.....	105
Figure 3.15: Representative Cryo-SEM images of treated and untreated samples.....	114
Figure 3.16: ESEM image of a treated sample (BC-I)	115
Figure 3.17: Representative optical images of dermal fibroblast proliferation on treated and untreated BC.....	116 - 121
Figure 3.18: MTT results for the viability of human dermal marrow fibroblasts after 6 and 10 days on BC with different treatments. Absorbance readings at 540 nm.....	122
Figure 2.19: Representative optical images of Day 6 (a) Dermal cells and (b) Bone marrow cells	124
Figure 3.20: Representative optical images of human bone marrow fibroblast proliferation on treated and untreated BC.....	125 - 130
Figure 3.21: MTT results for the viability of human bone marrow fibroblasts after 6 and 10 days on treated BC. Absorbance readings at 540 nm.....	132

Figure 3.22: TEM of bacterial cellulose whiskers after 48 hours magnification x10,000 ...	133
Figure 3.23: TEM images of BC whiskers after 48 hours magnification x50,000	134
Figure 3.24: TEM images showing BC whiskers after acid hydrolysis for (a) 2h, (b) 4h, (c) 6h, (d) 8h, (e) 12h and (f) 24h.....	135
Figure 3.25: Electrospun PCL collected on aluminium foil.....	136
Figure 3.26: SEM images of PCL, PCL-BC 2wt%, PCL-BC 4 wt. %, PCL-BC 6 wt. %, PCL-BC 8 wt. % and PCL-BC10 wt. %.....	137 - 142
Figure 3.27: Interferometry images of PCL, PCL-BC4 wt. % and PCL-BC10 wt. %.....	144
Figure 3.28: The effect of BC content on the crystallinity of PCL.....	146
Figure 3.29: DSC curves for PCL and PCL-BC electrospun composites.....	147
Figure 3.30: Phase contrast images of Bone marrow and Dermal cells after 24 hours	149
Figure 3.31: Phase contrast images of Bone marrow and dermal cells after 48 hours.....	150
Figure 3.32: MTT results of the viability of human dermal fibroblasts and bone marrow fibroblasts after 24 hours. Absorbance readings at 540 nm.....	151
Figure 3.33: MTT results of the viability of human dermal fibroblasts and bone marrow fibroblasts after 48 hours. Absorbance readings at 540 nm.....	151
Figure 3.34: Structure for 3D printing.....	153
Figure 3.35: Yield strength of PCL and PCL-BC composites.....	154
Figure 3.36: Ultimate tensile strength of PCL and PCL-BC composites.....	155

Figure 3.37: Young's modulus of PCL and PCL-BC composites.....	156
Figure 3.38: TGA curve for PCL and PCL-BC composites.....	158
Figure 3.39: TGA curve 300-500°C of PCL and PCL-BC composites.....	159
Figure 3.40: TGA curve 0-300°C of PCL and PCL-BC composites.....	159
Figure 3.41: Melting point curves of PCL and PCL-BC composites.....	160
Figure 3.42: Melting points for PCL and PCL-BC composites.....	160
Figure 3.43: Area under the melting curve.....	161
Figure 3.44: DSC curves showing decomposition of PCL and PCL-BC composites.....	162

List of Tables

Table 1.3: Properties of plant cellulose and BC.....	35
Table 1.4: Immersion times of BC in NaOH.....	47
Table 1.5: Production yield of BC based on the various carbon sources.....	50
Table 1.6: Bacterial cellulose composites and their applications.....	58
Table 2.1: Treatment period and % concentration for the BC pellicles.....	77
Table 3.1: Crystallinity indices ($1373/2900\text{ cm}^{-1}$) for treated and untreated BC.....	97
Table 3.2: Absorbance ratio $1430\text{ to }900\text{ cm}^{-1}$ for treated and untreated samples.....	99
Table 3.3: FTIR band assignments of cellulose I and II.....	101

Table 3.4: Mechanical properties of treated and untreated bacterial cellulose.....	102
Table 3.5: Decomposition temperature, weight loss at 300°C and temperature at 20% weight loss for treated and untreated BC.....	106
Table 3.6: Treatment period and % composition for the bacterial cellulose pellicles.....	106
Table 3.7: Treatment period and % composition for the bacterial cellulose pellicles.....	123
Table 3.8: Treatment period and % concentration for the BC pellicles.....	124
Table 3.9: Numerical values of Sa and Sq	145
Table 3.10: Tensile test values for PCL and PCL-BC composites.....	157

List of Abbreviations

3D	Three-dimensional
aceQ	Angiotensin I converting enzyme
aceR	Angiotensin I converting enzyme
BC	Bacterial cellulose
CNC	Cellulose nanocrystals
DSC	Differential scanning calorimetry
DTGA	Derivative Thermogravimetric analysis
FESEM	Field emission scanning electron microscope
FTIR	Fourier transform infrared spectroscopy
HA	Hydroxyapatite
HClO	Hypochlorous acid
MEM	Minimum essential medium
MFC	Micro-fibrillated cellulose
MTT	3-(4,5-dimethylthiazol-2-yl)-2,5-diphenyltetrazolium bromide
NaClO	Sodium hypochlorite
NaOH	Sodium hydroxide
NFC	Nano-fibrillated cellulose
PBH	Polyhydroxybutyrate
PBS	Phosphate buffer solution
PCL	Polycaprolactone

PLA	Polylactic acid
SEM	Scanning Electron microscopy
S-RPMI	Cell culture medium
TCP	Tissue culture plastic
TEM	Transmission electron microscopy
XRD	X-ray powder diffraction

CHAPTER 1

Introduction and Literature Review

1.1 Biomaterials and tissue engineering

The term tissue engineering was devised at a national science workshop in 1988. The field of tissue engineering is highly multidisciplinary and combines many biochemical factors and the knowledge of biomaterials to create substitutes for replacement or restoration of damaged tissue for clinical use (O'Brien, 2011; Liu et al., 2007; Langer and Vacanti, 1993).

In early biomaterial design, the goal was to match mechanical and material properties and to achieve a level of functional outcome that adequately matched the native tissue without causing tissue damage or a negative host response (Keane et al., 2014). There has been an enormous increase in the use of biomedical materials over the last few decades. The use of successful biomaterials has led to the increase of patients experiencing pain relief and an improved quality of life. The developments in biomedical materials has allowed the growth of living constructs outside the body for the use as engineered tissues for repair or replacement of damaged tissues (Hench et al., 2004). It can be argued that the most important measure of a scaffold material is not its composition, shape, mechanical properties, porosity, or ability to support cell growth, but rather the host response to the scaffold material (Keane et al., 2014).

Every year, millions of people suffer from tissue loss or organ failure (Langer and Vacanti, 1993). Current surgical therapies include reconstructive surgery and organ transplantation. However, the problem in reconstructive surgery is that mechanical devices are

not complete substitutes for functional tissue. Therefore, the shortage of donor organs, together with the side effects of the permanent use of immunosuppressive medications in organ transplantation implies that these are imperfect solutions (Tabata., 2009; Langer and Vacanti., 1993). The concept of tissue engineering has been introduced to resolve the issues faced with reconstructive surgery. Tissue engineering relies extensively on the use of porous 3D scaffolds to provide the appropriate environment for the cells, which are taken from different sources (autologous cells from the patient; allogeneic cells from another human with a different immune system; xenogeneic cells from a different species), proliferated *in vitro* and then seeded onto a scaffold (Griffith and Naughton, 2002). With the application of chemical, biological, mechanical and electrical stimuli, new tissue is formed and implanted into the patient's body, where natural tissue regeneration takes place, new blood vessels form and grow into the scaffold (angiogenesis). The scaffold degrades over time, leaving regenerated tissue in its place (Liu et al., 2007). Figure 1.1 illustrates the general process of tissue engineering (Rabkin and Schoen, 2002; Liu et al, 2007). Scaffolds play an important role in the tissue engineering process. They serve three key purposes:

- First, they provide a space for tissue regeneration (Hollister et al., 2002; Tabata, 2009). As a defect is produced in the body, the defect space is rapidly filled with fibrous tissue generated by fibroblasts, and ingrowth of this fibrous tissue into that space impairs regeneration of the target tissue (Tabata, 2009).
- Second, scaffolds provide a temporary function at the defect site until tissue regeneration is complete (Hollister et al., 2002).
- Third, they encourage the ingrowth of tissue and allow for the migration of oxygen and nutrients (Hollister et al., 2002; Liu et al., 2007). This is done through a network of

interconnected pores; therefore, pore size, shape, interconnectivity and total porosity all affect tissue regeneration. A suitable microstructure encourages cells to attach and proliferate, and an appropriate molecular structure induces the specific and desired cell response.

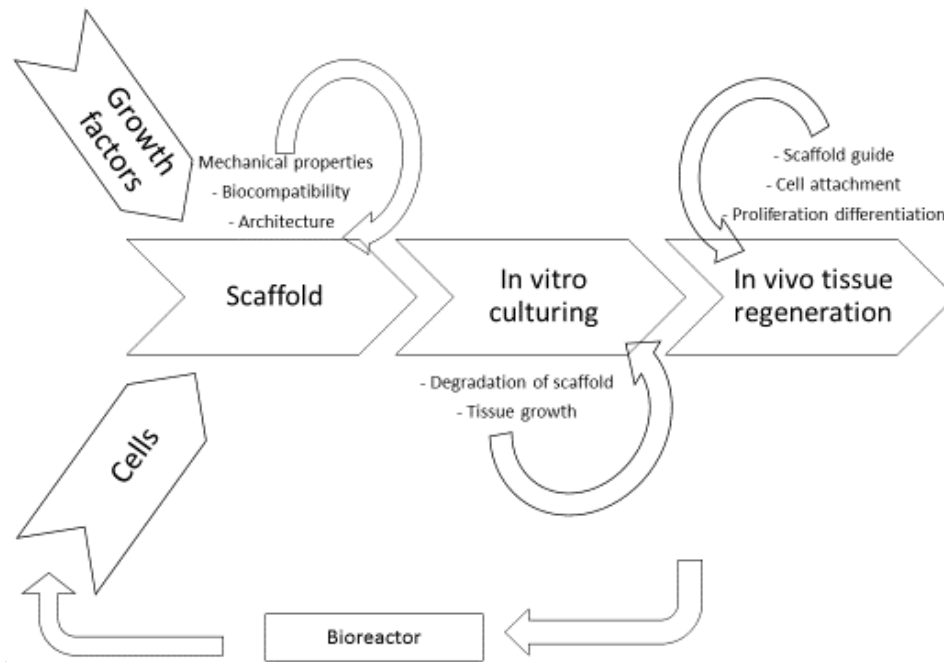


Figure 1.1: General process of tissue engineering (Rabkin and Schoen, 2002; Liu et al, 2007).

For a scaffold to allow tissue regeneration, it should have a three-dimensional template for tissue growth, which stimulates new growth in the shape of the scaffold. The template should mimic the host tissue and allow the 3D growth of cells. For a tissue to be able to grow in 3D, there needs to be a network of large pores (minimum 100 μ m diameter) connected to each other. The interconnected pore network is necessary for cell migration and the passage of nutrients through the scaffold to promote tissue growth. Surface topography also plays a key role in the cell behaviour and surface roughness at a nanoscale can increase cell activity. Therefore, the

optimisation of scaffold pore size and surface topography is important (Hollister et al., 2002; Gatenholm et al., 2010).

Bioactivity of an implant material is usually essential to avoid formation of scar tissue around the implant. Bioinert scaffolds prevent the regeneration of tissue by isolating the scaffold from the host. Therefore, a bioactive scaffold material should be used to prevent the scar tissue response.

Tissue engineering aims to regenerate tissue to restore original state and function as much as possible. Therefore, the characteristics of an ideal scaffold could be summarised as high porosity, biocompatibility, appropriate mechanical strength, stiffness, surface chemistry, high degradation rate with non-toxic by-products and permeability (Hollister et al., 2002; Rabkin and Schoen, 2002; Liu et al., 2007).

1.2 Bio-composites

The word composite means consisting of two or more distinct parts which are combined in a controlled way to achieve a mixture having more useful properties than any of the constituents on their own (Powel, 1983). In engineering design, composites consist of one or more discontinuous phases embedded within a continuous phase. Depending on the purpose of the composite, the discontinuous phase, which is usually stiffer and stronger than the continuous phase, is called either the reinforcement or filler, while the continuous phase is termed the matrix. The term 'reinforcement' is often used when the aim is the improvement of mechanical properties of the composites, while 'filler' is used when the main objective is cost reduction or the modification of other (non-mechanical) properties. Fibre-reinforced composite materials consist of fibres of high strength and modulus embedded in or bonded to a matrix with distinct interfaces

between them. The properties of composites are strongly influenced by the properties of their constituent materials, their distribution, processing condition and the interaction between them. The properties of a composite are not only dependent on the filler concentration but also on the size, shape (aspect ratio), interfacial interaction between filler and matrix, and filler orientation (Ratner et al., 1996; Agarwal et al., 1980). For many years, synthetic polymer composites have been developed and applied in various fields such as industrial, domestic equipment, the automotive industry, and even in aerospace. However, these synthetic materials come from non-renewable sources which are limited and difficult to decompose by microorganism present in nature (Wool and Sun, 2005).

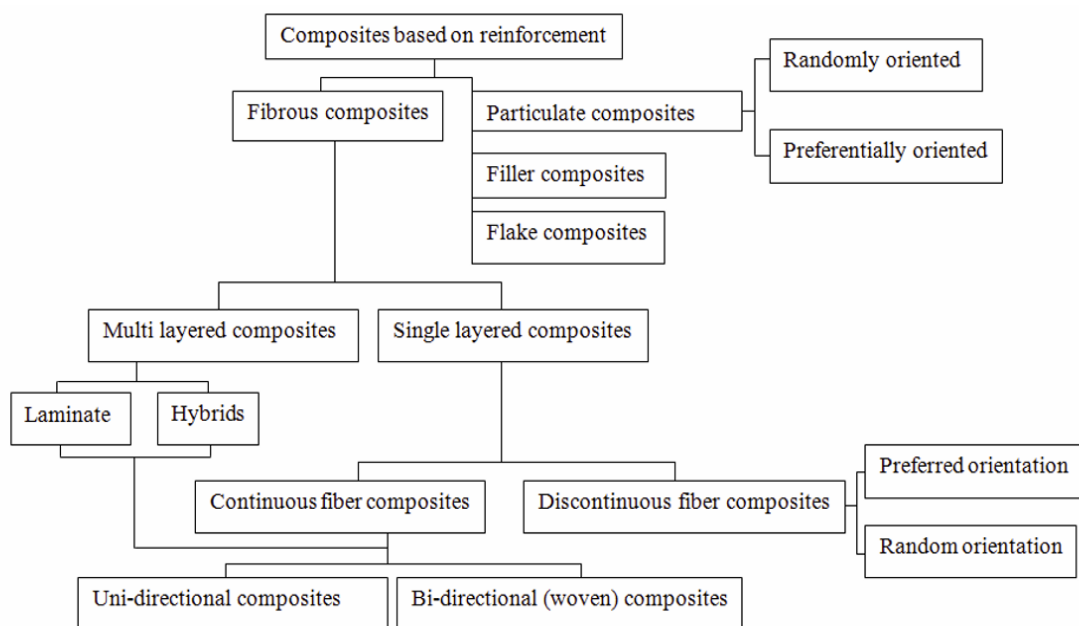


Figure 1.2: Classification of composite materials (Aizenberg et al., 2005; Agarwal and Broutman, 1980).

A worldwide growing environmental awareness has encouraged researchers and industrialists to consider natural plant fibres as an alternative reinforcing agent or filler to produce composite materials known as bio-based composites. The idea of using plant-based fibre as reinforcement has been around since the beginning of human civilization. Plant fibres have also been used to reinforce biodegradable polymers such as cellulose ester, polyhydroxybutyrate (PHB), polyesteramide, polylactic acid (PLA) and starch derivatives and blends (Peijs, 2000). A common choice for reinforcement of bio-based composites is cellulose. The cellulose fibre family, including kenaf, flax, ramie, hemp and jute has been widely used as a composite reinforcement for its outstanding properties including good mechanical and thermal stability, non-abrasiveness and biocompatibility (Geyer et al., 1994; Bullions et al., 2005; Lin et al., 2014). However, because of their hydrophilic nature, these fibres make imperfect bonds with the polymer matrix, which is generally of hydrophobic nature. Various ways of improving the interface to overcome this problem have been used, such as by the addition of surfactants or compatible agents, and by grafting a matrix-compatible polymer onto the fibre surface (Chance Escamilla et al., 1999; Viet et al., 2007; Lina et al., 2013).

1.3 Cellulose

Cellulose is an abundant polymer which is produced by plants, bacteria and animals. It is a semi crystalline high molecular weight homopolymer of β -1,4-linked anhydroglucose (Fengel and Wegener, 1983). The hydroxyl groups of cellulose form inter and intra molecular hydrogen bonds. These hydrogen bonds obstruct the free rotation of the ring (cellulose linking glucosidic bond) resulting in the chain becoming stiff. The hydrogen bonds also contribute to the insolubility of the cellulose chains in common solvents. Cellulose is a hydrophilic polymer, with three main

hydroxyl groups per glucosidic unit available for water adsorption (Saka, 2001; Haigler and Brown, 1986). The base cellulose molecule is essentially structured on a regular unbranched linear sequence of D-anhydroglucopyranose units which are linked together by β (1-4)-D-glucosidic with a syndiotactic homopolymer configuration (Theo et al., 2013; Jin et al., 2013). Its chemical formula is $(C_6H_{10}O_5)_n$.

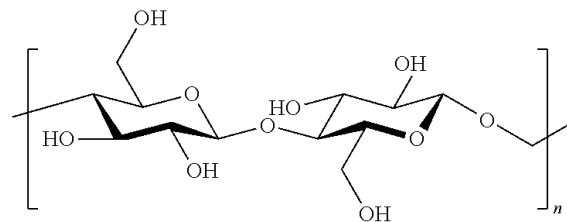


Figure 1.3: The cellulose polymer chain structure (Theo et al., 2013; Jin et al., 2013).

In the last few years the use of cellulose in composites has increased due to its relative low price compared to conventional fibre materials such as glass and aramid fibres, the fact that they can be burned with energy recovery, and the fact that they compete well in terms of mechanical behaviour (Eichhorn et al., 2001; Hon and Shiraishi, 1991; Ding and Himmel, 2006). To extend the application of and to achieve better chemical and physical properties, cellulose has been transformed into various derivatives including acetate cellulose, cellulose sulphate and cellulose palmitate among others (Heinze and Glasser, 1996).

1.3.1 Sources of Cellulose

Cellulose is most frequently isolated from plant cell walls; the most common commercial sources of cellulose include wood pulp and cotton linters. Cotton fibres are about 98% cellulose, whereas wood is 40-50% cellulose (Whistler, 1997; Ockerman, 1991). Cellulose can also be

produced from various other plant fibres, such as sugar cane stalks, wheat straw, rice hull, sugar beet, wheat straw, bamboo, and fibres such as flax and ramie as well as others, which is illustrated in Figure 1.3.1 (Franz, 1990; Hanna, 2001, Lin et al.,2014).

The second source of cellulose is biosynthesis by different micro-organisms for example, bacteria, algae and fungi (Klemm et al., 2001; Eichhorn et al., 2001). Biosynthesis by the bacteria *Gluconacetobacter xylinus* is the only species which is known to be capable of producing cellulose in a commercially achievable quantity.

1.3.1.1 Cellulose derived from plants

Plant cellulose is never found pure in nature. Cellulose is associated with other substances such as lignin and hemicelluloses, both in considerable quantities. Hemicellulose is a common name for a large number of different carbohydrate heteropolymers, of which xylans and glucommans are the main components. Unlike cellulose which has high crystallinity, and is strong and resistant to hydrolysis, hemicellulose is a highly-branched and amorphous structure with little inherent strength. Hemicelluloses are more closely associated with lignin than cellulose, and exist in amorphous state.

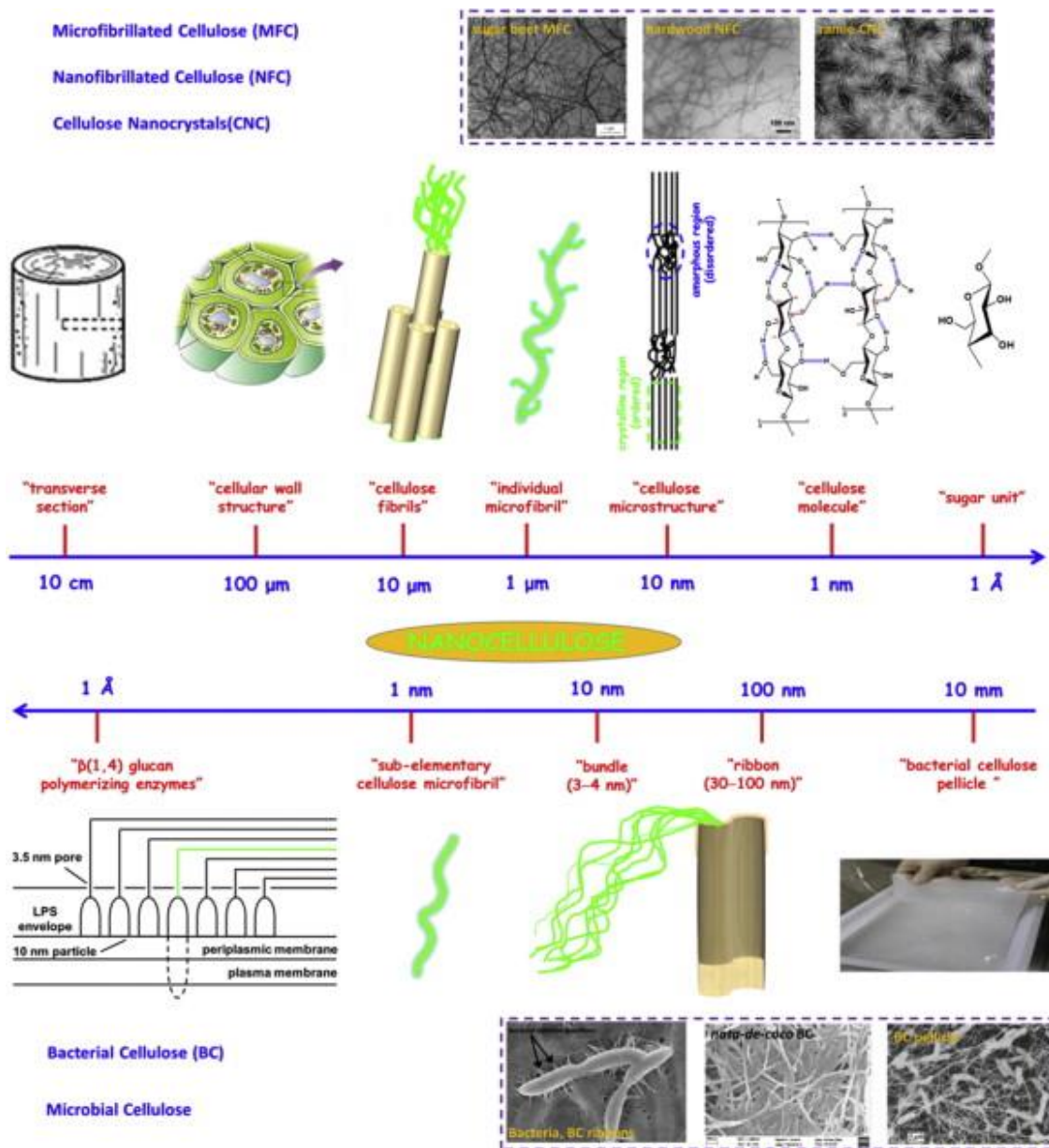


Figure 1.3.1: Structure of cellulose; Cellulose nanocrystals (CNC), micro/nanofibrillated cellulose (MFC and NFC; bacterial cellulose (BC)). TEM of sugar beet MFC, hardwood MFC, ramie CNC; and SEM of BC ribbons, nata-de-coco BC, BC pellicle (Lin et al., 2014).

The amorphous state of the hemicelluloses is evidently due to the presence of many side groups, which inhibit the close link between molecules that is necessary for the formation of crystalline regions (Klemm et al., 1998). The chemical structure of hemicelluloses is shown below in Figure 1.3.2.

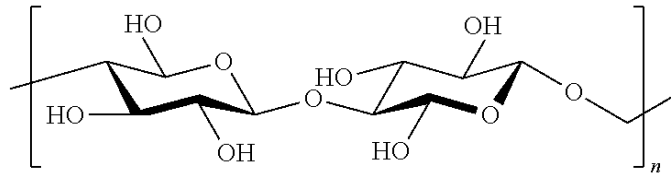


Figure 1.3.2: Chemical structure of hemicellulose (Jin et al., 2013).

The walls of a plant cell most commonly consist of primary and secondary cell wall layers as shown in Figure 1.3.3. The secondary layer is composed of three sub-layers known as S1, S2, and S3. These sub layers are based on differences in microfibril orientation.

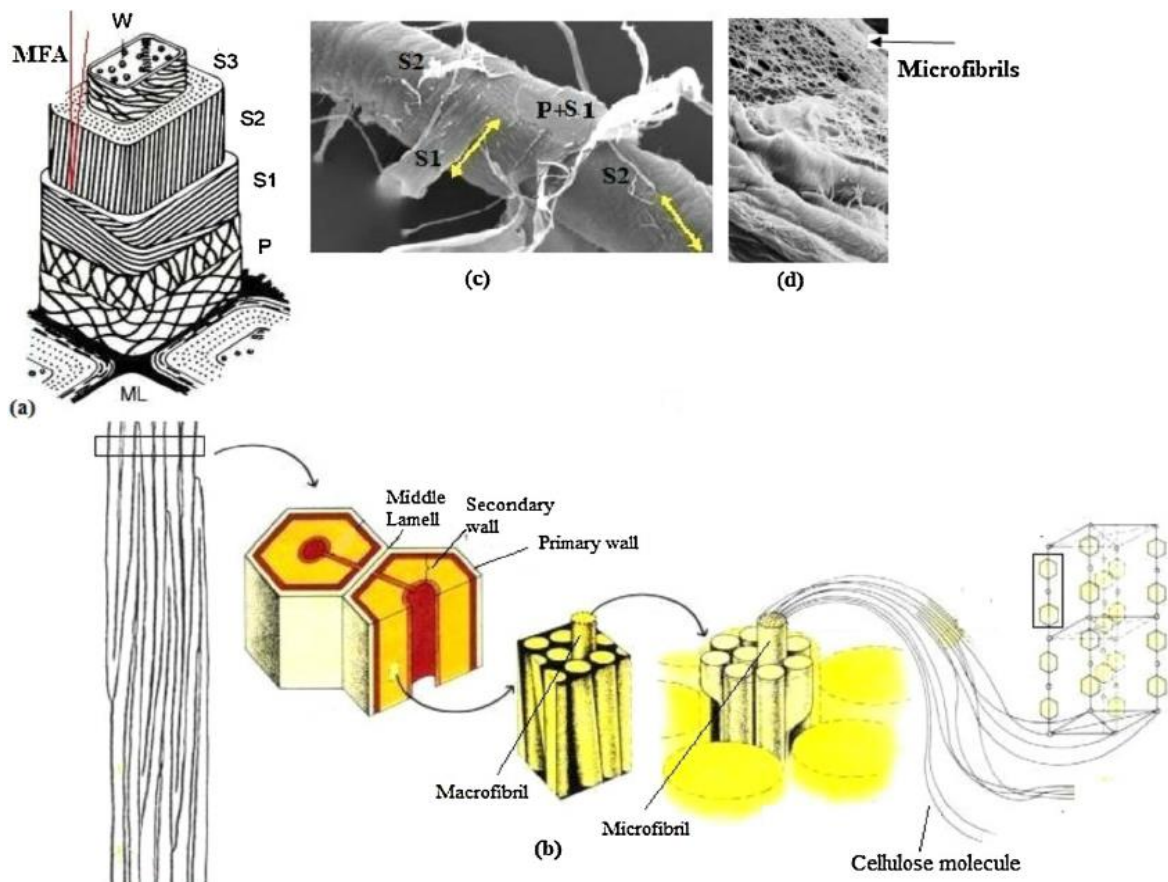


Figure 1.3.3: Schematic of cell wall (Chinga-Carrasco, 2011; Fardim, Liebert & Heinze, 2013; Fellers & Norman, 1998; Sixta, 2008).

The middle lamella is a layer which forms during cell division and is situated between cells. Figure 1.3.4 shows the middle lamella and the primary cell wall which consists of a stiff skeleton made up of randomly arranged layers of cellulose. The secondary cell wall is formed after cell expansion and it is set down in multi layers inside the wall of the primary cells.

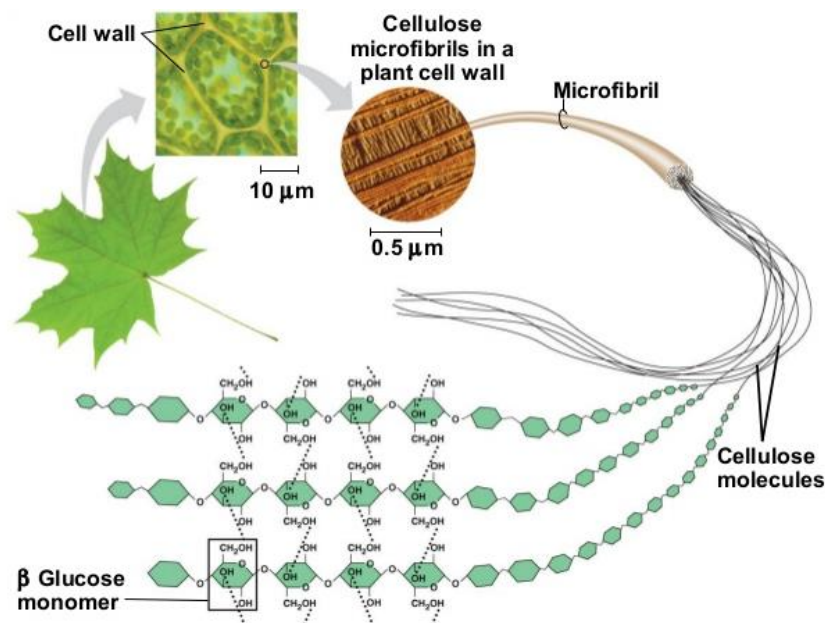


Figure 1.3.4: Assembly of plant cellulose chains into microfibrils that build up the plant cell wall (Djerbi, 2005).

The layers S1, S2 and S3, within the secondary cell wall are made up of microfibrils placed in a well-ordered and parallel organisation (Timell, 1969). These layers vary in thickness and up to 80 % of the total cell wall thickness is made up by S2 (Plomion et al., 2001; Timell, 1969).

Although cellulose is more readily available from plants, the major problem found in plant-derived cellulose is that it is highly bound to lignin, which forms lignocellulose (Sukara and Meliawati, 2014). Therefore, cellulose has to be separated from lignin before it can be used in industry, which is a difficult and expensive task requiring sophisticated technology and high energy input.

1.3.1.2 Bacterial Cellulose

Bacterial cellulose is a polymer produced by some gram-negative bacteria species of the genera *Acetobacter*, *Agrobacterium*, *Aerobacter*, *Achromobacter*, *Azotobacter*, *Salmonella*, *Escherichia*, *Rhizobium*, *Pseudomonas*, *Alcaligenes* and gram-positive species of the genus *Sarcina* (Shoda and Sugano, 2005). The most common and effective bacteria species producer of cellulose are *G. xylinus*, *A. hansenii* and *A. pasteurianus* (Bielecki et al., 2005). These possess the ability to produce cellulose at the surface of a medium containing carbon and nitrogen as a food source (Deinema and Avenhuizen, 1971). Bacterial cellulose is synthesised by strains of bacterium *Gluconacetobacter xylinus* (previously *A. xylinus*), reclassified as the genus *Gluconacetobacter*. It is a Gram negative, rod shape, aerobic bacterium (Joseph, 2001). Bacterial cellulose exists as a fibril structure consisting of β -1 \rightarrow 4 glucan with molecular formula $(C_6H_{10}O_5)_n$ (Esa et al, 2014). The glucan chains are held together by inter- and intra- molecular hydrogen bonding (Ul, Islam et al, 2012). Bacterial cellulose has many advantages, such as; high purity, better crystalline property, simple polymerisation, high strength, high water absorbency and high bio-compatibility, fibre networks with diameter of 20-100nm and stronger biological adaptability (Sukara and Meliawati, 2014, Bläckdahl et al., 2006, Klemm et al., 2006, Iguchi et al, 2000, Wan et al, 2006).

1.3.1.2.1 History of bacterial cellulose

A. J. Brown was the first to publish a scientific paper in 1886, describing an extracellular gelatinous mat, also referred to as a pellicle produced by *Gluconacetobacter xylinus* (Brown, 1886). The solid mass referred to as 'vinegar plant' was later identified as bacterial cellulose and the bacteria which produced the cellulose was called *Gluconacetobacter xylinus*. This has since

become the official name according to the International Code of Nomenclature of Bacteria. In scientific literature this bacterium is treated as a separate species but for the purpose of strict classification, it is considered a sub-species of *Gluconacetobacter aceti* (Cannon and Anderson, 1991). Between 1946 and 1963 bacterial cellulose production and its characterization was described using microscopic examination (Aschner and Hestrin, 1946), closely followed by the formation of a thin layer of bacterial cellulose on the surface of the medium (Hestrin et al., 1947). This showed that BC could be produced by *Gluconacetobacter xylinus* by taking advantage of various substrates other than glucose. The formation of gas bubbles within the submerged cellulose mesh prior to surface film formation was also observed and it was concluded that the gas probably floated the cellulose and the bacteria to the surface (Schramm and Hestrin, 1954). Observations of the structure, morphology and modification of BC were also conducted. X-ray analysis indicated that cellulose strands have a random orientation and are ribbon-like with a cross section of 100 x 200 Å, 40 µm in length (Frey-Wyssling and Muhletahler, 1946).

Cellulose that is produced in a bacterial cell forms an ultra-fine structure of microfibrils. During the culture process, the cell extrudes approximately 14 to 72 molecules of cellulose into the culture medium through pores on the cell surface (Zaar, 1979). Cellulose molecules bind to each other via hydrogen bonds after biogenesis near the surface of the cell and produce cellulose in a pure form (Ross et al., 1991). It is generally accepted that the synthesis of crystalline microfibrils by *Gluconacetobacter xylinus* is an extracellular process. In which the fibrous structure consists of a three-dimensional, non-woven nanofibril network, which shares the same chemical structure as a plant cellulose. This structure is held together by inter and intrafibrillar hydrogen bonds, resulting in a high strength hydrogel (Chawala et al., 2009; Esa et al., 2014; Lina et al., 2013).

Later research has applied more complex and advanced analysis. Some researchers, for instance, have mixed BC with resin to obtain a useful novel composite. By impregnating BC sheet with a phenolic resin and compressing it at high pressure, a high strength composite has been produced (Nakagaito et al., 2004) while impregnating BC sheet with acrylic resin gave an optically-transparent bacterial cellulose-based composite as shown in Figure. 1.3.5. (Yano et al., 2012).



Figure 1.3.5: *Optically transparent bacterial cellulose based composite (Yano et al, 2012).*

The latest research shows that bacterial cellulose can be used in tissue engineering and is safe to be implanted into the bodies of living creatures. Through chemical modification, *i.e.* phosphorylation and sulphation, bacterial cellulose has been converted to a new scaffold material for tissue engineering of cartilage (Svensson et al., 2005). Composites of hydroxyapatite and bacterial cellulose have been synthesised through biometric methods and can be used as artificial bone. Through pre-treatment by soaking the BC in 0.1 M CaCl₂ solution at 37 °C for 3 days apatite is more easily dispersed on the surface of the organic polymer. To trigger hydroxyapatite

growth, the treated bacterial cellulose was immersed in de-ionized water and further soaked in a 1.5 x simulated body fluid (Hong et al., 2006).

1.3.1.2.2 Mechanisms of bacterial cellulose production

The methods for producing bacterial cellulose can be either, static culture, rotating disk system or shake culture. There are advantages and disadvantages for each method, static culture is a simple traditional method but produces a smaller number of pellicles on the surface compared to other methods (Son et al., 2001). This is because the bacteria which produces cellulose is an aerobic organism and requires sufficient oxygen for growth (Budhiono et al., 1999). Therefore, the reason for the slow growth of these aerobic organisms is that the pellicles at the air/liquid interface form a barrier between the oxygen in the atmosphere and the nutrient in the culture. This reduces the rate at which oxygen penetrates the pellicle to the cells (Dudman, 1960). Increasing growth time allows increased bacterial cellulose formation and therefore increase in hydrogen and C-H bonding (Sheykhnazari et al., 2011). In shake culture and the rotating disk system bacterial cellulose can be produced in a bioreactor or in a flask. These methods are more efficient and preferred for the production of bacterial cellulose on a large scale as it increases the productivity of bacterial cellulose rather than a process which is continuous (Çakar et al., 2014).

However, gram negative and rod-shaped *Gluconacetobacter xylinus* is the only species known to be able to produce cellulose in marketable quantities. Particularly in this study, bacterial cellulose (BC) produced in static culture is composed of a number of microfibrils in the longitudinal axis of its envelope by *Gluconacetobacter xylinus*. Due to its remarkable mechanical properties and ability to form homogeneous membrane sheets after drying under certain synthesis conditions and an ultra-fine network structure, bacterial cellulose is useful for a number of

applications (Iguchi et al., 2000, Yamanaka et al., 1989) The methods of producing BC have been further developed with the intention of improving the structure and yield, as well as other physical properties (Ruka et al., 2012; Geyer et al., 1994; Jonas, 1998; Yamanaka et al., 2000). Apart from using different methods for production, the pH level, culture medium and the source of carbon and nitrogen as the main food for *Gluconacetobacter xylinus* have all been varied (Masaoka et al., 1993). Researchers also focused on the characteristics of BC, carrying out physical, thermal, and morphological analysis.

Previous research has focused on ensuring that the *Gluconacetobacter xylinus* does not undergo genetic mutation (Saxena and Brown, 1995; Wulf et al., 1996). The implications of mutation occurring are the growth of a wild type organism which can reduce the ability of *Gluconacetobacter xylinus* to produce cellulose (Schramm and Hestrin, 1954; Valla and Kjosbakken, 1982). Other side-effects include affecting the morphological and physiological properties of BC (Coucheron, 1991) and a fall in the Young's modulus of the BC sheet produced because of the growth of a by-product known as acetan (Watanabe et al., 1998). Various biosynthesis-related methods of ensuring a high productivity of BC from the *Gluconacetobacter xylinus* have been used (Nakai et al., 1999, Krystynowicz et al., 2002). The most recent was through cloning of the *Gluconacetobacter xylinus* whereby the resulting yield of BC was far more than that produced by the original bacteria itself (Kawano et al., 2002; Bae et al., 2004).

Cellulose produced by *Gluconacetobacter xylinus* does not occur randomly, the highly ordered synthesis begins with small glucan chains aggregating by a self-assembly mechanism into 3 to 4nm microfibrils. This is followed by the banding of microfibrils into bundles, which then form into the complete ribbon with a width (parallel to the longitudinal axis of the cell) between 40 and 60nm as seen in Figure 1.3.6 (Cannon and Anderson, 1991; Brown, 1992).

Bacterial cellulose synthesised extra-cellularly consists of nano-size extrusions, which results in greater hydrogen bonding between fibrils than with plant cellulose. The hydrogen bonds due to the hydroxyl group give rise to properties such as a high degree of crystallinity, high water-holding capacity and high tensile strength. Since BC has unique properties, including high hydrophilicity, as well as having a high water-holding capacity and a fine fibre network which can be easily shaped into three-dimensional structures during synthesis, it is an excellent candidate for use as a scaffold for tissue engineering (Svensson et al., 2005; Helenius et al., 2006). The porosity of BC, which is necessary to support cell ingrowths and effective mass transport of tissue such as cartilage, makes it a natural medium for growing cells.

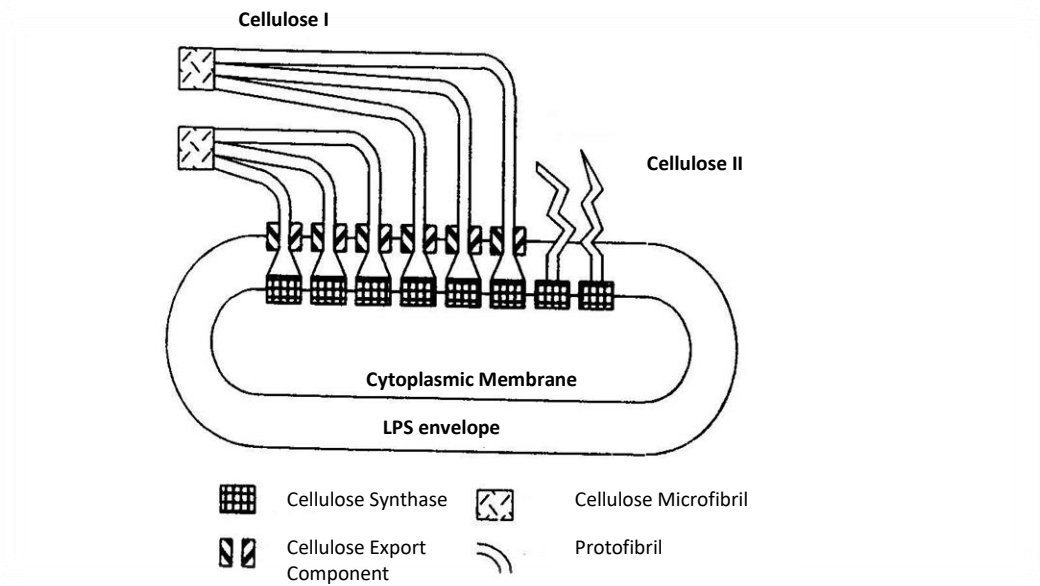


Figure 1.3.6: Assembly of microfibrils by *Gluconacetobacter xylinus* (Iguchi et al., 2000, Chawla et al., 2009).

It has been recognised that there are four different structural types of cellulose, different properties have been identified:

- ❖ **Cellulose I**: consists of β -1,4 glucan chains which are aligned parallel to each other. Typically found in nature. It is the cellulose produced in pellicle form by *Gluconacetobacter xylinus*. In a wet state, cellulose I can be referred to as ‘native’ cellulose (Ross *et al.*, 1991).
- ❖ **Cellulose II**: consists of anti-parallel β -1,4 glucan chains. It is found in shaken cultures of *Gluconacetobacter xylinus* or after re-crystallization or mercerisation of cellulose I (Ross *et al.*, 1991).
- ❖ **Cellulose III**: chemically treated cellulose I (Haigler and Weimer, 1991).
- ❖ **Cellulose IV**: can be derived from chemically treating cellulose II and is found in the cell wall of higher plants (Haigler and Weimer, 1991).

In the last two decades key advances have been made into the cellular activators that cause *Gluconacetobacter xylinus* to secrete cellulose. The initial breakthrough was the discovery that cellulose I actually has two allomorphs that had been confusing crystallography work by causing different diffraction patterns (Atalla & Vander Hart, 1984 and 1986). Cellulose I α is produced predominantly by many algae and bacteria while cellulose I β is derived from plants. All native cellulose contains measures of both allomorphs (Sugiyama *et al.*, 1991). This led to the suggested of a parallel orientation model of the cellulose chains with I α containing a triclinic unit cell and I β monoclinic unit cell (Hieta *et al.*, 1984).

In contrast to cellulose extracted from plant cells, bacterial cellulose is completely pure because 99.8% of its mass is water and 0.2% is an inert polysaccharide, while it contains no lignin, hemicelluloses, pectin, and waxes (Klemm et al., 2001). BC has a higher degree of crystallinity (above 65%) compared with plant cellulose (<65%). The fibre cross section diameter ranges from 2-4nm (Nakagaito et al., 2005), the length is several 100µm (Gindle et al., 2004) and the degree of polymerisation ranges between 2000 and 6000 (Iguchi et al, 2000). BC fibres exhibit high water absorption, excellent shape and strength retention, high mechanical strength and good chemical stability (Klemm et al., 2001). The crystalline structure of bacterial cellulose is generally cellulose I. Bacterial cellulose is reported to be more crystalline than plant cellulose due to the presence of predominant cellulose I α (Bielecki et al., 2001). The pellicle produced in static culture has an ultra-fine network structure, producing ribbons 500nm wide and 10nm thick (Brown et al., 1976; Gindle, 2004), thickness of 3-4nm (Bielecki et al., 2004) and diameter of 24-86nm (Chanliaud et al., 2002). BC is composed of nanosized fibres and the nanofibre structuring determines the product properties, this polymer is described as nanocellulose (Klemm et al., 2003). Table 1.3 below briefly shows the comparison between the physical properties of bacterial cellulose and plant cellulose.

Table 1.3: Properties of plant cellulose and BC.

Properties	Plant cellulose	Bacterial cellulose	Literature
Fibre width	1.4-4.0 x 10 ⁻² mm	70-80 nm	Pecoraro et al, 2008
Crystallinity	56-65%	65-79%	Pecoraro et al, 2008
Degree of polymerisation	13,000-14,000	2,000-6,000	Pecoraro et al, 2008
Young's modulus	Cotton 5.5-13 GPa	BC sheet 15-30 GPa	Bielecki et al, 2004
	Jute 27 GPa	BC fibre ~120 GPa	Yamanaka et al, 1998
	Flax 28 GPa	BC crystal ~138 GPa	Sakurada et al, 1962 Eichhorn et al, 2010
Water content	60%	98.50%	Pecoraro et al, 2008

The chemical and physical structure of BC enables it to be modified by various methods to improve its mechanical and thermal properties. The modulus of bacterial cellulose sheets can be increased by carrying out purification as a result of using alkaline and oxidative agents (Guhados et al., 2005). The Young's modulus of BC fibres is higher than the plant cellulose fibres because mainly the latter contain other products such as lignin and waxes, that render the properties of the fibres inferior to the purer BC fibres (Bielecki et al, 2004).

1.3.1.2.3 Bacterial cellulose purification

Once bacterial cellulose is produced at the surface of the medium, it is collected and purified using NaOH and NaOCl to clear it from impurities. If impurities such as nucleic acid, culture medium and protein in the cellulose matrix are removed, there will be an increase in the intrafibrillar and interfibrillar hydrogen bonds in the network due to the contact between cellulose fibrils (Yamanaka et al., 1989). The purification process of bacterial cellulose is different to that

of plant cellulose because it involves the removal of only the remaining organic material, which is a source of food for the microbes in the medium (George et al., 2005).

The purification of bacterial cellulose by NaOH and NaOCl has been extensively studied by Gea et al., to observe the effect on mechanical properties and to see if the structure of bacterial cellulose changes from cellulose I to cellulose II. Gea et al., reported two stages in the purification of bacterial cellulose, first, washing the pellicle in a 2.5 wt. % NaOH solution and then with a 2.5 wt. % NaOCl solution overnight sequentially. The use of an alkaline solution followed by the NaOCl solution, allows the removal of non-cellulose materials such as proteins and nucleic acids from the pellicle to form strong inter and intrafibrillar bonds (Nishi et al., 1990. Gea et al., 2011). They found an increase in the Young's modulus and in tensile strength after treatment with both chemicals. A change in the orientation of the microfibrils was also observed but there were no changes in the structure of cellulose I to cellulose II (Gea et al., 2011). Purified bacterial cellulose can be stored for a longer period without experiencing changes in its quality or colour.

Studies have shown that using NaOH with concentrations of 6 wt. % and over can theoretically change the crystal structure of bacterial cellulose from cellulose I to cellulose II (Dinand et al., 2002; Gomes et al., 2007; Mansikkämäki et al., 2005; Oh et al., 2005; Shibazaki et al., 1997). It was reported by Laszkiewicz (1997) and Gea et al., 2011, that structural changes in BC are also accompanied by molecular changes. Therefore, the structural change in bacterial cellulose from cellulose I to cellulose II as a result of the alkalisation process also involves breakage of inter and intramolecular hydrogen bonds that are present in cellulose (Laszkiewicz, 1997. Gea *et al.*, 2011).

1.3.1.2.4 Synthesis of Bacterial Cellulose

There are two main mechanisms involved in the synthesis of bacterial cellulose; the production of uridine diphosphoglucose (UDPGlc), followed by the polymerisation of glucose into long and unbranched chains (the β -1 \rightarrow 4 glucan chain). Despite the high value and widespread use of cellulose, the mechanism of its synthesis is relatively poorly understood. This is due to the difficulty in directly observing *in vitro* with higher plant enzyme preparation and identifying the proteins involved in the synthesis of cellulose (Delmer and Amor, 1995). To overcome this difficulty, for the reason of high purity and crystallinity, BC has been extensively used as a model for studying cellulose biogenesis of linear β -1,4 glucan chains and their crystallization into cellulose fibrils, and also for studying metabolic processes occurring in the bacteria.

The most important factor for the growth of the bacteria is the acidity of the culture medium. Several studies have reported the optimum pH for cellulose production by *Gluconacetobacter xylinus* to be less than pH 7 (Glasser et al., 1958; Hestrin, 1952; Masaoka et al., 1993). When a culture medium of pH 4 was used, this strain of bacteria was susceptible to mutagenesis, making it a gluconate negative mutant of its parent strain. Therefore, making it a potentially non-cellulose producing, or a wild type product (Hwang et al., 1999; Valla and Kjosbakken, 1982) or native-band cellulose (Ohad et al., 1962). The change of bacterial cellulose structure from I α to folded-chain cellulose II is a result of the mutagenesis of *Gluconacetobacter xylinus* (Kuga et al., 1993).

In the initial stage, the bacteria population increases by taking up dissolved oxygen and producing a certain amount of cellulose in the entire liquid phase. When there is a lack of dissolved oxygen, only the bacteria existing in the area of the surface are able to maintain their

production of cellulose. Although they may undergo cell division, the population size in the surface area does not increase exponentially but reaches equilibrium as the excess are obstructed and sink in the pellicle (Iguchi et al., 2000). The bacteria increase by forming a new branch (Brown et al., 1976; Zaar, 1977). The fibrils of BC are formed by the bundling of microfibrils that are excreted from the aligned pores on the cell surface along the longitudinal axis. There are two reasons for *Gluconacetobacter xylinus* to produce cellulose; as an environmental defence mechanism which allows the bacteria to float at the air/liquid interface so it can access oxygen and the media and as a by-product of its metabolism (Nishi, 1990). Kinetically the production of cellulose by bacteria has been studied since the 1950s. The yield of the cellulose production increases exponentially with time assuming that, during its generation time, the bacteria produce a certain number of chain initiators. Monomer units are added to the chain initiators, forming cellulose, given that the bacteria obey the law of bacteria growth (Brown et al., 1962; Budhiono et al., 2000).

The advantages of using the bacteria as a model system are that they grow fast under controllable conditions and produce cellulose from various carbon sources, such as glucose, ethanol, sucrose, and glycerol. Another advantage is that genetic analysis of the bacteria is aided by the isolation of a large number of mutants affected in cellulose biosynthesis, and these mutants have allowed identification of specific genes involved in this process. In order to understand the formation of cellulose ribbon, materials such as hemicelluloses and carboxymethyl cellulose (Brown et al., 1976; Haigler et al., 1980), xyloglucan (Hayashi et al., 1989; Whitney et al., 1995) were directly added into inoculated-bacteria medium to disrupt the growth of BC crystals. The presence of carboxymethyl cellulose in the medium delayed the growth formation of visible aggregates of BC and hence the rate of cellulose synthesis increases (Ben-Hayim and Ohad,

1965). The inhibition of crystallization, but not polymerization, shows that both processes took place consecutively and not simultaneously. From this data, Zaar comes to the conclusion that there are two processes involved in the biosynthesis of bacterial cellulose. The first is biosynthesis of linear β -1,4, glucan chains catalysed by the enzyme cellulose synthase, followed by the biological mechanism of their crystallization to form cellulose microfibrils (Zaar, 1977).

Brown et al. showed how the synthesis of cellulose is in close contact with the bacterial envelope and each bacterium produces a flat ribbon which contains cellulose on its surface (Brown et al., 1976). These ribbons are assembled side by side in a horizontal axis producing a flat ribbon like structure. It was reported by Haigler and Benziman that the cellulose synthesising sites on the cell surface are arranged in a linear row and are made of 3.5 nm pores (Haigler and Benziman, 1982). Each of these pores can cover up to a 10 nm particle, which consists of enzymes that synthesise cellulose and are involved in the polymerisation reaction. A number of glucan chains are produced by each 10 nm particle, these chains form a sub elementary fibril of 1.5 nm which together form the microfibril. These microfibrils are connected together by hydrogen bonding to create flat layers and pellicle structures. As the microfibrils are very fine in size, they are therefore in very close contact with each other. This results in the increased density of the interfibrillar and intrafibrillar hydrogen bonding. It is thought that the strong hydrogen bonding leads to high water retention and high strength of bacterial cellulose (Iguchi et al., 2000; Klemm et al., 2001).

Various methods have been intensively studied to determine the biosynthetic pathway of carbon metabolism in *Gluconacetobacter xylinus*. The pathway from substrate glucose to cellulose involves at least four stages of biochemical reaction. First, the enzyme gluconase converts glucose to glucose-6-phosphate; this is followed by the isomerisation of glucose-6-

phosphate into glucose-1-phosphate by phosphoglucomutase. Thirdly, glucose-1-phosphate is converted into UDP-glucose-1-phosphate, before being converted into pyrophosphorylase (Lee et al., 2014).

In *Gluconacetobacter xylinus* this enzyme is activated by cyclic nucleotide (c-di-GMP) which is synthesised in *Gluconacetobacter xylinus* by the enzyme diguanylate cyclase. Its concentration is regulated by the action of phosphodiesterase. UDPG is polymerized into cellulose by cellulose synthase (Tal et al., 1998). Figure 1.3.7 shows the schematic pathway of carbon metabolism in *Gluconacetobacter xylinus*. The cellulose synthase enzyme plays the most important part in the synthesis of cellulose (Brown et al., 1976; Ross et al., 1987 Lee et al., 2014). This nucleotide is synthesized from guanosine triphosphate (GTP) by diguanylate cyclase and is degraded by phosphodiesterase A and B. This shows that cellulose synthase is further regulated at the genetic level (Saxena et al., 1994; Volman et al., 1995). Genetic cloning is a way to improve the yield of bacterial cellulose, as results from genetic complementation tests and gene disruption studies showing that all four genes in the operon are required for maximal bacterial cellulose synthesis in *Gluconacetobacter xylinus* (Wong et al., 1990). *Gluconacetobacter xylinus* secretes water-soluble polysaccharide acetan during bacterial cellulose production (Lee et al., 2014, Couso et al., 1987). The acetan is produced from UDPGIc, which is the starting compound for the production of cellulose. Therefore, inhibiting the production of acetan is likely to increase the concentration of UDPCIc, which in turn increases the yield of bacterial cellulose (Lee et al., 2014).

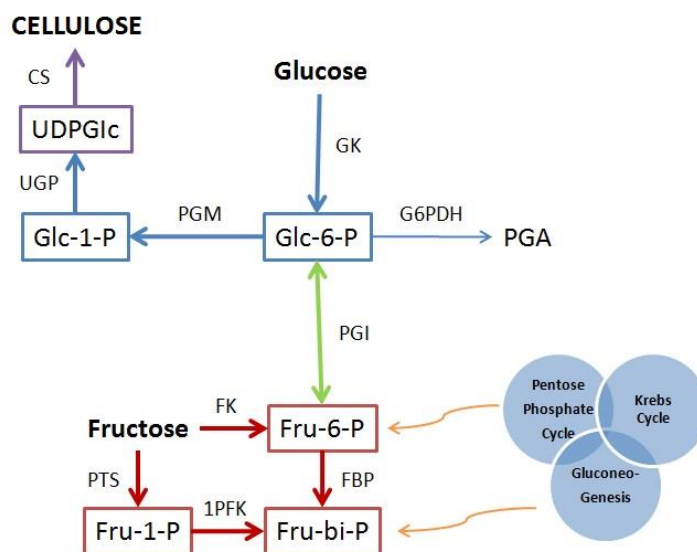


Figure 1.3.7: Pathways of carbon metabolism in *Gluconacetobacter xylinus* (Klemm et al., 2001).

1.3.2 Crystalline structure of cellulose

Cellulose is an aggregate of glucan chains that are arranged in a specific manner to give rise to a crystalline state. Despite the fact that all celluloses, whether produced by plants, bacteria or other organisms, have the same chemical composition, there are stark differences between celluloses from different sources, especially in terms of physical properties such as the glucan chain, the crystallinity and the crystalline form of the cellulose product. The crystalline state, which defines the physical properties of the product such as its strength, solubility in various solvents, and accessibility to various modifying reagents, differs from organism to organism (Saxena et al., 1995).

The crystalline structure of cellulose has been one of the most studied structural problems in polymer science. Cellulose consists of both amorphous and crystalline regions (Thygesen et al., 2005). It is well known that cellulose can exist as crystalline microfibrils of cellulose I, II, III

and IV (Marchessault et al., 1962; Walton et al., 1973). The crystalline fraction is expressed as a percentage as the crystallinity index. Various methods of assessing the crystallinity are available, X-ray diffraction; CP/MAS C13 solid-state NMR, and Fourier Transform IR-spectroscopy (Vander Hart et al., 1984; Segal et al., 1959; Nelson et al., 1964).

Cellulose I is a native form of cellulose. Based on NMR studies, native celluloses are composed of species-specific compositional ratio of two crystalline allomorphs, designate cellulose I α and I β (Vander Hart et al., 1984). The two forms of cellulose I have different intermolecular hydrogen bonding patterns, although the configurations of the heavy atoms are similar. Investigation using electron microbeam diffraction and combined X-ray and neutron diffraction has revealed that cellulose I α has a triclinic unit cell, and that it is predominant in celluloses from bacteria and non-charophycean algae, whereas cellulose I β has a monolithic unit cell and it is the predominant form in higher plant cellulose such as cotton ramie types (Horii et al., 1987; Bielecki et al., 2005). These differences may influence the physical properties of the cellulose. Cellulose I β is more stable than I α , as is evident from the fact that cellulose I α is easily converted to cellulose I β when dissolved in hydrolysis acid (Atalla, 1989), or subjected to steam annealing or a solid-state chemical transformation (Horii et al., 1987). A series of investigations by Meyer and co-workers led to the postulation of a monoclinic unit cell as shown in Figure 1.3.9 with axes of $a = 8.35\text{\AA}$, $b = 10.3\text{\AA}$, $c = 7.9\text{\AA}$ and $\beta = 84^\circ$. The unit cell most probably belongs to the space group $P2$, and contains four glucose residues (Ott *et al.*, 1954).

Cellulose II, which is seldom found in nature, is produced by the mercerisation of native cellulose or regeneration from cellulose I dissolved in a solvent followed by re-precipitation by dilution in water (Kono et al., 2004). Mercerisation involves intracrystalline swelling of cellulose in concentrated aqueous NaOH followed by washing and recrystallization. Regeneration involves

either preparing a solution of cellulose in an appropriate solvent or the preparation of an intermediate derivative followed by coagulation and recrystallization (Langan et al., 2001).

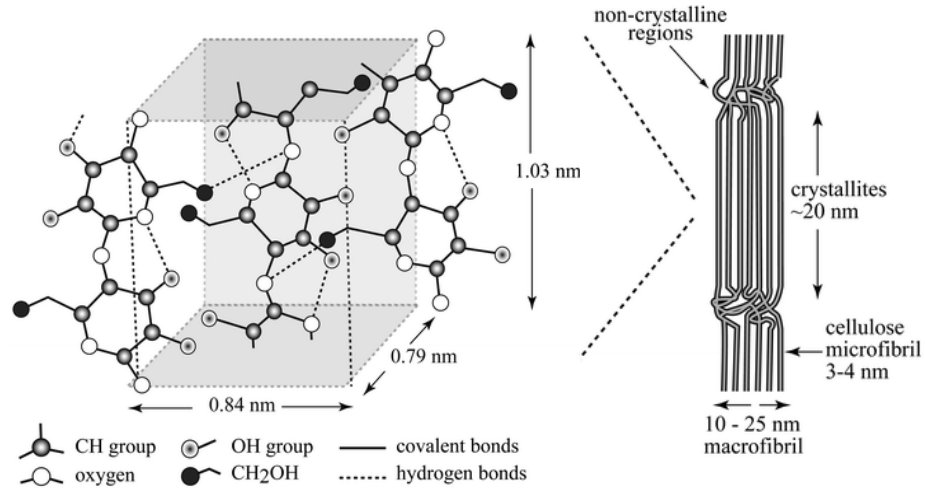


Figure 1.3.8: Cellulose unit cell (Gibson et al., 2010).

The multiple glucan chains in cellulose I are arranged in parallel (Koyama et al., 1997), whereas cellulose II is composed of anti-parallel chains, thought to be as a result of chain folding (Kolpack and Blackwell, 1976; Langan et al., 2001; Kuga et al., 1993) as shown in Figure 1.3.8.

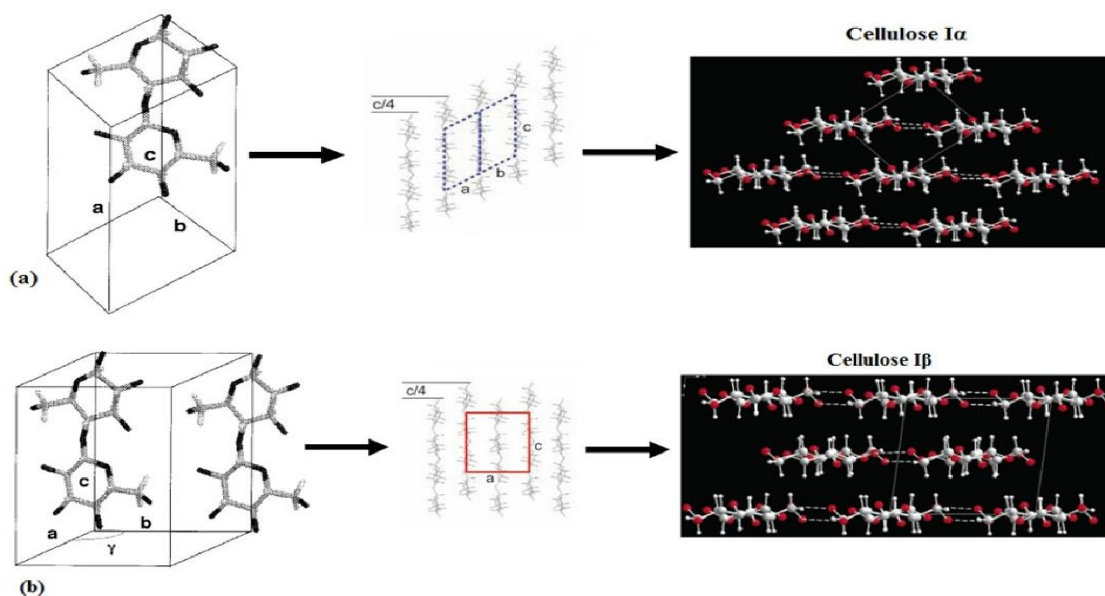


Figure 1.3.9: Crystal structure models of celluloses Ia (a) and Ib (b) assignable to the one-chain triclinic and two chain monoclinic crystals, respectively (Moon et al., 2011; Koyama et al., 1997).

The lattice structure of cellulose II is usually based on the monoclinic unit cell found by Andress with axes: $a = 8.14 \text{ \AA}$, $b = 10.3 \text{ \AA}$, $c = 9.14 \text{ \AA}$ and $\beta = 62^\circ$. Like cellulose I, this unit cell contains four anhydroglucose units and most probably belongs to space group $P2$. The arrangement of molecules in the crystal structure of cellulose II is shown in Figure 1.3.10. Cellulose II is formed naturally by a mutant bacteria strain of *Gluconacetobacter xylinus* and occurs in the algae *Halicysdetis*. Both sources are very useful in providing an insight into the crystal structure of cellulose II (Klemm et al., 2003; Zugenmaier, 2001).

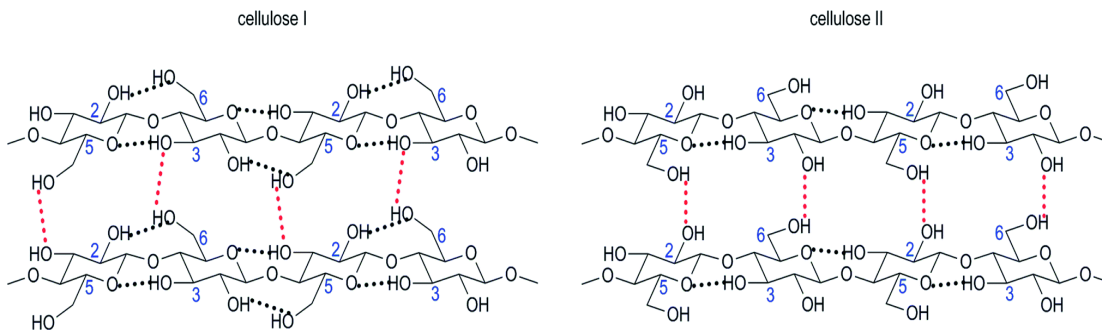


Figure 1.3.10: Suggested arrangement of molecules in crystal of (a) cellulose I and (b) cellulose II (Credou et al., 2014).

Cellulose III and IV are derived from cellulose I and II, and they are called III₁, IV₁, III₁₁, and IV₁₁, respectively (Ishikawa et al., 1997). Cellulose III₁ and III₁₁ are formed in a reversible process from cellulose I and II by treatment with liquid ammonia or small amounts of amines, and the subsequent evaporation of excess ammonia. Meanwhile, VI₁ and IV₁₁ may be prepared by heating cellulose III₁ and III₁₁ respectively at 260 °C in glycerol as shown in Figure 1.3.11. Published cell parameters for cellulose III₁ are $a = 1.025$; $b = 0.778$; $c = 1.034$ nm; and $V = 122.4$. The model does not show strict *P21* chain symmetry (Sarko et al., 1976). Based on ¹³C NMR spectrum of III₁ it can be seen that there is no hydrogen bonding in cellulose III₁ to increase the flexibility of the chains, and the lateral order of the crystallization was eventually lost (Wada et al., 2004).

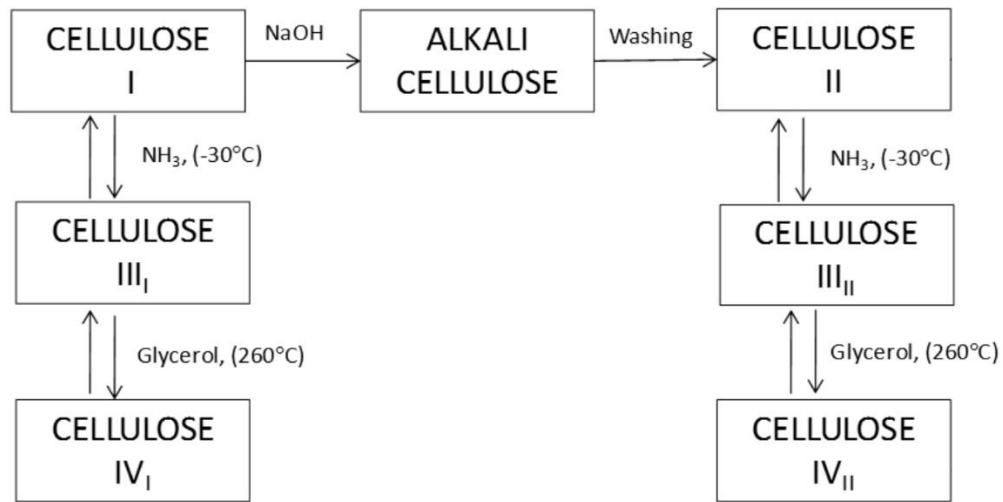


Figure 1.3.11: Inter-conversion of the polymorphs of cellulose (Theo et al., 2013)

1.3.3 Converting cellulose I to cellulose II

One of the most important steps in the production of any cellulose product is the purification, known as pulping in the paper making industry. The purification process removes all of the residue and chemicals bound to the cellulose fibre. It also removes the impurities that occur during processing and converts them into soluble compounds. It is important to remove lignin to prevent the discolouration of paper with age, which can be caused by photo-oxidation (Robert, 1996). Consequently, many different methods have been developed using different chemicals to produce a good quality paper and overcome the possibility of low pulp yields (Rashidova et al., 2003; Bajpai, 2005).

The most commonly used chemicals in the mercerisation process are alkaline due to their ability to hydrolyse cellulose and remove the impurities present in cellulose. The mercerisation process is usually accompanied by the unwanted transformation of cellulose I to cellulose II. The transformation of the crystal structure from cellulose I to cellulose II depends on the

concentration of NaOH. Researchers have reported that the transformation of cellulose I to cellulose II occurs at concentrations of NaOH above 6 % (Borysiak, 2003; Moigne, 2009). Many studies have researched the purification of cellulose and the effect of immersion time on the purification (Table 1.4). There is still ongoing research into the change of cellulose I to cellulose II as a result of alkalisiation (Oh et al., 2005; Zhou et al., 2004).

Table 1.4: *Immersion times of BC in NaOH.*

NaOH Immersion Time	Researchers
8 min	Moharram, 2008
30 min	George et al., 2005
1 hours	Mansikkamäki et al., 2007; Oh et al., 2005; Shibazaki et al., 1997
2 hours	Nakagaito and Yano, 2008
4 hours	Gelin et al., 2007
24 hours	Nishi et al., 1990
48 hours	Saibuatong and Philasapong, 2010, Aziz and Ansell, 2004

The transformation of cellulose I to cellulose II consists of some essential steps, the fibre swells due to water absorption, which leads to a considerable increase in the mobility of the cellulose chains and then the alkaline solution enters the amorphous areas. It then saturates the cellulose and disrupts the crystalline region, forming a new lattice. This new crystalline lattice is formed after the mercerisation alkaline solution is washed off (Lee et al., 2004; Liu et al., 2008). The amorphous and crystalline regions covering the upper surface of the cellulose structure usually react with the alkali solution. They are removed when the solution is washed off (Gassan & Bledzki, 1999; Liu et al., 2008). The transformation from cellulose I to cellulose II is a polymorphic transformation in which a change in the conformation occurs from parallel to anti

parallel. This transformation is accompanied by the breaking of many primary inter- and intramolecular hydrogen bonds in cellulose I. This transformation is a secondary occurrence, which would not take place without first breaking the primary hydrogen bonds in cellulose I (Laszkiewicz, 1997). As a result of this transformation, there is a significant decrease in mechanical properties. It was reported that Young's modulus of a single ramie fibre decreased from 27 GPa (cellulose I) to 21 GPa (cellulose II) (Ishikawa and Okano, 1997). The use of wide angled X-ray diffraction can easily detect the appearance of cellulose polymorphs (Mansikkamäki et al., 2005; Zugenmaier, 2008). X-Ray diffraction method was used by Matsuo et al., (1990) to measure single cellulose fibres. It was observed that the cellulose I fibre had a modulus of 120-135 GPa and cellulose II had a modulus of 106-112 GPa. The moduli of both polymorphs have also been reported to be 130-137 GPa and 71-90 GPa for cellulose I and II, respectively (Kroon-Batenburg and Kroon, 1997).

An enhancement in mechanical and thermal properties of processed bacterial cellulose sheets is visualised by preserving the more high-performance cellulose I crystal phase in the bacterial cellulose microfibrils (George et al., 2005; Hsieh et al., 2008; Nishi et al., 1990; Shibazaki et al., 1997; Yamanaka et al., 1989),

1.3.4 Surface modification of Bacterial Cellulose

Bacterial Cellulose (BC) is one of the materials showing potential for use as a scaffold. BC is a polysaccharide (Backdahl et al., 2006) and is a form of completely pure cellulose synthesized extracellularly as nanofibrils by *Gluconacetobacter xylinus*. In BC, a network of these fibrils generates high mechanical strength and water content. Hydrogen bonds from the

hydroxyl groups hold the cellulose chains together and produce materials with a high degree of crystallinity, low solubility and very low degradation rate (Helenius et al., 2006).

The structural modification of cellulosic materials can be achieved by alkali treatment. The bacterial cellulose produced by *Gluconacetobacter xylinus* is in the form of cellulose I allomorph (Yu and Atalla, 1996), which is the predominant form of native cellulose. However, cellulose I can be converted into the more stable polymorph, cellulose II, by mercerisation. Mercerisation is the swelling of cellulose I fibres in sodium hydroxide solution, allowing for reorganisation of the chains and subsequent conversion of cellulose I to cellulose II when the solution is removed. In this conversion, additional interchain hydrogen bonding is formed, which leads to higher stability and improvement of the properties of cellulose II (Kolpak et al., 1978). Various modifications have been made to improve the mechanical, chemical, structural and biological properties and production yield of BC. Some researchers have altered the synthesis of bacterial cellulose using different carbon resources such as fructose, mannitol, corn syrup, alcohol, organic acid and glucose as shown in Table 1.5. Tonouchi et al., found that glucose enhances cellulose yield by activating phosphoglucose isomerase and UDPGLc pyrophosphorylase (Tonouchi et al., 1996). BC production using fructose as a carbon source was 10% lower than in a glucose containing medium. In other studies, molasses were used as a carbon source. As a result, the yield increased by 76% and the specific growth rate increased two-fold compared with untreated molasses (Bae and Shoda., 2004). With carboxymethylated cellulose and glucose added into the medium as a carbon source, the process produces an extracellular polysaccharides carboxymethylated-BC. This material has the capability to act as an ion exchange with enhanced specific adsorption for lead and uranyl ions (Sakairi et al., 1998b). Another way to increase the yield of production of bacterial cellulose on the static culture is to

use a cylindrical fermentation vessel. The bottom of the container can be lined with a silicone sheet of ~100 µm thickness. To facilitate the absorption of oxygen by the medium, the apparatus is equipped with tortuous airflow silicone constructed from a silicone framework of 0.5 mm thickness, of which both sides are attached to a silicone membrane of 100 µm thickness. The rate of BC production increased to approximately five times higher than usual.

Table 1.5: Production yield of BC based on the various carbon sources (Masaoka et al., 1993).

Carbon Source		Cellulose yield (relative %)
Monosaccharides:	D-fructose	92
	D-galactose	15
	D-glucose	100
	D-mannose	3
	D-xylose	11
	L-arabinose	14
	L-sorbose	11
	Disaccharides:	lactose
maltose		7
sucrose		33
Polysaccharides:	Starch	18
Alcohols:	Ethanol	4
	Ethylene glycol	1
	Diethylene glycol	1
	Propylene glycol	8
	Glycerol	93
	Myo-inositol	17
Organic acids:	Citric acid	20
	l-Malic acid	15
	Succinic acid	12
Other:	D-glucono lactone	62
No carbon source		2

The mechanical properties of BC can be improved by adding agents which allow the bacteria to produce cellulose fibrils that are much longer and thinner than usual into the medium during culture. Adding agents such as chloramphenicol or nalidixic acid allows the shape of the BC fibre

to be lengthened by 2-4 times from its original size, giving a BC with superior mechanical properties (Ishihara and Yamanaka, 2002).

1.3.5 Applications of Bacterial Cellulose

Bacterial cellulose can, in general, be applied in areas where plant cellulose is used. As a result, it has many useful applications in biotechnology and biomedical science and has a wide range of applications in tissue engineering (George et al., 2005; Jonas, 1998; Chang et al., 2011; Lina et al., 2013). Because of its unique properties, such as ability to absorb fluids, good histocompatibility with living tissue and high purity with a crystalline structure, it has great value in medicine, particularly as artificial skin and as a wound dressing.

The use of bacterial cellulose as a wound healing dressing has been successful due to bacterial cellulose having high water holding capacity (Sulaeva et al, 2015). The ability to absorb water also provides the possibility of loading liquid drugs and bioactive compounds into the structure of the bacterial cellulose dressing material (Shah et al, 2013). Bacterial cellulose wound dressings are also favoured more due to their ability to retain a wet environment, preventing the dressing from sticking to the wound. Therefore, protecting the wound as well as reducing pain during change of dressing and it also shortens the healing time or wound closure when compared to standard care for non-healing ulcers (Czaja et al., 2006, Czaja et al., 2007, Ovington, 2007). For example, Biofill®, Gengiflex®, and XCell® are developed for such purposes (Fontana et al., 1991; Novae et al., 2000). Modifying BC with the aim to improve wound dressing characteristics are generally related to enhancing its properties, such as; biocompatibility, liquid holding and release capacity and impregnation with antimicrobial components (Sulaeva et al, 2015). There are many studies outlining the numerous parameters that affect the formation of the bacterial

cellulose network (Chawla et al, 2009. Dufresne, 2012. Keshk, 2014. Krystynowicz et al, 2002). The scope of BC utilisation in the biomedical field can be extended by controlling the characteristics of the material (Sulaeva et al, 2015. Ul-Islam et al, 2012).

It is also used as a controllable delivery system and other applications in tissue engineering, sensor, blood purification, agriculture, and water purification (Lina et al., 2013, Chang et al., 2011).

The application of bacterial cellulose in commercial food production is a traditional dessert in the Philippines known as ‘nata de coco’. It is prepared using sucrose as the growth medium for the bacterial cellulose producing bacteria, with either coconut water or coconut milk (Figure 1.3.12). Nata de coco is becoming increasingly common beyond Asia and it is believed that the consumption of the dessert pellicles protects against, arteriosclerosis, bowel cancer, and coronary thrombosis, and also prevents the sudden increase of glucose level in the urine (Bielecki et al., 2005).



Figure 1.3.12: Nata de coco (<https://nurfaiyah33.files.wordpress.com/2010/04/127.gif>)

Disintegrated bacterial cellulose makes an excellent component in the production of paper, resulting in paper with superior mechanical properties. Microfibrils of the BC (are connected by hydrogen bonds) polymer form a great number of hydrogen bonds when the paper is subjected to drying, therefore giving improved chemical adhesion and tensile strength, leading to a stronger paper. BC-containing paper shows a more elastic, air permeable and better retention of solid additives, such as filler and pigments. It is also resistant to forces such as tearing and bursting (Iguchi et al., 2000). Bacterial cellulose-based composites have been made, with water-soluble polymers for special applications such as a filtration material, using carboxymethyl chitin, carboxymethyl cellulose, and other cellulose-based polymers. These polymers were added into the medium by *in situ* processes (Shibazaki et al., 1993; Takai, 1994).

An edible bacterial cellulose is produced by treating BC with alginate or ethanol. This makes the bacterial cellulose softer and gives it a texture similar to fruit and other foods. This mechanism forms a gel by immobilising the water, which leaves it easier to chew and bite (Okiyama et al., 1992). Bacterial cellulose can also be used as a thickener in food and cosmetics to maintain its viscosity (Jonas and Farah, 1998; Kent et al., 1991).

There has been much work focused on designing an ideal biomedical device from bacterial cellulose, such as artificial; blood vessels, skin, cornea, urethra, bone, heart valve prosthesis, cartilage, drug delivery, hormones and protein (Lina et al., 2013; Halib et al., 2009; Oshima et al., 2011; Peterson et al., 2011; Wang et al., 2010).

1.3.6 Bacterial Cellulose composites

Bacterial cellulose has a natural porous arrangement of fibres which acts as a matrix for framing particles from a variety of different reinforcement materials (Esa et al., 2014). The

generation of composites is another way of utilising bacterial cellulose based materials (Sulaeva et al, 2015). The approach of composite formation usually occurs through reinforcement of nanoparticles or liquid into the BC structure (Sulaeva et al, 2015. Hu et al, 2014). Physico-chemical interactions of these substances with the BC interfibrillar network are the main mechanisms of composite formation (Hu et al, 2014). Favier et al., were the first to apply cellulose whiskers extracted from marine life as a reinforcing phase, which they added to latex obtained by the copolymerization of styrene (35 wt.%) and butyl acrylate (65 wt.%) as a matrix to make a new nanocomposite. Even with a small percentage of cellulose whiskers (1 to 12 wt. %) added into the matrix, the mechanical properties of this nanocomposite were improved substantially (Favier et al., 1995). The tensile strength properties of whiskers are believed to be far beyond those of the current high-volume content reinforcement and allows composites to be processed with the highest possible strengths (Samir et al., 2005). This invention opened the way to cellulose nanocomposite technology, which is widely used in various applications, such as agro-based composites, automotive parts, aircraft, railways, furniture, and sports clothing and equipment (Dahlke et al., 1998; Herrmann et al., 1998).

As mentioned by Klemm et al., (2000), bacterial cellulose is composed of nanosized fibres, described as nanocellulose, and the nanofibre structuring determines the properties of the product. Nishi et al., (1990) reported a strikingly high dynamic Young's modulus close to 30 GPa for dried sheets acquired from processed bacterial cellulose pellicle. Due to this incredible modulus, bacterial cellulose is an ideal candidate as raw material to further enhance the Young's modulus of high strength biobased nanocomposites. The microfibril ribbons are roughly 3-4 nm (thickness) x 10-130 nm (width) (Bielecki et al., 2005; Jonas and Farah, 1998; Yamanaka et al., 2000). The model created by Iguchi et al., (2000), as shown in Figure 1.3.6 assists in the

understanding of bacterial cellulose microfibrils and has been cited by a number of researchers interested in this field.

The use of cellulose microfibrils obtained from bacterial cellulose in various applications has been reported in a great deal of publications. Nakagaito and Yano, have produced optically transparent composites based on both bacterial cellulose and micro-fibrillated plant cellulose. Their composites have a remarkable strength comparable to magnesium alloy (over 400 MPa) (Nakagaito and Yano, 2006). By mixing acrylic resin with bacterial cellulose acetylated nanofibres, Ifuku et al., produced optically transparent composites (Ifuku et al., 2007). In biomedical applications, fibrillated bacterial cellulose has been used as reinforcement for poly(vinyl alcohol) (PVA) as a matrix (Wan et al., 2006). In contrast, there has so far been very limited literature regarding the preparation of nanocomposites using nanocellulose fibres obtained from bacterial cellulose. This is because of the difficulties in extracting nanocrystals from bacterial cellulose, the result of which being that the cost of production is higher than for plant cellulose. However, some researchers have extracted cellulose nanocrystal from commercial bacterial cellulose by following the classic method, i.e. acid hydrolysis, which was developed by Rånby and Ribi in the early 1950s. It is now the most widely used procedure for the extraction of cellulose nano-whiskers (CNW) and involves acid treatment with sulphuric acid, followed by a filtration or centrifugation process. Acid hydrolysis leads to a stable aqueous suspension of cellulose nanocrystals. These cellulose nanocrystals are negatively charged, therefore they do not have a tendency to aggregate. In the course of the hydrolysis process, esterification of the surface hydroxyl groups from cellulose takes place, introducing sulfate groups as a result (Rånby, 1949). Regardless of the advantage of attaining a stable suspension, the presence of the sulfate groups in the outer surface of the material has proven to decrease the

thermal stability of the material (Roman, 2004). This is also an important factor when planning to use cellulose nano whiskers for nano-reinforcement. A common method for the extraction of cellulose nano whiskers involves centrifugation after the hydrolysis process to remove acid and the degraded material. Cellulose nano whiskers are usually acquired from the liquid supernatant after several centrifugation cycles, leaving behind the larger cellulosic material fractions and some impurities in the solid precipitate. Taking into consideration that in the there is no hemicellulose or lignin to remove from bacterial cellulose, previous research has proposed an extraction method in which bacterial cellulose nanosized whiskers are obtained in the centrifugation precipitate instead of the supernatant. Therefore, the yield can be as high as 90% based on the dry weight of bacterial cellulose (Martínez-Sanz et al., 2010; Olsson et al., 2010) compared to around 1–5% when the whiskers are obtained from the liquid supernatant. However, in comparison to this, strong hydrolysis condition are needed to break down the fibril bundles in the highly crystalline network structure of bacterial cellulose. Individual nanofibrils cannot be produced without degradation and partial carbonization of the material (Olsson et al., 2010).

Grunet and Winter, successfully produced cellulose whiskers from bacterial cellulose using cellulose acetate butyrate (CAB) as a matrix to produce the nanocomposite (Grunet and Winter, 2002). In combination with the same matrix, Roman and Winter, were able to extract nanocrystal cellulose from bacterial cellulose (Roman and Winter, 2006). Orts et al., also hydrolysed needle-like nanocrystal cellulose from bacterial cellulose and used these in combination with starch as a matrix (Orts et al., 2005). One important point mentioned by the latter is that the addition of reinforced microfibrils obtained from bacterial cellulose does not always improve the modulus to the same extent as cotton or soft wood fibre. As unmodified microcrystalline cellulose (MCC) is generally hydrophobic in nature, it is likely to be difficult to

get a good degree of compatibility using bacterial cellulose-nano-cellulose as a reinforcement agent with a hydrophilic matrix. In order to reduce its hydrophobic nature, cellulose nanocrystals from BC have been topochemically Trimethylsilylated (Grunet and Winter, 2002; Roman and Winter, 2006). Degradable polymers are thoroughly explored as biomaterials in the field of reconstructive surgery (Sarasam et al., 2005). Polycaprolactone (PCL) is a semi-crystalline biodegradable thermoplastic polymer with low melting point ($\sim 67^{\circ}\text{C}$) and a glass transition temperature in the range of -65 to -60°C . PCL has received a lot of attention due to its biodegradability, favourable miscibility with other polymers and low temperature adhesiveness (Wu, 2005; Chandra et al., 1998; Zhong et al., 2001; Jimenez et al., 1997; Corradini et al., 2004). PCL is relatively hydrophobic and has a slow degradation rate, ideal for use as bone substitutes and sustained release drug carriers (Chen, 2005).

Many attempts have been made in the past to blend plastic materials such as PCL with cheaper, biodegradable natural biopolymers such as cellulose, starch and chitin (Wu, 2005; Olabarrieta et al., 2001; Li et al., 2002; Suryadiansyah, 2002; Wu et al., 2002). Interest in the production of biodegradable polymers using these renewable resources is growing (Cho et al., 2000). A great deal of research has been carried out on improving the properties of PCL (Zhong et al., 2001; Jimenez et al., 1997; Corradini et al., 2004; Hao et al., 2002). Zhong et al., investigated the properties of soy protein isolate/polycaprolactone blends (SPI/PCL) compatibilized by methylene diphenyl diisocyanate (MDI). It was found, that mechanical properties of 50/50 (SPI/PCL) blends increased with increasing MDI concentrations and elongation increased with increasing PCL concentration (Zhong et al., 2001).

In a study by Jimenez et al., the structure and properties of PCL-clay blends were investigated. From isothermal crystallisation experiments, it was found that a small amount of

clay in the blend accelerated the crystallisation of PCL, whereas a large amount of clay delayed it (Jimenez et al., 1997). However, in a study by Corradini et al., blends of PCL with zein (PCL/zein) were produced and the mechanical and thermal properties were investigated. Zein represents about 80% of the total proteins in corn grains; due to its hydrophobicity, thermoplasticity and impermeability to gases it is a potential material for use in the production of biodegradable polymers. Blends of PCL/zein showed a reduced tensile strength and elongation at break, but the Young's modulus had increased when compared to the pure polymers. Analysis of the morphology revealed good dispersion of the zein in the polymers, but weak interfacial adhesion between PCL and zein. Therefore this experiment showed that PCL and zein were incompatible (Corradini et al., 2004). Hao et al., used a solvent-cast technique to produce nanocomposites of PCL and hydroxyapatite (PCL/HA). The study showed that the melting point increases with increasing HA content, while the tensile modulus for the nanocomposites also increases with increasing HA content. The yield stress was almost invariant with composition (Hao et al., 2002).

The main limitation of PCL is the low melting temperature ($T_m \sim 65^\circ\text{C}$), which can be overcome by blending it with other polymers. Blending two polymers is an approach to developing new biomaterials exhibiting combinations of properties that could not be obtained by individual polymers (Sarasam et al., 2005). Blends made of synthetic and natural polymers can consume the wide range of physicochemical properties and processing techniques of synthetic polymers as well as the bio-compatibility and biological interactions of natural polymers. The addition of relatively small amounts of nano-sized fillers in PCL can lead to dramatically improved mechanical properties and heat distortion temperatures. Several synthetic and mineral nano-fillers (as layered silicate montmorillonite) (Pantoustier et al., 2002; Chen and Evans.,

2006) have already been studied as reinforcement for PCL, but an increasing interest is rising in bio-nanocomposites in which bio-sourced nano-scaled fillers are used as reinforcement (Berglund and Peijs, 2010; Eichhorn et al., 2010; Bordes et al., 2009).

Due to its abundance, renewability, hydrophilic nature and good mechanical properties, cellulose is the main fibre source for the preparation of such bio-nanocomposites (Peijs, 2000; Berglund et al., 2010; Bledzki and Gassan, 1999; John et al., 2007). Over the last few years, researchers have developed procedures to isolate nano-crystals of cellulose, known as cellulose whiskers, which are derived from various origins such as plants and tunicates (Favier, 1995; Oksmann, 2001). Chitin whiskers, have already been used as reinforcement fillers for PCL bio-nanocomposite (Wu et al., 2007). Cellulose nanofibres can also be directly obtained from some bacteria (e.g. *Gluconacetobacter xylinus*), which under special static culturing conditions produce a fine fibrous network of cellulose nanofibres. Elastic moduli of bacterial cellulose nanofibrils between 78GPa (Guhados et al., 2005) as measured by AFM nano-bending tests, and 114 GPa (Hsieh et al., 2008) as measured using Raman spectroscopy, have already been reported. The nano-structured network of bacterial cellulose nanofibrils, which interact with a high density of hydrogen bonds, is as important as the characteristics of isolated nanofibrils and can justify some interesting physical properties. Young's moduli and stress to failure of as much as 30 GPa and 200 MPa, respectively, have been found for 2D-isotropic bacterial cellulose films (Iguchi et al., 2000; Gea et al., 2007).

Yano et al., have reported bacterial cellulose composites prepared via impregnation of thermoset resins (up to 70 wt. % bacterial cellulose content), which showed optical transparency, low coefficient of thermal expansion (comparable with silicon) and mechanical strength comparable with mild steel (Yano et al., 2005). A non-trivial challenge is how to transfer the BC

nanofibres into a thermoplastic matrix and at the same time preserving the fibrous network structure. Impregnation by a polymer solution is a viable route (Righdal et al., 1983) but it requires long preparation times and the use of solvents, which can draw environmental concerns. Bacterial cellulose has been applied in different fields such as; blood vessel regeneration and wound dressings, (Wippermann., 2009, Muangman et al., 2011). Table 1.6 below shows bacterial cellulose composites and their various functions (Esa et al., 2014).

Table 1.6: *Bacterial cellulose composites and their applications (Esa et al., 2014)*

Application Field	Reinforcement material	Function	References
Electronic	Graphite nanoplatelet	Electrical conductivity	Zhou et al., 2013
Electronic	Poly-4-styrene sulfonic acid	Redox flow battery	Gadim et al., 2014
Biomedical/Industrial	Chitosan	Nanofilm	Fernandes et al., 2009
Biomedical	Hydroxyapatite	Bone tissue engineering	Tazi et al., 2012
Biomedical	Silver nanoparticles	Antimicrobial wound dressing	Wu et al., 2014, Zhang et al., 2014
Biomedical	Paraffin	Bone scaffolding	Zaborowska et al., 2001
Electronic	Polyurethane	Film substrate of light emitting diode	Ummartyotin et al., 2012

1.3.7 Bacterial cellulose based scaffolds for tissue engineering.

Tissue engineering is a field that combines the knowledge and technology of cells, suitable biochemical factors, and engineering materials to regenerate damaged tissue and create artificial tissues and organs (Langer et al., 1993, Liu et al., 2007). Scaffolds can be synthetic or natural materials. Synthetic biopolymers do offer an advantage over natural materials because they can be specially tailor made to serve a wide range of properties and there are many methods which can process biomaterials into scaffolds. Some techniques are conventional, such as

impregnation and sintering ceramic scaffold, phase separation, solvent casting and fibre knitting to name a few. Techniques such as fibre networking, use biodegradable fibres to fabricate scaffolds by either fibre binding routes or knitting (Cooper et al., 2005, Freed et al., 2006).

Electrospinning is a method reported to fabricate polymer fibres which range from a few nanometres to microns (Xu et al., 2004). Another great potential in electrospun fibres is in the region of bioengineering. In biomedical applications, the materials used have to be biocompatible. Therefore, natural polymers have an advantage over synthetic because most natural polymers can be degraded by naturally occurring enzymes. It can be used in drug delivery or in applications where temporary implants are required. The degradation rate of the implanted polymer can also be controlled by chemical crosslinking or other chemical modifications, which allow greater versatility in the design of the implant (Atala et al., 2002).

Electrospun fibres form nanostructured networks that are expected to influence mechanical properties such as the tensile strength, elongation, etc. Elastomer-based electrospun fibres have shown a 40% reduction in the peak tensile strength and 60% reduction in elongation at maximum applied stress. Wang et al., reported that mechanical properties of electrospun nanofibres are closely related to the fibre orientation, bonding between fibres and fibre slippage rather than the mechanical properties of individual fibres within the web (Wang et al., 2008; Favier et al., 1997).

Previous studies have demonstrated that 2D and 3D micro/nanofibrous scaffolds can improve cell attachment and spread significantly due to surficial nano-topography and an enlarged inner surface of the structure (Kim et al., 2010; Park et al., 2008). In particular, 3D scaffolds with oriented fibres or microgrooves could induce a uniform cell alignment as well as

directional cell migration and even guide the cell outgrowth (Badrossamay et al., 2010; Uttayarat et al., 2010; Wang et al., 2009).

Electrospinning process creates nanofibres through an electrically charged jet of polymer solution or polymer melt. In electrospinning, a high voltage is applied to a polymer fluid such that the fluid will induce charges. When charges within the fluid reach a critical point/amount, a fluid jet will erupt from the drop that is formed at the tip of the needle which results in the formation of a Taylor cone (Sun et al., 2014).

The electrospinning jet travels towards the region of lower potential, which in most cases is the ground collector. Many parameters influence the morphology of the resulting electrospun fibres, from beaded fibres to fibres with pores on its surface (Lyons et al., 2004; Larrondo and Manley, 1981). Most electrospinning is carried out using polymer solutions. Therefore, the parameters affecting electrospinning of polymer solutions is of great interest. Varying the parameters can create nanofibres with different morphology (Huang et al., 2003). The Surface tension has a part to play in the formation of beads along the fibre length. The viscosity of the solution and its electrical properties will determine the extent of elongation of the solution; this will affect the diameter of the resultant electrospun fibres. One of the factors affecting the viscosity of the solution is the molecular weight of the polymer. When a polymer of higher molecular weight is dissolved in a solvent, its viscosity will be higher than a solution of the same polymer but of a lower molecular weight. One of the conditions necessary for electrospinning to occur where fibres are formed is that the solution must consist of a polymer of sufficient molecular weight and the solution must be of a sufficient viscosity (Ramakrishna et al., 2005, Sun et al., 2014).

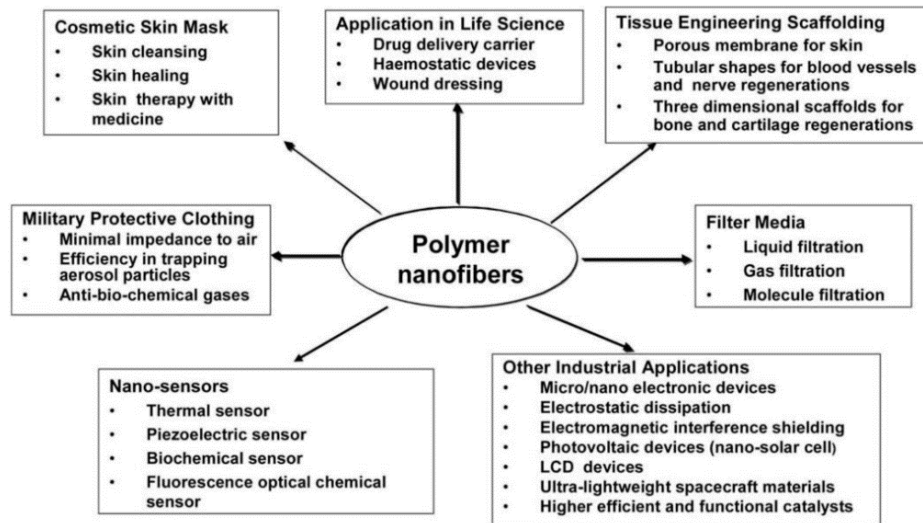


Figure 1.3.13: Potential applications of electrospun polymer nanofibers (Huang et al., 2003).

The electrospinning technique can serve various purposes, such as the fine control of the fibre diameters, the production of defect-free or defect-controllable fibre surface, and the formation of continuous single nanofibres (Jin et al., 2005). The outstanding properties of polymer nanofibres include their extensive surface area, flexibility of surface functionalities, and good mechanical performance (Kim et al., 2005). Polymer nanofibres can be used in a broad range of applications such as artificial tissue for membrane separation, texturing filters, porous electrodes, biomaterials and composite reinforcement (Jin et al., 2005; Kim et al., 2005; Vepari et al., 2006). Three-dimensional printing is an innovative technology which is pioneering in engineering, manufacturing and product design. It has also been a great promise to for ground breaking medical research. The process of 3D printing involves printing a single material or a combination of multiple materials in a layer by layer manner to generate the shape of every individual layer which eventually results in a 3D complex structure that has limited restrictions on its spatial arrangements (Chia et al., 2015; Bose et al., 2013). There are many different types of 3D printing techniques, such as stereolithography (SLA) which was one of the first in 3d

printing technology (Hull, 1986; Chia et al., 2015), Selective laser sintering (SLS) and fused deposition modelling (FDM) (Chia et al., 2015).

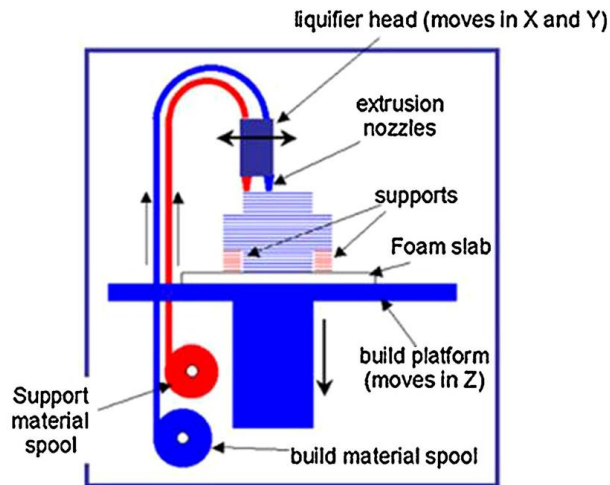


Figure 1.3.14: Fused deposition modelling schematic (Van, 2012; Chia et al., 2015)

FDM involves the use of a computer aided file (CAD) to provide information for the production of the 3D printed object. It involves heating an amorphous thermoplastic filament to a semi-liquid viscous state, which is then extruded through two heated extrusion heads with a small orifice and deposited slowly through an aperture onto a non-sticky substrate to build objects layer by layer in a specific laydown pattern (Figure 1.3.14) (Zein et al., 2002).

The 3D printing approach offers significant advantages for tissue engineering and biomedical devices due to be able to produce specific and distinct parts (Chia et al., 2015). Although 3D printing offers excellent potential for applications in the medical field, there are still issues that need to be overcome before it can be considered as a common bio fabrication technology in medicine.

1.3.8 Cellular interactions with bacterial cellulose

BC has been studied for use as a scaffold in skin tissue engineering (Sanchavanakit et al., 2006), blood vessels (Klemm et al 2001), tissue engineered blood vessels (TEBV) in small calibre grafts (Backdahl et al., 2006) and cartilage tissue engineering (Svensson et al., 2005), as well as in bone in the form of a HA/BC nanocomposite (Wan et al., 2006).

Research on the growth of human skin fibroblasts on BC shows that fibroblasts attach together over time and detach from the BC scaffold. This suggests insufficient adhesion between the fibroblasts and BC surface. In order for cells to integrate into a scaffold, they must first adhere to the surface to be able to grow and proliferate (Svensson et al., 2005); however, if the surface charges are too strong, the proliferation is inhibited. The network density of the hydrogel nanofibrils can also affect the attachment and proliferation of the cells.

Other studies have reported that different cells such as human embryonic kidney cells (Grande et al., 2009), human smooth muscle cells (Petersen et al., 2011), bone forming osteoblasts and fibroblasts (Chen et al., 2009), can grow in the presence of bacterial cellulose scaffolds. Human vein endothelial cells have also shown great proliferation in a bacterial cellulose hydrogel (Jeong et al., 2010; Recouvreux et al., 2011). Hu et al., studied the growth of human osteoblast cells on bacterial cellulose and showed that the osteoblast cells were able to attach and spread well on larger bacterial cellulose particles (Hu et al., 2014). Studies have demonstrated that 2D and 3D micro/nanofibrous scaffolds can improve cell attachment and spread significantly due to surface nano-topography and an enlarged inner surface of the structure (Kim et al., 2010; Park et al., 2008).

1.4 Aims and Objectives

The aim of this study was to grow and characterise bacterial cellulose (BC) from *Gluconacetobacter xylinus* and then carry out appropriate modification of the bacterial cellulose (BC) for use as a potential scaffold in tissue engineering. BC has a positive charge that would repel proteins from attachment on the surface, therefore one option would be to chemically modify the bacterial cellulose surface and consequently change the positive surplus to negative one. To achieve this, the bacterial cellulose surface was treated by varying concentrations of NaOH (5, 7 and 9%) over different time periods (5, 10 and 12 hours) to achieve a negative surface charge. The surfaces were then characterised in order to identify any chemical changes in the structure of bacterial cellulose. The main objectives of this research are listed below:

- To grow and preserve bacterial cellulose from *Gluconacetobacter xylinus*.
- To purify bacterial cellulose by eliminating bacteria and other bacterial components
- To characterise bacterial cellulose before and after purification.
- To determine the mechanical properties of bacterial cellulose before and after purification.
- To modify the surface of purified BC by mercerisation in varying concentrations of NaOH aqueous solutions.
- To study the effect of the above modifications on the properties and structure of BC.
- To observe transformation of cellulose I to cellulose II caused by mercerisation.
- To observe and compare Cell-cellulose interactions on BC and NaOH Surface modified BC.

The BC was grown and the morphology of the bacteria was observed using SEM analysis. The mechanical properties and morphology were also investigated after the purification treatment to study the effect of the purification steps and to prove that the purification steps do not transform cellulose I to cellulose II.

Surface modification of BC using varying concentrations of NaOH (5, 7 and 9%) was investigated at different time intervals (5, 10 and 12 hours). The morphology of the treated and untreated samples was observed using SEM analysis. FTIR was used to analyse the chemical changes and conversion of cellulose I to cellulose II with the treatment of NaOH. Surface topography was assessed using white light interferometry.

The cellular compatibility was tested on treated and untreated samples and analysed using phase contrast imaging and MTT assay.

A preliminary study in the use of BC as an electrospun nanocomposite with PCL is also studied. BC and PCL composites were also produced in order to study the effect of BC as a filler and observe changes in the mechanical properties. A thermal analysis was also conducted for both PCL-BC composites (electrospun nanocomposites and micro composites) to determine the effect of increased bacterial cellulose content on the thermal stability of composites.

CHAPTER 2

Materials and Methods

2.1 Culturing Bacteria

Bacterial cellulose was produced from *Gluconacetobacter xylinus* strains supplied by the Microbiology Laboratory of the Institute of Agriculture, Indonesia. The culture medium (prepared at University of Birmingham metallurgy and materials) was made up using the following chemicals; magnesium sulphate, ammonium sulphate, potassium hydrogen orthophosphate, glucose and yeast extract (Sigma Aldrich). The chemicals used for the agar solid media were mannitol, peptone and agar powder (Sigma Aldrich) as a setting agent. The chemicals used in the purification process, sodium hydroxide and sodium hypochlorite were received from VWR. Additional vitamins such as B1, B3 and B5 (Sigma Aldrich) were used to promote growth following Iguchi et al., (1988).

2.1.1 Preservation of the *Gluconacetobacter xylinus*

To ensure ease of storage and longevity, the bacteria were kept in a solid agar medium (the preservation was carried out at Queen Mary University in London). For every 3 litres of distilled water, 5g of yeast extract, 3g of peptone, and 25g of mannitol were added, with 15g of agar powder as a hardener. Glacial acetic acid was added into the medium to adjust its acidity. After being sterilised, the medium was placed in a laminar flow hood equipped with UV light under aseptic conditions where the bacteria were transferred to fresh medium. After being refreshed three times, the bacteria should be tested by isolation of individual colonies and

verification of the phenotype. If a colony of different morphology is detected, this shows that the bacteria have been contaminated.

Another way to store the bacteria is by placing them in a vial of 2-5 ml volume which is then frozen in liquid nitrogen and kept in cold storage at -70 °C. This allows storage of the bacteria for up to one year. The observation of the *Gluconacetobacter xylinus* colony obtained from the surface of the Petri dish or tilted tube (as shown in fig 2.2) was carried out using optical microscopy. In order to maintain the integrity of the colony, part of the agar medium containing the colony was removed using a sharp knife and transferred to a glass slide. Here it was spread evenly over the glass slide in order for it to be viewed under an optical microscope.

A lot of research has been carried out into BC with the aim of improving the quality and properties, as well as the production methods. Previous researchers have described some physiological parameters and investigation related to the metabolism of glucose in the Schramm-Hestrin medium and modified media. The strain of the bacteria, source of carbohydrates, acidity, temperature and culture methods are all important parameters for the production of cellulose by *Gluconacetobacter xylinus* (Masaoka et al., 1993; Geyer et al., 1994).

The strain of *Gluconacetobacter xylinus* used was a stock supply from the Laboratory of Microbiology, Institute of Agriculture, Bogor. This strain was originally supplied by the National Institute of Science and Technology, Manila, and is usually used for commercial purposes in the processing of 'nata de coco', a low calorie dessert in South East Asia (Budhiono et al., 1999). There was no further treatment applied and it was used as received.

For the preparation of a new starter or broth seed, a colony of *Gluconacetobacter xylinus* (Figure 2.1 and Figure 2.2) was gently transferred from the surface of solid agar, using an inoculating-hand loop and then transferred into culture medium. This is done to replenish the

bacteria and also to keep them viable and in good condition. Based on experience, the bacteria can be kept for 2 months in the agar solid in a fridge. If the colour of the agar solid turns pale, it indicates that the viability of the bacteria has decreased and they must be transferred to a new medium.



Figure 2.1: Transfer process of the bacteria onto the surface of solid agar media by an inoculating - hand loop under aseptic condition.



Figure 2.2: Bacteria kept in tilted test tubes to provide a larger surface area of solid agar media.

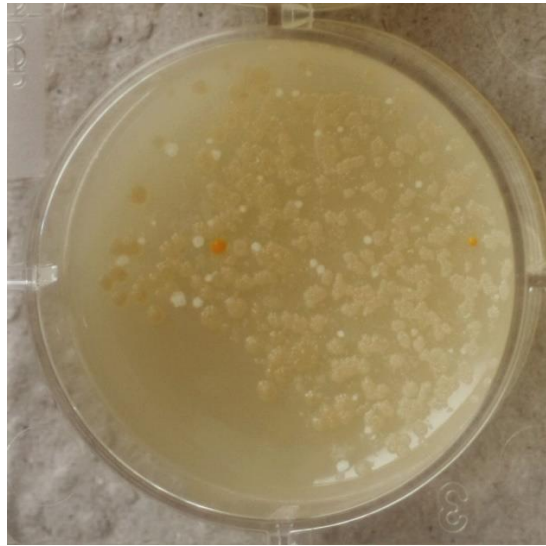


Figure 2.3: *Gluconacetobacter xylinus* bacteria colony growing and can be observed by eye (https://www.uni-weimar.de/kunst-und-gestaltung/wiki/images/1-1_Gluconacetobacter_xylinus.jpg).

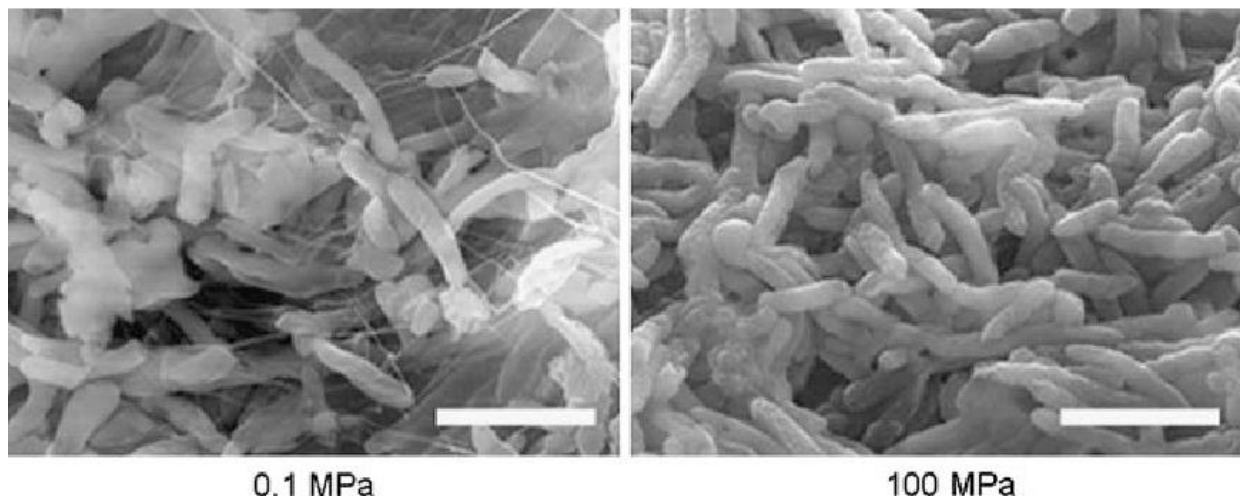


Figure 2.4: SEM Micrograph of *Gluconacetobacter xylinus* bacteria (Kato et al., 2007).

2.1.2 Gram staining

Gram staining reflects fundamental differences in the biochemical and structural composition of bacteria and it is used to identify possible contamination of the bacteria cell culture. *Gluconacetobacter xylinus* is a gram-negative bacterium with a rod-shaped cell (Deinema et al., 1971; Zaar et al., 1979; Sutherland, 2001; Saxena et al., 2005; Barud et al., 2008). Gram staining was carried out to check that the organisms were Gram negative rods and were not contaminated as shown in *Figure 2.5* below.

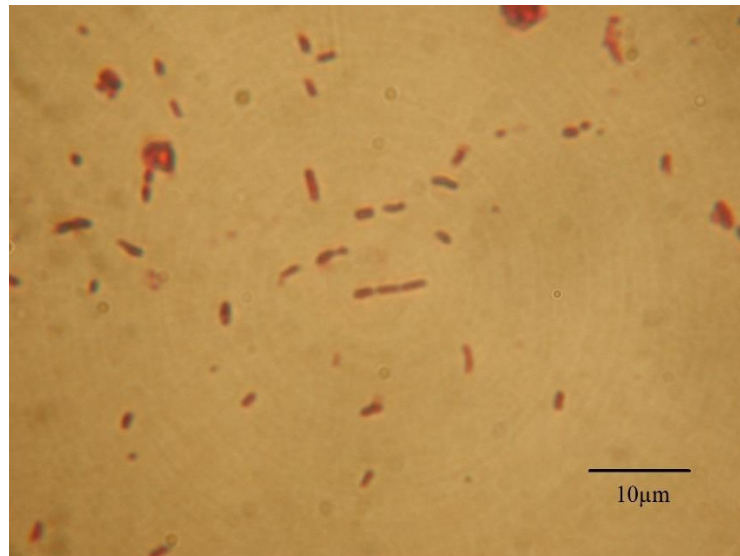


Figure 2.5: Gram stain of individual cells from after gram staining the colony of bacteria obtained from the surface of solid agar media from a tilted test tube or a Petri dish.

2.2 Culture medium

The culture medium was prepared according to the method outlined by Iguchi *et al.*, (2000) and Gea *et al.*, (2011). For every litre of distilled water, 5g of ammonium sulphate, 4g of potassium hydrogen orthophosphate, 0.1g of magnesium sulphate, 50g of glucose and 5g of yeast extract were added. Once prepared, the culture medium was then autoclaved for 2 hours at 121°C. It was then cooled to ambient temperature before the vitamins B1, B2, and B5 were added following the method by Iguchi *et al.*, (1998). Glacial acetic acid was used to adjust the acidity of the medium to pH 4. This type of medium will be referred to hereafter as medium 1. This medium can be stored for several months in a dark bottle covered by sterilised cotton and a layer of aluminium foil (Iguchi *et al.*, 1988 and 1998).

2.2.1 Preparing the seed broth

In a laminar flow hood, 100 ml of medium 1 was placed in a sterilised container. The agar containing the *Gluconacetobacter xylinus* was sterilised using UV light. A handle loop was used to sweep bacteria from the surface of the agar and mixed into the medium. In order to ensure that the bacteria was distributed well, the container was shaken for 4 hours, before it was placed in an incubator at 28 °C for 4 days. After 4 days in the incubator, a thin white layer appeared on the surface of the medium. The white layer was removed from the container and this remaining broth could be used as a starter to grow the bacterial cellulose pellicle again. This bacteria containing medium is referred to as medium 2 (Iguchi *et al.*, 1988).

2.2.2 Pellicle of BC

Medium 2 was added into the culture medium (medium 1) in a ratio of 1:10 and the glass covered by porous paper that had been placed in an autoclave at 121 °C for 2 h. The resultant medium (medium 3) was kept at a temperature between 28°C-30°C for 21 days. The culture time can be adjusted depending on the required thickness of the pellicle.

2.3 Purification Treatment of Bacterial Cellulose

After collection some of the bacterial cellulose pellicles were left on a sieve to allow drainage of the liquid growth medium from the pellicles without any treatment. These samples were then labelled untreated BC. However, the purification of the remaining pellicles involved firstly washing the pellicles under running tap water for 6 hours before immersing them overnight in 2.5 wt. % NaOH. The final purification step was to prepare the samples in the same way as the NaOH treated bacterial cellulose and then treat them with 2.5 wt% NaOCl. After the final step, the BC pellicles were washed under running tap water to remove the solvent until neutral pH conditions were achieved. This method was followed from Gea *et al.*, 2011.

2.4 Preparation of BC Sheet

The bacterial cellulose samples were prepared in the form of sheets for experiments such as thermal, structural and mechanical analysis. However, the samples were left in the form of a pellicle for morphological analysis specimen preparation. Bacterial cellulose sheets were prepared by placing a pellicle between two, 20mm thickness stainless steel plates with a wire mesh, at 115°C, up to 70MPa pressure for 5 minutes to squeeze out any water.

2.5 Morphological analysis

Morphological analysis of all the bacterial cellulose samples was investigated by using a cryo-field emission scanning electron microscope (FESEM) Quanta 3D ESEM FEI. Samples were carefully cut and mounted onto a sample holder and then frozen in liquid nitrogen. This sample was then transferred into the cryo-SEM sample preparation chamber under vacuum. The temperature of the sample was constantly maintained at -150°C via a cold stage and the anti-contaminator in the sample preparation chamber was maintained at a temperature of -190°C . A clean surface of frozen BC was revealed by fracturing the sample using a cold knife (kept at -150°C). Once the sample temperature was steady at -135°C , it was then sputter-coated for 1 minute at 11mA to deposit a fine layer of conductive platinum onto the sample surface. The sample was then imaged at an accelerating voltage of 2 kV and at a working distance of 6-8 mm.

2.6 Tensile testing

Tensile testing was undertaken at room temperature and at a speed of $10\text{mm}\cdot\text{min}^{-1}$ using an Instron 5566 equipped with a 1kN static load cell. The sheets (0.2-0.4mm thick) were cut into strips (30mm by 5mm). All measurements and tensile tests were performed at room temperature and at five samples were used to calculate the average value.

2.7 Thermogravimetric analysis (TGA)

A thermogravimetric analyser (TA Instrument Q500 thermal analyser) was used to measure the effect of the chemical treatment on the mass loss and decomposition of BC and PCL-BC composites. The initial weight of each sample was approximately 5mg. The samples were kept in alumina crucibles and heated from 30°C to 700°C in a furnace, flushed with argon gas at

the rate of 100ml/min. The percentage weight loss and derivative weight loss were plotted against the temperature.

2.8 X-ray diffraction analysis

Bacterial cellulose sheets were mounted onto the sample holder directly to analyse the crystalline structure (Siemens D5000 XRD). The scanning step was 0.02° with a scan time of 2.5 seconds per step and the aperture slits were set at 0.1° . The X-ray beam was Ni-filtered Cu $K\alpha$ ($\lambda=0.154\text{nm}$) and radiation operated at 40 kV with a filament of 40 mA.

2.9 FT-IR analysis

Samples of BC sheet were mounted in the sample holder and spectra were obtained in the mid infrared region ($4000\text{-}800\text{cm}^{-1}$) at 8 cm^{-1} resolution and averaging of 128 scans. Fourier transfer infrared (FT-IR) spectra was obtained using a Nicolet 8700 FT-IR spectrometer (Thermo Electron Corporation, UK) in combination with an MTEC Photoacoustic Spectrum (PAS) cell.

For the FTIR and thermal analysis of the surface modified samples, the samples were dried between filter papers in an oven at $80\text{ }^\circ\text{C}$ for 10-12 hours and the FT-IR spectra were obtained in the mid infrared region ($4000\text{-}800\text{cm}^{-1}$) at 8 cm^{-1} resolution and averaging of 128 scans.

2.10 Surface modification treatment of Bacterial Cellulose

In this study, BC used was produced as described in 2.2. The purification and treatment was carried out using sodium hydroxide (NaOH) and sodium hypochlorite (NaOCl) as described in 2.3. The BC pellicles were treated using sodium hydroxide (NaOH) to modify the surface

charge and structure. The pellicles were immersed in three different concentrations (5%, 7% and 9% w/v) for 5, 10 and 12 hours. They were washed with tap water for several minutes to remove the excess of NaOH and to achieve pH neutrality. Table 2.1 shows the treatment period and concentration for each sample.

Table 2.1: Treatment period and % concentration for the BC pellicles

NaOH Concentration (W/v %) Treatment Period (hrs)	5	7	9
5	BC-A	BC-D	BC-G
10	BC-B	BC-E	BC-H
12	BC-C	BC-F	BC-I
Untreated BC-J			

2.11 Cell Culture

Samples were cut into 5mm x 5mm squares using scissors and a scalpel and autoclaved at 120°C at 18 psi for 20 minutes in deionised water. Before seeding the cells, the sterilised samples were cut into very small sections and aseptically transferred to 96-well plates. Care was taken to ensure uniformity of sample size. Human primary cells, Synovial, bone marrow and skin fibroblast cells were taken from a male donor of Age 35 with rheumatoid arthritis. These cells were provided by the Wellcome Trust at the University of Birmingham by Dr Andrew Filer who had already obtained ethical approval. The details of the ethical approval are as follows:

- The ethics is still current and samples are still being analysed
- Ethical committee: West Midlands Black Country Research Ethics Committee

- Name of Project: Origins and roles of stromal cells in chronic inflammatory Arthritis
- REC Reference: 07/H1204/191.

2.11.1 Cell culture medium

The cells were grown in complete fibroblast medium (S-RPMI), which was made up of; RPMI 1640 and supplemented with the addition of 10% foetal calf serum, 1% MEM non-essential amino acids, 1% sodium orthopyruvate, 2mM glutamine, 100U/ml penicillin and 100µg/ml streptomycin (Sigma Aldrich).

2.11.2 Cell seeding

The cells were grown in the culture medium until they were sufficiently confluent to seed onto the scaffolds. The cells were removed from the culture substrate by first removing the medium and then washing twice with 10ml 1% PBS to remove the excess medium and dead cells. The cells were then incubated at 37°C for 1 minute with 1ml trypsin and 9ml of S-RPMI. The suspension was centrifuged at 1000rpm for 3 minutes, after which the trypsin and S-RPMI were removed via pipette. The resulting pellet was then re-homogenised with 10ml of S-RPMI.

The cells were then seeded on the samples at a density of 2.4×10^6 cells/cm². During preparation, 100µl of S-RPMI were added to each well and an additional 100 µl were added every 48 hours for the duration of the experiment.

2.12 Phase-contrast imaging

The morphology of the dermal and bone marrow cells seeded on the scaffolds was examined using an inverted optical microscope (Zeiss Axiovert 200) in Phase Contrast mode, controlled by Simple PCI version 5.0.0.1503.

2.12.1 Preparation of cells for Phase contrast imaging

The cells were grown directly on a cover slip immersed in cell culture medium to form a monolayer. The cell culture medium provided all the nutritional requirements for the cells to divide and grow. When the cells reached the preferred population, the cover slip was removed from the cell culture medium and mounted upside down on a microscope slide. The specimen was then viewed in the microscope.

2.13 MTT Assay

In the MTT assay, a yellow tetrazolium salt (dimethylthiazol diphenyl tetrazolium bromide) (supplied by sigma) is reduced to purple formazan crystals by dehydrogenase enzymes in metabolically active cells. The amount of produced formazan is directly proportional to the number of viable cells.

The substrates were placed in 96-well plates and seeded as described above. An MTT solution was prepared in PBS using 5 g/mL and sterilised by filtration. The culture medium was then aspirated and replaced by 25 μ L MTT solution. The samples were incubated at 37 °C in a 5% CO₂ atmosphere for 4-5 hours. The samples were removed to clean wells (days 6 and 10 only). The S-RPMI and MTT solution were removed from the wells and 150 μ L dimethyl sulfoxide (DMSO) was added to dissolve the formazan crystals. The samples were placed on a

shaker for 5 minutes to ensure complete dissolution of the formazan and then the absorbance was measured at 540 nm using a Multiscan Ascent 96-well plate reader (Thermo Labsystems).

Triplicate samples were used for the cell culture studies in the analysis of cell viability. The statistical significance was tested by ANOVA-single factor. $P < 0.05$ was considered highly significant for dermal cells. $P < 0.05$ was not significant for bone marrow cells.

2.14 Cell count

The haemocytometer and cover slip were firstly prepared by spraying with 70% alcohol and then carefully drying with tissue. The coverslip was then fixed on the haemocytometer by moving it back and forth whilst exerting slight pressure until Newton's rings (rainbow effect) appear at the sides of the cover slip. A small aliquot (20 μ l) of cell suspension was removed to a microfuge tube and a same volume (20 μ l) of trypan blue was added to the tube and mixed thoroughly. A pipette was used to place a small volume of the cell mixture onto the counting platform, allowing it to run under the cover slip. The number of cells present in the 5-square counting grid were counted. Dead cells were also excluded from the count as indicated by the deep staining. The number of cells per ml in the total suspension was calculated using the steps shown in Figure 2.8.

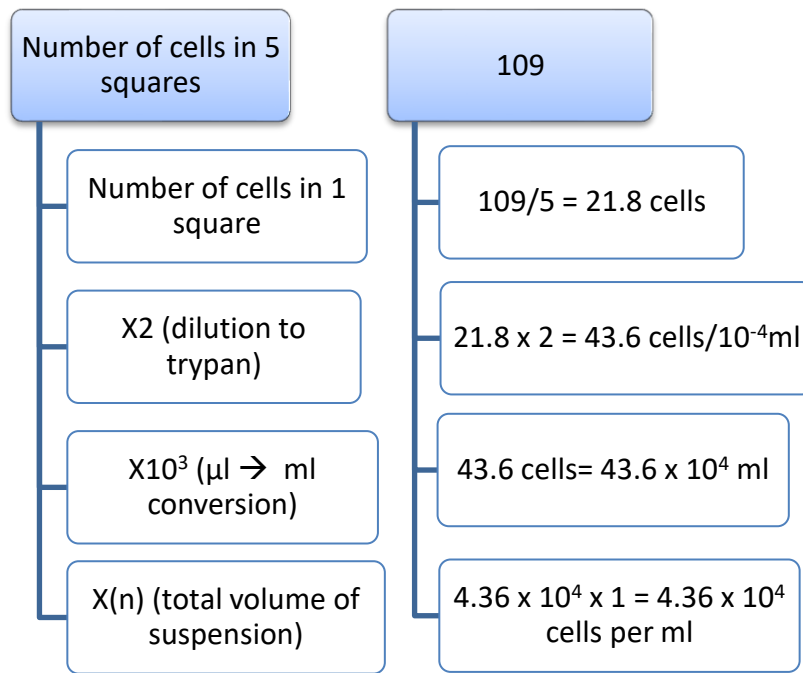


Figure 2.8: Calculation of cell density.

2.15 Differential scanning calorimetry for composites

The Differential scanning calorimetry (DSC), works on the principle of relative heat flow between two chambers, the aluminium pan containing the polymer sample (sample pan) and an empty pan (reference pan). The DSC results are in the form of curves showing the amount of heat energy put into the sample pan to keep both pans at the same temperature. When the polymer sample crystallises, it is an exothermic process, therefore the heat energy required to keep the sample pan temperature the same as the reference pan drops, hence a trough is seen on the DSC graphs (Hone, 1996). DSC was performed using water as the cooling fluid. Each sample was heated from -60°C to 120°C at a heating rate of $10^{\circ}\text{C min}^{-1}$. The melting temperature (T_m) will be taken as the peak temperature of the melting endotherm. Then, the sample was cooled down to -60°C and heated again to 120°C at a heating rate of $10^{\circ}\text{C min}^{-1}$. The area under the melting

endotherm will be used to determine the degree of crystallinity of the nanocomposite. The degree of crystallinity was calculated using the equation below assuming that 100% crystalline PCL has a value of $\Delta H = 136\text{J/g}$.

$$\text{Degree of crystallinity (x\%)} = (\Delta H_1/\Delta H) \times 100$$

Where $\Delta H_1 = \text{integral/sample weight}$ and $\Delta H = 136\text{J/g}$. The integral value is obtained from the DSC curves produced.

2.16 Extraction of bacterial cellulose whiskers

The bacterial cellulose whiskers were extracted by acid hydrolysis in 65wt% sulphuric acid at 40°C for 16 hours with continuous stirring. The reaction was quenched by dipping the flask in cold water. The cellulose whiskers were acquired by centrifugation and dialysis.

2.17 TEM of BC whiskers

Cellulose whiskers were examined using transmission electron microscopy (Phillips CM 200 instrument). A droplet of the diluted suspension was placed onto a copper grid covered with a carbon film and samples were then stained by allowing the grids to float in a 2wt% solution of uranyl acetate for 3 min.

2.18 Electrospinning nanocomposites

The bacterial cellulose whiskers/PCL blends were prepared at Queen Mary University by dissolving PCL in chloroform and adding the extracted BC whiskers (wt. %) to the dissolved PCL. The PCL/BC solutions were prepared at different concentrations (2wt. %, 4wt. %, 6wt. %, 8wt. %, 10wt.%) for electrospinning. Electrospinning was performed using a steel capillary tube

with a 1.5mm diameter tip mounted on an electrically insulated stand. The capillary tube was connected to a syringe filled with 10ml of a bacterial cellulose/PCL blend.

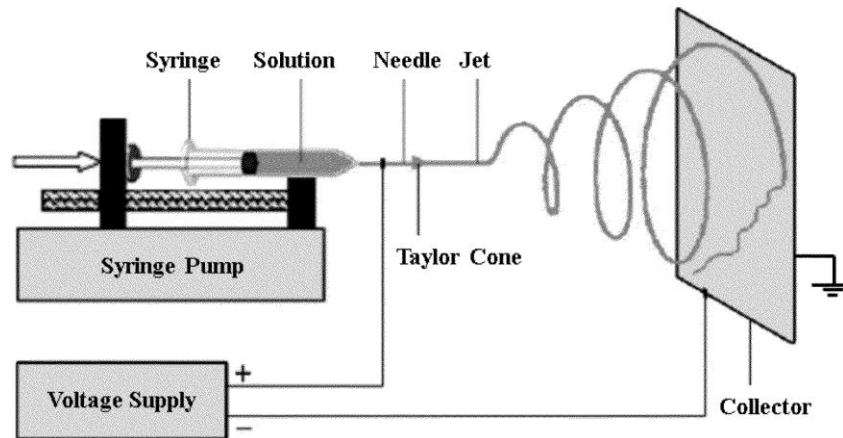


Figure 2.9: Schematic diagram of electrospinning method (Bhardwaj et al., 2010).

The distance between the tip and the collector (aluminium foil) was 20 cm, and flow rate of the fluid was 0.03 mL/min. The potential difference between the capillary tip and the aluminium foil was gradually increased from 10 to 25 kV/cm.



Figure 2.10: Electrospinning setup used for this study (Queen Mary University equipment).

Electrospinning is a process that creates nanofibers through an electrically charged jet of polymer solution or polymer melt.

2.19 Composite samples for mechanical testing

Composites for mechanical testing were made by twin extrusion and this work was carried out using the HAAKE minilab Thermo scientific mini twin-screw extruder at Warwick University/ Warwick Manufacturing Group (WMG). The extruder temperature was 135°C and the screw-speed was 50 RPM. The extruded samples were then injection moulded into test samples using the following conditions; Cylinder temperature, 135°C, Mould temperature, 40°C, Pressure was 80bar. The composites were made up using microcrystalline (approximately 100 µm in length and 10 µm in diameter) bacterial cellulose and PCL for the following compositions; PCL-BC 2, 4, 6, 8 and 10 wt.%.

At least 5 samples were tested for each composition. Width and thickness of each sample was measured before testing and they had an average thickness of 3.20mm, width of 3.20mm and gauge length of 15.3mm. A speed of 10 mm.mm⁻¹ was used throughout the testing.

CHAPTER 3

Results and Discussion

3.1 Bacterial cellulose

3.1.1 Formation of BC pellicles

Medium used in the fermentation process was inoculated with medium containing bacteria, which had previously undergone inoculation with bacteria stored in agar in a ratio of 1:10 v/v. This previous inoculation serves to control the number and growth of bacteria in the medium, which is indicated by the same thickness of pellicle. Four days after inoculation, a thin white layer called pellicle (gel-like substance) appears on the surface of medium (Figure 3.1). This layer is then removed and the remaining solution is used as a starter (seed broth).



Figure 3.1: The white layer appeared on medium after four days of inoculation in static conditions.

By culturing *Gluconacetobacter xylinus* into the medium containing glucose as a main source of food of the bacteria, bacterial cellulose pellicles have been successfully produced by a static culture method. Using an agar media in a Petri dish or a tilted test tube, the bacteria are

easily collected or transferred to another container to prepare a new seed broth which becomes a new starter for further culturing. In order to guarantee that the bacteria retain a high level of viability and to avoid genetic mutation, the bacteria were continually transferred to new agar media. The results of tests confirmed that the *Gluconacetobacter xylinus* used in this work is a rod-shaped Gram-negative bacterium (see section 2.1.2). The length of culturing depends on the required thickness of the BC pellicle.

3.2 Characterisation of Bacterial Cellulose

3.2.1 Purification of BC

The rod-shape bacteria of *Gluconacetobacter xylinus*, which is shown in Figure 3.2 can be seen on the surface of untreated bacterial cellulose pellicle.

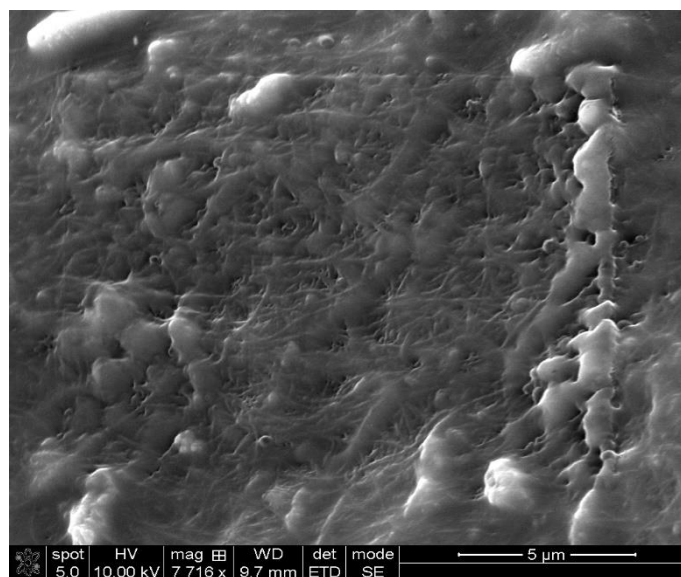


Figure 3.2: Cryo-Field Emission Scanning Electron Microscopy micrograph of untreated BC.

The purification method was chosen to maintain the three-dimensional structure of the bacterial cellulose pellicle, which allows easier observation of the internal structural network. It is impossible to directly study the internal structure/network of untreated bacterial cellulose due to the surface being opaque, as seen in Figure 3.3 (a and b).

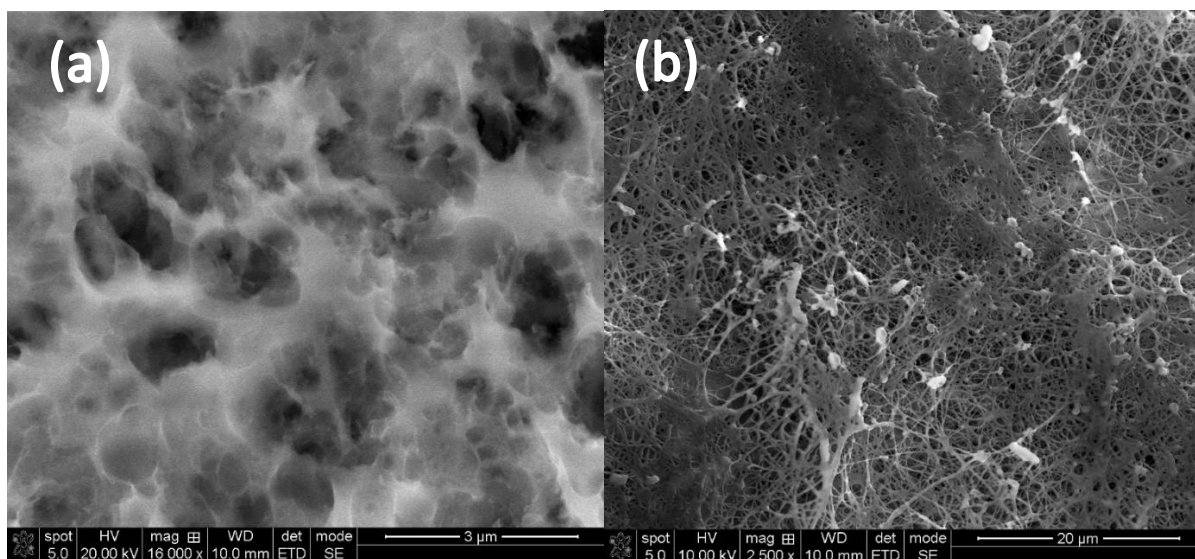


Figure 3.3: (a) Cryo-Field Emission Scanning Electron Microscopy micrograph of NaOH treated BC; (b) Cryo-Field Emission Scanning Electron Microscopy micrograph of NaOH + NaOCl treated BC.

The pores of the surface were covered in organic impurities from the medium used in the culture process, as well as the rod-shaped *Gluconacetobacter xylinus*. This prevented contact between fibres in the network, resulting in a dramatically reduced number of hydrogen bonds, therefore reducing the strength of bacterial cellulose sheets (Yamanaka et al., 1989). Investigation of the untreated bacterial cellulose by Gea et al., (2011), confirmed this theory. Young's modulus values reported by Gea et al., 2011 were compared with the 2.5 wt.% NaOH treated bacterial cellulose

in Figure 3.3.a, where the rod-like shape of *Gluconacetobacter xylinus* and other impurities were no longer seen on the surface, revealing the internal structure of the pellicle. Nanofibres of bacterial cellulose was clearly seen in the pellicle, which was then further treated with the 2.5 wt. % NaOCl (shown in Figure 3.3.b). This displayed the effectiveness of NaOCl as a bleaching agent and its ability to remove impurities, which were unable to be removed by the single treatment with NaOH. To reinforce this argument, Tomasino et al. reported that when NaOCl dissolves in water, hypochlorous acid (HOCl) is formed (Tomasino, 1995). Hypochlorous acid is a major inorganic bactericidal compound of innate immunity, which is effective against a broad range of microorganisms (Wang et al., 2007).

3.3 Surface modification of BC by mercerisation

3.3.1 FT-IR analysis

The samples were treated with NaOH for surface modification as described in section 2.10. The FTIR spectra of treated (surface modified) and untreated samples are shown in two separate regions, 3500-1600 cm^{-1} and 1500-870 cm^{-1} in Figures 3.4 and 3.5 respectively. The infrared spectra can be used as a measure of the degree of crystallinity, as well as a measure of the lattice type change (conversion of cellulose I to cellulose II) of the components consisting of cellulose I, cellulose II or a mixture of both lattices (Nelson and O'Connor 1964).

The effect of NaOH treatment and purification of bacterial cellulose has been extensively studied as mentioned earlier (section 1.3). A more closely related study by Gea et al., (2011) is

used as a reference in this study to support the findings and further reiterate the purpose of modification of bacterial cellulose.

FT-IR spectroscopy of bacterial cellulose and surface modified bacterial cellulose was carried out in order to determine any changes in the peaks that could be accredited to NaOH treatment for purification and mercerisation for surface modification. Gea et al. reported that the hydrogen-bonded O-H stretching vibrations at 3800 – 2900 cm^{-1} in BC shifted to a higher wave number and the intensity of O-H stretch of cellulose type I at 3345 cm^{-1} increased due to the purification process using NaOH. A shift in the peak area was also observed in this region, which could be due to the disappearance of the N-H stretch related peak from amino acids and proteins at 3150- 3220 cm^{-1} (Gea et al., 2011). The peaks at 3488 cm^{-1} and 3447 cm^{-1} assigned for –OH stretching intramolecular hydrogen bonding as typical for cellulose II (Carillo et al., 2004) were not found in the spectrum shown in Figure 3.5. The purification of bacterial cellulose led to an increase in the intensity of 1156 cm^{-1} assigned to the asymmetric stretch of C-O-C and CH_2 deformation. FTIR of the mercerisation of bacterial cellulose are shown in Figure 3.5 and 3.6.

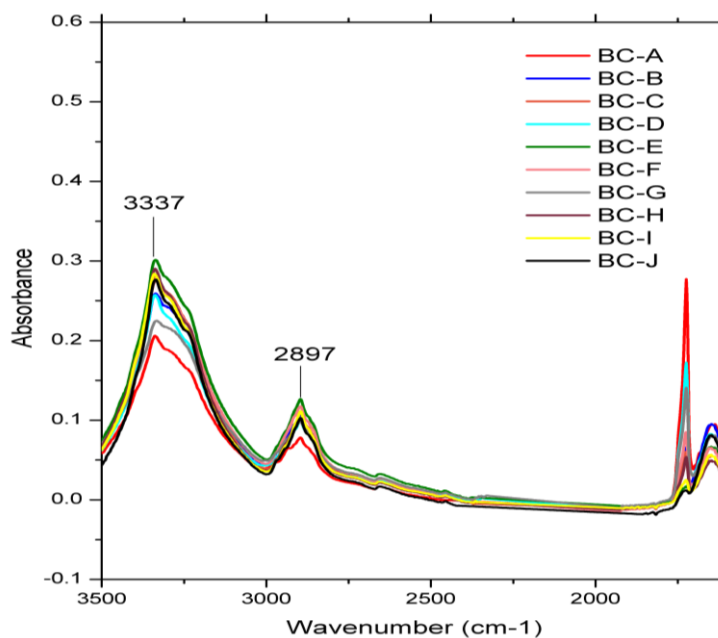


Figure 3.4: FT-IR spectra of NaOH treated and untreated BC ($3500-1600\text{ cm}^{-1}$).

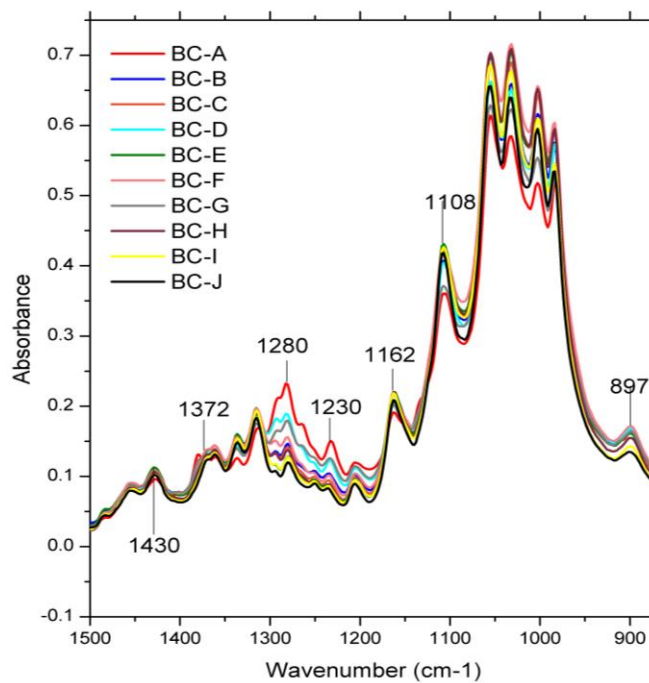


Figure 3.5: FT-IR spectra of NaOH treated and untreated BC ($1500-870\text{ cm}^{-1}$).

Nelson & O'Connor proposed a ratio of infrared bands located at 1375 cm^{-1} and 2900 cm^{-1} to measure the crystallinity of cellulose samples. They proved that the values of this ratio ranks the cellulose samples in the same order as the crystallinity parameters derived from X-ray diffraction (Nelson and O'Connor 1964a). They noted that the absorbance of the group of bands in the $1200\text{-}1400\text{ cm}^{-1}$ region were affected by the crystallinity and not by the lattice type (cellulose I and II). From the four bands in this region (1315 , 1335 , 1372 and 1429 cm^{-1}), which were assigned to C-H and O-H bending and CH_2 wagging, the band at 1372 cm^{-1} (assigned to C-H bending) was chosen to be the most suitable indicator of crystallinity. The band at 1335 cm^{-1} assigned to O-H in plane bending could be affected by the amount of water absorbed and the bands at 1315 and 1429 cm^{-1} (CH_2 wagging and CH_2 scissoring, respectively) could be affected by the change in the lattice type.

The absorbance ratio of this band to 2900 cm^{-1} (C-H and CH_2 stretching) was calculated by drawing a convenient baseline. For the band at 1372 cm^{-1} , a line was drawn between the minima at approximately 1300 and 1400 cm^{-1} , to give a common baseline for the three bands in this region. For the band at 2900 cm^{-1} , the adjacent minima at 3000 cm^{-1} was chosen as the base (Nelson and O'Connor 1964a). Values for this ratio total Crystallinity Index (TCI) (Carrillo et al 2004) are listed in Table 3.1 (refer to table 2.1 for treatment time and concentration).

The TCI values were plotted in two separate figures in order to study the effects of both the sodium hydroxide concentration and the period of treatment on BC scaffolds. As shown in Figure 3.6 by increasing the concentration of sodium hydroxide, the crystallinity of the samples tended to increase. As shown in Figure 3.7, as the period of treatment with 5 w/v\% NaOH increased, the crystallinity tended to decrease slightly; whereas, for treatment with 7 and 9 w/v\% NaOH , the TCI tended to increase slightly. The fitting of the trend lines for crystallinity is not as

exact as one may desire, particularly for samples treated for 10 hours and those treated at a concentration of 5%. However, it shows that, overall, the general trend was a slight increase in crystallinity after each treatment. As the bacterial cellulose is highly crystalline cellulose I, this conversion to cellulose II would mean transformation of one crystalline lattice to another, and not an amorphous phase to a crystalline one. This could be the reason that the increase in crystallinity is very small.

Table 3.1: Crystallinity indices ($1373/2900\text{ cm}^{-1}$) for treated and untreated BC

Sample	TCI(A_{1372}/A_{2900})
BC-A	0.88
BC-B	1.43
BC-C	0.64
BC-D	0.61
BC-E	0.73
BC-F	0.57
BC-G	0.69
BC-H	0.66
BC-I	0.63
BC-J	0.60

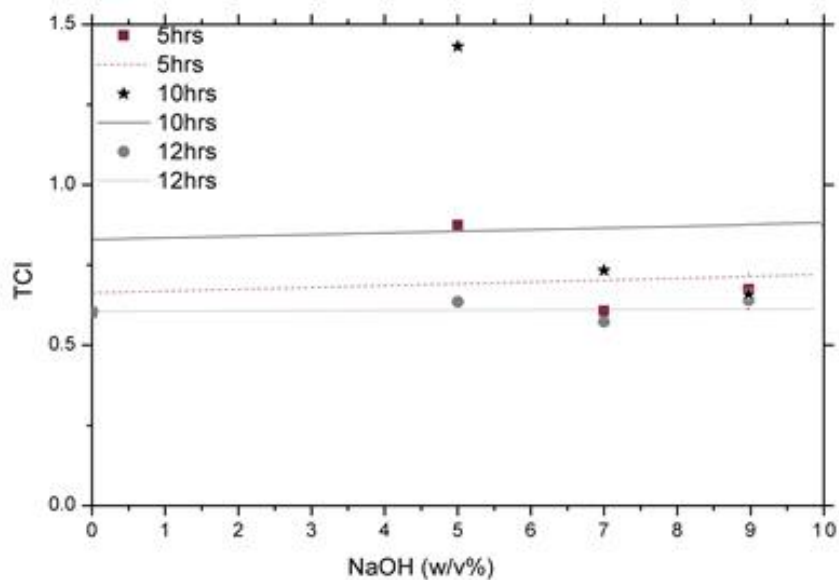


Figure 3.6: Effect of sodium hydroxide concentration on the crystallinity of scaffolds treated for 5, 10 and 12 hours.

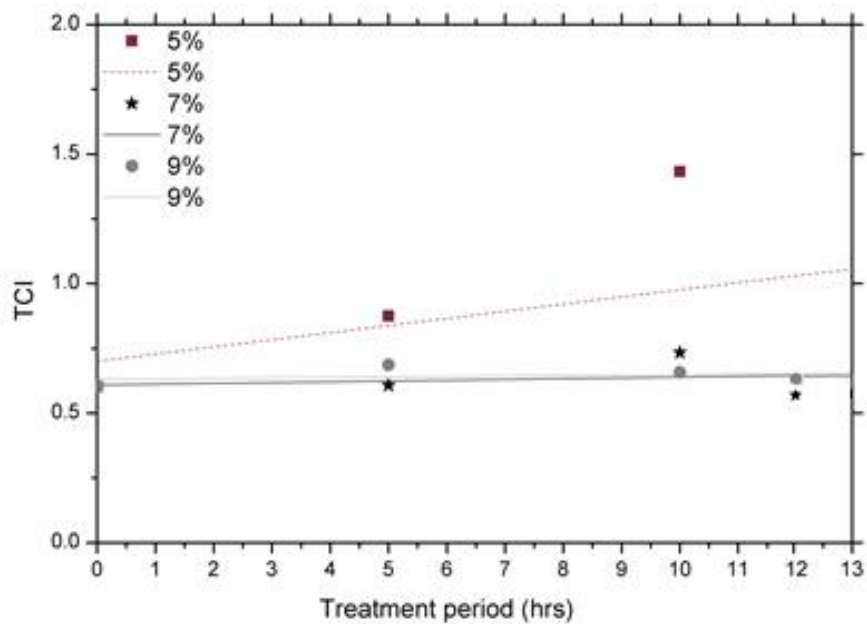


Figure 3.7: Effect of sodium hydroxide treatment period on the crystallinity of scaffolds treated with 5, 7 and 9% NaOH.

XRD of the treated and untreated bacterial cellulose samples exhibit three main peaks, located at $2\theta = 14.7^\circ$, 16.2° and 22.4° (Gea et al., 2011). These are in agreement with previously reported data which relates to the primary diffraction of the (1 $\bar{1}$ 0), (110) and (200) planes of cellulose I polymorphs (Klechkovskaya et al., 2003; Sugiyama et al., 1991; Zugenmaier., 2008). This exhibits that the initial two step purification process does not alter the structure of bacterial cellulose from cellulose I to cellulose II. However, a change that appears in the diffractograms of single-step treated bacterial cellulose and two-step treated bacterial cellulose after purification is an increase in the intensity of their peaks compared with untreated bacterial cellulose. This means that during the purification process a change in orientation of the cellulose fibre takes place (Gea et al., 2011).

3.3.2 Lattice Type (Cellulose I and Cellulose II)

By comparing the infrared spectra of highly crystalline cellulose I and II, Nelson and O'Connor, showed that the spectra of cellulose I differs distinctively from cellulose II at 1430, 1111 and 897 cm^{-1} . These bands were observed in cellulose I, while they were shifted to 1420, 1007 and 893 cm^{-1} , respectively, in cellulose II (Nelson and O'Connor, 1964). It was also suggested that the band at 1155 cm^{-1} for cellulose I shifts to 1162 cm^{-1} in cellulose II (Carillo et al., 2004). These bands, therefore, can be used to study the type of crystalline lattice in treated and untreated scaffolds.

The band at 1430 cm^{-1} assigned to the symmetric bending of CH_2 at C-6 (Oh et al, 2005), was observed at 1427-1428 cm^{-1} for all of the treated and untreated samples. This suggested the predominant presence of cellulose I. If the amount of cellulose II was significant, then this band would shift to 1420 cm^{-1} . The band at 1111 cm^{-1} (ring asymmetric stretching) was observed at

1106-1107 cm^{-1} , and the band at 897 cm^{-1} assigned to COC stretching at the β -glycosidic linkage, COC stretching, CCO stretching and CCH stretching at C-5 and C-6 (Oh et al, 2005) was detected at 897-900 cm^{-1} , which confirmed the predominance of crystalline cellulose I.

In addition, the hydrogen bonding is different in cellulose I and II and this difference is shown by the intensities and frequencies of the absorption bands in the O-H stretching region. In cellulose I, the band assigned to intra-chain hydrogen bonded hydroxyls is located at 3350 cm^{-1} , while for cellulose II, it is located at 3488 cm^{-1} (Nelson and O'Connor, 1964). This band was observed for all of the samples at 3333-3340 cm^{-1} . The absorbance bands at 3488, 3447 and 3175 cm^{-1} are typical of the -OH stretching intra-molecular hydrogen bonds and are only observed in cellulose II. These bands were not detected in either the treated or untreated samples in this study. However, the band at 1155 cm^{-1} , assigned to C-O-C asymmetric stretching at the β -glucosidic linkage, was observed at 1162 cm^{-1} in all treated and untreated samples. Bands at 1315, 1280 and 1205 cm^{-1} , characteristic of cellulose II, were also observed in all treated and untreated samples. These indicated a mixture of cellulose I and II lattices.

The absorbance ratio of the bands at 1430 and 900 cm^{-1} can be used to follow any transformation in crystalline lattice structure from cellulose I to cellulose II. This ratio was proposed by O'Connor and named Lateral Order Index (LOI) by Hurtubise and Krassig in 1960. Later, by comparisons with the diffraction patterns, Oh et al. (2005) confirmed that the ratio A_{1430}/A_{900} is related to the proportion of cellulose I. Values of this ratio for all treated and untreated samples are listed in Table 3.3. As with crystallinity, these values were used to evaluate both the effect of time and concentration of the treatments on the transformation of cellulose I to cellulose II.

Table 3.2: Absorbance ratio 1430 to 900 cm^{-1} for treated and untreated samples

Sample	LOI (A_{1430}/A_{900})
BC-A	0.65
BC-B	0.87
BC-C	0.91
BC-D	0.66
BC-E	0.94
BC-F	0.75
BC-G	0.63
BC-H	0.78
BC-I	0.97
BC-J	1.20

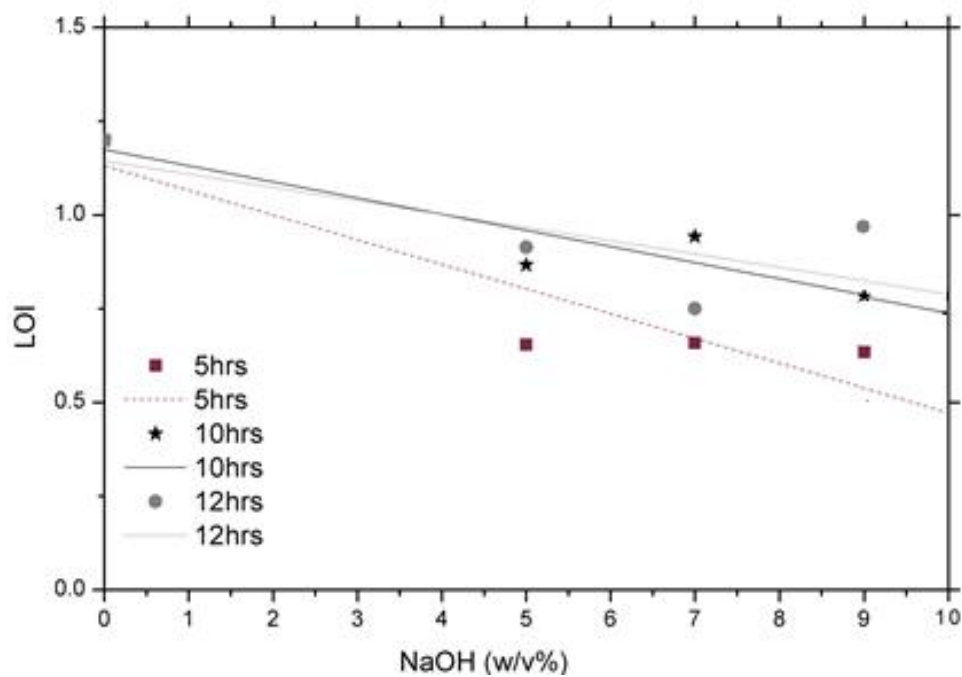


Figure 3.8: Effect of sodium hydroxide concentration on the proportion of cellulose I after 5, 10 and 12 hours.

As shown in Figure 3.8, the proportion of cellulose I tended to decrease with the increasing concentration of sodium hydroxide. As can be seen from Figure 3.9, with the increased period of treatment with NaOH, the amount of cellulose I followed a decreasing pattern, and therefore, conversion to cellulose II increased, as expected.

The FTIR spectra of BC samples treated with 5, 7 and 9 w/v% NaOH for 10 hours (B, E and H, respectively) were compared with the untreated sample (J) in the 1500-870 cm^{-1} region, as shown in Figures 3.10, 3.11 and 3.12 respectively.

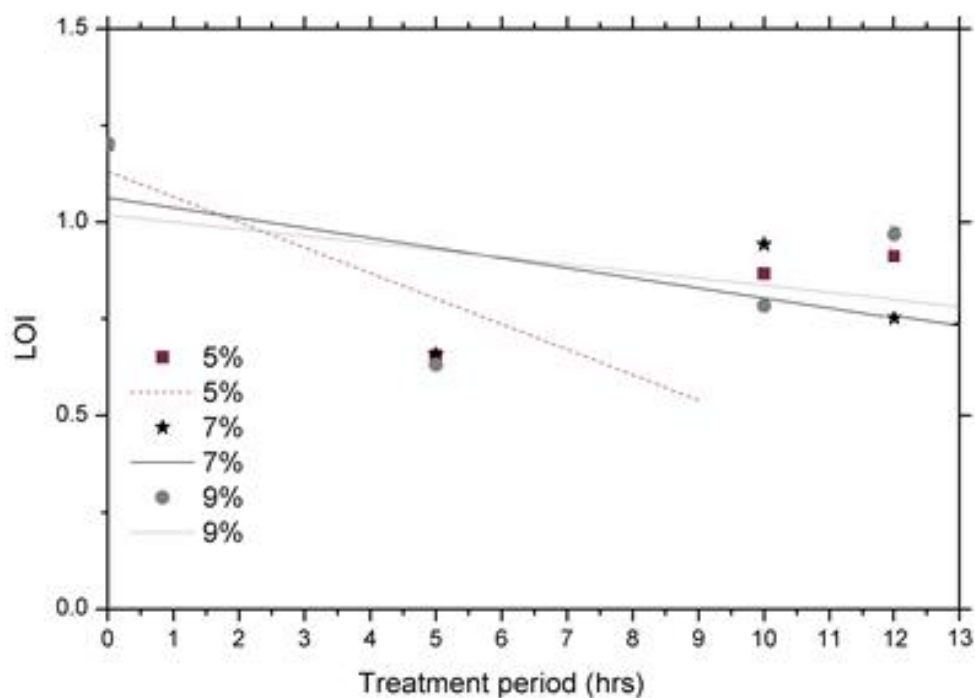


Figure 3.9: Effect of sodium hydroxide treatment period on proportion of cellulose I with 5, 7 and 9% NaOH.

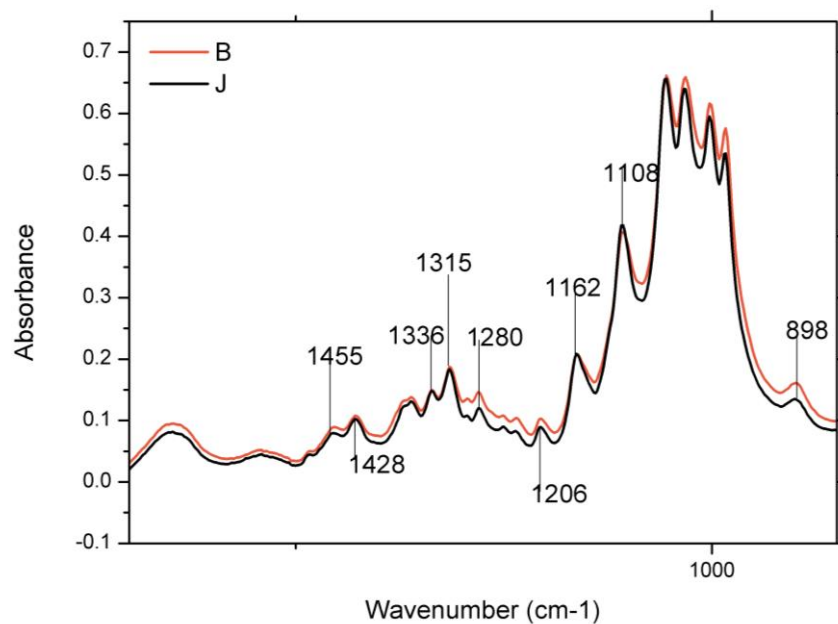


Figure 3.10: Comparison of FTIR spectra - samples B and J in 1500-879 cm^{-1} .

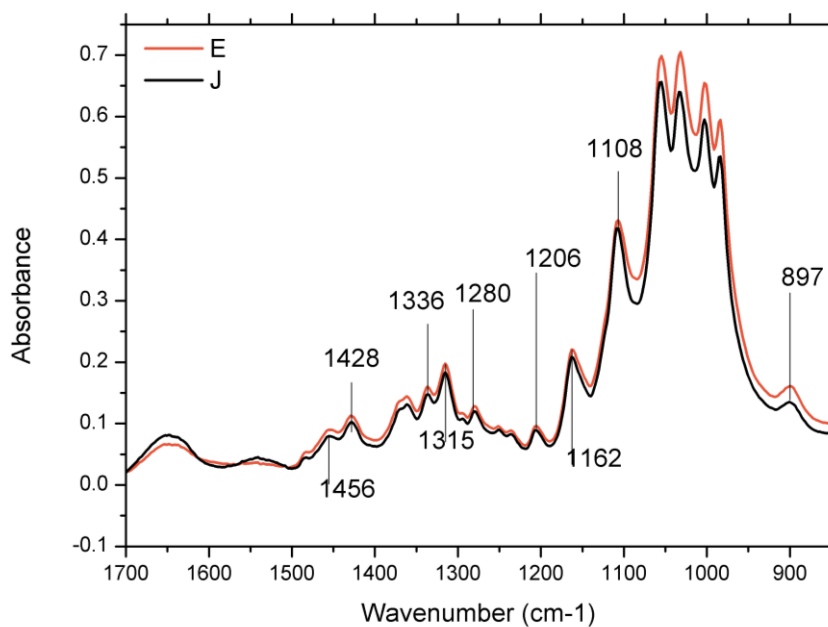


Figure 3.11: Comparison of FTIR spectra - samples E and J in 1500-879 cm^{-1} .

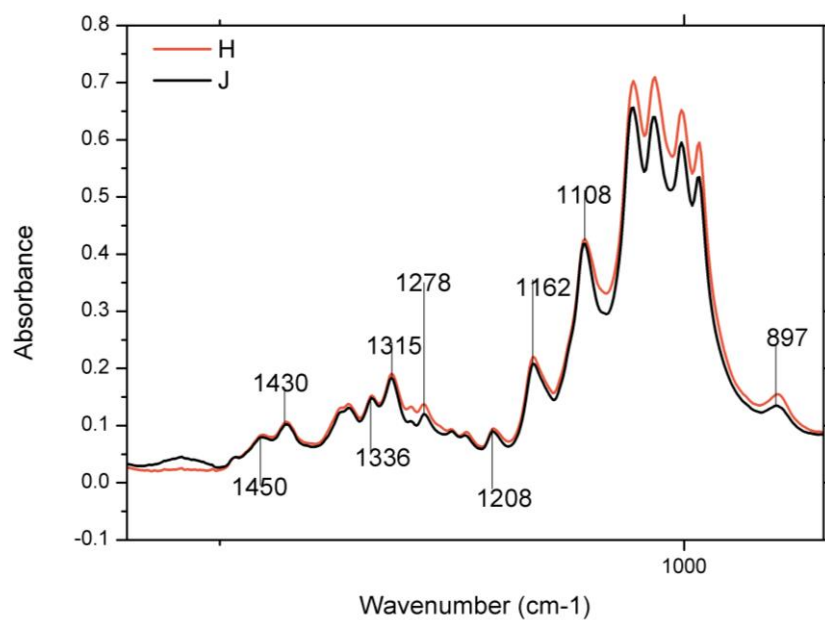


Figure 3.12: Comparison of FTIR spectra - samples H and J in 1500-879 cm⁻¹.

Table 3.3: FTIR band assignments of cellulose I and II

Wavenumber (cm-1)	Assignment	Reference
3352	stretching OH (hydrogen bonded) in Cellulose I	Oh et al. 2005
2892	stretching CH in Cellulose II	Oh et al. 2005
1431	bending CH ₂ (sym) at C-6 in Cellulose I	Oh et al. 2005
1373-1376	bending C-H	Oh et al. 2005
1278	bending C-H in Cellulose I	Oh et al. 2005 Colom & Carrillo 2002
1236	bending COH in plane at C-6 → Cellulose I	Oh et al. 2005 Colom & Carrillo 2002
1162	stretching COC at beta-glucosidic linkage in Cellulose I	Oh et al. 2005
1100-1111	stretching (C-O), stretching (C-O) – ring symmetric stretching	Marta Kacurakova et al. 2002 Colom & Carrillo 2002
895	stretching (C-1-H) → Beta-anomeric link → origin C, COC in plane, symmetric stretching	Marta Kacurakova et al. 2002 Colom & Carrillo 2002

The two-step purification process is able to produce purified bacterial cellulose samples, which are shown by SEM images, FTIR and TGA. This purification process greatly improved the mechanical and thermal performance of native BC. The structure of cellulose did not change from cellulose I to cellulose II by using a concentration of 2.5 wt. % NaOH followed by 2.5 wt. % NaOCl. The FTIR spectrum gave no suggestion of the formation of cellulose II. In addition,

the Young's modulus of NaOH-treated BC increased when compared to untreated bacterial cellulose because there was no disruption of the intermolecular and intramolecular hydrogen bonding between and within the fibres in the H-bonded network. As expected, a further increase in tensile strength was observed for the two-step treated BC, since the polymorphic transformation from cellulose I to other less performing cellulose types was prevented, while at the same time a stronger network was formed (Gea et al., 2011; Chiaoprakobkij et al., 2011). One of the most important steps in improving mechanical properties of bacterial cellulose is the purification of the pellicle (Yamanaka et al., 1989; Gea et al., 2011). Young's modulus, tensile strength, and strain at break of every sample are revealed in Table 3.4 below.

Table 3.4: Mechanical properties of treated and untreated Bacterial Cellulose.

Bacterial Cellulose	Young's Modulus (GPa)	UTS (MPa)	Elongation at break (-)
Untreated	8.7	90.0	0.013
Treated with 2.5 wt% NaOH	15.2	140.1	0.014
Treated with 2.5 wt% NaOH and 2.5 wt% NaOCl	20.1	209.1	0.016

The mechanical properties increased significantly after purifying bacterial cellulose. BC pellicles treated with 2.5 wt.% NaOH release impurities which are still trapped at the surface and in the pellicle. As a result, increased hydrogen bonding within these BC pellicles can occur because of the absence of impurities that will hinder bonding between BC fibrils. Gea et al., reported that the Young's modulus of 2.5 wt.% NaOH treated BC was doubled compared to

untreated BC and the best properties of the samples were observed after further overnight purification with 2.5 wt. % NaOCl (Gea et al., 2011). This is in agreement with the results in Table 3.4 above, which shows that the Young's modulus and the ultimate tensile strength both increased after treatment with NaOH and then NaOCl. This further confirms that purification of bacterial cellulose does improve the mechanical properties.

3.3.3 Thermal Analysis

Thermogravimetric analysis (TGA) can be used to characterise a material which displays weight change when it is heated and to also detect phase change due to the process of decomposition. The TG weight loss curves and the corresponding derivative curves were obtained by plotting the percentage of weight loss and percentage of weight loss per minute against temperature, respectively. The maximum decomposition temperature, which is known as a criterion for thermal decomposition, was obtained from DTG (derivative TG) data. Figure 3.14 below, indicates that the bacterial cellulose which was not modified by mercerisation started to degrade at 240 °C, while the treated/modified samples started degradation at significantly higher temperatures. This is in agreement with the investigation by Gea et al., (2011).

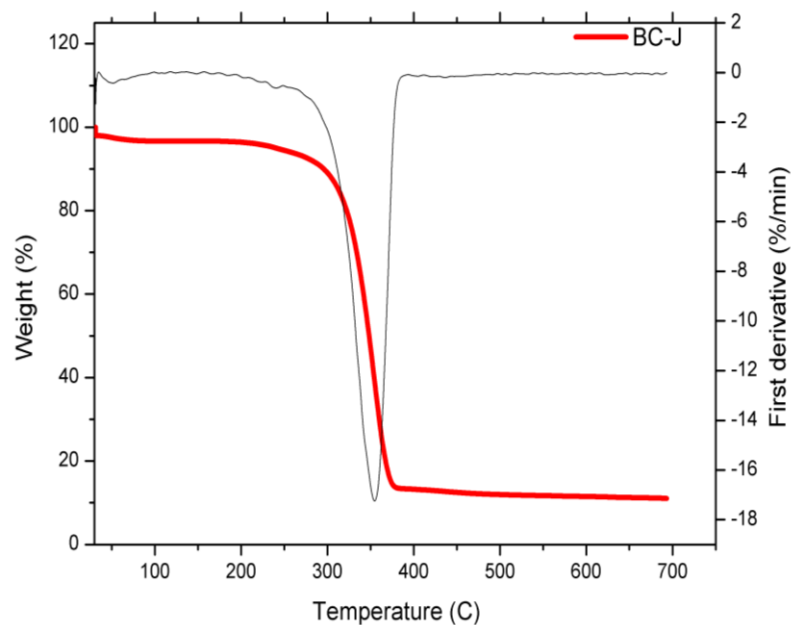


Figure 3.13: TGA curve of untreated (purified) bacterial celliulose, sample J.

Purified bacterial cellulose endures a main degradation at around 360 °C, which is typical of cellulose breakdown apart from a small loss of mass at around 100 °C, which may be the result of water evaporation (Roman, 2004, Gea et al., 2011).

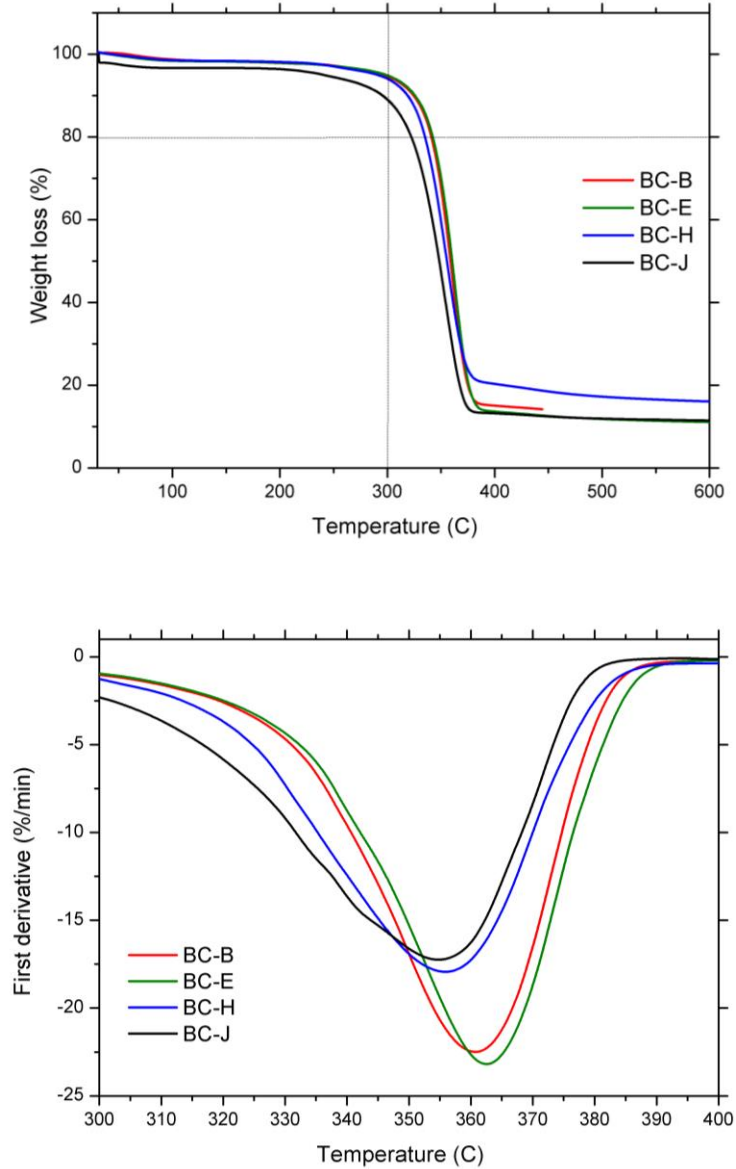


Figure 3.14: (a) TG curves for samples B, E and H (treated with 5, 7 and 9% NaOH for 10 hours) and untreated BC (b) DTG curves.

The NaOH treated samples tolerate a lower temperature before the main degradation takes place (320 °C), with a shoulder at around 400 °C (Gea et al., 2011). The degradations between 145 °C and 255 °C can be due to protein impurities, whereas the main degradation of cellulose can be

found at a temperature as low as 290 °C. The residue value decreases from around 35% for untreated bacterial cellulose to 16% for purified bacterial cellulose. This can be due to the presence of phosphorous compounds, which can greatly enhance the char formation. According to Table 3.5, by increasing the intensity of treatment, the temperature at 20% weight loss and the decomposition temperature increased before a slight decline in sample H (NaOH 9 w/v% treated for 10 hours).

Table 3.5: Decomposition temperature, weight loss at 300 °C and temperature at 20% weight loss for treated and untreated BC.

Sample	Temperature at 5% weight loss (°C)	Temperature at 20% weight loss (°C)	Weight loss (%) at 300 (°C)	Decomposition temperature (°C)
BC-J	240.42	321.67	10.77	355.57
BC-B	296.219	341.019	5.36	356.97
BC-E	298.72	342.32	5.12	362.57
BC-H	290.87	335.068	5.93	360.72

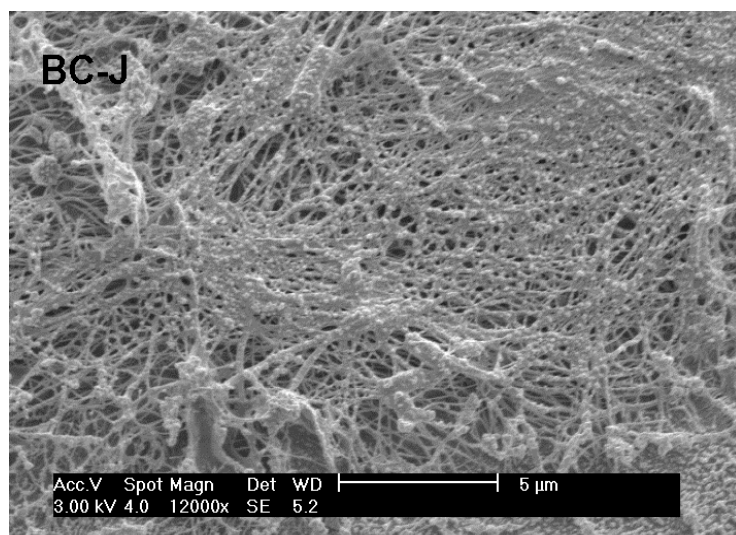
Table 3.6: Treatment period and % concentration for the bacterial cellulose pellicles

Treatment Period (hrs) \ NaOH Concentration (W/v %)	NaOH Concentration (W/v %)		
	5	7	9
5	BC-A	BC-D	BC-G
10	BC-B	BC-E	BC-H
12	BC-C	BC-F	BC-I
Untreated BC-J			

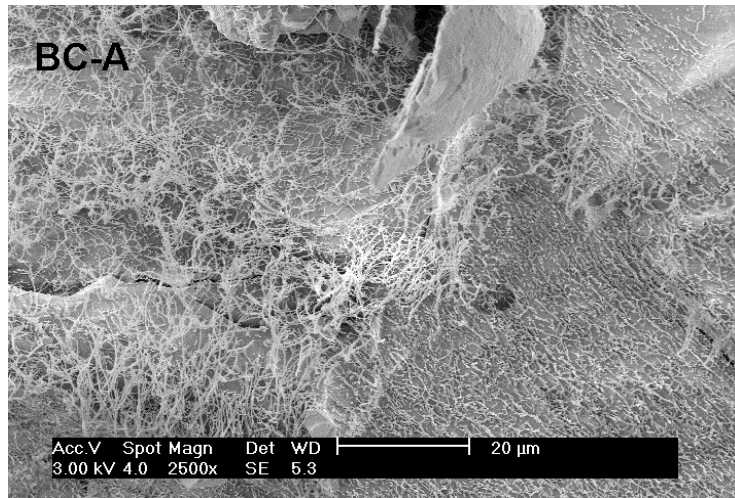
Thermal degradation behaviour is influenced by factors such as molecular weight, crystallinity and orientation of the chains (George et al., 2005). The initial increase in the decomposition temperature of treated samples compared to untreated samples confirms an increase in crystallinity and/or increase in the proportion of cellulose II polymorph, as discussed in the FTIR results. Cellulose II is the most thermodynamically stable allomorph of cellulose (Brown, 1999), which corroborates the increase in thermal stability with alkali treatment. The slight decrease in decomposition temperature for the most extensively treated sample (here H) may suggest degradation or a collapse in cellulose structure caused by this treatment.

3.3.4 Cryo-SEM characterisation

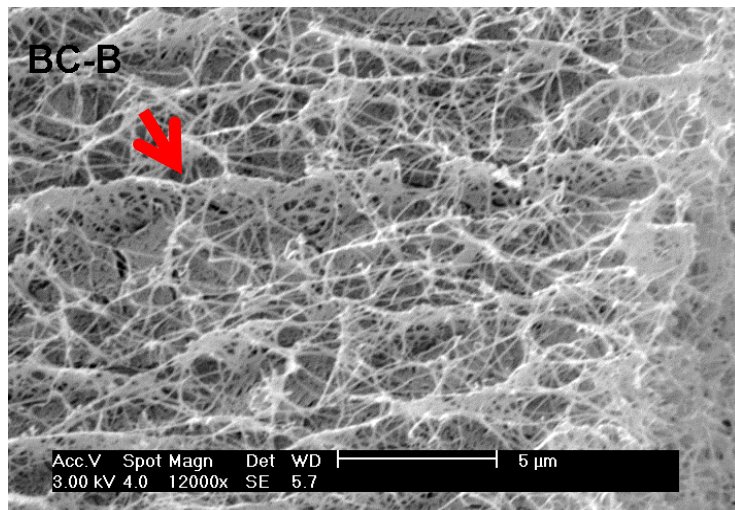
Figure 3.15 show the effect of NaOH on the morphology of treated (BC-A to BC-I) and untreated BC (BC-J) samples studied by cryo-SEM.



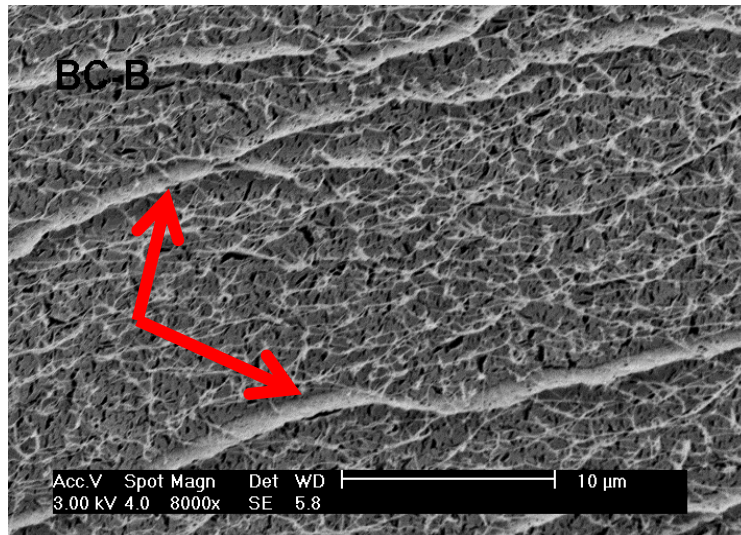
BC-J (untreated bacterial cellulose)



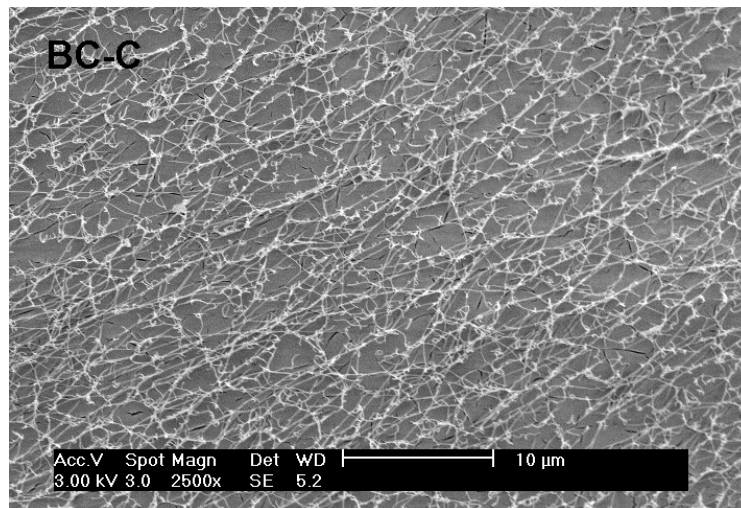
BC-A (5 w/v% NaOH treated for 5 hours)



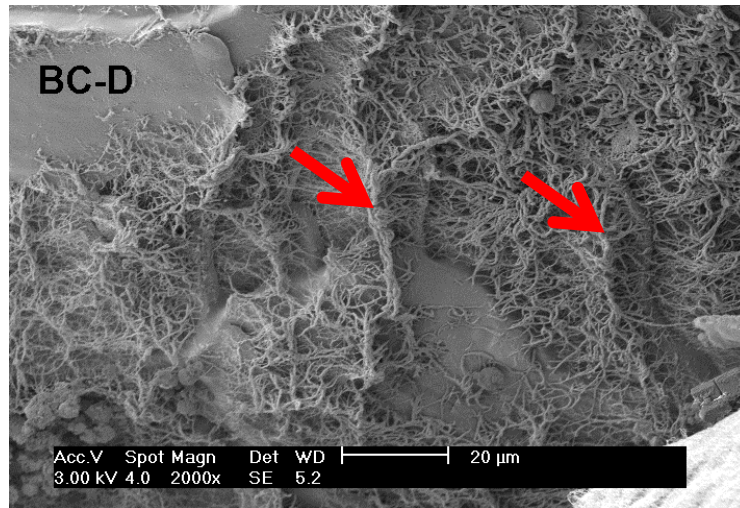
BC-B (5 w/v% NaOH treated for 10 hours) Red arrow indicates lamellae-like structure with parallel layers of compact fibres and looser fibres in between.



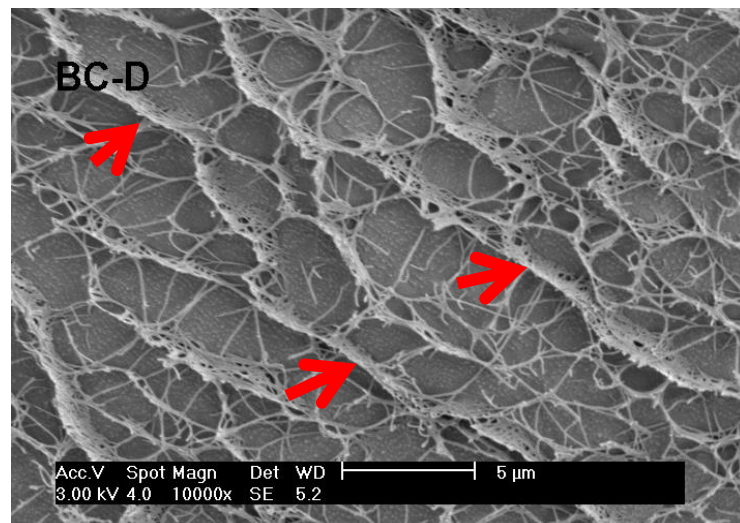
BC-B (5 w/v% NaOH treated for 10 hours) Red arrows indicate lamellae-like structure with parallel layers of compact fibres and looser fibres in between.



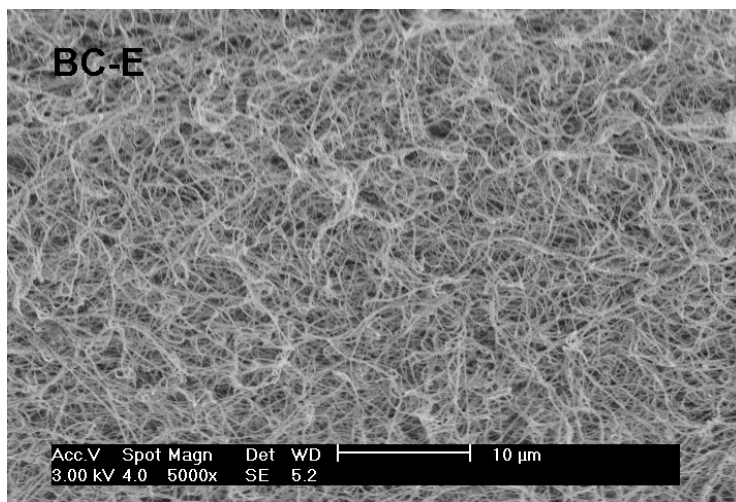
BC-C (5 w/v% NaOH treated for 12 hours)



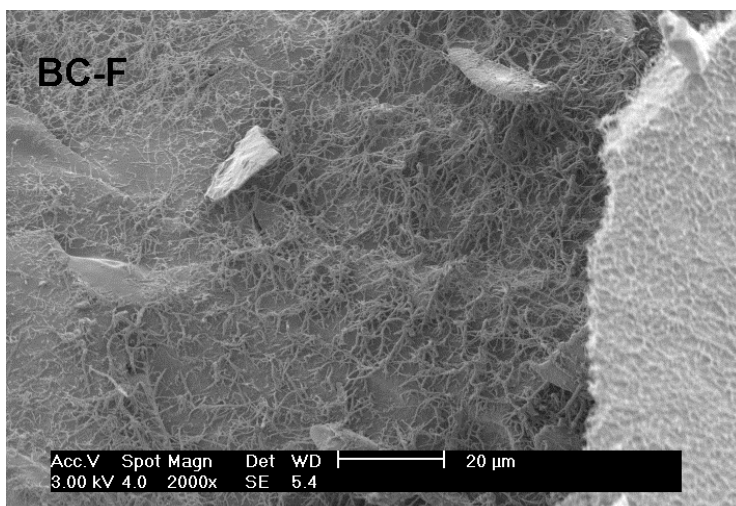
BC-D (7 w/v% NaOH treated for 5 hours) Red arrows indicate lamellae-like structure with parallel layers of compact fibres and looser fibres in between.



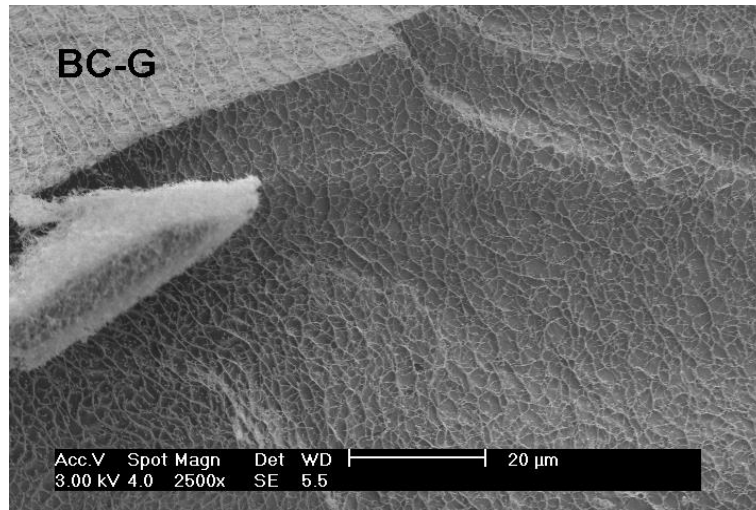
BC-D (7 w/v% NaOH treated for 5 hours) Red arrows indicate lamellae-like structure with parallel layers of compact fibres and looser fibres in between.



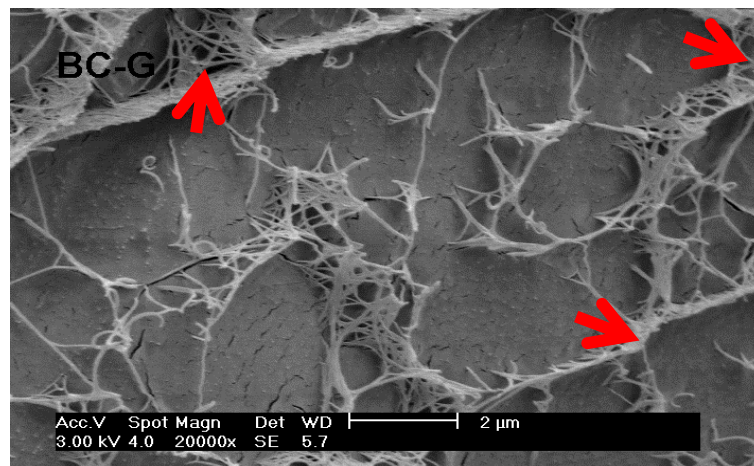
BC-E (7 w/v% NaOH treated for 10 hours)



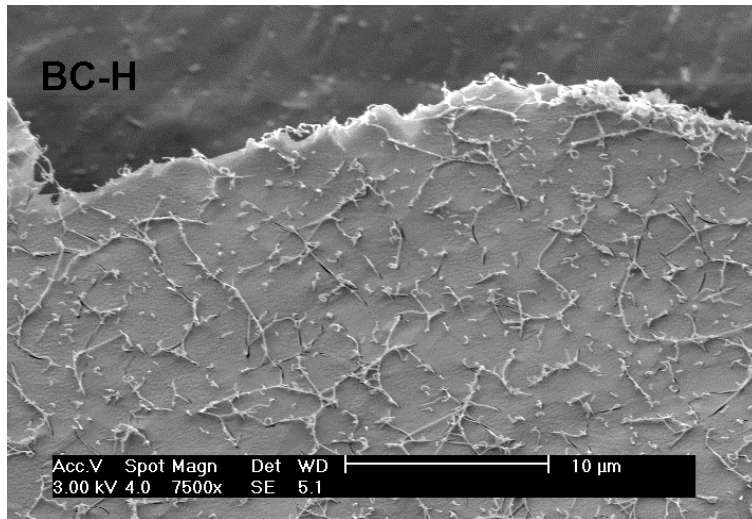
BC-F (7 w/v% NaOH treated for 12 hours)



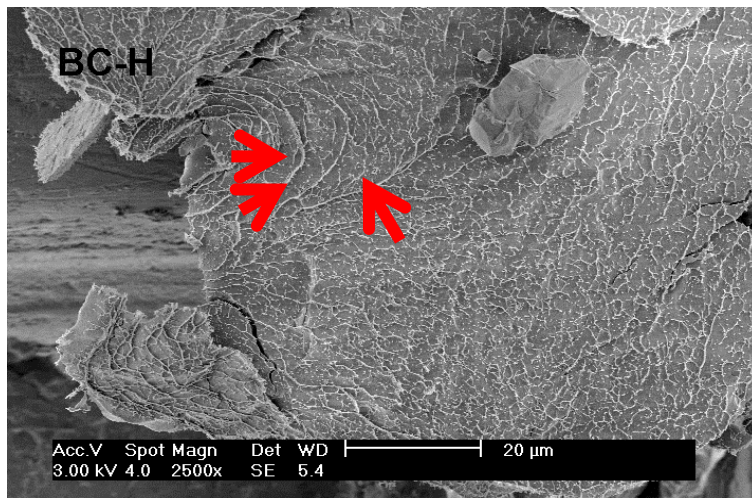
BC-G (9 w/v% NaOH treated for 5 hours)



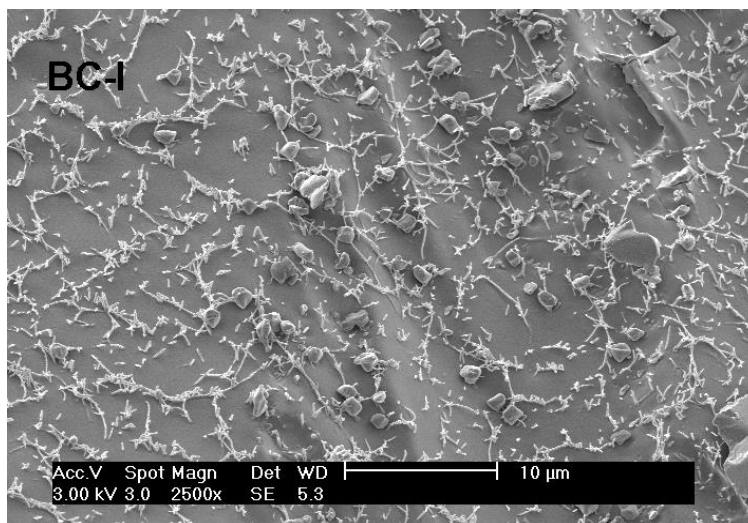
BC-G (9 w/v% NaOH treated for 5 hours) Red arrows indicate lamellae-like structure with parallel layers of compact fibres and looser fibres in between.



BC-H (9 w/v% NaOH treated for 10 hours)

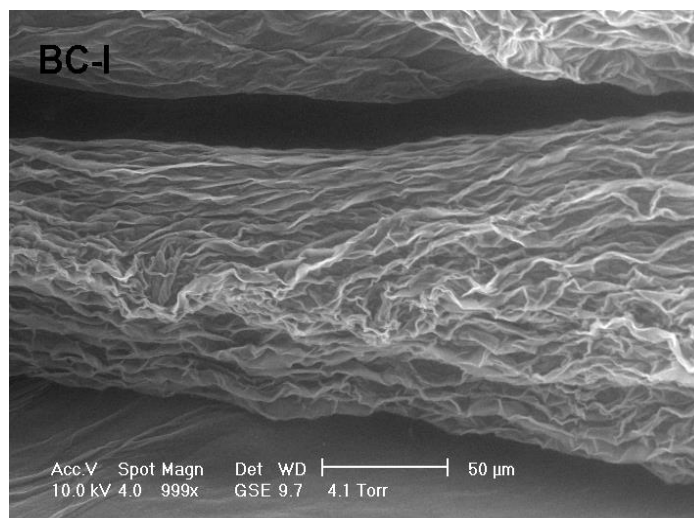


BC-H (9 w/v% NaOH treated for 10 hours) Red arrows indicate lamellae-like structure with parallel layers of compact fibres and looser fibres in between.



BC-D (9 w/v% NaOH treated for 12hours)

Figure 3.15: Representative Cryo-SEM images of treated and untreated samples.



BC-I (9 w/v% NaOH treated for 12 hours)

Figure 3.16: ESEM image of a treated sample (BC-I) clearly showing the layers of fibres in the swollen state.

Figure 3.15 BC-J (untreated BC) shows the structure of the untreated sample with a dense interconnected network of fibres. From Figure 3.15 BC-B, it is clear that the bacterial cellulose scaffold consisted of a lamellae-like structure with parallel layers of compact fibres indicated by red arrows (seen also in Figure 3.16 an ESEM image of BC structure) with looser fibres in between. As the concentration/period of treatment increased, the loose fibres tended to degrade while the layers remained intact. This can be seen by comparing Figure 3.15-BC-D with Figures 3.15-BC-H and BC-I, which were treated with higher concentrations of sodium hydroxide. Therefore, it is possible to conclude that the compact layers of fibres were crystalline regions with amorphous areas between them. The amorphous and crystalline regions covering the surface of the cellulose structure reacted with the alkali solution and were removed when the solution was washed off (Gassan & Bledzki, 1999; Liu et. al., 2008). Haigler et al., proposed that *Gluconacetobacter xylinus* extrudes cellulose in the form of 1.5 nm nanofibrils (Haigler et al, 1980; Yu and Atalla 1996), as also observed in the Cryo-SEM images in this study. An interconnective channel of pores, a fibrous fracture surface and a relatively dense network of fibrils were observed in samples J to F (refer to Table 3.6 for sample treatment times), while this network tended to collapse in samples G, H and I, which were treated with higher concentrations of NaOH. Images of samples H and I clearly showed a less dense network of fibres with a greater number of broken fibrils.

3.3.5 Cell Culture

3.3.5.1 MTT Assay & Phase-contrast Imaging of Dermal Fibroblasts

As can be seen from the representative phase-contrast images in Figure 3.17, dermal fibroblasts adhered and proliferated on all of the samples and most had grown to or near confluence after 10 days.

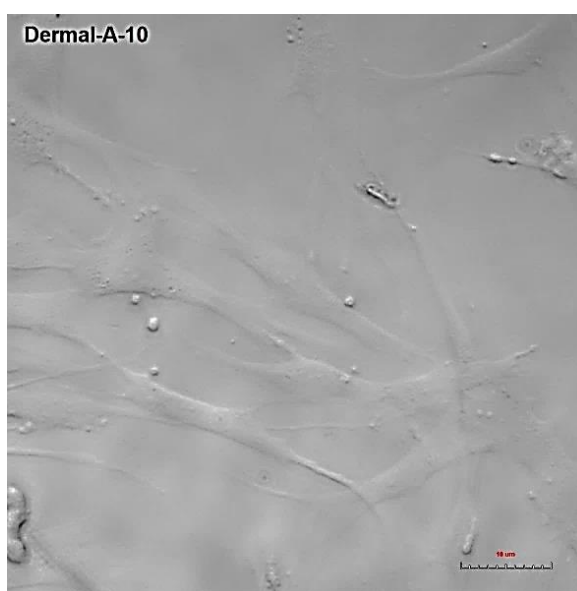


Figure 3.17 (a): Representative optical images of dermal fibroblast proliferation, sample A (5 wt.% NaOH for 5 hours), day 10 (scale bars represent 10 μm).

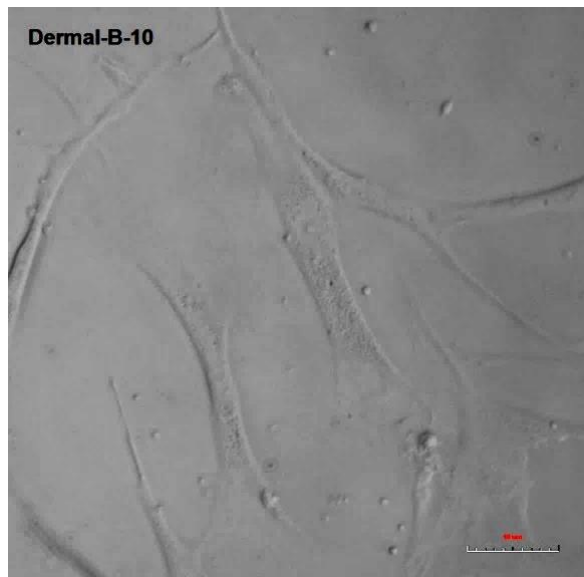


Figure 3.17 (b): Representative optical images of dermal fibroblast proliferation, day 10, sample B, 5 wt.% NaOH for 10 hours (scale bars represent 10 μm).

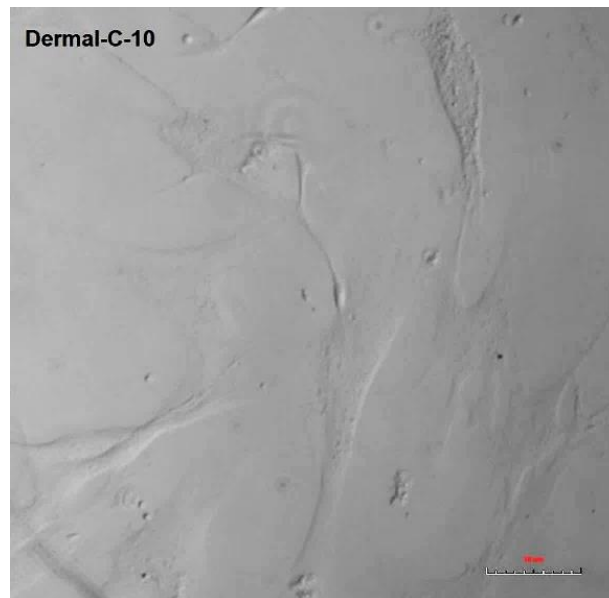


Figure 3.17 (c): Representative optical images of dermal fibroblast proliferation, sample C (5 wt.% NaOH for 12 hours), day 10 (scale bars represent 10 μm).



Figure 3.17 (d): Representative optical images of dermal fibroblast proliferation, sample D (7 wt.% NaOH for 5 hours), day 10 (scale bars represent 10 μm).

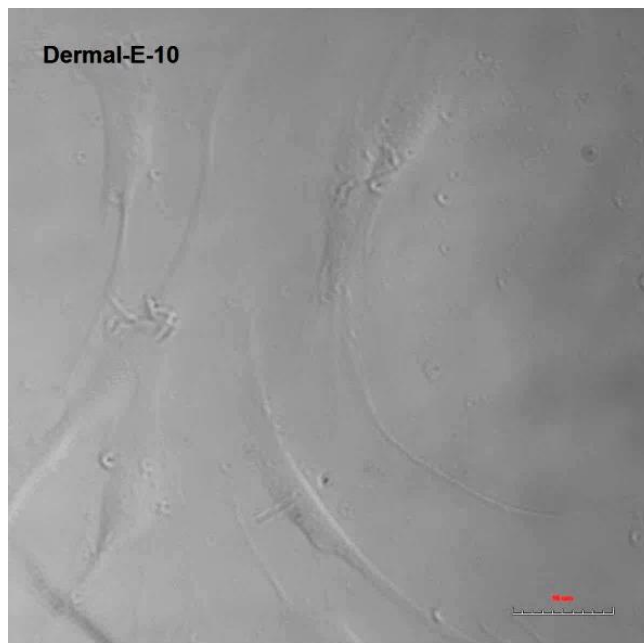


Figure 3.17 (e): Representative optical images of dermal fibroblast proliferation, sample E (7 wt.% NaOH for 10 hours), day 10 (scale bars represent 10 μm).

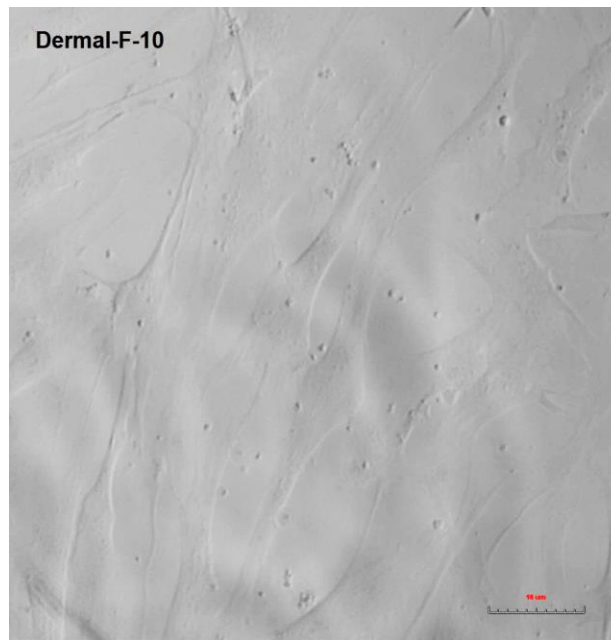


Figure 3.17 (f): Representative optical images of dermal fibroblast proliferation, sample F (7 wt.% NaOH for 12 hours), day 10 (scale bars represent 10 μm).

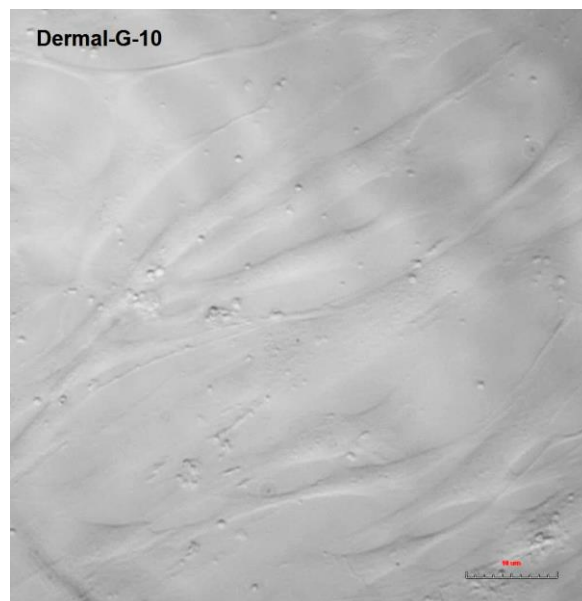


Figure 3.17 (g): Representative optical images of dermal fibroblast proliferation, sample G (9 wt.% NaOH for 5 hours), day 10 (scale bars represent 10 μm).

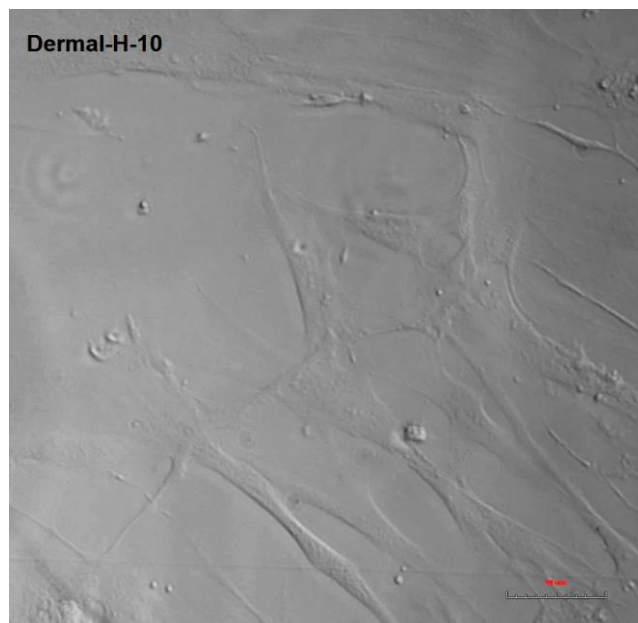


Figure 3.17 (h): Representative optical images of dermal fibroblast proliferation, sample H (9 wt.% NaOH for 10 hours), day 10 (scale bars represent 10 μm).

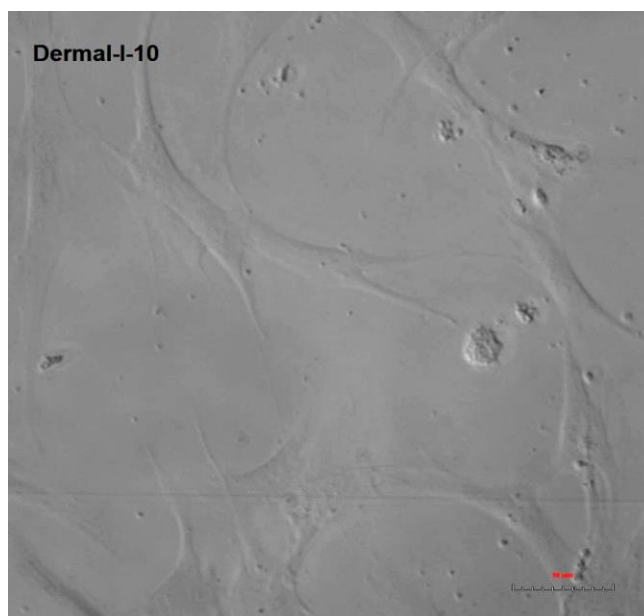


Figure 3.17 (i): Representative optical images of dermal fibroblast proliferation, sample I (9 wt.% NaOH for 12 hours), day 10 (scale bars represent 10 μm).

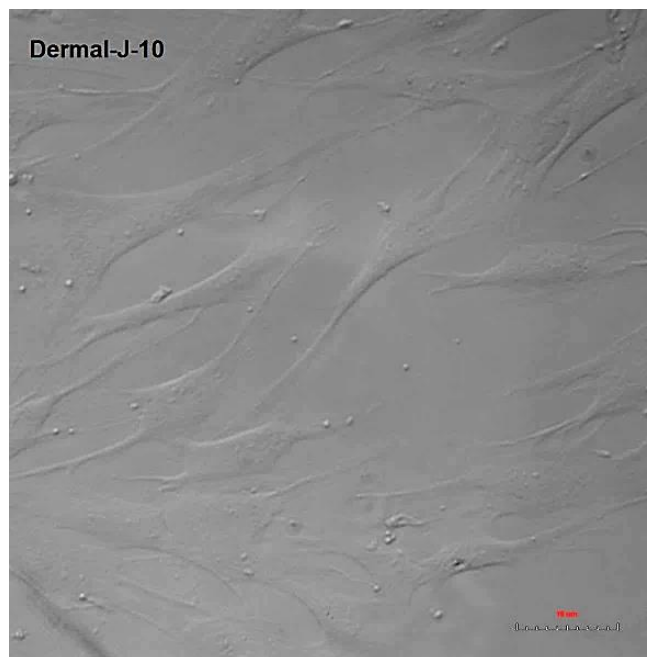


Figure 3.17 (j): Representative optical images of dermal fibroblast proliferation, sample J (untreated), day 10 (scale bars represent 10 μm).

The MTT results showed the relative viability of dermal fibroblasts growing on scaffolds with different alkali treatments. The results are comparable because the same number of cells was seeded onto all samples. It can be seen from Figure 3.18 that the viability of the dermal cells growing on tissue culture plastic was significantly higher than those on the BC samples. It can be seen that the viability of cells after 6 days of cultivation was higher on all of the treated samples (except for sample I, with the most extensive treatment) compared to the untreated sample J. After 10 days, the scaffolds treated with 9 w/v% NaOH for 5, 10 and 12 hours showed lower viability than the untreated sample J.

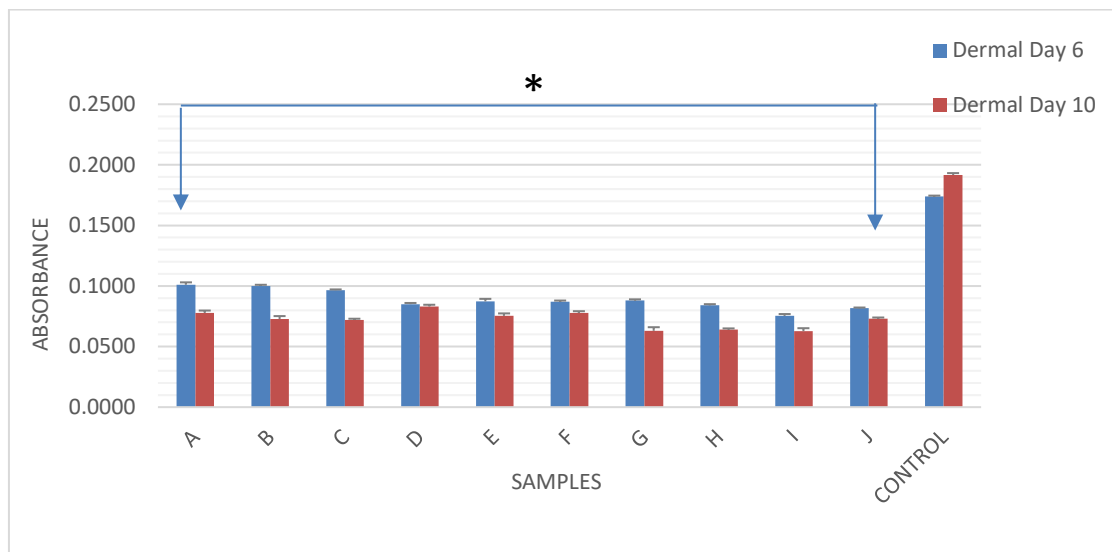


Figure 3.18: MTT results of the viability of human dermal fibroblasts after 6 and 10 days on BC with different treatments. Absorbance readings at 540 nm. $*p < 0.05$ compared with the control.

Comparing the MTT results and optical images with the images obtained from the Cryo-SEM, it appeared that the rather dense network of fibres in sample A had the most suitable microstructure for cell attachment and proliferation at day 6. However, this network of dense fibres might be responsible for the significant decrease in the viability of cells on scaffold A at day 10. A study by Backdahl et al., suggested that the definition of a pore size in a fibrous hydrogel is not relevant, because the migrating cells can push aside the nanofibrils and grow into the hydrogel. Since their experiment was done with Smooth Muscle Cells (SMCs), the ability to push the fibrils aside might depend on the strength of the migrating cells. However, they proposed that the density of the nanofibrils network affect the extent to which the cells could migrate into the scaffold. Therefore, although a dense network of fibrils is beneficial for cell attachment, a

more porous scaffold with more free space more readily allows the ingrowth of cells and their further proliferation (Backdahl et al., 2006).

The dense network of fibrils in scaffold A could have inhibited the ingrowth of the cells, and the fibroblast cells could simply not be strong enough to push the fibrils aside. Therefore, the fibroblast cells easily attached to the surface of scaffold A, proliferated until the surface was covered, but were not able to migrate into the scaffold and, hence, the proliferation stopped. The best balance of free spaces and network density of nanofibrils was exhibited by scaffold D, as it showed the highest viability of cells after 10 days.

Table 3.7: Treatment period and % concentration for the BC pellicles

NaOH Concentration (Wt %) Treatment Period (hrs)	5	7	9
5	BC-A	BC-D	BC-G
10	BC-B	BC-E	BC-H
12	BC-C	BC-F	BC-I
Untreated BC-J			

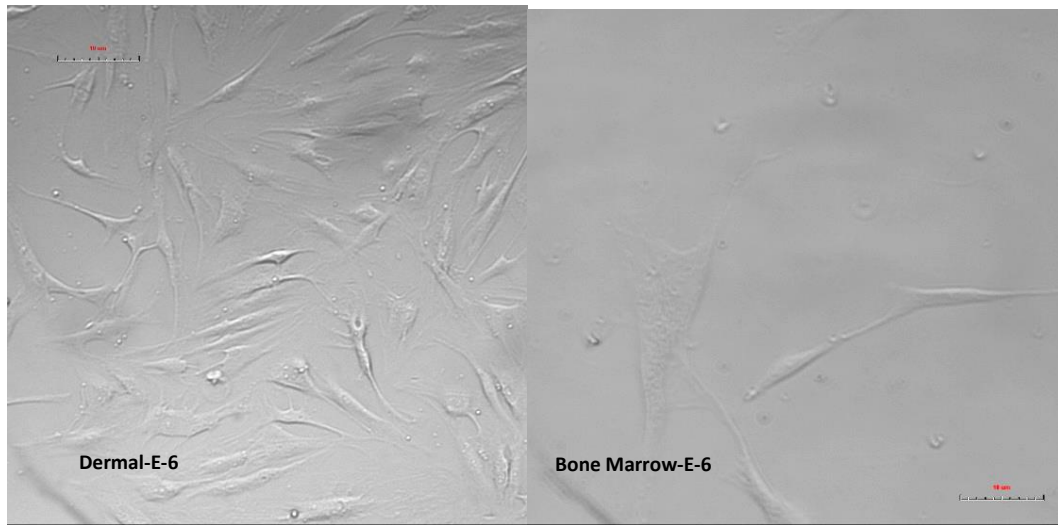


Figure 3.19: Representative images for Day 6 (a) Dermal cells (b) Bone marrow cells (scale bars represent 10 μm).

Figure 3.19 show dermal cells (a) and bone marrow cells (b) proliferating on sample E on day 6, the images for all samples looked similar, therefore only two were selected to represent day 6 cell culture.

The surface charges of treated BC may have led to stronger adherence of cells on the scaffold, but if the adhesion is too strong, the growth and proliferation is inhibited (Svensson et al., 2005). Therefore, in addition to the surface morphology, this may also justify the higher cell viability on samples treated with lower intensities compared with higher intensities (especially on day 10 where proliferation is the dominant factor).

3.3.5.2 MTT Assay & Phase-contrast Imaging of Bone Marrow Fibroblasts

As can be seen from the representative phase-contrast images of bone marrow fibroblasts on the treated and untreated samples in Figure 3.20 (a-j), the cells appear to have attached to the scaffold and proliferated, however, to a lesser extent than the dermal cells.

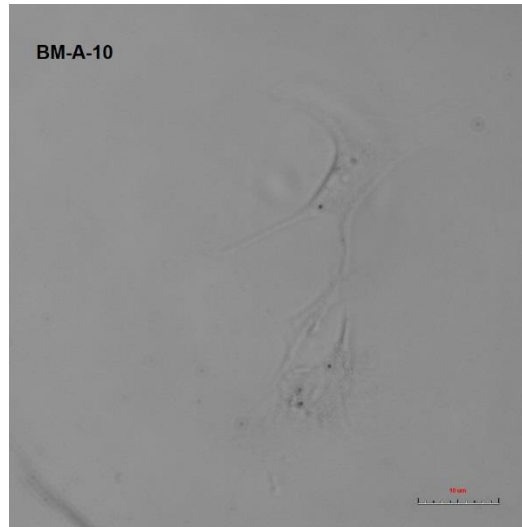


Figure 3.20: (a) Representative optical images of bone marrow fibroblast proliferation, sample A (5wt.% NaOH for 5 hours), day 10 (scale bars represent 10 μm).

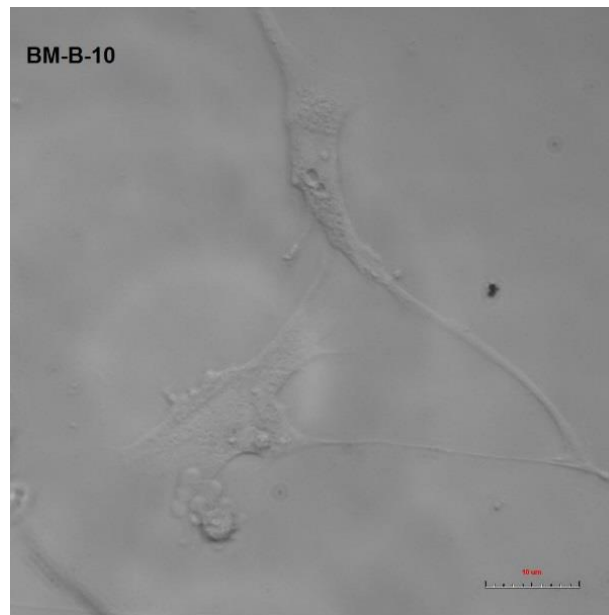


Figure 3.20: (b) Representative optical images of bone marrow fibroblast proliferation, sample B (5wt.% NaOH for 10 hours), day 10 (scale bars represent 10 μm).

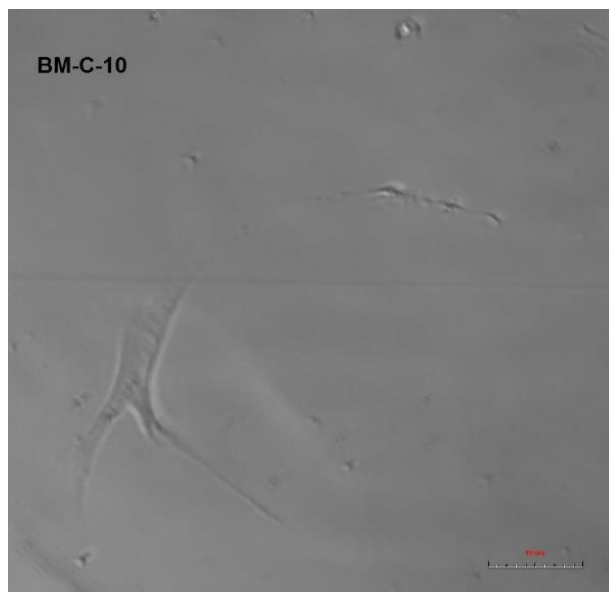


Figure 3.20: (c) Representative optical images of bone marrow fibroblast proliferation, sample C (5wt.% NaOH for 12 hours), day 10 (scale bars represent 10 μm).

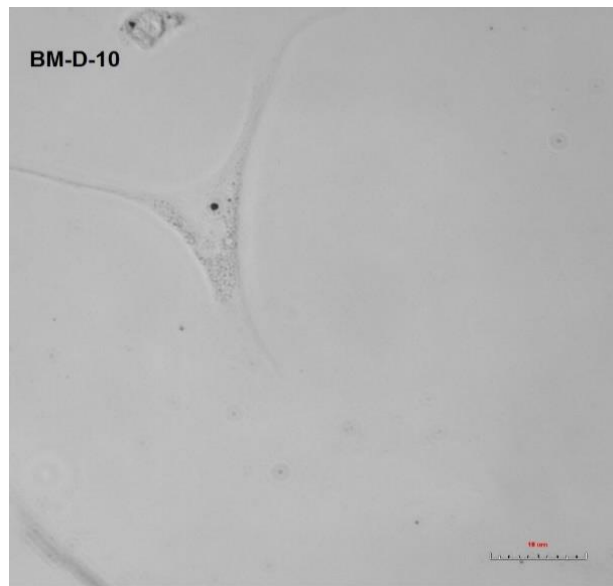


Figure 3.20: (d) Representative optical images of bone marrow fibroblast proliferation, sample D (7 wt.% NaOH for 5 hours), day 10 (scale bars represent 10 μm).

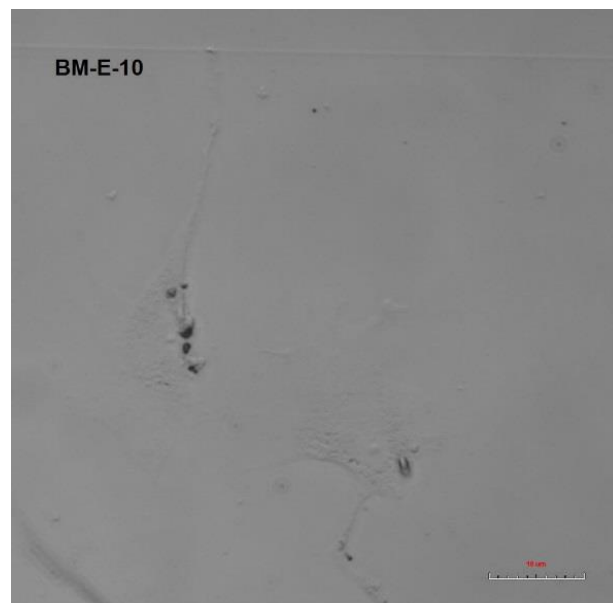


Figure 3.20: (e) Representative optical images of bone marrow fibroblast proliferation, sample E (7 wt.% NaOH for 10 hours), day 10 (scale bars represent 10 μm).

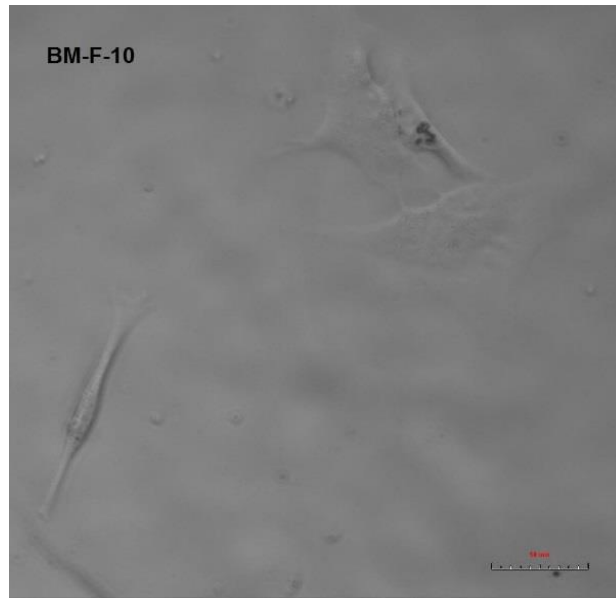


Figure 3.20: (f) Representative optical images of bone marrow fibroblast proliferation, sample F (7 wt.% NaOH for 12 hours), day 10 (scale bars represent 10 μm).

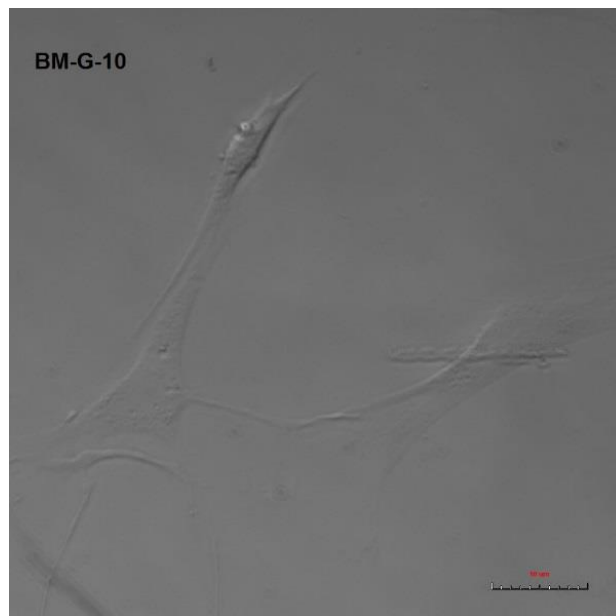


Figure 3.20: (g) Representative optical images of bone marrow fibroblast proliferation, sample G (9 wt.% NaOH for 5 hours), day 10 (scale bars represent 10 μm).

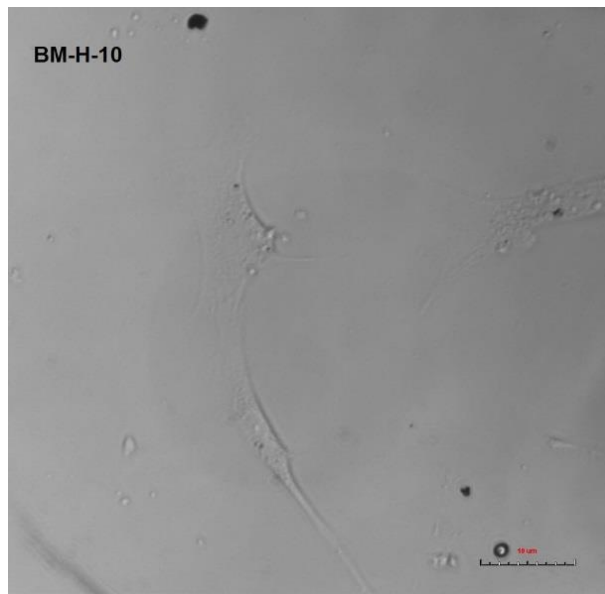


Figure 3.20: (h) Representative optical images of bone marrow fibroblast proliferation, sample H (9 wt.% NaOH for 10 hours), day 10 (scale bars represent 10 μm).

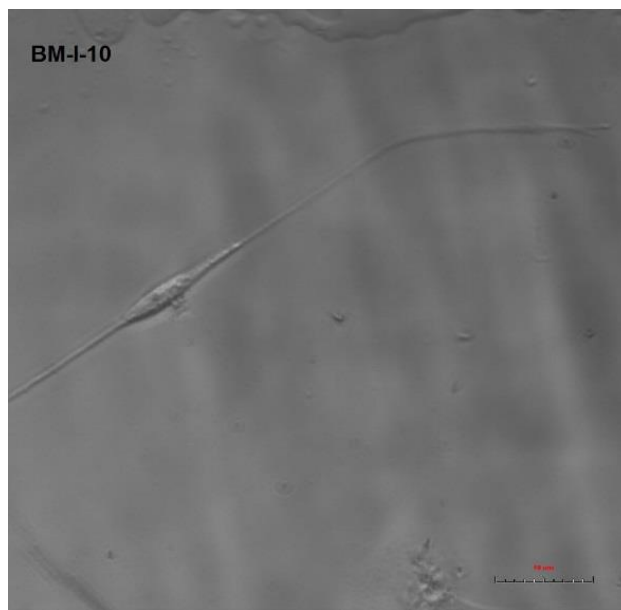


Figure 3.20: (i) Representative optical images of bone marrow fibroblast proliferation, sample I (9 wt.% NaOH for 12 hours), day 10 (scale bars represent 10 μm).

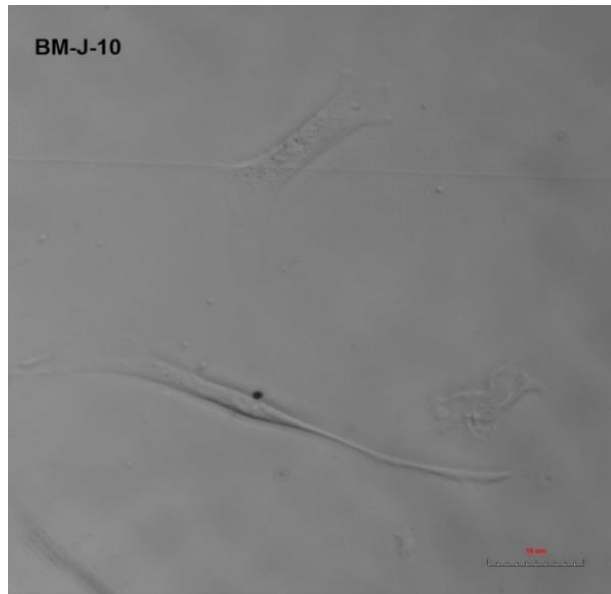


Figure 3.20: (j) Representative optical images of human bone marrow fibroblast proliferation on treated and untreated BC.

The MTT cell viability results from the different samples are shown in Figure 3.21. It can be seen that after 6 days of cultivation, all of the treated samples showed fairly similar, or higher, cell viability than the untreated sample. The viability of fibroblasts growing on sample D was very similar to that of tissue culture plastic (TCP), a frequently used substrate for cell cultivation (Svensson et al, 2005). It was noted that after 10 days of cultivation, the viability of cells on all of the treated samples was higher than that of the untreated sample, this may be due to low seeding density.

The same argument that applies to dermal cells can also be applied to bone marrow fibroblasts. From the MTT result in Figure 3.21, it is clear that after 6 days, the cells showed the highest viability on scaffold D, and after 10 days on scaffold H. Cryo-SEM images in Figure 3.15 show the differences in morphology of these two samples. This again suggests that the least dense

network of sample H (9 w/v% NaOH for 10 hours) provided a better environment for proliferation of bone marrow cells and showed the most viable cells. The slight decrease in survival of the cells on the control sample from day 6 to day 10 suggested that proliferation of bone marrow fibroblasts is generally more difficult. Higher cells viability on sample H compared to TCP implies that 9 w/v% NaOH (sample H) for 10 hours could be proposed as an optimum treatment for cultivation of bone marrow cells.

The results were very similar in both cell types apart from the significantly higher survival rate of the bone marrow cells on sample H, and the dermal cells showing slightly higher viability in general on the control cultures. It can be concluded that while the samples treated with lower concentrations of NaOH were beneficial for survival of dermal cells, higher NaOH concentrations promoted higher viability for bone marrow cells. There was a significant difference (t-test statistical analysis values are shown in appendix) between the cells treated with higher NaOH for bone marrow cells on day 6 and day 10.

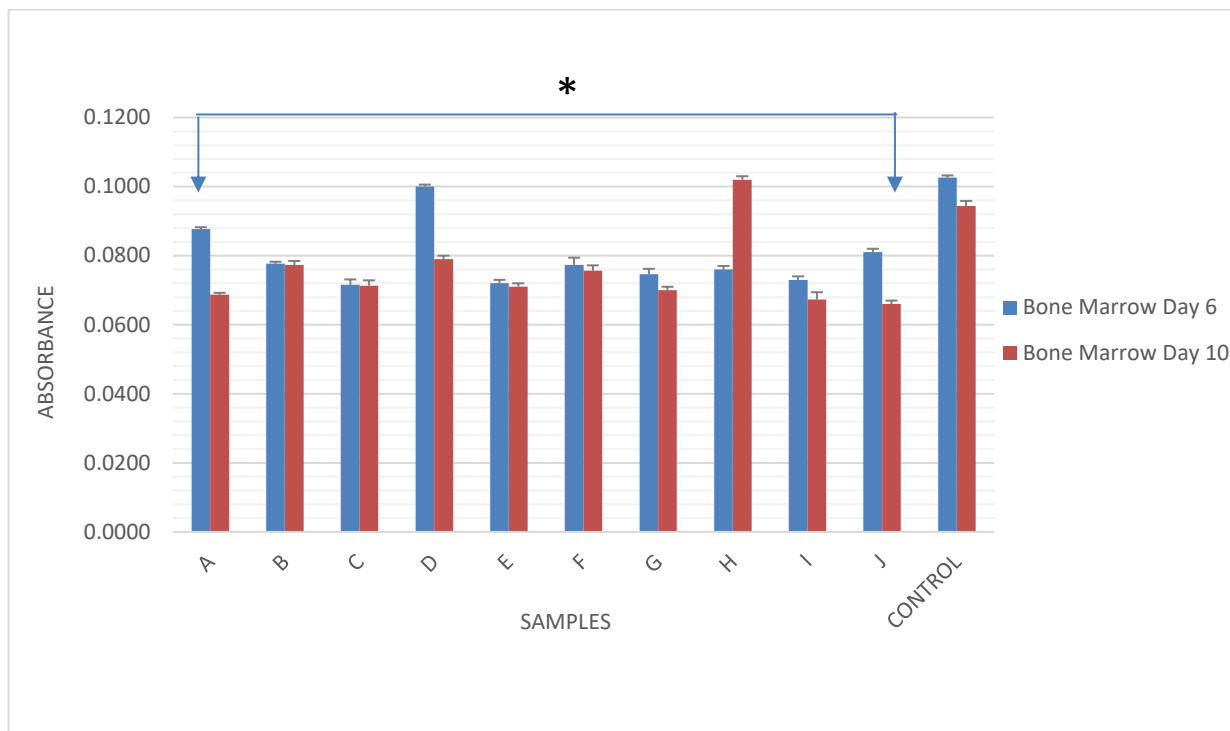


Figure 3.21: MTT results for the viability of human bone marrow fibroblasts after 6 and 10 days on BC with different treatments. Absorbance readings at 540 nm. * $p < 0.05$ compared with the control.

When conducting MTT assays on days 6 and 10, the scaffolds were removed to new wells in order to avoid false signals from the cells at the bottom of the well. However, the MTT data for day 3 represents the viability of cells both on the scaffold and in the well. Therefore, this data is not directly comparable to the viability on days 6 and 10. Cells were not growing maybe due to low seeding density.

3.4 Polycaprolactone-Bacterial Cellulose nanocomposites

3.4.1 Acid hydrolysis of BC

The treatment of bacterial cellulose/cellulose materials with sulfuric acid is an extensively used method of extraction for cellulose nanocrystals. This is because it causes a preferential hydrolysis of disordered or amorphous regions of the material by surface reactions (De-Souza et al., 2004).

Figure 3.22 and Figure 3.23 show TEM images of BC whiskers prepared from a diluted suspension of BC whiskers by acid hydrolysis for 24 hours. The suspension displayed colloidal behaviour due to the existence of the positive charges on the surface of the whiskers.

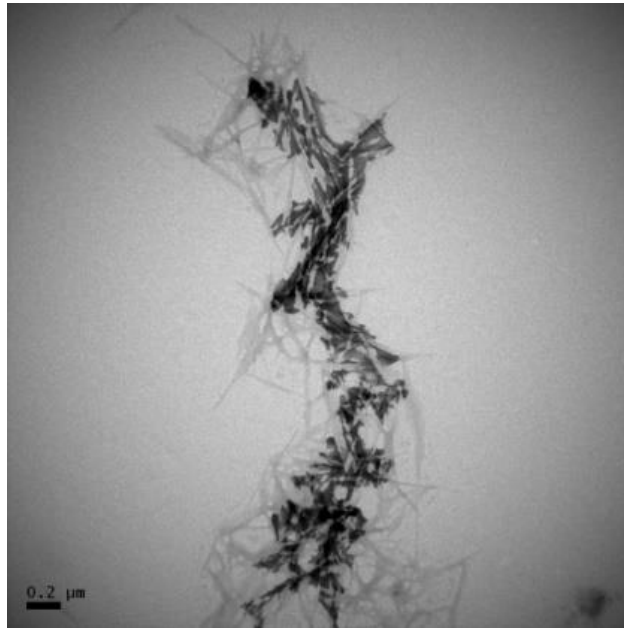


Figure 3.22: TEM of bacterial cellulose whiskers after 48 hours magnification $\times 10,000$.

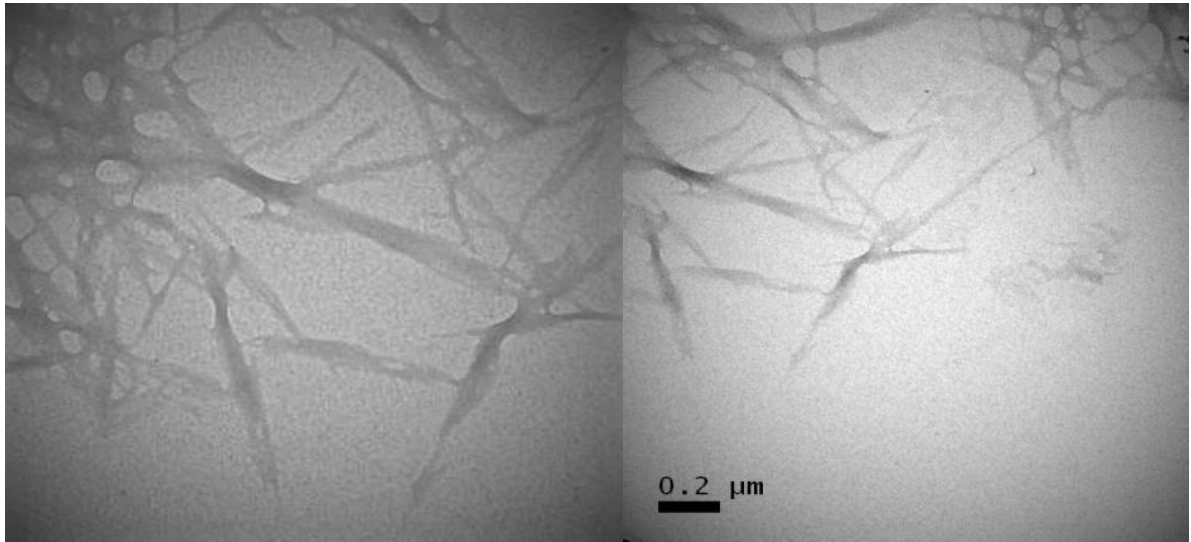


Figure 3.23: TEM of bacterial cellulose whiskers after 48 magnification x50,000.

In this work, a trend of decreasing bacterial cellulose nano whiskers length was observed when increasing the hydrolysis time (Figure 3.24). This has been previously reported when cellulose samples were treated with strong acids, which produce disordered regions along the cellulose fibrils, consequently resulting in shorter nanocrystals (Azizi et al., 2005). Martines et al., also reported a trend of decreasing bacterial cellulose nanowhiskers length with increasing hydrolysis time (Martines-Sans et al., 2011).

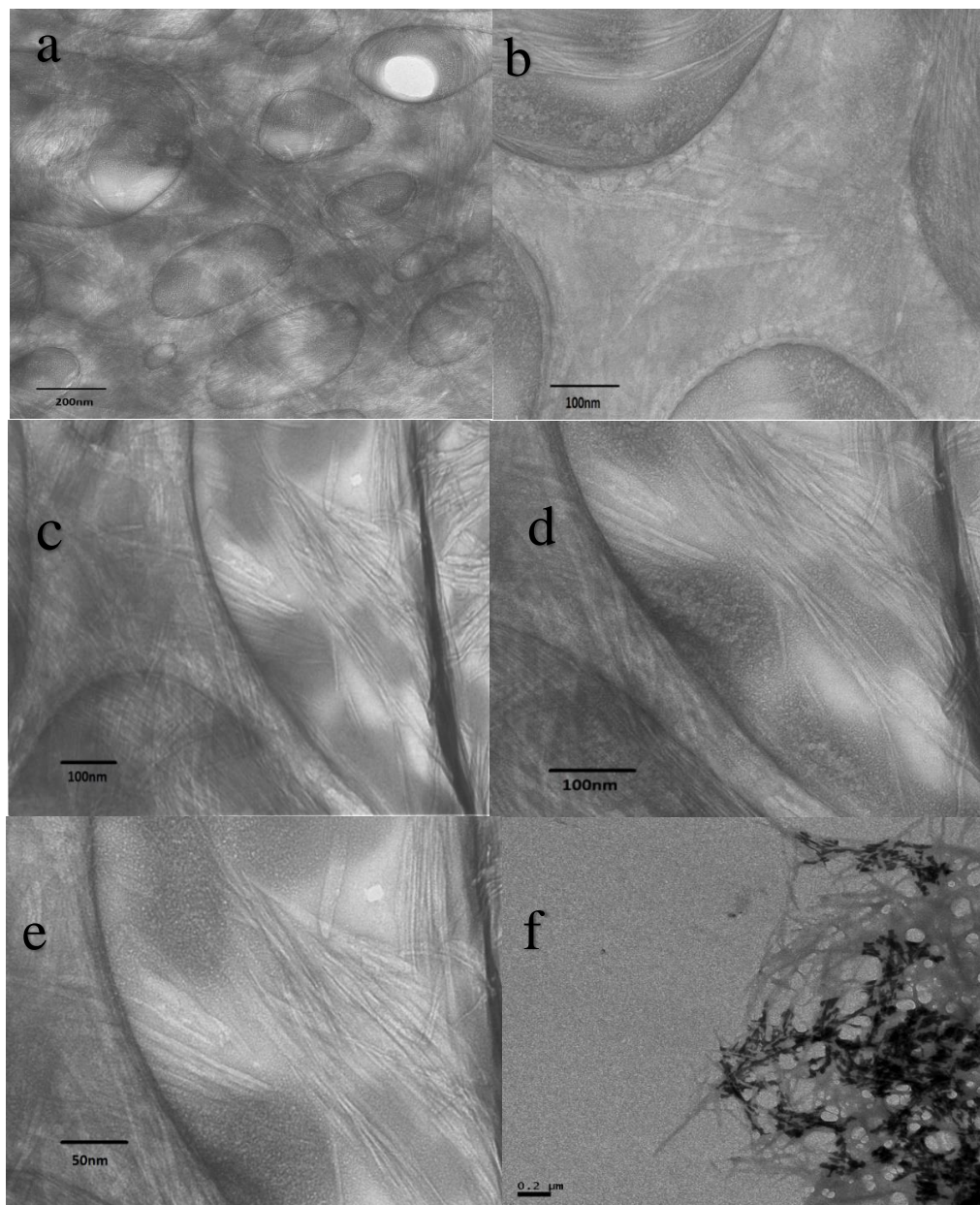


Figure 3.24: TEM of BC whiskers after acid hydrolysis for (a) 2h, (b) 4h, (c) 6h, (d) 8h, (e) 12h and (f) 24h.

Extraction of the whiskers was performed at different time intervals to examine the effect of the acid hydrolysis on the whisker length. The samples show a change in the whisker length

as the time of immersion increases. TEM analysis of the whisker suspension was analysed at different time interval to observe any changes that occurred in the whisker length. Figure 3.24 shows the distribution of whiskers after (a) 2h, (b) 4h, (c) 6h, (d) 8h, (e) 12h and (f) 24h of acid hydrolysis.

3.4.2 Electrospinning PCL-BC fibres

Fibres of polycaprolactone (PCL) and bacterial cellulose whiskers (BC) with varying compositions were prepared using electrospinning (Figure 3.25).



Figure 3.25: Electrospun PCL collected on aluminium foil.

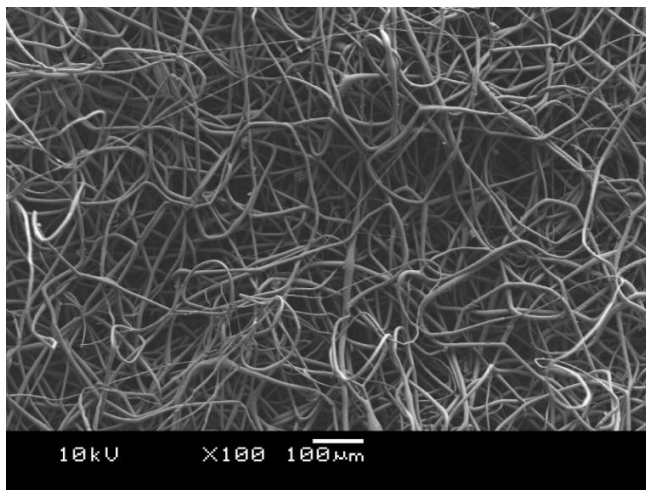
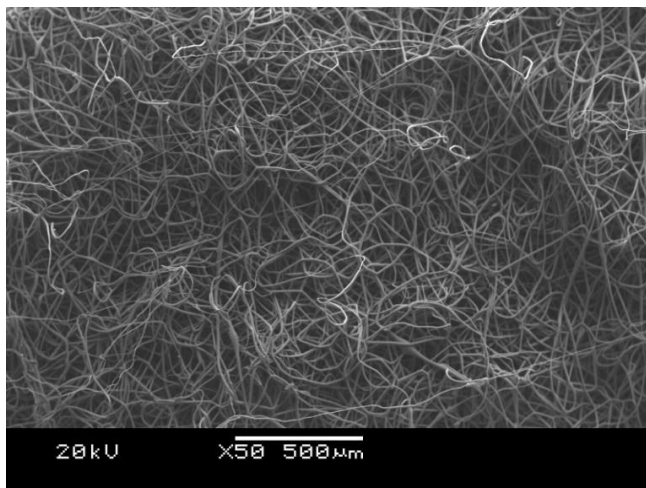
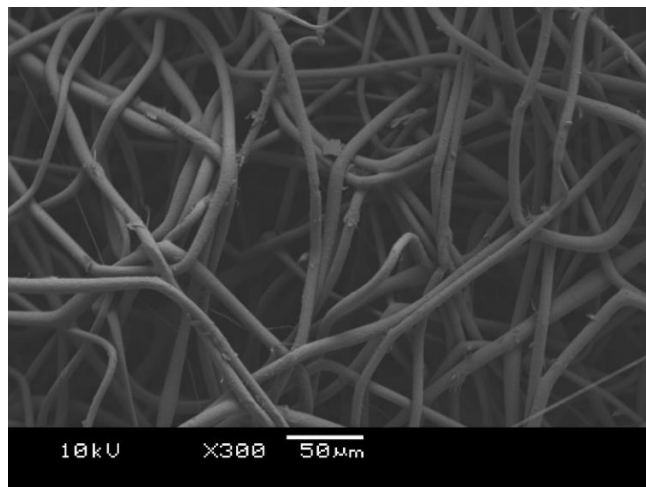


Figure 3.26 (a): Scanning electron microscope images of electrospun PCL.

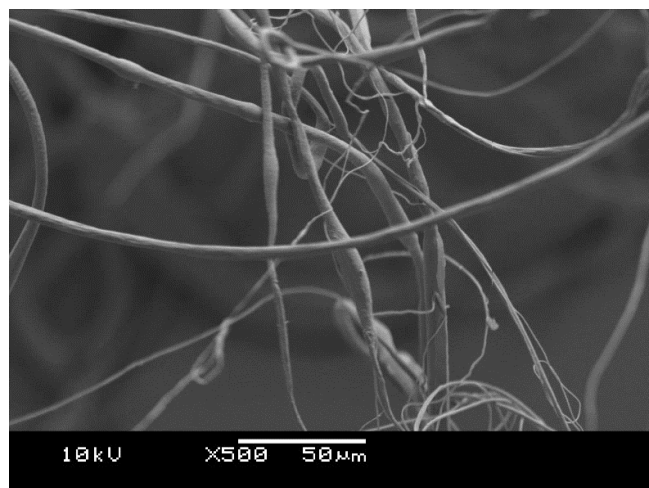
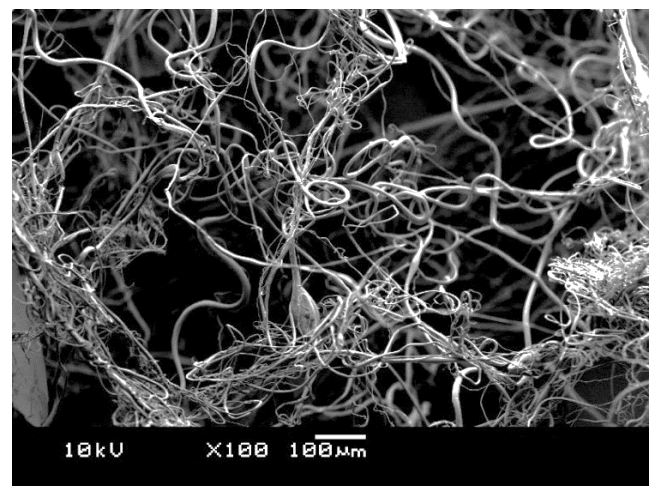
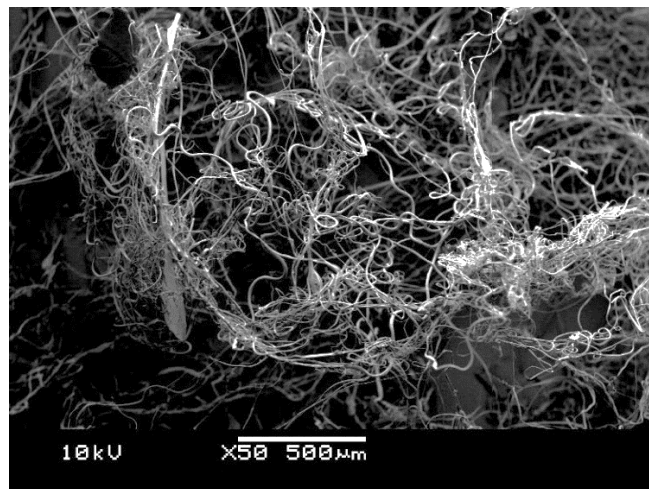


Figure 3.29 (b): Scanning electron microscope images of electrospun PCL-2%BC.

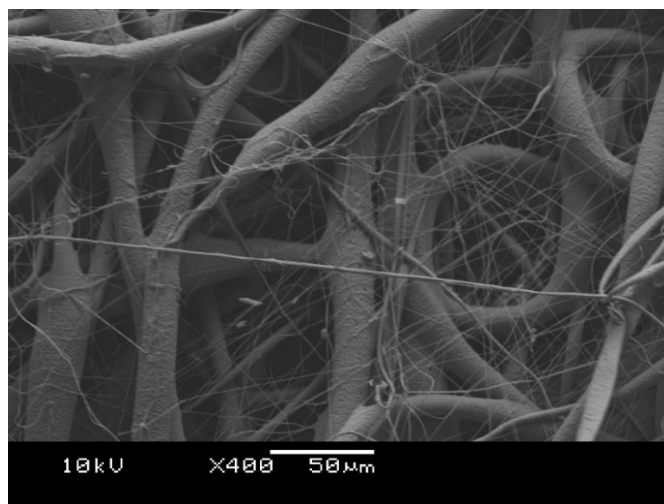
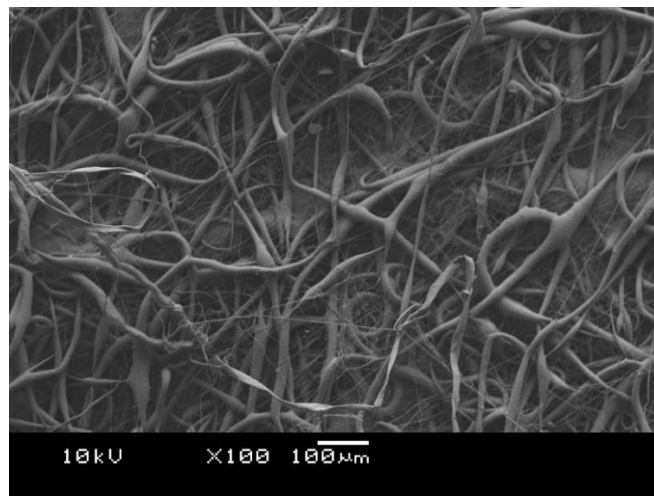
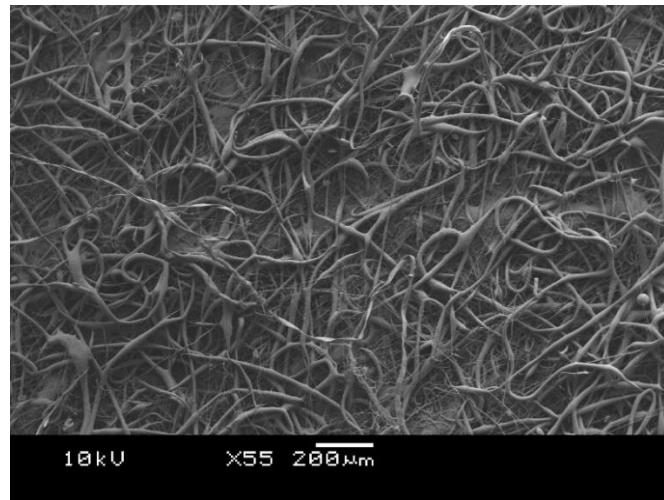


Figure 3.29 (c): Scanning electron microscope images of electrospun PCL-4%BC.

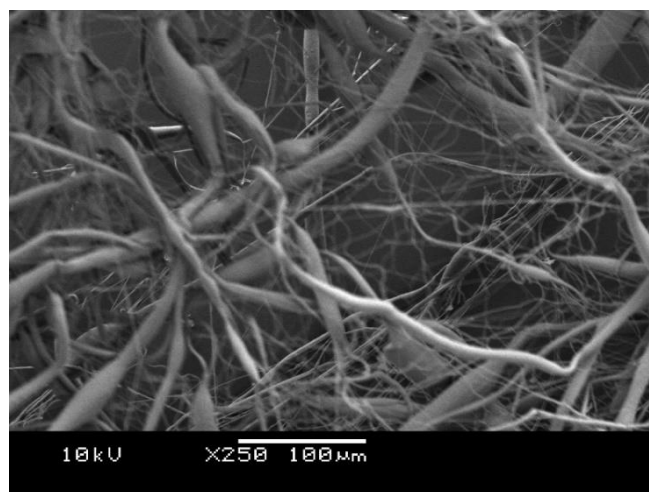
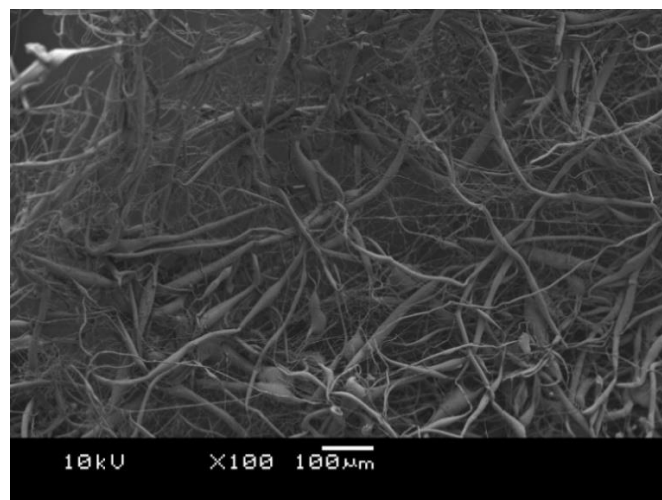
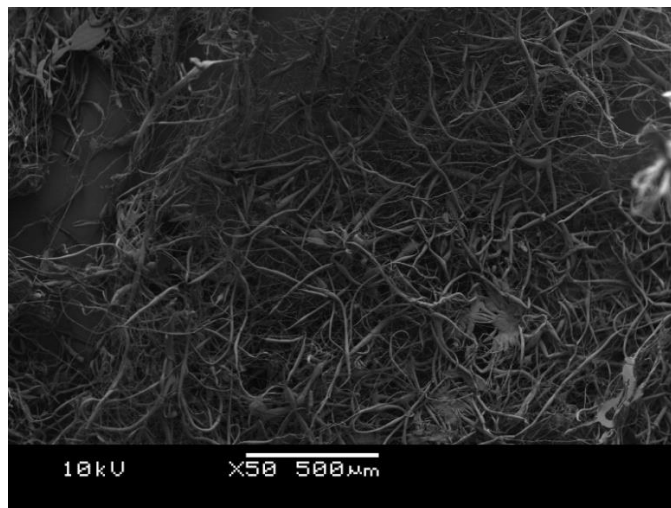


Figure 3.29 (d): Scanning electron microscope images of electrospun PCL-6%BC.

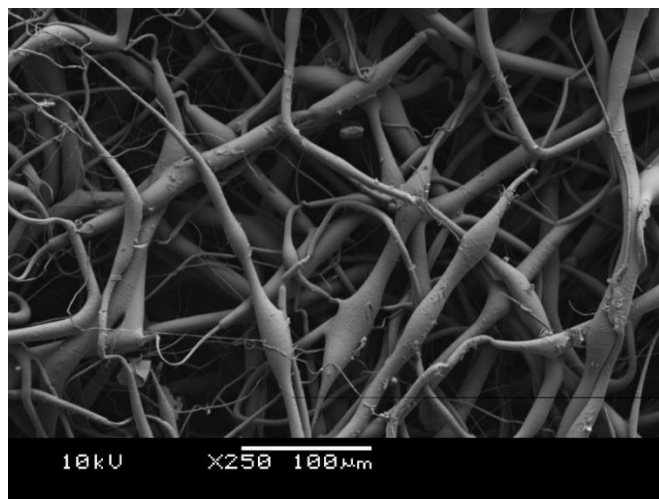
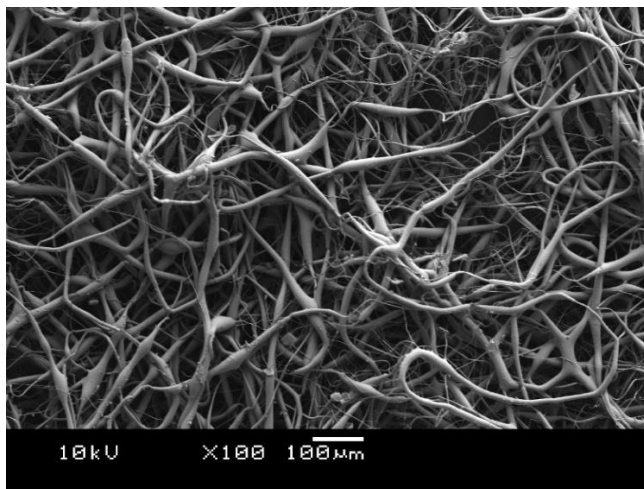
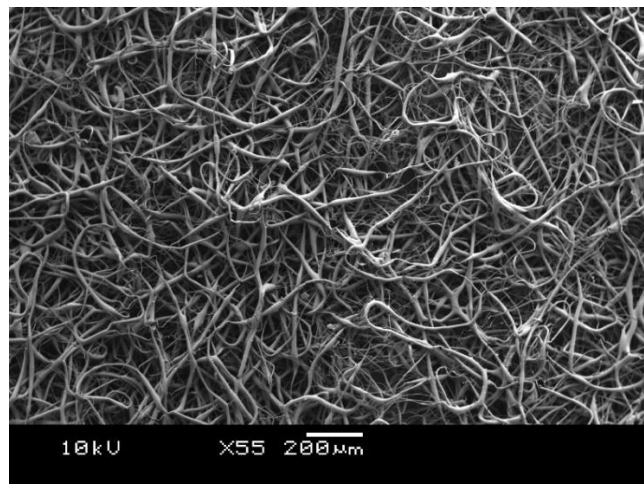


Figure 3.29 (e): Scanning electron microscope images of electrospun PCL-8%BC.

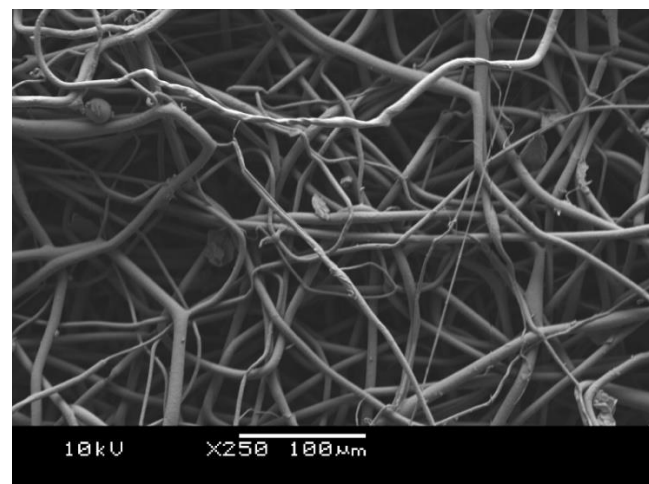
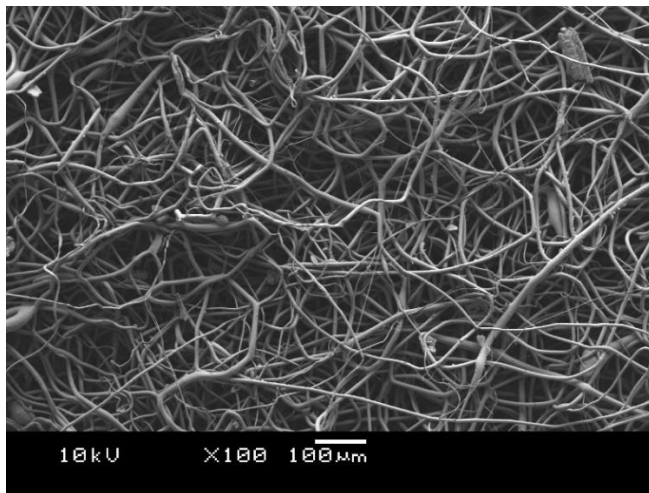
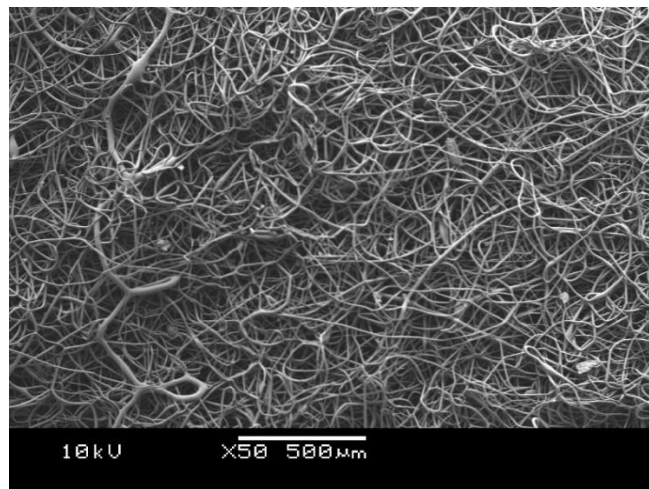


Figure 3.29 (e): Scanning electron microscope images of electrospun PCL-10%BC

Analysis of the images in Figure 3.29 (a) - (e), revealed that the diameter range of fibres from PCL solution was about 100-200 μm . However, an increased fibre diameter was observed as the BC content in the nanocomposites increased, leading to a broader size distribution. Figure 3.29 (a, b, c, d and e) show an uneven size distribution amongst the fibres produced. This indicates that the parameters for the electrospinning setup are not fully optimised and therefore need more experimental work to be able to produce electrospun fibres of even size distribution. The formation of beads which can be seen along some of the electrospun fibres, may be a result of the viscoelastic relaxation. It may also be due to the surface tension upon the reduction of the coulombic force once the fibres are in contact with the grounded target that drives the formation of beads (Arayanarakul et al., 2006).

3.4.3 White light interferometry

The surface roughness of PCL and PCL-BC composites was observed using white light interferometry. The topography of the materials is shown in Figure 3.30 and the numerical values of the measurements are presented in Table 3.13.

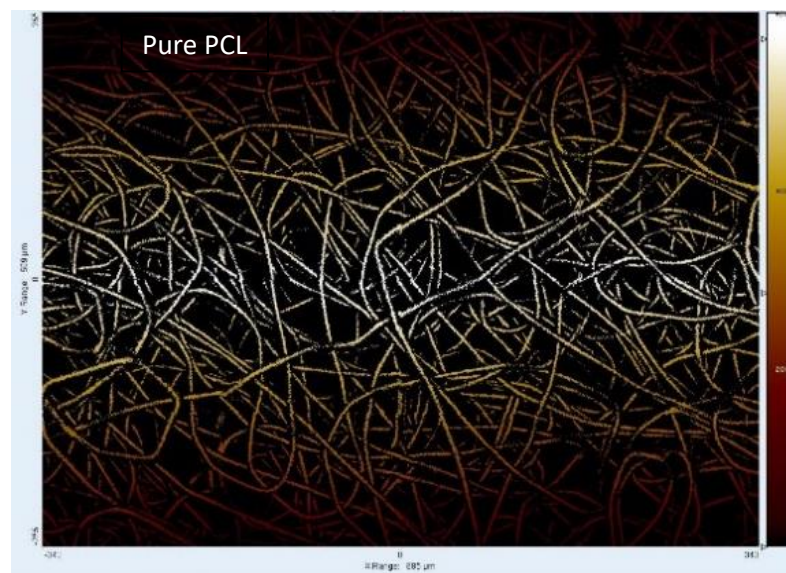




Figure 3.27: Interferometry images of PCL, PCL-BC4 wt. % and PCL-BC10 wt. % showing surface of electrospun sheets.

Figure 3.27 shows that there is a visible difference in the appearance of the samples as the BC content increases. The numerical values in Table 3.9 also highlight the changes in surface roughness as the BC content increases, therefore indicating that the fibres are not as uniform as they were in pure PCL.

Table 3.9: Numerical values of Sa and Sq

Sample	Sa (nm)	Sq (nm)
PCL	98.7	142
PCL-BC4%	325	413
PCL-BC10%	382	486

The surface roughness of the PCL-BC composites increases as the BC content increases. The Sa difference between PCL and PCL-BC4 wt. % is 226.3nm, the Sq difference 271nm, respectively. The Sa difference between PCL and PCL-BC10 wt. % is 283.3nm, the sq difference is 344nm, respectively. The increase in roughness may be a result of the changes in fibre diameter as the content of BC is increased in the nanocomposites. This may play an important role in the cell adhesion and proliferation.

It has been suggested that suspension instabilities cause aggregation by the reduction in the polarity of the dispersion of electrospun nanofibers (Zoppe et al., 1996) and it may be that the electrospinning conditions are optimised for the high-molecular-weight PCL matrix but may not be the optimum conditions suitable for the BC whiskers. The conditions required to preserve the integrity of the electrospun PCL-BC nanofibers are expected to be different because of the different respective rheological behaviour. Therefore, different morphologies that have been observed by increasing the BC content for composite fibres can be a consequence of the different crystallization rates for different PCL chains.

3.4.4 DSC of PCL nanocomposites

The addition of relatively small amounts of nano-sized fillers in PCL can lead to dramatically improved mechanical properties and heat distortion temperatures. Several synthetic

and mineral nano-fillers (Pantoustier et al., 2002; Chen and Evans, 2006) have already been studied as reinforcement for PCL, but an increasing interest is rising in bio-nanocomposites in which bio-sourced nano-scaled fillers are used as reinforcement (Berglund and Peijs, 2010; Eichhorn et al., 2010; Bordes et al., 2009). It can be observed in Figure 3.28 that there is a decrease in PCL crystallinity as the content of BC increases in the nanocomposites.

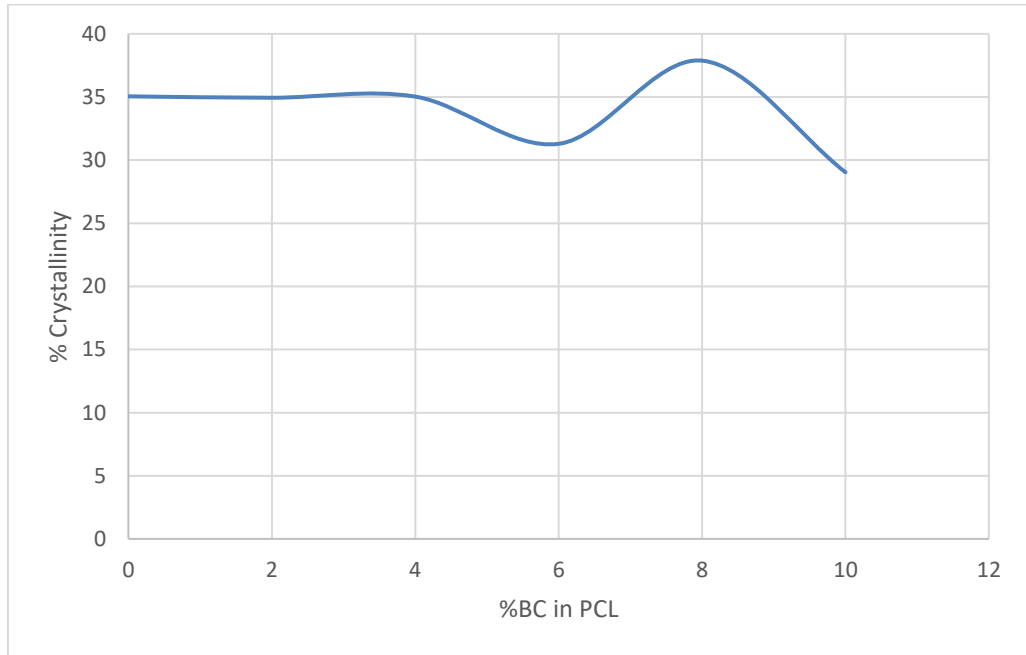


Figure 3.28. *The effect of BC content on the crystallinity of PCL.*

In Figure 3.28 pure PCL shows a crystallinity of 35.05% during heating in the DSC. However, increasing the BC content, the crystallinity decreases. These results are in agreement with the results found by Wu et al., (2005). The decrease in the degree of crystallinity could be due to the fact that BC might slow the crystallisation kinetics of PCL.

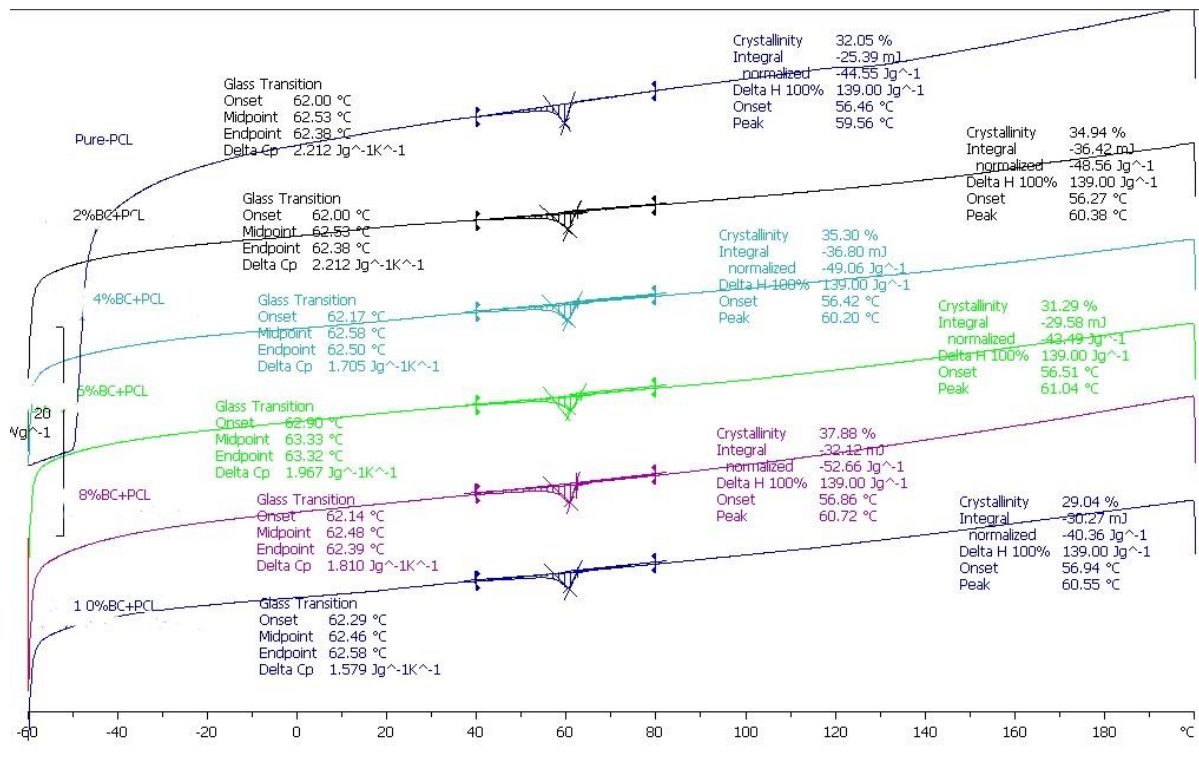
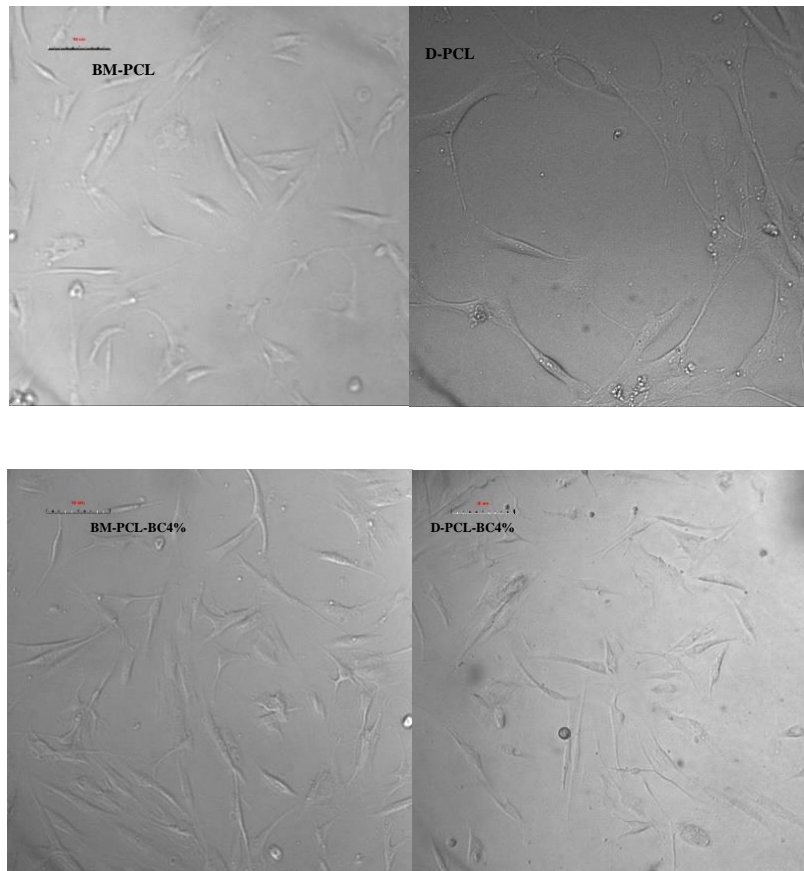


Figure 3.29: DSC curves for PCL and PCL-BC electrospun composites.

Due to the presence of intermolecular hydrogen bonds between the carbonyl groups of PCL and hydrogen donating groups of BC, hydroxyl, amide and amine groups are formed. With increasing concentration of BC, the intermolecular hydrogen bonds might become strong enough to prevent the crystallisation of the polymer. The hydrogen bonding interaction leads to the formation of a miscible phase between the PCL and BC, resulting in the suppression of PCL crystallisation. Another factor other than hydrogen bonding, which lowers the degree of crystallinity of PCL, is the difference in the molecular mobility between PCL and BC (Yang et al, 2003 and Senda et al, 2002).

3.4.5 MTT Assay & Phase-contrast Imaging

Cell culture experiments with human bone marrow and dermal fibroblast cells were carried out in order to assess the biocompatibility of the electrospun nanocomposites and to evaluate the ability and extent to which the cells are able to attach to the materials surfaces and remain viable. MTT was carried out after 24 and 48 hours of culture to evaluate viable cell numbers. MTT assay data and microscopic observations of the cells seeded on the samples, confirmed that the PCL and PCL-BC composites did appear to support the growth and spreading of human fibroblasts (Dermal cells and bone marrow cells). Phase contrast images of cell proliferations at 24 hours and 48 hours after seeding of human dermal and bone marrow fibroblast cells on the PCL and PCL-BC scaffolds are shown in Figure 3.30 and 3.31, respectively.



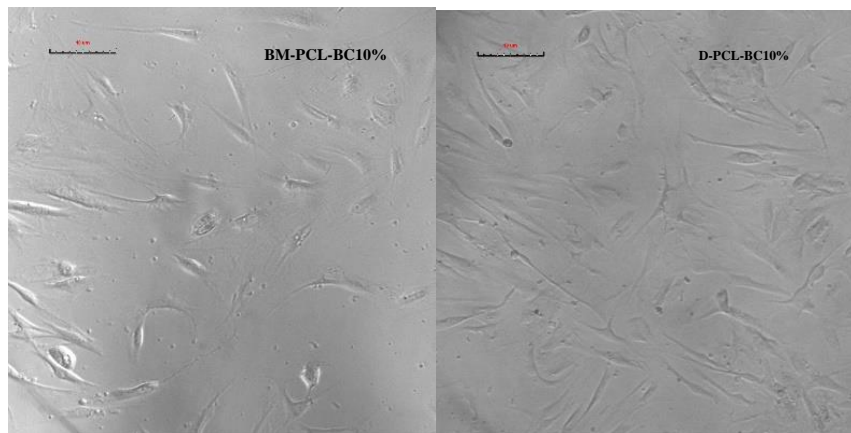
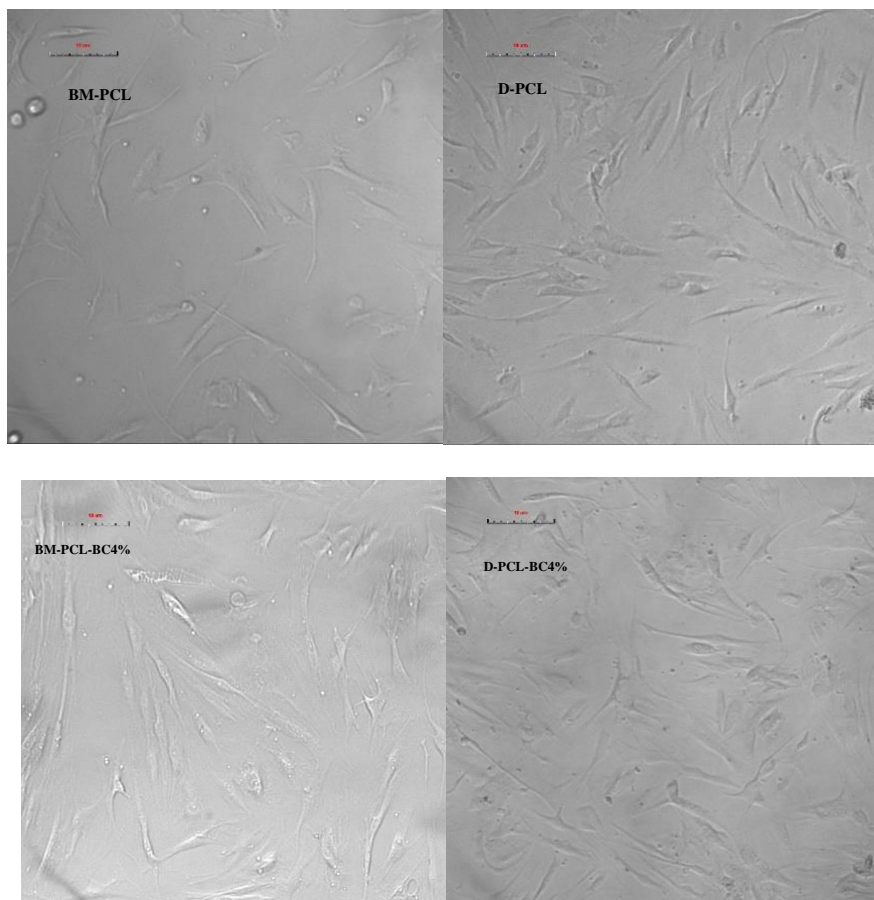


Figure 3.30: Phase contrast imaging of Bone marrow and Dermal fibroblast cells after 24 hours (scale bars represent 10 μ m).



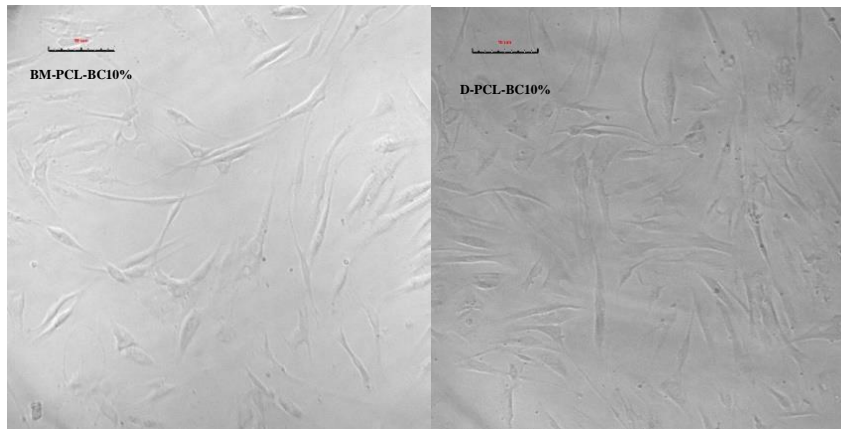


Figure 3.31: Phase contrast images of Dermal and bone marrow cells after 48 hours (scale bars represent 10 μ m).

Dermal and bone marrow cells show a higher or more successful proliferation on all the samples when compared with the culture plastic (control). This is in agreement with a study by Svensson et al., where the proliferation tests of bovine chondrocytes showed that the percentage of relative cell viability on BC scaffolds were greater than those on tissue culture plastic and calcium alginate (Svensson et al., 2005).

The distribution of dermal cells seemed to be denser than the bone marrow cells (figures 3.30 and 3.31) and all the cells had a flat appearance with clear extended processes attached to the surface of the PCL-BC composites. This indicated healthy cells with a good adherence to the material. If the cells achieve confluence it is a good indicator that they are proliferating and remaining viable. MTT analysis also shows that there is an obvious difference in the high percentage of dermal cell viability in all the samples in comparison to the bone marrow cells (Figure 3.17 and 3.20).

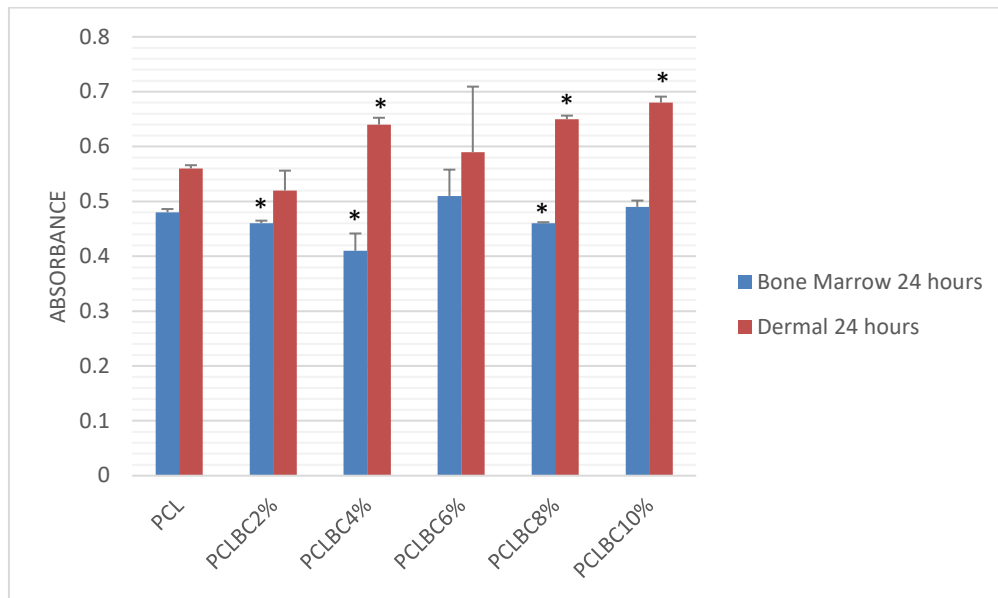


Figure 3.32: MTT results of the viability of human dermal fibroblasts and bone marrow fibroblasts after 24 hours. Absorbance readings at 540 nm. * $p < 0.05$ compared with the control.

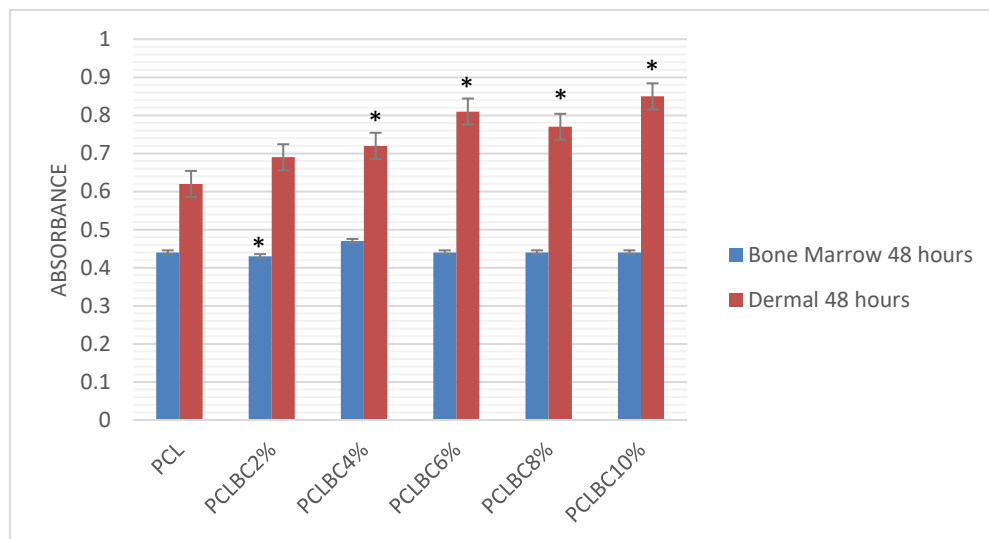


Figure 3.33: MTT results of the viability of human dermal fibroblasts and bone marrow fibroblasts after 48 hours. Absorbance readings at 540 nm. * $p < 0.05$ compared with the control.

Longer cell culture times could allow the cells to synthesise and release some kinds of extracellular matrix (ECM), which could promote cell proliferation and migration on the surface of the scaffolds (Sun et al., 2014). Comparing the images in Figure 3.30 and Figure 3.31 it can be observed that there is an increase in cell proliferation after 48 hours of cell culture in the PCL-BC composites with increasing BC content.

Other studies have confirmed that different cells such as human embryonic kidney cells (Grande et al., 2009), human smooth muscle cells (Petersen et al., 2011), bone forming osteoblasts and fibroblasts (Chen et al., 2009), can grow in the presence of bacterial cellulose scaffolds. Therefore, suggesting that bacterial cellulose has great potential as a scaffold for tissue engineering purposes.

The outcome of this study further reiterates the importance of continued research into BC and BC related materials as potential tissue engineering scaffolds. The microscopic analysis after 24 and 48 hours of cell seeding, showed that cells were as adherent and confluent on the PCL-BC as on the control substrate, which is known to have successful fibroblast adherence.

3.4.6 PCL-BC composites

In order to 3D print, homogeneous filaments were required with a diameter of 1.75mm. A large twin extruder and filament machine were used at the University of Warwick (Prof. Tony McNally, Nanocomposite Research Group at WMG), where numerous problems were faced due to the size and processing of the machine. The correct dimensions of the filaments were not easily achieved for the FDM. A smaller filament diameter (1.75mm) gives better flexibility with 3D printing flow rates as it has a higher surface to volume ratio, which also allows faster melting in

the nozzle. The reason the filaments were required to be made and not bought from suppliers was in order to maintain the consistency of the experimental PCL used in this study. The attempts to produce the correct filament diameter were not successful as it was a large industrial sized machine. This was time consuming and further led to the unsuccessful use of the FDM. There were attempts made to trial any small amounts of filament which measured close enough to the required diameter for the FDM. However, this was also not successful. Figure 3.34 shows the structure that was aimed to be replicated for the 3D scaffolds.

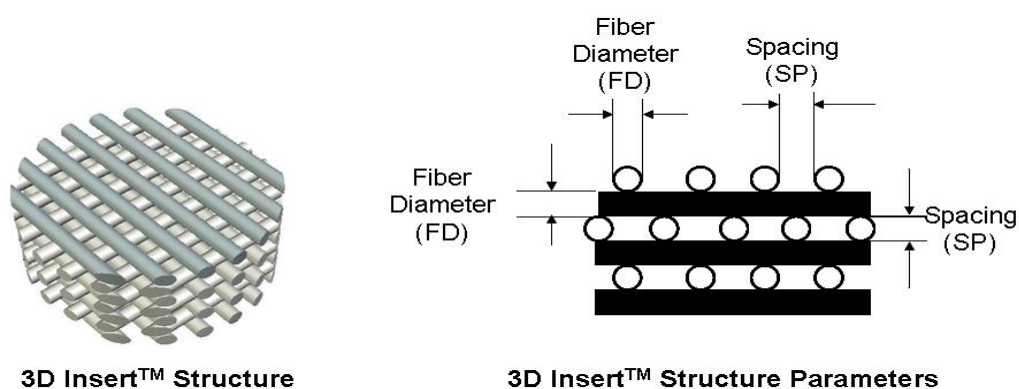


Figure 3.34: Structure that was aimed to be replicated for 3D printing PCL-BC scaffolds (http://www.3dbiotekstore.com/index.php?main_page=index&cPath=10).

PCL and bacterial cellulose composites were extruded and then injection moulded, to produce samples for mechanical testing. Tensile testing and TGA were performed on the composite samples. The samples tested were Pure PCL, PCL-2% BC, PCL-4% BC, PCL-6% BC, PCL-8% BC and PCL-10% BC (% wt).

3.4.7 Tensile testing PCL-BC composites

Bacterial cellulose and PCL composites were prepared for tensile testing by extrusion and injection moulding. All samples were repeated 5 times and the gauge length and thickness were individually measured. The effect of bacterial cellulose on the mechanical properties of PCL is shown in the figures below. From Figure 3.35 and 3.36, it can be observed that there is a decrease in the ultimate tensile strength with increasing the BC content, whereas the yield strength does not show much change. This may be due to the mixing process that did not allow even distribution of BC in PCL. A combination however of PCL and bacterial cellulose gives an advantage as far as biocompatibility is concerned (Torres et al., 2012; Limongi et al., 2015).

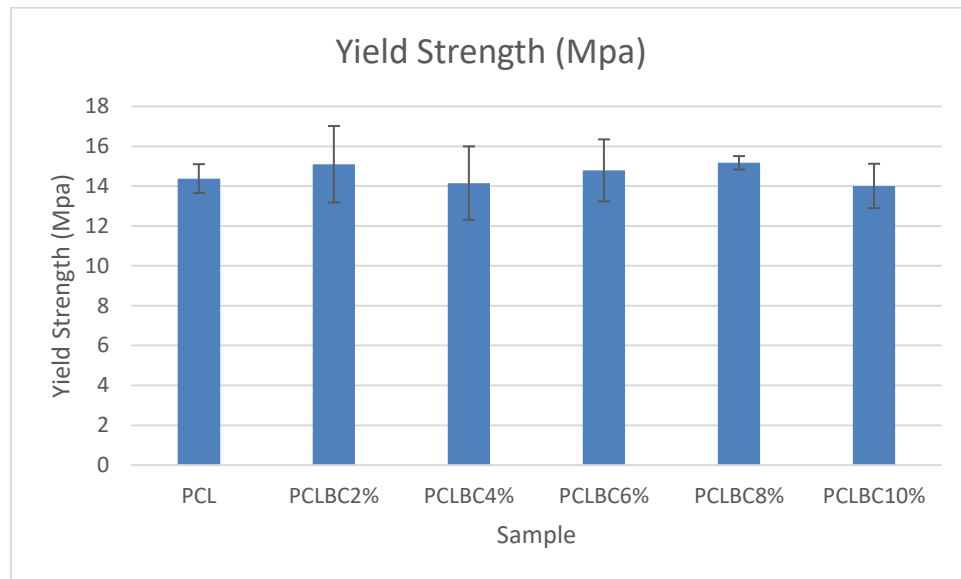


Figure 3.35: Yield strength of PCL and PCL-BC composites.

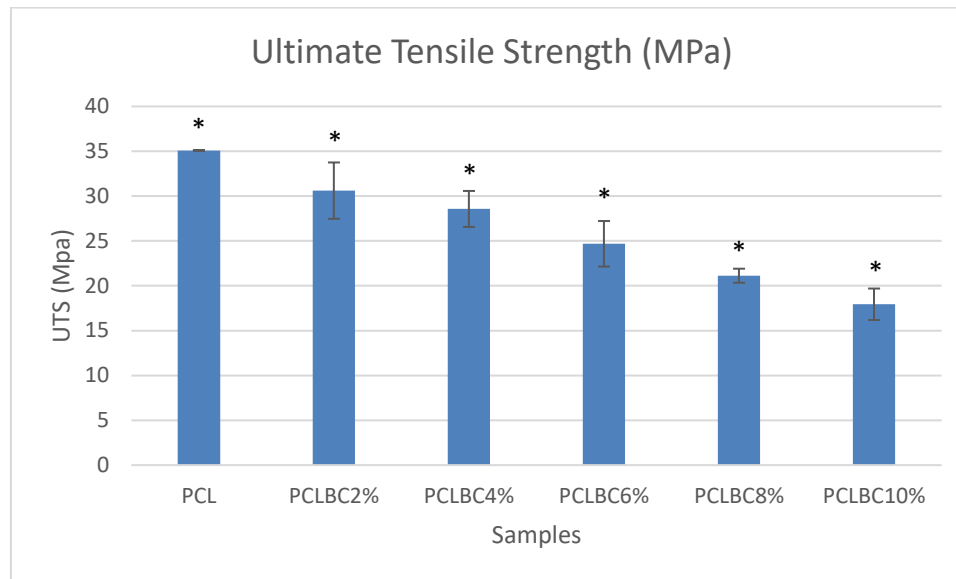


Figure 3.36: Ultimate tensile strength of PCL and PCL-BC composites. * $p < 0.05$ compared with the control.

There is a general decrease in the ultimate tensile strength which may be due to the intermolecular Interactions in the composites. There is a significant difference in the decrease in ultimate tensile test values for all the samples (which are shown in the appendix) showing statistical analysis of t-test values $p < 0.05$. Chiaoprakobkij et al., studied BC-Alginate composites and tested mechanical properties, reporting that bacterial cellulose composites show a decrease in their mechanical properties (Kanjanamosit et al., 2010; Phisalaphong et al., 2008; Wu et al., 2004). This suggests that the hydrogen bonding of cellulose may be disrupted or broken down to form cellulose-alginate hydrogen bonds. These intermolecular hydrogen bonds can reduce the crystallinity and mechanical strength of the composite material (Chiaoprakobkij et al., 2011). Gea et al., investigated bacterial cellulose and PCL composites with bacterial cellulose content as high as 50 vol%. They observed an improvement in the mechanical properties of PCL.

A higher tensile strength and strain at break were observed but the Young's modulus wasn't reported to have much change (Gea et al., 2010).

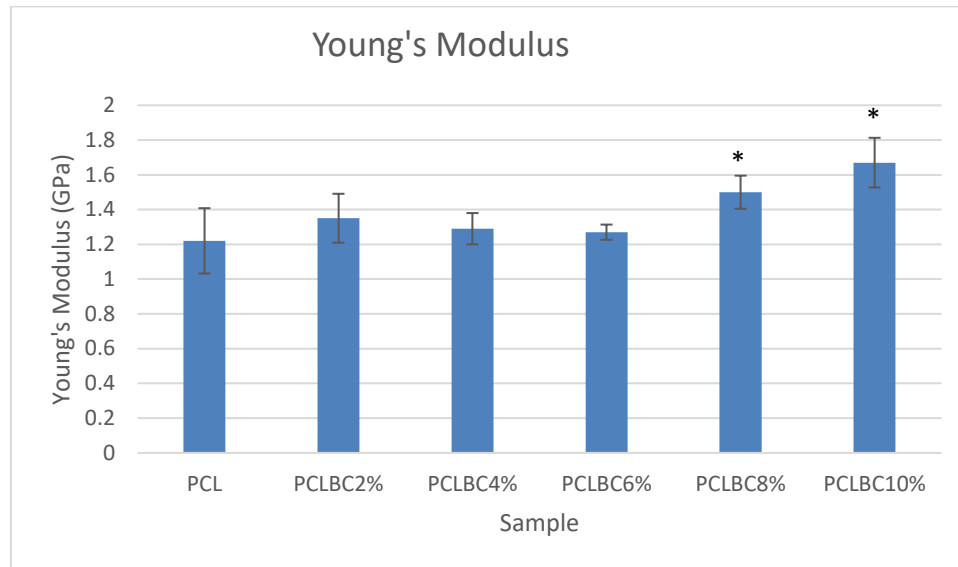


Figure 3.37: Youngs Modulus of PCL and PCL-BC composites. * $p < 0.05$ compared with the control.

Figure 3.37 shows that Young's modulus increases with higher bacterial cellulose content in the composites. There was a significant difference (t-test statistical analysis values are also shown in appendix) in Young's modulus, comparing composites with higher BC content with the lower bacterial cellulose content. PCL-BC composites were prepared by extrusion and injection moulding for mechanical testing. Tensile testing was carried out to observe the effect of bacterial cellulose on the mechanical properties of PCL. The samples showed a decrease in the ultimate tensile strength with increasing BC content. The yield strength did not show much change. This could be due to the nucleation effect of BC and the mixing process, which may not have allowed even distribution of the BC in PCL. The bacterial cellulose content may not be enough for the strengthening effect of PCL, which could be the reason for the mechanical properties. Fu et al.,

studied the effect of particle size, particle/matrix adhesion and particle loading on the composite stiffness, strength and toughness range of particulate composites containing micro and nano-fillers with small aspect ratios (Fu et al., 2008). It was reported that there is a critical particle size (usually nano size), below which the composite stiffness is greatly enhanced due to the significant effect of the particle size, probably caused by the much larger surface areas (Fu et al., 2008).

Table 3.14: Tensile test results for PCL and PCL-BC composites

Sample	Yield Strength (Mpa)	UTS (MPa)	Youngs Modulus (GPa)
PCL	14.38	35.09	1.22
PCLBC2%	15.1	30.61	1.35
PCLBC4%	14.15	28.57	1.29
PCLBC6%	14.79	24.68	1.27
PCLBC8%	15.17	21.12	1.5
PCLBC10%	14.01	17.94	1.67

3.4.8 Thermogravimetric analysis PCL-BC composites

Thermal degradation of PCL and PCL-bacterial cellulose composites was investigated by thermogravimetric analysis under argon flow. The curves of mass loss at a heating rate of 20°C.min⁻¹ are shown below in Figure 3.38.

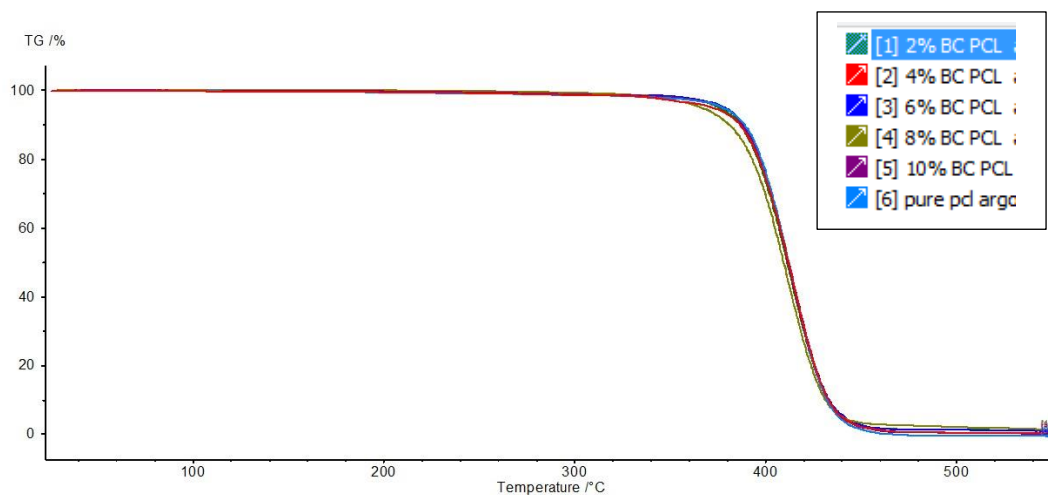


Figure 3.38: TGA curve for PCL and PCL-BC composites.

Figure 3.38 indicates that there is not much difference in the degradation pattern for the composites in comparison to Pure PCL. Thermal degradation behaviour is influenced by factors such as molecular weight, crystallinity and orientation of chains (George et al., 2005). From the thermogravimetric curves it can be seen that bacterial cellulose is less thermally stable than PCL, with a main degradation present at about 375°C. The curves do not show much improvement in the thermostability as the bacterial cellulose content is increased. In section 3.4.4 (Figure 3.28) it can be observed that the increase in BC content in the composite has an effect on the crystallinity of PCL. The crystallinity on heating shows a general decrease as the content of BC increases in the PCL-BC composites made by electrospinning (Figure 3.27).

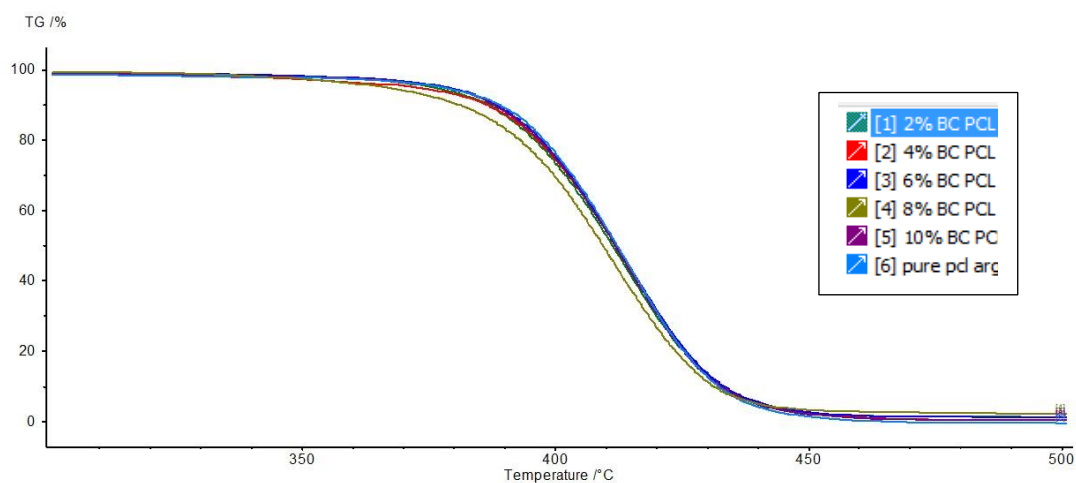


Figure 3.37: TGA curve 300-500°C of PCL and PCL-BC samples.

There is a slight shift in the curve showing 8% BC content in PCL, this seems to decompose earliest. The complete thermal degradation of the samples occurs in the range of 430°C and 550°C, when chemical bonds of polymer chains break.

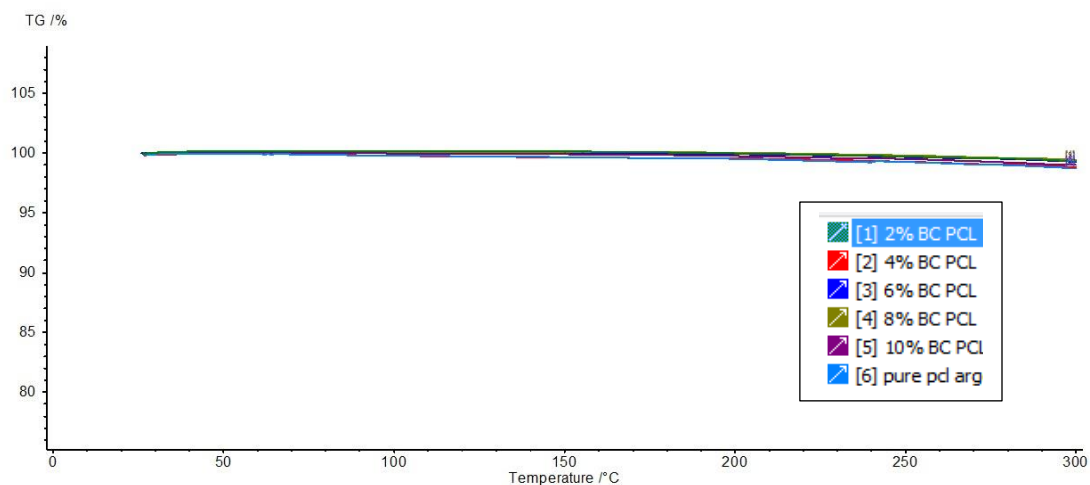


Figure 3.40: TGA 0-300°C curves of PCL and PCL-BC composites.

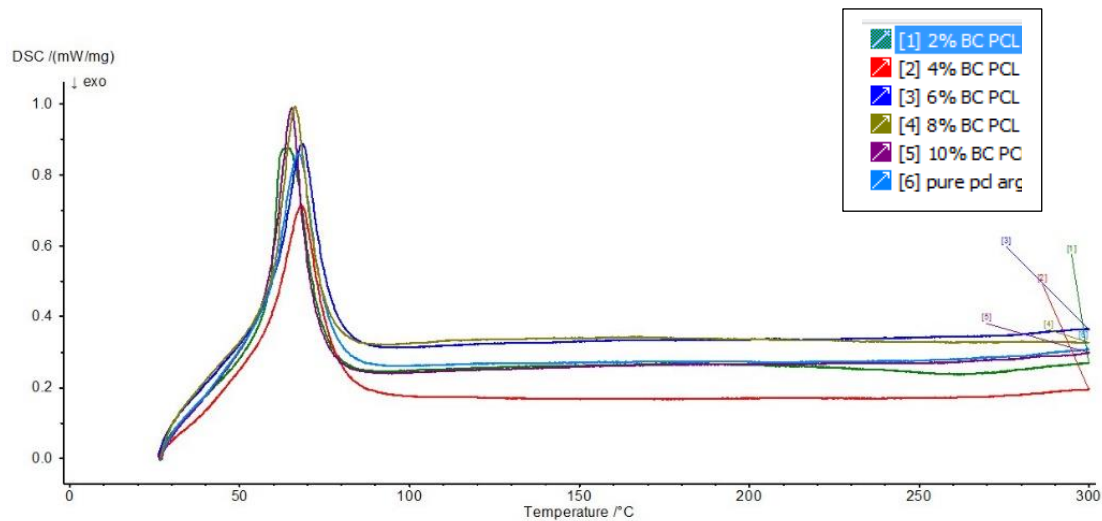


Figure 3.41: Melting point curves of PCL and PCL-BC composites.

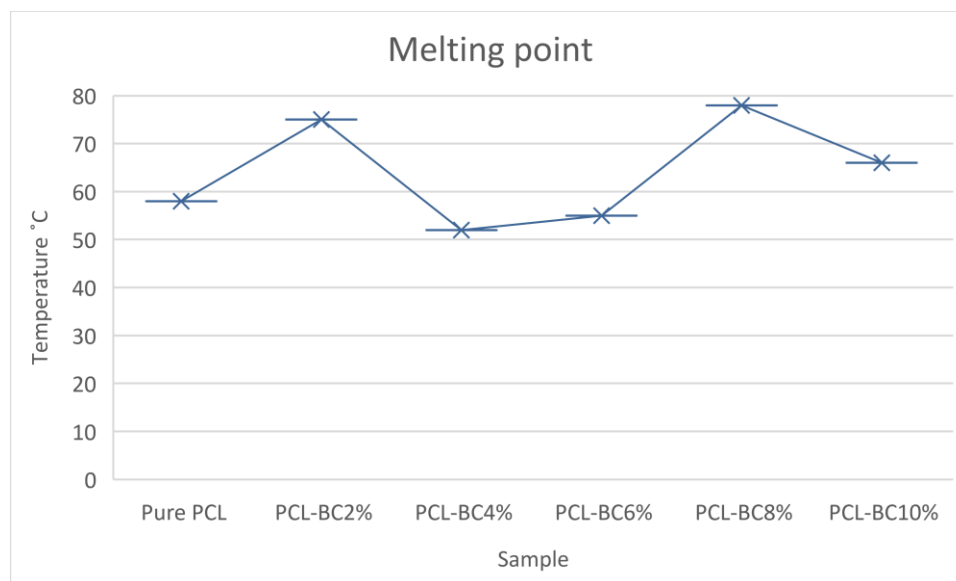


Figure 3.42: Melting points for PCL and PCL-BC composites.

The melting temperature shows a general increase with increased bacterial cellulose content, with the exception of PCL-BC4% and PCL-BC6%, which show a lower melting point than PCL. It has been previously reported that melting temperature shows an increase with

cellulose incorporation with PCL, due to the formation of crystals and the crystallinity index of the corresponding nanocomposite (John et al., 2002).

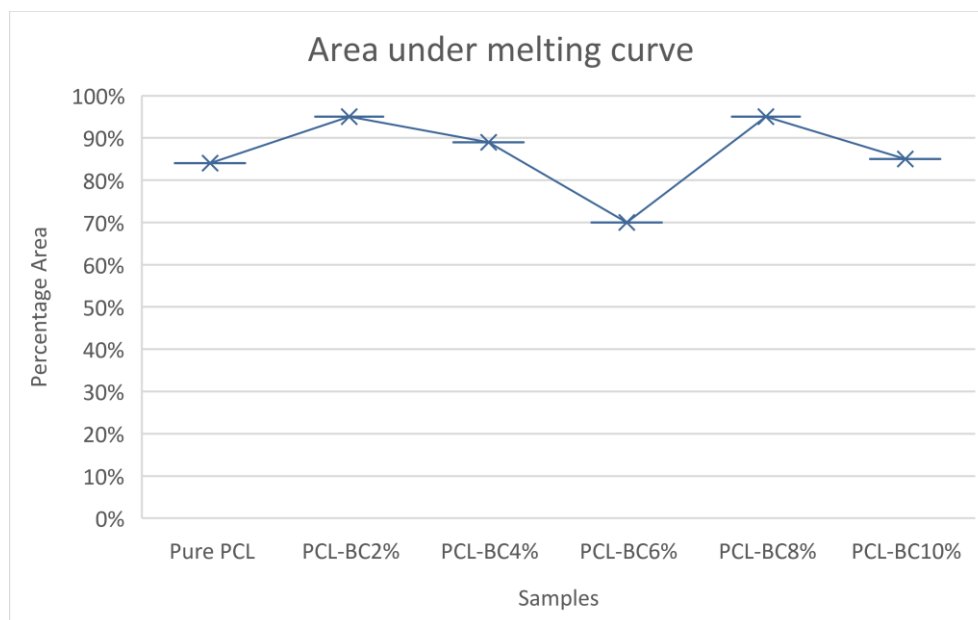


Figure 3.43: Area under the melting curve.

Area under the curve increases with increasing bacterial cellulose content in the PCL-BC composites, which could indicate that the degree of crystallinity increases.

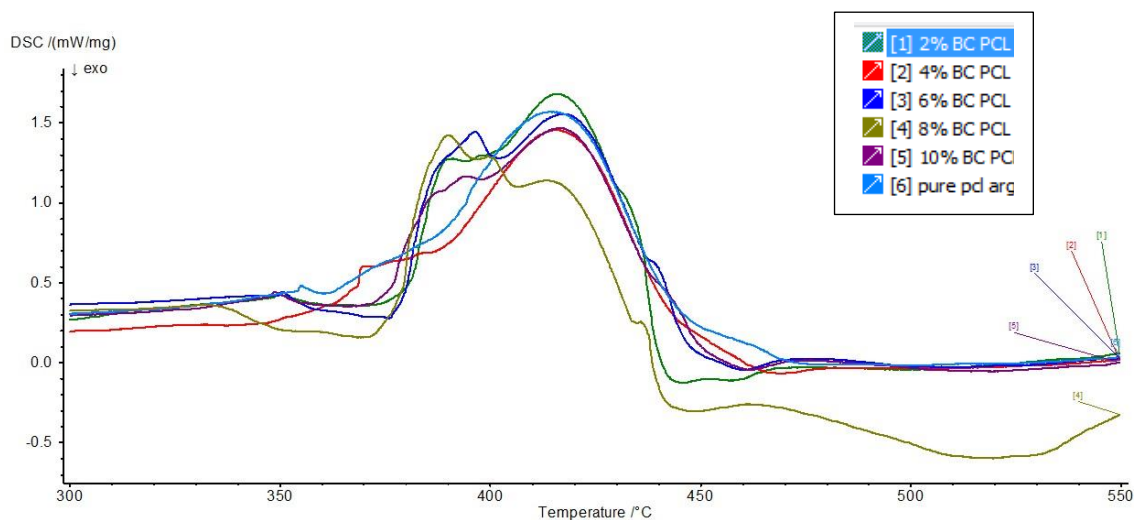


Figure 3.44: DSC curves showing decomposition of PCL and PCL-BC composites.

PCL has mainly one peak in the region of 300°C-550°C whereas the composites show a number of peaks and shoulders. This may be because bacterial cellulose degrades earlier than PCL, which can also be noted in Figure 3.44 above that the composite peaks all show earlier degradation in comparison to the PCL sample.

The variations in the results are most likely caused by the poor dispersion of bacterial cellulose in the PCL, however this may not be the only factor contributing to the results. It should be taken into consideration that the samples were processed through extrusion and injection moulding, which can contribute to the possible decrease in the properties and ageing of the polymer. This cause the various peaks and shoulders in the decomposition region between 300°C and 550°C.

GENERAL DISCUSSION

Successful biosynthesis of bacterial cellulose was achieved, and the purification process was assessed in order to observe any changes in the internal structure and properties. From Figure 3.15 and Table 3.4, it is clear that the mechanical properties increased significantly after the purification. The FTIR spectra did not suggest cellulose II formation, therefore indicating that the structure of bacterial cellulose did not change from cellulose I to cellulose II after the purification process. When bacterial cellulose was treated with 2.5 wt.% NaOH, impurities were released from the surface of the pellicle. The absence of these impurities resulted in increased hydrogen bonding between the bacterial cellulose fibrils. Gea et al., reported an increase in Young's Modulus when comparing unpurified bacterial cellulose and purified bacterial cellulose (Gea et al., 2011).

Studies have shown that using a higher concentration of NaOH with concentrations of 6 wt.% and over can cause changes in the crystal structure of bacterial leading to transformation from cellulose I to cellulose II (Dinand et al., 2002, Gomes et al., 2007, Manisikkamaki et al., 2005, Oh et al., 2005, Shibazaki et al., 1997). Changes at the molecular level also accompany structural changes in bacterial cellulose. Therefore, the changes in the structure from cellulose I to cellulose II involved breaking of inter and intramolecular hydrogen bonds that are present in cellulose (Laszkiewicz, 1997, Gea et al., 2011). Bacterial cellulose was further treated with higher concentrations of NaOH (5, 7 and 9 wt.%) to study changes in the mechanical and structural properties. Each treatment with a higher concentration of NaOH resulted in a slight increase of the crystallinity of bacterial cellulose which was expected as bacterial cellulose is already a highly crystalline material. Conversion of cellulose I to cellulose II was clearly

observed by FTIR (Figure 3.4 and 3.5) and TCI (Table 3.1) studies that showed clearly transformation from the one type of crystal structure to the other. The absorbance ratio of the bands at 1430 and 900 cm^{-1} was used to follow any transformation in crystalline lattice structure from cellulose I to cellulose II. The values for this ratio A_{1430}/A_{900} are listed in Table 3.2 and were used to evaluate crystallinity and effect of time of treatment and concentration of NaOH solution on bacterial cellulose. The proportion of cellulose I decreased with increasing the concentration of NaOH treatment solution (Figure 3.8 and 3.9). The formation of cellulose II from cellulose I was also evidenced by the thermal decomposition temperature (Table 3.5) that increased in the case of treated cellulose compared with the untreated cellulose suggesting an increase in crystallinity and increase in the proportion of cellulose II. The thermal degradation behaviour is influenced by factors such as crystallinity and orientation of chains as reported by George et al. (George et al., 2005). Cellulose II is the most thermodynamically stable allomorph of cellulose (Brown, 1999), which is in agreement with the results showing an increase in thermal stability with alkali treatment.

The SEM micrographs (Figure 3.15) showed that the modified bacterial cellulose consisted of micro- and nano-fibres, which formed a three-dimensional network. Comparing the cryo-SEM images of the treated bacterial cellulose samples shown in Figure 3.15, it can be concluded that samples treated with lower concentration of NaOH showed a denser network compared to the samples treated with higher concentrations of NaOH. Haigler et al. proposed that *Gluconacetobacter xylinus* extrudes cellulose in the form of nanofibrils (Haigler et al., 1980). This is in good agreement with the Cryo-SEM images in Figure 3.15. Bacterial cellulose has a natural porous arrangement of fibres which acts as a matrix for framing particles from a variety of different reinforcement materials (Esa et al., 2014). Santos et al. observed an increase in the

porosity of bacterial cellulose structure after alkali treatment with NaOH which is in agreement with previous studies suggesting that the purification helps to release space which is usually occupied by microorganisms/impurities (Nishi et al., 1990, Gea et al., 2011, Santos et al., 2015). This can lead to the conclusion that the purification conditions for harvesting bacterial cellulose membranes can also affect the porosity of the final product.

According to Vincent and Engler, the biocompatibility of a material can be determined by its physical properties, such as; porosity, surface morphology, fibre structure and elasticity (Vincent and Engler, 2011). In vivo and in vitro studies on bacterial cellulose have shown successful cell viability and cell proliferation. However, this depends on the physical and chemical characteristics of bacterial cellulose, such as fibre morphology (Helenius et al., 2006), pore size distribution (Zaborowska et al., 2001) and the presence of reactive sites introduced through chemical modifications (Pertile et al., 2010). Hue et al., studied the growth of human osteoblast cells on bacterial cellulose and showed that the osteoblast cells were able to attach and spread well on the larger bacterial cellulose particles (Hue et al., 2013). Other studies have confirmed that different cells such as human embryonic kidney cells (Grande et al., 2009), human smooth muscle cells (Petersen et al., 2011), bone-forming osteoblasts and fibroblasts (Chen et al., 2009), can grow in the presence of bacterial cellulose scaffolds suggesting that bacterial cellulose has great potential as a scaffold for tissue engineering purposes. The results presented in Figures 3.17 and 3.18 are in agreement with these studies, as human cells were successfully grown, and cells were still viable after ten days of culture. The results were very similar in both cell types apart from the significantly higher survival rate of the bone marrow cells on sample H. The dermal cells showed slightly higher viability in general for the control cultures. It can be concluded, that while the samples treated with lower concentrations of NaOH were beneficial for

the survival of dermal cells, higher NaOH concentrations promoted higher viability for bone marrow cells. There was a significant difference (t-test statistical analysis values are shown in Appendix) between the viability of bone marrow cells on days 6 and 10 for the samples treated with higher NaOH concentration. This could be attributed to the formation of more attachment sites due to the treatment that created more lamellar-like structures on the surface as well as exposed looser fibres in between parallel layers of compact fibres. Previous studies have demonstrated that 2D and 3D micro/nanofibrous scaffolds can improve cell attachment and spread significantly due to surface topography and an enlarged inner surface of the structure (Kim et al., 2010; Park et al., 2008). In addition, Innala et al. and Jonsson et al. reported that chemical modifications (e.g., phosphorylation, acetylation, mercerisation) and protein coating of cellulose materials can improve significantly the cell-scaffold interactions (Innala et al., 2014, Jonsson et al., 2015). Svensson et al. reported that chemical sulphation and phosphorylation of bacterial cellulose can add a surface charge to the surface of bacterial cellulose and mimic the glycosaminoglycans of the *in vivo* cartilage tissue. This however, did not enhance chondrocyte growth (Svensson et al., 2005).

The approach of composite formation usually occurs through reinforcement of nanoparticles or liquid into the BC structure (Sulaeva et al., 2015. Hu et al., 2014). Physico-chemical interactions of these substances with the BC interfibrillar network are the main mechanisms of composite formation (Hu et al., 2014). Polycaprolactone - Bacterial cellulose composites (PCL-BC) produced in this project by electrospinning and by injection moulding showed that even a slight amount of filler in PCL can lead to changes in the mechanical properties. The mechanical characteristics of bacterial cellulose can complement and also

enhance the biological properties of the components and also extend their potential to be used in biomedical applications (Hu et al., 2014). Electrospinning composites have been favoured due to being able to produce fibres which can mimic the extracellular matrix and therefore aid wound healing (Mogosanu and Grumezescu, 2014). Electrospun PCL-BC samples were produced and Figure 3.26 (a-e) shows that the diameter range of fibres was about 100-200 μ m. A broader size distribution was observed with increasing BC content, which suggested that the parameters were not fully optimised. Figure 3.28 showed that there was a decrease in PCL crystallinity as the content of bacterial cellulose increased in the electrospun composite. Bacterial cellulose has a hydrophilic nature, which can lead to the conclusion that the decrease in the degree of crystallinity may be due to the bacterial cellulose slowing down PCL crystallisation kinetics (Wu et al., 2005). Bone marrow and dermal cells both showed a higher and successful cell proliferation on all samples when compared with the control. This may be due to the increased roughness as the BC content increases (Table 3.9).

A combination of PCL and bacterial cellulose fibres gives an advantage as far as biocompatibility is concerned (Torres et al., 2012; Limongi et al., 2015). It was noted, that bacterial cellulose was less thermally stable than PCL, and there was not much improvement seen in the thermal stability with increasing bacterial cellulose content, as shown in Figure 3.37 and 3.38, respectively. There was a significant decrease in the ultimate tensile strength values for all samples with increasing BC concentration from 2-10% as shown in Table 3.10. This was likely attributed to the mixing process (extrusion followed by injection moulding) that resulted in uneven distribution of bacterial cellulose in PCL. Gea et al., produced PCL composites with higher BC loading (up to 50 wt. %) and reported improved mechanical properties of PCL-BC composites (Gea et al., 2010). Therefore, this can suggest that the loading of bacterial cellulose

in this study may not have been enough to provide a good strengthening effect in the composite. On the other hand, the Young's modulus increased (Figure 3.35) with increasing bacterial cellulose content. This may have been due to the nucleation effect in the PCL matrix provided by the fine particles of bacterial cellulose (Gea et al., 2010). Fu et al., reported that composite strength increased with decreasing particle size for a given particulate volume fraction because smaller particles have a higher total surface area for a given particle loading, indicating that strength increases with increasing surface area of the particles (Fu et al., 2008). However, Fu et al., also noted that larger particles (larger than 80 nm), reduced composite strength with increasing particle size (Fu et al., 2008). It can be related to this study where the ultimate tensile strength decreased with increasing BC content, as suggested earlier this can be due to the mixing process, which caused uneven particle distribution.

There have been many approaches to influence the structure of bacterial cellulose to improve its biocompatibility towards desired cell lines. Improving the biocompatibility can define the primary direction of bacterial cellulose as a scaffold for tissue engineering, a wound dressing material or as a substitute for damaged cartilage, skin or blood vessels (Sulaeva et al, 2015). Observing the growth of dermal and bone marrow cells (Figure 3.17 and 3.20) on mercerised bacterial cellulose has shown that bone marrow cells grow better on BC treated with higher concentrations of NaOH. This may be due to the changes in the surface morphology of the bacterial cellulose, therefore allowing better cell adhesion.

Overall, bacterial cellulose structure can provide ideal features for potential as a tissue engineering scaffold. There has been sufficient evidence in this study to suggest that BC has great potential as a tissue engineering scaffold. Studies have reported many applications of bacterial cellulose for medical uses, such as; a nano composite using BC and Poly (vinyl alcohol) for soft

tissue replacement applications (Wan and Millon, 2005), BC complexes with many different materials, for example, nano-silver (Wang et al., 2011a, Wang et al., 2011b), collagen (Zheng et al., 2012). As well as soft tissue repair, BC can also be used for hard tissue repair and for tissue engineering scaffolds. Composites based on BC, collagen and hydroxyapatite have been used for applications in bone and connective tissue repair (Saska et al., 2011b). Despite the substantial progress in the field of tissue engineering, there still aren't any materials which can completely capture the intricate nature of the native tissue or restore function to an ideal level. Therefore, the challenges remain, to invent new composite materials with nanoscale engineering to make fully biomimetic tissues. Advances in the use of bacterial cellulose in the medical field are ongoing and the characteristics of bacterial cellulose can be improved to meet the demands of required applications (Haung et al., 2014). Current advances include development of drug delivery systems (Saska et al., 2011b), wound dressings (Yang et al., 2011, Cai et al., 2011), artificial skin (Lin et al., 2011) and preparation of implants and grafts, such as vascular (Fink et al., 2010, Esguerra et al., 2010) and bone repair (Wang et al., 2010). Many companies have introduced commercial bacterial cellulose products, especially in wound healing.

CHAPTER 4

Conclusions

By culturing *Gluconacetobacter xylinus* into the medium containing glucose as a main source of food of the bacteria, BC pellicles were successfully produced by a static culture method.

A two-step purification process is required to produce purified bacterial cellulose (BC) samples as demonstrated by SEM images, TGA and FTIR. This resulted in improved mechanical and thermal performance of native BC. A purification treatment with a 2.5 wt. % NaOH followed by 2.5 wt. % NaOCl, did not affect the structure of cellulose I as native cellulose as indicated by the FTIR studies. Further treatment with higher concentrations of NaOH and for longer time periods, resulted in an obvious conversion of cellulose I to cellulose II as shown by the FTIR studies. The amount of cellulose II increased with increasing concentrations of NaOH and increasing duration of the treatment period, as expected during mercerisation. However, cellulose I remained the predominant structure in all of the scaffolds.

The change in the crystallinity of scaffolds treated with sodium hydroxide was very small. The suggested reason is that the bacterial cellulose in its native form is a highly crystalline cellulose I, and alkali treatment can partially change the structure from one crystalline form to another (cellulose II), without involving transformation of amorphous phase to the crystalline phase and therefore, a very slight increase in crystallinity was observed.

The Young's modulus of NaOH-treated BC sheets increased by a factor of two compared to the untreated BC sheets. This was because there was no disruption of the intermolecular and intramolecular hydrogen bonding between and within the fibres in the H-bonded network. As

expected, a further increase in tensile strength was observed for the two-step treated BC sheets, since the polymorphic transformation from cellulose I to other less performing cellulose types was prevented, while at the same time a stronger network was created. Some change of orientation of the BC ribbons was revealed as indicated by a difference in the intensity of the peaks of the diffractograms, as shown by XRD data.

The onset of decomposition temperature and the maximum decomposition temperature of bacterial cellulose increased significantly with treatment. This confirmed the conversion of cellulose I to II, as cellulose II is the most thermally stable form of cellulose.

Cryo-SEM images showed a two phase lamellae-like structure of compact layers of fibres with some entangled fibres between them. The treatment affected the entangled fibres first and, therefore, it is possible to designate this phase as the amorphous phase and the layers as the crystalline phase. Samples treated with lower concentrations of NaOH, showed a higher density of fibre networks, while this network appeared to collapse for samples treated with higher concentrations of NaOH, where more loose-end fibres were observed.

Cell culture studies using NaOH treated BC showed that the viability of the cells was dependent on a combination of surface charges and the morphology of the BC pellicle. Surface charges are necessary for the attachment of cells but if too strong, they prevent proliferation. The cell study showed that a dense network of fibres enhanced cell attachment, while a more porous one improved cell proliferation.

Dermal cells attached and proliferated on both treated and untreated samples, with higher viability on most of the treated ones. The scaffold treated with 5 w/v% NaOH for 5 hours and with 7 w/v% NaOH for 5 hours showed the highest viability on day 6 and day 10, respectively and therefore the above treatments are the optimum for cultivation of dermal fibroblasts.

Bone marrow cells showed the highest viability on the scaffold treated with 7 w/v% NaOH for 5 hours after 6 days of cultivation and on the scaffold treated with 9 w/v% NaOH for 10 hours after 10 days. The latter was even higher than the tissue culture plastic, hence proposed as the optimum alkali-treatment for cultivation of bone marrow fibroblasts.

Bacterial cellulose whiskers were extracted by acid hydrolysis. The hydrolysis time was varied to study the effect of acid on the length of the whiskers. This showed that the length of bacterial cellulose whiskers decreased with increased hydrolysis time. TEM analysis of the whisker suspension was analysed at varied time (2, 4, 6, 8, 12 and 24 hours) intervals to observe the changes in whisker length.

Electrospinning was used to prepare PCL-BC composite nanofibres. SEM images of the fibres showed that the electrospun fibres produced had randomly distributed tangled fibres with a broad diameter range. There was a slight difference in the fibres produced using PCL compared with PCL-BC composites. An increased fibre diameter was observed as the bacterial cellulose content increased, leading to a broader size distribution. This indicated that the electrospinning parameters were not optimised to achieve the best possible scaffold with uniform fibres and even size distribution. White light interferometry was used to observe the surface roughness of the electrospun composites. This showed that surface roughness increased as the content of BC increased in the electrospun composites. This may be due to the changes in fibre diameter and the formation of beading along fibre lengths.

The effect of bacterial cellulose on the crystallinity of PCL was studied by DSC analysis. There was a general decrease in the degree of crystallinity as the BC content increased. With

increasing the concentration of bacterial cellulose, the intermolecular hydrogen bonds might become strong enough to prevent the crystallization of the polymer.

Cell culture experiments with human bone marrow and dermal fibroblast cells were carried out to assess the biocompatibility of the electrospun nanocomposites and to evaluate cell viability and attachment. Phase contrast imaging and MTT assay was carried out to evaluate cell viability after 24 and 48 hours. It was observed that bone marrow and dermal cells both showed successful cell proliferation and the cells were viable. The distribution of dermal cells was seen in the images by phase contrast microscopy to be denser than bone marrow cells. MTT analysis also showed that there was an obvious difference in the high percentage of dermal cell viability in all the samples in comparison to the bone marrow cells. It was also noted that the cell viability was higher for the dermal cells for composites with a higher BC content. The outcome of this study further reiterates the importance of continued research into BC and BC related materials as potential tissue engineering scaffolds.

There was an attempt to produce 3D scaffolds by FDM. The 3D printer required a specific filament diameter (1.75mm). This was not successfully achieved as the extruder used was a large industrial sized machine.

PCL-BC composites were formed by extrusion and injection moulding to form samples for mechanical testing. A decrease in the ultimate tensile strength was observed as the bacterial cellulose content increased, whereas the yield strength did not show much change. The Young's modulus increased with increasing bacterial cellulose content in the composites. However, increasing bacterial cellulose content within the PCL composites did not improve the

thermostability of the samples. Thermal degradation behaviour of the PCL-BC composites was studied. There was not much noticeable difference between the curves. It was noted that BC is less thermally stable than PCL, with a main degradation present at around 375°C. Overall, the curves did not show much improvement in the thermal stability as the bacterial cellulose content increased. There was a slight shift in the curve for PCL-8%BC, showing an early decomposition. The melting points on the DSC curves showed a general increase in melting temperature with an increase in the bacterial cellulose content. However, the variations in the results is most likely caused by the poor dispersion of bacterial cellulose in the PCL. This may not be the only contributing factor, it should be noted that the samples were processed through extrusion and injection moulding, which can contribute to the possible decrease in the properties and decomposition.

CHAPTER 5

Future work

Surface modification of bacterial cellulose study needs some extensive research into mechanical properties by making sheets. The effect of surface modification on surface charge is also an area of interest as this would affect the ability of cells to attach and proliferate. Further cell culture with SEM images to show cell attachment and proliferation is necessary to assess the biocompatibility of modified bacterial cellulose.

Further extensive research is still needed to expand the electrospinning study and produce directional fibres. This is still a challenge for tissue engineering of nanocomposite fibres, therefore a greater focus on the parameters involved with electrospinning is required for the optimisation of electrospun fibres. This would further help determine the range of diameter size that can be produced/achieved and the effect of this on cell adhesion. Further research on the physical and chemical as well as the mechanical properties would be required as well as a more detailed cell culture study. Bacterial cellulose nanocomposites need further development with higher concentrations of bacterial cellulose in PCL to evaluate the effect of particle loading on mechanical properties and the effect of the nano filler aspect ratio and particle size.

The challenge to produce successful 3D printed nanocomposite scaffolds needs to be overcome with varying structures and dimensions for tissue engineering. This needs to be followed up with cell culture and analysis to see the potential of bacterial cellulose nanocomposites as scaffolds. 3D scaffolds are of great interest for the future of biomedical

research and therefore needs more attention. Using bacterial cellulose as the filler, many alternative polymers can be explored and extensively studied to determine the best nanocomposite for particular tissue engineering applications. However, obstacles such as the issue of biocompatibility and material properties may hinder the combination of BC and any other material. This is an area of great interest and can be further investigated to extend the study and possibly look to produce biodegradable scaffolds for tissue engineering.

References

Agarwal, D., Broutman, j., Shekhara, C., (1980). Analysis and performance of fiber composites. 3rd edition, John Wiley and sons.

Arsug, S., Takagi, S., Brown, R. (1993). Native-folded chain cellulose II. Polymer, 34, 3293-3297.

Atala, A., Lanza, R., (2002), Methods of tissue engineering, Gulf professional publishing, Elsevier academic press 1285Rama.

Atalla, R.H., (1996). Production of cellulose II by *Gluconacetobacter xylinum* in the presence of 2,6-dichlorobenzonitrile. International Journal of Biological Macromolecules, 19(2), 145-146.

Atalla, R. H., Vander Hart, D.L., (1989). In: C. Schuerch (Eds). Cellulose and Wood, Chemistry and Technology, Proceedings of the 10th Cellulose Conference. Wiley Interscience, John Wiley & Sons, New York, p.169-188.

Aziz, H., Ansell, P. (2004). The effect of alkalization and fibre alignment on the mechanical and thermal properties of kenaf and hemp bast fibre composites: part 2- cashew nut shell liquid matrix. Composites Science and Technology, 64, 1231-1238.

Azizi Samir, F. Alloin, A. Dufresne (2005) Review of recent research into cellulosic whiskers, their properties and their application in nanocomposite field, Biomacromolecules, 6, pp. 612–626.

Backdahl, H. et al., (2006). Mechanical properties of bacterial cellulose and interactions with smooth muscle cells. Biomaterials, 27(9), 2141-2149.

Badrossamay, R., McIlwee, A., Goss, A., Parker, K. (2010) Nanofiber assembly by rotary jet-spinning. Nano Letters, 10, 2257-2261.

Bae, S., Shoda, M. (2004). Bacterial cellulose production by fed-batch fermentation in molasses medium. *Journal of Bioscience and Bioengineering*, 97 (1), 33-38.

Bajpai, P. (2005) *Environmentally benign approaches for pulp bleaching*. Vol.1, Elsevier, Amsterdam

Bajgai, P., Aryal, S., Bhattarai, R., Bahadur, R., Kim, W., Kim, J. (2008) Poly(caprolactone) grafter dextran biodegradable electrospun matrix: a novel scaffold for tissue engineering. *Journal of Applied Polymer Science*. 108, 1447–1454.

Barud, S., Ara'ujo, J., Santos, B., Rosana, N., Assunc, N., Meireles, S., Cerqueira, A., Filho, R., Cl'ovis, A., Ribeiro, A., Messaddeq, Y., Sidney, L., Ribeiro, L. (2008). Thermal behaviour of cellulose acetate produced from homogeneous acetylation of bacterial cellulose. *Thermochimica Acta*, 471, 61–69.

Becker, A., Katzen, F., Puhler, A., Ielpi, L. (1998). Xanthan gum biosynthesis and application: a biochemical/genetic perspective. *Applied Microbiology and Biotechnology*, 50, 145-152.

Beck-Candanedo, M., Roman, G., (2005) Effect of reaction conditions on the properties and behaviour of wood cellulose nanocrystal suspensions, *Biomacromolecules*, 6, pp. 1048-1054.

Ben-Hayim, G., Ohad, I. (1965). Synthesis of cellulose by *Gluconacetobacter xylinum* VIII. On the formation and orientation of bacterial cellulose fibrils in the presence of acidic polysaccharides. *Journal of Cell Biology*, 25, 191-207.

Berglund, A., Peijs, T. (2010). Cellulose bio-composites from bulk mouldings to nanostructured systems. *MRS Bulletin*, March, 35, 201-207.

Bianco, P., Robey, G. (2001) Stem cells in tissue engineering. *Nature* 414.118–121.

Bielecki, S., Krystinowicz, A., Turkiewicz, C., Kalinowska, H. (2005). Bacterial cellulose, in: Polysaccharides and polyamides in the food industry: Properties, production and patents, Wiley VCH, Weinheim.31-85

Bläckdahl, H., Helenius, G., Bodin, A., Nannmark, U., Johansson, B., Reisberg, B., (2006) Mechanical properties of bacterial cellulose and interactions with smooth muscle cells. *Biomaterials*. 27, 2141-2149.

Bledzki, K., Gassan, J. (1999). Composites reinforced with cellulose based fibres. *Progress in Polymer Science*, 24, 221-274.

Bohn, A., Fink, H. P., Ganster, J., Pinnow, M. (2000). X-ray texture investigation of bacterial cellulose. *Macromolecules Chemistry and Physics*, 201, 1913-1921.

Boldizar, A., Klason, C., Kubat, J., Naslund, P., Saha, P. (1987). Prehydrolyzed cellulose as reinforcing filler for thermoplastics. *International Journal of Polymer Materials*, 11, 4, 229- 262.

Bosworth, L. Clegg, P. Downes, S. (2007), Electrospun nanofibres of polycaprolactone, and their use for tendon regeneration. *Int. J. Nano Biomater.* 1, 3, 263–279.

Brown, M., Willison, J., Richardson, L. (1976). Cellulose biosynthesis in *Gluconacetobacter xylinum*: visualisation of the site of synthesis and direct measurement of the in vivo process. *Proceedings of National Academic of Sciences of U. S. A*, 73, 4565-4569.

Brown, J. (1886). An acetic ferment which form cellulose. *Journal of Chemical Society*, 49, 432-439.

Brown, M. (1962). The mechanism of cellulose biosynthesis by *Gluconacetobacter xylinum*. *Journal of Polymer Science*, 59, 155-169.

Brown. M. (1999). Cellulose structure and biosynthesis. *Pure Applied Chemistry*, 71(5), 767-775.

Borysiak, S., & Garbarczyk, J., Applying the WAXS method to estimate the supermolecular structure of cellulose fibres after mercerisation. *Fibres & Textile in Eastern Europe*, 11, 5 (44), 104-106.

Budhiono, A., Rosidi, A., Iguchi, M. (1999). Kinetic aspects of bacterial cellulose formation in nata-de-coco culture system. *Carbohydrate Polymer*, 40, 137–143.

Bullion, A., Hoffman, D., Gillespie, A., Brien, P., Loos, C., (2006). Contributions of feather fibers and various cellulose fibers to the mechanical properties of polypropylene matrix composites. *Composites Science and Technology*, 66, 102–114.

Cai, Z., Hou, C., Yang, G., Kim, J., (2011). Bacterial cellulose as a template for the formation of polymer/nanoparticle nanocomposite. *Am Soc Mech Eng* 2. (3).

Çakar, F., Ozer, I., Aytekin, A., Sahin, F. (2014) Improvement production of bacterial cellulose by semi-continuous process in Molasses Medium. *Carbohydrate Polymers* 106, 7-13.

Canche-Escamilla, G., Cauich-Cupul, I., Mendizábal, E., Vázquez-Torres. E., Puig, E., Herrera-Franco, J. (1999). Mechanical properties of acrylate-grafted henequen cellulose fibers and their application in composites, *Composites: Part A*, 30, 349-359.

Canche-Escamilla, G., Cauich-Cupul, I., Mendizábal, E., Vázquez-Torres. E., Puig, E., Herrera-Franco, J. (1999). Mechanical properties of acrylate-grafted henequen cellulose fibres and their application in composites, *Composites: Part A*, 30, 349-359.

Cannon, E., Anderson, M., (1991). Biogenesis of BC. *Critical Reviews in Microbiology*, 17(6), 435-447.

Carillo, F., Colom, S., Suñol, J., Saurina, J. (2004). Structural FTIR analysis and thermal characterisation of lyocell and viscose-type fibres. *European Polymer Journal*, 40, 2229-2234.

Chandra, R., Rustgi, R. (1998) Extrusion of thermoplastic starch: effect of Green and common polyethylene on the hydrophobicity characteristics, *progress in polymer science*, 23, 1273-1335.

Chang, Y., Zhang, N. (2011). Cellulose based hydrogels: Present status and applications prospects. *Carbohydrate polymers*, 84, 40-53.

Chanliaud, E., Burrows, M., Jeronimidis, G., Gidley, J. (2002). Mechanical properties of primary plant cell wall analogues. *Planta*, 215, 989–996.

Chawla, R., Bajaj, B., Survase, A., Singhal, S. (2009) Microbial Cellulose; Fermentative production and applications. *Food technology and biotechnology* 47 (2), 107-124.

Chen. B., Sun. K., Ren. T., (2005). Mechanical and viscoelastic properties of chitin fiber reinforced poly(ϵ -caprolactone). *European polymer journal*, 41, 453-457.

Chen, B., Evans, R. G. (2006). Poly (ϵ -caprolactone) nanocomposites: structure and mechanical properties. *Macromolecules*, 39, 747-754.

Chen, Y., Xi, T., Zheng, Y., Guo, T., Hou, J., Wan, Y. (2009) In vitro cytotoxicity of bacterial cellulose scaffolds used for tissue engineered bone. *Journal of bioactive and biocompatible polymers: biomedical applications*, 24, 5137-5145.

Chiaoprakobkij, N., Sanchavanakit, N., Subbalekha, K., Pavasant, P., Pjaisalaphong, M., (2011) Characterization and biocompatibility of bacterial cellulose/alginate composite sponges with human keratinocytes and gingival fibroblasts. *Carbohydrate polymers* 85, 548-553.

Cho.Y, Han.S, Ko.S, (2000). PVA containing chito-oligosaccharide side chain, *Polymer* 41, 2033-2039.

Colom, X., Carrillo, F., (2002). Crystallinity changes in lyocell and viscose-type fibres by caustic treatment. *European Polymer Journal*, 38(11), 2225-2230.

Cooper, J., Luu, H., Ko, F., Freeman, J., Laurencin, C., 2005, Fiber- based tissue engineering scaffold for ligament replacement: design considerations and in vitro evaluation, *biomaterials*, 26, 1523-1532.

Corradini, E., Mattoso, L., Guedes, C., Rosa, D. (2004) Mechanical, thermal and morphological properties of Poly (-caprolactone)/zein blends, *polymers for advanced technology*, 15 (6), 340-345.

Coucheron, H. (1991). An *Gluconacetobacter xylinum* insertion sequence element associated with inactivation of cellulose production. *Journal of Bacteriology*, 173, 5723-5731.

Couso, O., Ielpi, L., Dankert, A. (1987). A xanthan-gum-like polysaccharide from *Gluconacetobacter xylinum*. *Journal of Microbiology*, 133, 2123-2135.

Czaja, W., Krystynowicz, A., Bielecki, S., Brown, R. (2006) Microbial cellulose-the natural power to heal wounds. *Biomaterials*, 27, 145-151.

Czaja, W., Young, D., Kawecki, M., Brown, R. (2007) The future prospects of microbial cellulose in biomedical applications, *Biomacromolecules*, 8, 1-12.

Dahlke, B., Larbig, H., Scherzer, D., Poltrock, R. (1998). Natural fibre reinforced foams based on renewable resources for automotive interior applications. *Journal of Cellular Plastic*, 4, 361-379.

De Souza Lima, R. Borsali (2004), Rod-like cellulose microcrystals: Structure, properties, and applications, *Macromolecular Rapid Communications*, 25, 771–787.

Deinema. M., Zevenhuizen. M., (1971). Formation of cellulose fibrils by gram negative bacteria and their role in bacterial flocculation. *Archiv fur Mikrobiologie*, 78, 1, 42-51.

Delmer, P., Amor, Y. (1995). Cellulose biosynthesis. *Plant Cellulose*, 5 (7), 987-1000.

Dinand, E., Vignon, M., Chanzy, H., Heux, L. (2002). Mercerization of primary wall cellulose and its implication for the conversion of cellulose I → cellulose II. *Cellulose*, 9, 7-18.

Ding, Y., Himmel, E., (2006). The maize primary cell wall microfibril: A new model derived from direct visualisation. *Journal of agricultural and food chemistry* 54: 597-606.

Djerbi, S., (2005). Cellulose synthases in populus –identification, experience analyses and in vitro synthesis, Ph.D. Thesis, Royal Institute of Technology, School of Biotechnology, Stockholm.

Dudman, F., (1960). Cellulose production by *Gluconacetobacter* strain in submerged culture. *Journal of General Microbiology*, 22, 25-39.

Dufresne, A., (2012), *Nanocellulose: from nature to high performance tailored materials*. Walter De Gruyter, Berlin.

Eichhorn, J., Baillie, A., Zafeiropoulos N., Mwaikambo, Y., Ansell, P., Dufresne, A., Entwistle, M., Herrera-Franco, J., Escamilla, C., Groom, L., Hughes, M., Hill, C., Rials, G., Wild, M. (2001). Review current international research into cellulosic fibres and composites. *Journal of Material Science*, 36, 2107-2131.

Eichhorn, J., Dufresne, A., Aranguren, M., Marcovich, E., Capadona, R., Rowan, J., Weder, C., Thielemans, W., Roman, M., Renneckar, S., Gindl, W., Veigel, S., Keckes, J., Yano, H., Abe, K., Nogi, M., Nakagaito, N., Mangalam, A., Simonsen, J., Benight, S., Bismarck, A., Berglund, A., Peijs, T. (2010). Review: current international research into cellulose nanofibres and nanocomposites. *Journal of Material Science*, 45, 1-33.

Esa, F., Tasirin, S., Rahman, N., (2014) Overview of bacterial cellulose production and application. *Agriculture and agricultural science procedia* 2, 113-119.

Esguerra. M., Fink. H., Laschke. M.W., Jeppsson. A., Delbro. D., Gatenholm. P., Menger. M.D., Risberg. B., (2010). Intravital fluorescent microscopic evaluation of bacterial cellulose scaffold for vascular grafts. *Biomedical materials research*. A93. 1. 140-149.

Favier, V., Canova, R., Cavaille, Y., Chanzy, H., Dufresne, A., Gauthier, C. (1995). Nanocomposite materials from latex and cellulose whiskers. *Polymer Advance Technology*, 6, 351-355.

Favier, V., Dendievel, R., Canova, G., Cavaille, Y., Gilormini, P. (1997) Simulation and modeling of three-dimensional percolating structures: Case of a latex matrix reinforced by a network of cellulose fibers, *Acta Mater.* 45, 1557–1565.

Fengel, D., Wegener, D. (1983). *Wood: Chemistry, Ultrastructure and Reactions*, Walter de Gruyter & Co., Berlin.

Fernandes, S., Oliveira, L., Freire, C., Silvestre, A., Neto, C., Gandinia, A., Desbrieres, J., (2009) Novel Transparent Nanocomposite Films based on chitosan and bacterial cellulose. *Green chemicals* 11, 2023-2029.

Fink. H., Faxe'lv. L., Molnar. G. F., Drotz. K., Risberg. B., Lindhal. T., Sellborn. A., (2010). Real time measurements of coagulation on bacterial cellulose and conventional vascular graft materials. *Acta Biomater.* 6. 3. 1125-1130.

Fontana, D., Franco, C., de Sousa, J., Lyra, N., Sousa, M. (1991). Nature of plant stimulators in the production of *Gluconacetobacter xylinum* ('tea fungus') biofilm used in skin therapy. *Applied Biochemistry Biotechnology*, 28 (29), 341-351.

Franz, G., Blaschek, W. (1990). Cellulose, in *Methods in Plant Biochemistry*, Vol. 2 Carbohydrates. 1990. Academic Press, Harcourt Brace Janovich, London. pp 291-322.833.

Freed, L., Guilak, F., Guo, X., Gray, M., Tranquillo, R., Holmes, J., Radisc, M., Sefton, M., Kaplan, D., Vunjak-Novakovic, G., 2006, Advanced tools for tissue engineering scaffolds, bioreactors and signalling, *Tissue Engineering*, 12 (12), 3285-3305.

Frey-Wyssling, A., Muhlethaler, K. (1946). Submicroscopic structure of cellulose gels. *Journal of Polymer Science*, 1, 172-174.

Fu, S., Feng, X., Lauke, B., Mai, Y. (2008). Effects of particle size, particle/matrix interface adhesion and particle loading on mechanical properties of particulate-polymer composites. *Composites, Part B*, 933-961.

Fu, L. Zhang, J. Yang, G. (2013), Present status and applications of bacterial cellulose-based materials for skin tissue repair, *Carbohydrate Polymers*, 92, 1432-1442.

Gadim, T., Figueiredo, A., Rosero-Navarro, N., Vilela, C., Gamelas, J., Barros-Timmons, A., Neto, C., Silvestre, A., Freire, C., Figueiredo, F., (2014) Nanostructured bacterial cellulose-poly(4-Styrene Sulfonic Acid) composite membranes with high storage modulus and protonic conductivity. *ACS Applied Materials interfaces* 6(10), 7864-7875.

Gassan, J., & Bledzki, K. (1999). Influence of fibre surface treatment on the creep behaviour of jute fibre-reinforced polypropylene. *Journal of Thermoplastic Composite Materials*. 12, 5, 388-398.

Gattenholm, P., Klemm, D., (2010) Bacterial nanocellulose as a renewable material for biomedical applications. *MRS bulletin* Volume 35, 208-213.

Gea, S., Torres, G., Tronscoso, P., Reynolds, T., Vilasecca, F., Iguchi, M., Peijs, T. (2007). Biocomposites based on bacterial cellulose and apple and radish pulp. *International Polymer Processing* 22, 5, 497-501.

Gea, S., Reynolds, C., Roohpour, N., Wirjosentono, B., Soykeabkaew, N., Bilotti, E., Peijs, T. (2010) Biodegradable composites based on poly(ϵ -caprolactone) and bacterial cellulose as reinforcing agent. *Journal of biobased materials and bioenergy*, 4 (7) 4, 384-390.

Gea, S., Reynolds, C., Roohpour, N., Wirjosentono, B., Soykeabkaew, N., Bilotti, E., Peijs, T. (2011) Investigation into the structural, morphological, mechanical and thermal behaviour of bacterial cellulose after a two-step purification process. *Bioresource technology*, 102, 9105-9110.

Gelin, K., Bodin, A., Gatenholm, P., Mihranyan, A., Edwards, K., & Stromme, M. (2007). Characterization of water in bacterial cellulose using dielectric spectroscopy and electron microscopy. *Polymer*, 48, 7623-7631.

George, J., Ramana, V., Sabapathy, N., Jagannath, H., Bawa, S. (2005). Characterization of chemically treated bacterial (*Gluconacetobacter xylinum*) biopolymer: some thermo-mechanical properties. *World Journal of Microbiology & Biotechnology*, 21, 1323-1327.

GeunHyung, K., Taijin, M., Su, P., Wan, K., Young, K. (2007), Fabrication of a biocomposite reinforced with hydrophilic eggshell protein *Biomed. Mater*, 2, 250–256.

Geyer, U., Heinze, T., Stein, A., Klemm, D., Marsch, S., Schumann, D., Schnauder, P., (1994). Formation, derivatization and applications of bacterial cellulose. *International Journal of Biological Macromolecules*, 16(6), 343-347.

Ghasemi-Mobarakeh, L., Prabhakaran, P., Morshed, M., Nasr Esfahani, H., Ramakrishna, S. (2008), Electrospun poly(ϵ -caprolactone)/gelatin nanofibrous scaffolds for nerve tissue engineering, *Biomaterials*, 29, 4532– 4539.

Gindle, W., Keckes, J. (2004). Tensile properties of cellulose acetate butyrate composites reinforced with bacterial cellulose. *Composite Science and Technology*, 64 (15), 2407-2413.

Glasser, L. (1958). The synthesis of cellulose in cell-free extracts of *Gluconacetobacter xylinum*. *Journal of Biological Chemistry*, 232, 627-636.

Gomes, A., Matsuo, T., Goda, K., Ohgi, J. (2007). Development and effect of alkali treatment on tensile properties of curaua fiber green composites. *Composite Part A*, 38, 1811-1820.

Grande, C., Torres, F., Gomez, C., Bano, M. (2009) Nanocomposites of bacterial cellulose/hydroxyapatite for biomedical applications, *Acta Biomaterialia*, 5, 1605-1615.

Griffith, G., Naughton, G., (2002). Tissue Engineering--Current Challenges and Expanding Opportunities. *Science*, 295(5557), 1009-1014.

Grunet, M., Winter, T., (2002). Nanocomposites of cellulose acetate butyrate reinforced with cellulose nanocrystals. *Journal of Polymer and the Environment*, 10, 1-2, 27-30.

Guhados, G., Wan, W., Hutter, L. (2005). Measurement of the elastic modulus of single bacterial cellulose fibres using Atomic Force Microscopy. *Langmuir*, 21(14), 6642-6646.

Haigler, Brown, Benziman, (1980). Cellulose Biogenesis- Polymerization and crystallization are coupled processes in *Gluconacetobacter-Xylinum*. *Proceedings of the National Academy of Sciences of the United States of America*, 77(11), 6678-6682.

Haigler. H., Benziman, M., Brown, M. (1982) (Eds): Cellulose and other natural polymer systems. Plenum Press, New York.

Haigler, H., Brown, M. (1986) Transport of rosettes from the golgi apparatus to the plasma membrane in isolated mesophyll cells of *zinnia elegans* during differentiation to tracheary elements in suspension culture. *Protoplasma* 134, 111-120.

Halib, N., Amin, M., Ahmed. I., Hasim, Z., Jamal. N (2009). Swelling of bacterial cellulose-acrylic acid hydrogels: sensitivity towards external stimuli. *Sains malaysiana*, 38 (5), 785-791.

Hanna, M., Biby, G., Miladinov, V. (2001). Production of microcrystalline cellulose by reactive extrusion. United States Patent 6228213.

Hao. J., Yuan. M., Deng. X., (2002). Biodegradable and biocompatible nanocomposites of poly (ϵ -caprolactone) with hydroxyapatite nanocrystals: thermal and mechanical properties. *Journal of applied polymer science*, 86, (3), 676-683.

Heinemann, S. (2015). Polymer based matrix composites. Makhlouf, A.S.H., Scharnweber, D. (Eds), Handbook of nanoceramic and nanocomposite coatings and materials. Butterworth-Heinemann. 3-27.

Helbert, W., Cavaille, Y., Dufresne, A. (1996). Thermoplastic Nanocomposite filled with heat straw cellulose whisker. Part I: processing and mechanical behaviour. *Polymer Composite*, 17 (14), 604-611.

Helenius, G., Backdahl, H., Bodin, A., Nannmark, U., Gatenholm, P., Reisberg B. (2006). In vivo biocompatibility of bacterial cellulose. *Journal of Biomedical and Research*, 76A, 431-438.

Hench. L., Jones. J., (2004) "Biomaterials, artificial organs and tissue engineering" Institute of materials and mining. *Polymers for advanced technologies*, 2004, 15 (6), 340-345.

Herrick, W., Casebier, L., Hamilton, K., Sandberg, L. (1983). Microfibrillated cellulose: morphology and accessibility. *Journal of Applied Polymer Sciences and Applied Polymer Symposia*, 37, 797.

Herrmann, S., Nickel, J., Riedel, U. (1998). Construction materials based upon biologically renewable resources - from components to finished parts. *Polymer Degradation and Stability*, 59, 1-3, 251-261.

Hestrin, S., Schramann, M. (1952). Synthesis of cellulose by *Gluconacetobacter xylinum*: 2. Preparation of Freeze-dried cells capable of polymerizing glucose to cellulose. *Biochemical Journal*, 58, 345-352.

Hollister, J., Maddox, D., Taboas, M. (2002). Optimal design and fabrication of scaffolds to mimic tissue properties and satisfy biological constraints. *Biomaterials*, 23(20), 4095-4103.

Hollister, J. (2005) Porous scaffold design for tissue engineering. *Nat Mater*. 4. 518–524.

- Hon, S., Shiraishi, N. (1991). Wood and cellulosic chemistry. New York, Marcel Dekker, Inc.
- Hong, L., Wang, Y., Jia, R., Huang, Y., Gao, C., Wan, Z. (2006). Hydroxyapatite/bacterial cellulose composite synthesis via a biomimetic route. *Materials Letters*, 60, 1710-1713.
- Horii, F., Yamamoto, H., Kitamaru, R., Tanahashi, M., Higushi, T. (1987). Transformation of native cellulose crystals induced by saturated steam at high temperatures. *Macromolecules*, 20, 2946–2949.
- Hsieh, C., Yano, H., Nogi, M., Eichhorn, J. (2008). An estimation of the Young's modulus of bacterial cellulose filaments. *Cellulose*, 15, 507-513.
- Hu, W., Chen, J., Li, Z., Wang, H., (2014). Functionalized bacterial cellulose derivatives and nanocomposites. *Carbohydrate polymer*, 101, 1043-1060.
- Huang, Z., Zhang, Y., Kotakic, M., (2003), A review on polymer nanofibres by electrospinning and their applications in nanocomposites, *composites science and technology*, 63, 2223-2253.
- Huang, Y., Zhu, C., Yang, J., Nie, Y., Chen, C., Sun, D., (2014). Recent advances in bacterial cellulose. *Cellulose*. 21. 1-30.
- Hubbell JA. (1995) Biomaterials in tissue engineering. *Nat Biotechnol*. 13. 565–576.
- Hurtubise, G., Krassig, H., (1960). Classification of Fine Structural Characteristics in Cellulose by Infrared Spectroscopy. Use of Potassium Bromide Pellet Technique. *Analytical Chemistry*, 32(2), 177-181.
- Hwang, W., Yang, K., Hwang, K., Pyn, R., Kim, S. (1999). Effects of pH and Dissolved Oxygen on Cellulose Production by *Gluconacetobacter xylinum* BRC5 in Agitated Culture. *Journal of Bioscience and Bioengineering*, 88, 2, 183-188.

Ifuku, S., Nogi, M., Abe, K., Handa, K., Nakatsubo, F., Yano, H. (2007). Surface modification of bacterial cellulose nanofibers for property enhancement of optically transparent composites: dependence on acetyl-group DS. *Biomacromolecules*.

Iguchi, M., Mitshuhasi, S., Ichimura, K., Nishi, Y., Uryu, M., Yamanaka, S., Watanabe, K. (1988). United States Patent 4742164.

Iguchi, M., Yamanaka, S., Budhiono, A. (2000). Review bacterial cellulose – a masterpiece of nature's arts. *Journal of Material Science*, 35, 261-270.

Innala, M., Riebe, I., Kuzmenko, V., Sundberg, J., Gatenholm, P., Hanse, E., (2014). 3D culturing and differentiation of SH-SY5Y neuroblastoma cells on bacterial nanocellulose scaffolds. *Artif. Cells Nanomedicine Biotechnol.* 42, 302-308.

Ishida, T., Sugano, Y., Nakai, T., Shoda, M. (2002). Effect of acetan and production of bacterial cellulose by *Gluconacetobacter xylinum*. *Bioscience, Biotechnology, and Biochemistry*, 66, 1677-1681.

Ishihara, M., Yamanaka, S. (2002). Modified bacterial cellulose, United States Patent Application No. 20020065409.

Ishihara, M., Yamanaka, S. (2003). Modified bacterial cellulose. United States Patent 662419 B2.

Ishikawa, A., Okano, T., (1997). Fine structure and tensile properties of ramie fibres in the crystalline form of cellulose I, II, III1 and IV1. *Polymer*, 38, 2, 463-468.

Jansson, E., Lindberg, J., Wimalasiri, S., Dankert, A. (1993). Structural studies of acetan, an exopolysaccharide elaborated by *Gluconacetobacter xylinum*. *Carbohydrate Research*, 245, 313-310.

Jimenez, G., Ogata, N., Kawai, H., Ogihara, T. (1997). Structure and thermal/mechanical properties of poly(ϵ -caprolactone) – clay blend. *Journal of applied polymer science*, 64 (11), 2211-2220.

John, J., Anandjiwala, D., Pothan, A., Thomas, S. (2007). Cellulosic fibre-reinforced composites. *Composite Interface*, 14, 733-751.

Jonas, R., Farah F., (1998). Production and application of microbial cellulose, *Polymer Degradation and Stability*, 59, 101-106.

Jonsson, M., Brackmann, C., Puchades, M., Brattas, K., Ewing, A., Gatenholm, P., (2015). Neuronal networks on nanocellulose scaffolds. *Tissue engineering Part C methods* 21, 1162-1170.

Kačuráková, M., Smith, C., Gidley, J., Wilson, H. (2002). Molecular interactions in bacterial cellulose composites studied by 1D FT-IR and dynamic 2D FT-IR spectroscopy. *Carbohydrate Research* 337, 1145-1153.

Kawano, S., Tajima, K., Uemori, Y., Yamashita, Erata, T., Munekata, M., Takai, M. (2002). Cloning of cellulose synthesis related genes from *Gluconacetobacter xylinum* ATCC23769 and ATCC53582: comparison of cellulose synthetic ability between strains. *DNA Research*, 9, 149–156.

Keane, T., Badylak, F. (2014) Biomaterials for tissue engineering applications, *Seminars in Paediatric surgery*, 23, 112-118.

Kent, R., Stephens, S., Westland, A. (1991). Bacterial cellulose fibre provides an alternative for thickening and coating. *Food technology*, June, 108-113.

Keshk, S.M., (2014). Vitamin C, enhances bacterial cellulose production in *Gluconacetobacter xylinus*. *Carbohydrate polymer*, 99, 98-100.

Kibbe, A.H. (ed). (2000). Handbook of Pharmaceutical Excipients, 3rd edition, pp 96–111.

Kim, J., Jang, H., Park, H., Min, M., (2010) Fabrication and characterisation of 3-dimensional PLGA nanofiber/microfiber composite scaffolds. *Polymer*, 51, 1320-1327.

Klechkovskaya, V., Baklagina, B., Stepina, D., Khripunov, K., Buffat, A., Suvorova, I., Zhanavskina, S., Tkachenko, A., Gladchenko, V. (2003). Structure of cellulose *Gluconacetobacter xylinum*. *Crystallography Report*, 48(5), 755-762.

Klemm, D., Philipp. B., Heinze. T., Heinze. U., Wagenknecht. (1998). *Comprehensive cellulose chemistry*. Vol.1. Wiley-VCH. New York.

Klemm, D. et al., (2001). Bacterial synthesized cellulose artificial blood vessels for microsurgery. *Progress in Polymer Science*, 26(9), 1561-1603.

Klemm, D., Schumann, D., Kramer, F., Hessler, N., Hornung, M., Schamuder, H.P., (2006). Nanocelluloses as innovative polymers in research and application. *Advances in polymer science*. 205. 49-96.

Kolpak, F., Weih, M., Blackwell, J., (1978). Mercerization of cellulose: 1. Determination of the structure of Mercerized cotton. *Polymer*, 19, 123-131.

Koyama, M., Helbert, W., Imai, T., Sugiyama, J., Henrissat, B. (1997) Parallel-up structure evidences the molecular directionality during biosynthesis of bacterial cellulose, *Proc National Academy of Science*, 94(17): 9091-9095.

Klemm, D., (2001). Bacterial synthesized cellulose-artificial blood vessel for microsurgery. *Progress in Polymer Science*, 26,9, 1561-1603.

Kono, H., Numata, Y. (2004). Two-dimensional spin-exchange solid-state NMR study of the crystal structure of cellulose II. *Polymer*, 45, 4541-4547.

Krystynowicz, A., Czaja, W., Wiktorowska-Jeziarska, M., Turkiewicz, M., Goncalves-Miszkiewicz, M., Biele, S. (2002). Factors affecting the yield and properties of bacterial cellulose. *Journal of Industrial Microbiology & Biotechnology*, 29, 189 – 195.

Langan, P., Nishiyama, Y., Chanzy, H. (2001). X-ray structure of mercerized cellulose II at 1 Å resolution. *Biomacromolecules*, 2, 410-416.

Langer, R., Vacanti, P., (1993). Tissue engineering. *Science*, 260(5110), 920-926.

Langer, R., Tirrell, A. (2000) Designing materials for biology and medicine. *Nature*. 428. 487–492.

Larrondo, L., Manley, R., (1981), Electrostatic fibre spinning from polymer melts. III. Electrostatic deformation of a pendant drop of a polymer melt. *Journal of polymer science. Part B*, 19 (6), 933-940.

Laszkiewicz, B. (1997). Solubility of bacterial cellulose and its structural properties. *Journal of Applied Polymer Science*, 67, 1871-1876.

Lee, H., Park, S., Yoo, J., & Hauser, J. (2004). Enhancing the durability of linen-like temperature mercerized cotton. *Textile Research Journal*, 74, 2, 146-154.

Lee, K., Buldum, G., Mantalaris, A., Bismack, A. (2014). More than meets the eye in bacterial cellulose: Biosynthesis, bioprocessing and applications in advanced fiber composites. *Macromolecular Bioscience*. 14, 10-32.

Li, Z., Zhuang, P., Liu, X., Guan, Y., Yao, K., (2002), “Study on antibacterial O-carboxymethylated chitosan/cellulose blend film from LiCl/N, N-dimethylacetamide solution” *Polymer* 43 (4), 1541-1547.

Li. J, Wan. Y, Li. L, Liang. H, Wang. J, (2009), Preparation and characterization of 2,3-dialdehyde bacterial cellulose for potential biodegradable tissue engineering scaffolds, *Materials Science and Engineering*, 29 1635–1642.

Li. D, Wu. T, He. N, Wang. J, Chen. W, He. L, Huang. C, El-Hamshary. H. A, Al-Deyab. S. S, Ke. Q, (2014), Three-dimensional polycaprolactone scaffold via needless electrospinning promotes cell proliferation and infiltration. *Colloids and Surfaces B*, 121, 432-443.

Limongi, T., Giugni, A., Tan, H., Bukhari, E., Torre, B., Allione, M., Marini, M., Tirinato, L., Das, G., Moretti, M., Falqui, A, Fabrizio, E. (2015) Fabrication, Mercury Intrusion Porosimetry Characterization and *In Vitro* Qualitative Analysis of Biocompatibility of Various Porosities Polycaprolactone Scaffolds. *J Tissue Sci Eng* 6:159-164.

Lin. Y-K., Chen. K-H., Ou. K-L., Liu. M. (2011). Effects of different extracellular matrices and growth factor immobilization on biodegradability and biocompatibility of microporous bacterial cellulose. *J Bioact Compat Polym* 26 (5) 508-518.

Lin. N., Dufresne. A, (2014), “Nanocellulose in biomedicine: current and future prospect” *European Polymer Journal*. 59, 302-325.

Lina. F, Zhang. J, Yang. G, (2013), “Present status and applications of Bacterial cellulose-based materials for skin tissue repair”. *Carbohydrate Polymers*, 92, 1432-1442.

Liu, C., Xia, Z., Czernuszka, J., (2007). “Design and Development of Three-Dimensional Scaffolds for Tissue Engineering”. *Chemical Engineering Research and Design*, 85(7), 1051-1064.

Liu, Y., & Hu, H. (2008). X-ray diffraction study of bamboo fibres treated with NaOH. *Fibers and Polymers*, 19, 6, 735-739.

Liu, C., Yang, D., Wang, Y., Shi, J., Jiang, Z., (2012) Fabrication of antimicrobial bacterial cellulose-Ag/AgCl nanocomposite using bacteria as versatile biofactory. *J.Nanoparticle Res.* 14, 1084-1095.

Lyons, J., Li, C., Ko, F., (2004). Melt electrospinning of polymers: A review, *Polymer News*, 30, 1-9.

MacCormick, A., Harris, E., Gunning, P., Morris, J. (1993). Characterization of a variant of the polysaccharide acetan produced by a mutant of *Gluconacetobacter xylinum* strain CR1/4. *Journal of Applied Bacteriology*, 74, 196-199.

Mansikkamäki, P., Lahtinen, M., Rissanen, K. (2005). Structure changes of cellulose crystallites induced by mercerisation in different solvent system; determined by powder X-ray diffraction method. *Cellulose*, 12, 233-242.

Marchessault, H., Sarko, A. (1962). X-ray structure of polysaccharides. *Advanced carbohydrate chemistry*, Wolfrom, M. L (Ed), Academic Press New York, 4221-4283.

Martínez-Sanz, M., Olsson, T., Lopez-Rubio, A., Lagaron, M. (2010). Development of electrospun EVOH fibres reinforced with bacterial cellulose nanowhiskers. Part I: Characterization and method optimization. *Cellulose*, doi:10.1007/s10570-010-9471-1.

Martinez-Sanz, M., Lopez-Rubio, A., Lagaron, J., (2011) Optimisation of the nanofabrication by acid hydrolysis of bacterial cellulose nanowhiskers, *Carbohydrate polymers*, 85, 228-236.

Masaoka, S., Ohe, T., Sakota, N., (1993). Production of cellulose from glucose by *Gluconacetobacter xylinum*. *Journal of Fermentation and Bioengineering*, 75, 1, 18-22.

Matsuo, M., Sawatarie, C., Iwai, Y., & Ozaki, F. (1990). Effect of orientation and crystallinity of the measurement by X-ray diffraction of the crystal lattice moduli of cellulose I and II. *Macromolecules*, 23, 3266-3275.

Milewski, V. (1994). Whiskers in *Concise encyclopaedia of composite materials*; Kelly A (Ed). Pergamon, New York. p 311-314.

Moharram, A., Osama, M. (2008). FTIR spectroscopic study of the effect of microwave heating on the transformation of cellulose I into cellulose II during mercerization. *Journal of Applied Polymer Science*, 107, 30-36.

Moigne, N., Navard, P. (2009). Dissolution mechanism of wood cellulose fibres in NaOH-Water. *Cellulose*, in-press.

Moon, J., Martini, A., Naim, J., Simonsen, J., Youngblood, J. (2011) Cellulose nanomaterials review: structure, properties and nanocomposites, *Chem Soc Rev.* 40 (7): 3941-3994.

Morton, E., Hearle, S. (1962). *Physical properties of textile fibres*. Butterworth & Co (Publisher) Ltd and the Textile Institute, London.

Movasaghi, Z., Rehman, S., Rehman, I. (2008). Fourier transform infrared (FTIR) spectroscopy of biological tissues. *Applied Spectroscopy Reviews*, 43134–179.

Muangman, P., Opananon, S., Suwanchot, S., Thangthed, O., (2011), Efficiency of microbial cellulose dressing in partial-thickness burn wounds, *the journal of the American college of certified wound specialists* 3(1), 16-19.

Nakagaito, N., Iwamoto, S., Yano, H. (2005). Bacterial cellulose: the ultimate nanoscalar cellulose morphology for the production of high strength composites. *Applied Physics A*, 80 (1), 93-97.

Nakagaito, N., Yano, H. (2006). Nanocomposites based on cellulose microfibril. In: Oksman, K., Sain, M. (Eds). *Cellulose nanocomposite; processing, characterisation and properties*. ACS symposium series, p. 151-168.

Nakagaito, N., & Yano, H. (2008). Toughness enhancement of cellulose nanocomposites by alkali treatment of the reinforcing cellulose nanofibers. *Cellulose*, 15, 323-331.

Nakai, Y., Fukuoka, E., Nakajima, S. (1977). Crystallinity and physical characteristics of microcrystalline cellulose. *Chemistry of Pharmacy Bulletin*, 25, 96-101.

Nakai, T., Tonouchi, N., Konishi, T., Kojima, Y., Tsuchida, T., Yoshinaga, F., Sakai, F., Hayashi, T. (1999). Enhancement of cellulose production by expression of sucrose synthase in *Gluconacetobacter xylinum*. *Applied Biological Sciences*, 96, 14-18.

Nelson, L., O'Connor, T. (1964). Relation of certain infrared bands to cellulose crystallinity and crystal lattice type. Part I. Spectra of lattice types I, II, III and amorphous cellulose. Part II. A new infrared ratio for estimation of crystallinity in cellulose I and II. *Journal of Applied Polymer and Science*, 18, 1311-1341.

Nelson, L., O'Connor, T. (1964a). Relation of certain infrared bands to cellulose crystallinity and crystal latticed type. Part II. A new Infrared Ratio for estimation of crystallinity in Cellulose I and II. *Journal of Applied Polymer Science*, 8(3), 1325-1341.

Nishi, Y., Uryu, M., Yamanaka, S., Watanabe, K., Kitamura, N., Iguchi, M., Mitsuhashi, S. (1990). The structure and mechanical properties of sheets prepared from BC. Part2: Improvement of the mechanical properties of sheet and their applicability to diaphragms of electro-acoustic transducer. *Journal of Material Science*, 25, 2997-3001.

Nogi, M., Handa, K., Nakagaito, N., Yano, H. (2005). Optically transparent bionanofibre composites with low sensitivity to refractive index of polymer matrix. *Applied Physics letter*, 87, 1, 1-3.

Novaes, A., Novaes, B., Grisi, M., Soares, N., Gabaraa, F. (1991). Gengiflex®, an alkali-cellulose membrane for GTR; histologic observation. *Brazilian Dentistry Journal*, 65-71.

O'Brien, J. (2011), "Biomaterials and scaffolds for tissue engineering", *Materials today*, Vol 14, issue 3, 88-95.

Oh, Y., Yoo, I., Shin, Y., Kim, C., Kim, Y., Chung, S., Park, H., Youk, H. (2005). Crystalline structure analysis of cellulose treated with sodium hydroxide and carbon dioxide by means of X-ray diffraction and FTIR spectroscopy. *Carbohydrate Research*, 340, 2376-2391.

Ohad, I., Danon, D., Hestrin, S. (1962). Synthesis of cellulose by *Gluconacetobacter xylinum*. V. Ultrastructure of polymer. *Journal of Cell Biology*, 12, 31-46.

Okiyama, A., Shirae, H., Kano, H., Yamanaka, S. (1992). Bacterial cellulose I. Two-stage fermentation process for cellulose production by *Gluconacetobacter aceti*. *Food Hydrocolloids*, 6, 471-477.

Oksmann, K., Wallstrom, L., Berglund, A., Filho, T. (2001). Morphology and mechanical properties of unidirectional sisal-epoxy composites. *Journal of Applied Science*, 84, 2358-2365.

Olabarrieta, I., Forsstrom, D., Gedde, W., Hedenqvist, S. (2001) "Transport properties of Chitosan and whey blended with poly(ϵ -caprolactone) assessed by standard permeability measurements and microcalorimetry" *Polymer*, 42, (2) 4401-4408.

Olsson, R. Kraemer, A. Lopez-Rubio, S. Torres-Giner, J., Ocio, M., Lagaron. (2010), Extraction of microfibrils from bacterial cellulose networks for electrospinning of anisotropic biohybrid fiber yarns, *Macromolecules*, 43 (2010), pp. 4201–4209.

Orts, J., Shey, J., Imam, H., Glenn, M., Guttman, E., Revol, F. (2005). Application of cellulose microfibrils in polymer nanocomposites. *Journal of Polymers and the Environment*, 13 (4), 301-306.

Oshima, T., Taguchi, S., Ohe, K., Baba, Y., (2011) Phosphorylated bacterial cellulose for adsorption of proteins. *Carbohydrate polymers*, 83 (2) 953-958.

O'Sullivan, C. (1997). Cellulose: the structure slowly unravels. *Cellulose*, 97 (4), 173–207.

Ott, E., Spurlin, M., Grafflin, W. (1954). Cellulose and cellulose derivatives. Interscience Publisher, London.

Ovington, L.G., (2007). Advances in wound dressings. *Clinical dermatology*, 25, 33-38.

Pantoustier, N., Lepoittevin, B., Alexandre, M., Kubies, D., Calberg, C., Jerome, R., Dubois, P. (2002). Biodegradable polyester layered silicate nanocomposites based on poly (ϵ -caprolactone). *Polymer Engineering Science*, 42, 1928-1937.

Park, H., Kim, G., Kim, C., Yang, Y., Park, G., (2008), Development of dual scale scaffolds via direct polymer melt deposition and electrospinning for applications in tissue regeneration. *Acta Biomaterials*. 4, 1198-1207.

Peijs, T. (2000). Natural fibre-based composites. *Materials Technology*, 15, 4, 281-285.

Peijs, T. (2003). Composites for recyclability. *Materials today*, April, 30-35.

Persson, P., (2004). Strategies for cellulose fiber modification. Royal Institute of Technology, School of Biotechnology, Stockholm.

Pertile, N., Andrade, F., Alves, C., Gama, M. (2010), Surface modification of bacterial cellulose by nitrogen-containing plasma for improved interaction with cells, *Carbohydrate Polymers*, 82 (3), 692-698.

Petersen, N., Gatenholm, P. (2011) Bacterial cellulose based materials and medical devices current state and perspectives. *Applied microbiology and biotechnology*, 91, 1277-1286.

Plomion, C., Leprovost, G., Stokes, A., (2001). Wood formation in trees. *Plant Physiology*, 124, 1513-1523.

Powel, P.C. *Engineering with polymer*. (1983), Chapman and Hall

Rabkin, E., Schoen, J., (2002). Cardiovascular tissue engineering. *Cardiovascular Pathology*, 11(6), 305-317.

Ramakrishna, S., Fujihara, K., Teo, W., Lim, T., Ma, Z., (2005) An introduction to electrospinning and nanofibres, ISBN: 981-256-415-2. Publisher; World scientific publishing Co. Pte. Ltd.

Rånby (1949), Aqueous colloidal solutions of cellulose micelles, *Acta Chemica Scandinavica*, 3, pp. 649–650.

Ratner, D., Hoffman, S., Schoen, J., Lemons, E., (1996). *Biomaterials Science: an introduction to materials in medicine*. Academic Press, New York.

Rigdahl, M., Westerlind, B., Hollmark, H., De Ruvo, A. (1983). Introduction of polymer into fibrous structure by solution impregnation. *Journal of Applied Polymer Science*, 28, 1599-1611.

Robert, C. (1996) *The chemistry of paper*. The Royal society of Chemistry. Cambridge.

Roman, M., Winter, T. (2004), Effect of sulfate groups from sulfuric acid hydrolysis on the thermal degradation behaviour of bacterial cellulose, *Biomacromolecules*, 5 (2004), pp. 1671–1677.

Roman, M., Winter, T. (2006). Cellulose nanocrystals for thermoplastic reinforcement: Effect of filler surface chemistry on composite properties. In: Oksman, K., Sain, M. (Eds). *Cellulose nanocomposite; processing, characterisation and properties*. ACS symposium series, p. 99-113.

Ross, P., Weinhouse, H., Aloni, Y., Michaeli, D., Weinberger-Ohana, P., Mayer, R., Braun, S., de Vroom, E., van der Marel, A., van Boom, H., Benziman, M. (1987). Regulation of Cellulose Synthesis in *Gluconacetobacter xylinum* by Cyclic Diguanylic acid. *Nature*, 325, 279 –281.

Ross, P., Mayer, P., Benziman, M., (1991) Cellulose biosynthesis and function bacteria. *Microbiology Review*, 55, 35-58.

Rowe, C., McKillop, G., Bray, D. (1994). The effect of batch and source variation on the crystallinity of microcrystalline cellulose. *International Journal of Pharmacy*, 101, 169-172.

Ruka, R., Simon, P., Dean, M. (2012) “Altering the growth conditions of *Gluconacetobacter xylinus* to maximise the yield of bacterial cellulose”, *Carbohydrate polymers*, 89, (2) 613-622.

Saibuatong, O., Philasapong, M. (2010). Novo aloe vera-bacterial cellulose composite film from biosynthesis. *Carbohydrate Polymer*, 79, 455-460.

Sakairi, N., Asano, H., Ogawa, M., Nishi, N., Tokura, S. (1998a). A method for direct harvest of bacterial cellulose filaments during continuous cultivation of *Gluconacetobacter xylinum*. *Carbohydrate Polymer*, 35, 233-237.

Sakairi, N., Suzuki, S., Ueno, K., Han, S.M., Nishi, N., Tokura, S. (1998b). Biosynthesis of hetero-polysaccharides by *Gluconacetobacter xylinum* – synthesis and characterization of metal-ion adsorptive properties of partially carboxymethylated cellulose. *Carbohydrate Polymer*, 37, 409-414.

Saka, S., (2001). Chemical composition and distribution. In: Hon, D. N. S., and Shirashi, N (Eds). *Wood and cellulosic chemistry*. Marcel Dekker, Inc. New York. P.51-81.

Samir, S., Alloin, F., Dufresne, A. (2005). Review of recent research into cellulosic whiskers, their properties in nanocomposite field. *Biomacromolecules*, 6, 612-626.

Sanchavanakit, N. et al., (2006). Growth of Human Keratinocytes and Fibroblasts on Bacterial Cellulose Film. *Biotechnology Progress*, 22(4), 1194-1199.

Santos. S.M., Carbajo, J.M., Quintana, E., Ibarra, D., Gomez, N., Ladero, M., et al., (2015). Characterisation of purified bacterial cellulose focused on its use on paper restoration. *Carbohydrate polymers*, 116, 173-181.

Sarasam, A., Sundararajan, V. (2005). Characterization of chitosan-polycaprolactone blends for tissue engineering applications. *Biomaterials*, 26, 5500-5508.

Sarko, A., Southwick, J., Hayashi, J. (1976). Packing analysis of carbohydrate and polysaccharides 7. Crystal structure of cellulose III₁ and its relationship to other cellulose polymorphs. *Macromolecules*, 9, 857-863.

Saska, S., Barud, H.S., Gaspar, A.M.M., Marchetto, S. J., Ribeiro, L., Messaddeq, Y., (2011a) Bacterial cellulose- hydroxyapatite nanocomposites for bone regeneration. *Int J Biomater.* 1

Saska, S., Marchetto, R., Messaddeq, Y., Ribeiro, S. J. L., Gaspar, A. M. M. (2011b). Methods for obtaining resorbable composites, composites, membrane, scaffold for tissue repair. WO2011150482.

Saxena, M., Brown, M., (1995). Identification of a Second Cellulose Synthase Gene (*acsAII*) in *Gluconacetobacter xylinum*. *Journal of Bacteriology*, Sept, 5276–5283.

Saxena, M., Brown, M. (2005). Cellulose biosynthesis: current views and evolving concepts. *Annals of Botany*, 96, 9-21.

Schramm, M., Hestrin, S., (1954). Factors affecting production of cellulose at the air/liquid interface of a culture of *Gluconacetobacter xylinum*. *Journal of General and Microbiology*, 11, 123-129.

Segal, L., Creely, J., Martin, E., Conrad, M. (1959). An empirical method of estimating the degree of crystallinity of native cellulose using the x-ray diffractometer. *Textile Research Journal*, 29, 786-794.

Shah, N., Ul-Islam, W., Khattak, W.A., Park, J.K., (2013). Overview of bacterial cellulose composites: A multipurpose advanced material. *Carbohydrate polymers*, 98, 1585-1598

Sheykhazaria, S., Tabarsaa, T., Ashorib, A., Shakeric, A., Golalipourd, M., (2011). Bacterial synthesised cellulose nanofibers, effects of growth times and culture mediums on the structural characteristics. *Carbohydrate Polymers* 86, 1187-1191.

Shibazaki, H., Kuga, S., Onabe, F., Usuda, M. (1993). Bacterial cellulose membrane as separation medium. *Journal of Applied Polymer Science*, 50, 965-969.

Shibazaki, H., Kuga, S., Okano, T. (1997). Mercerization and acid hydrolysis of bacterial cellulose. *Cellulose*, 4, 75-87.

Shoda, M., Sugano, Y., (2005). Recent advances in bacterial cellulose production. *Biotechnol. Bioprocess Eng.* 10(1), 1-8. *Biotechnology and Bioprocess Engineering*. 10. 1-8.

Sjöström, E., (1993). *Wood chemistry. Fundamental and application*. Academic Press, Sandiego.

Son, J., Heo, S., Kim, G., Lee, J. (2001). Optimization of fermentation condition for the production of BC by a newly isolated *Gluconacetobacter* sp. A9 in shaking culture. *Biotechnology and Applied Biochemistry*, 33, 1-5.

Sugiyama, J., Vuong, R., Chanzy, H. (1991). Electron diffraction study on the two crystalline phases occurring in native cellulose from an algae cell wall. *Macromolecules*, 24, 4168-4175.

Sukara, E., Meliawati, R., (2014), Potential values of bacterial cellulose for industrial applications. *Journal selulosa* 4, 7-16.

Sulaeva, I., Henniges, U., Rosenau, T., Potthast, A., (2015) Bacterial cellulose as a material for wound treatment: Properties and modification. A review. *Biotechnology Advances*

Sun, B., Long, Z., Zhang, D., Li, M., Duvail, L., Jiang, Y., Yin, I., (2014), Advances in three-dimensional nanofibrous macrostructures via electrospinning, *Progress in polymer science*, 39, 862-890.

Suryadiansyah, H., (2002), "Thermoplastic elastomers based on polypropylene/natural rubber and polypropylene/recycle rubber blends" *Polymer Testing*, Volume 21, (4) 389-395.

Svensson, A., Nicklasson, E., Harrah, T., Panilaitis, B., Kaplan, D. L., Brittberg, M., Gattenholm, P. (2005). Bacterial cellulose as a potential scaffold for tissue engineering of cartilage. *Biomaterials*, 26, 419-431.

Tabata. Y., (2009). Biomaterial technology for tissue engineering applications. *Journal of the Royal Society Interface*, 6(Suppl 3), S311-S324.

Takai, C. (1994). Composite in 'Cellulose polymer, blend and composite, Ed. By Gilbert R. D, Hanser/Gardner Publication, Cincinnati.

Tal, R., Wong, C., Calhoon, R., Gelfand, D., Fear, A., Volman, G., Mayer, R., Ross, P., Amikam, D., Weinhouse, H., Cohen, A., Sapir, S., Ohana, P., Benziman, M. (1998). Three cldgoperons control cellular turnover of cyclic di-GMP in *Gluconacetobacter xylinum*: genetic organization and occurrence of conserved domains in isoenzymes. *Journal of Bacteriology*, 180, 4416-4425. *National Academic of Sciences of U. S. A*, 87, 8130-8134.

Talaro, P., Talaro, A. (2001). *Foundations in microbiology*. 4th edition, Pasadena City College, McGraw-Hill.

Tazi, N., Zhang, Z., Messaddeq, Y., Almeida-Lopes, L., Zanardi, L., Levinson, D., Rouabhia, M., (2012). Hydroxyapatite bioactivated bacterial cellulose promotes osteoblast growth and the formation of bone nodules. *AMB Express* 2, 61.

Theo. V, Louis. G, (2013) Preparation and characterisation of novel bacterial cellulose/gelatin scaffold for tissue regeneration using bacterial cellulose hydrogel, *Cellulose-Fundamental aspects*, chapter 6, ISBN: 978953-51-1183-2.

Timell, E., (1969). The chemical composition of tension wood. *Svensk Papperstidning*, 173-181.

Tomasino, C. (1995). *Chemistry & Technology of fabric, preparation & finishing*. North Carolina State University.

Torres, F., Commeaux, S., Troncoso, O. (2012) Biocompatibility of bacterial cellulose based biomaterials, *Journal of functional biomaterials* 3(4) 864-878.

Ul-Islam, M., Khan, T., Park, J.K., (2012) Water holding and release properties of bacterial cellulose obtained by in situ and ex situ modification. *Carbohydrate polymers* 88(2), 596-603.

Ummartyotin, S., Juntarob, J., Sainb, M., Manuspiyaa, H., (2012). Development of transparent bacterial cellulose nanocomposite film as substrate for flexible organic light emitting diode (OLED) display. *Industrial crops and products* 35, 92-97.

Uttayarat, P., Perets, A., Li, M., Pimton, P., Stachelek, J., Alferiev, I., Composto, J., Levy, J., Lelkes, I. (2010) Micropatterning of three-dimensional electrospun polyurethane vascular grafts. *Acta Biomaterialia*, 6. 4229-4237.

Valla, S., Kjosbakken, J. (1982). Cellulose-negative mutants of *Gluconacetobacter xylinum*. *Journal of General Microbiology*, 128, 1401-1408.

Vander Hart, L., Atalla, H. (1984). Studies of macromolecules in native cellulose using solid-state C13 NMR. *Macromolecules*, 17, 1465-1472.

Viet, D., Candanedo, B., Gray, G., (2007). Dispersion of cellulose nanocrystals in polar organic solvents. *Cellulose*, 14, 109-113.

Vincent, L., Engler, A.J., (2011). Effect of substrate modulus on cell function and differentiation. Ducheyne, P. (Ed.) *Comprehensive Biomaterials*. Elsevier, Oxford. 5, 504.

Walton, G., Blackwell, J. (1973). *Biopolymers*. Academic Press, New York.

Wan, Y. et al., (2006). Synthesis and characterization of hydroxyapatite-bacterial cellulose nanocomposites. *Composites Science and Technology*, 66 (11-12), 1825-1832.

Wan, W., Millon, L., (2005) Poly (vinyl alcohol) – based cellulose nanocomposite. Us Patent 2005/0037082 A1.

Wang, W., Itoh, S., Konno, K., Kikkawa, T., Ichinose, S., Sakai, K., Ohkuma, T., Watabe, K. (2009), Effects of schwann cell alignment along the oriented electrospun chitosan nanofibers on nerve regeneration. *Journal of biomedical materials research part A*, 91, 994-1005.

Wang. J., Valmikinathan. C.M., Liu. W., Laurencin. C.T., Yu. X., (2010). Spiral-structured, nanofibrous, 3D scaffolds for bone tissue engineering. *J Biomed Mater Res A*. 93 (2). 753-762.

Wang, H., Gao. C., Zhang, Y, Wan. Z., (2010) Preparation and in vitro characterisation of BC/PVA hydrogel composite for its potential use as artificial Cornea biomaterial. *Materials science and engineering C; Materials for biological applications*, 30 (1), 214-218.

Wang, L., Bassiri, M., Najafi, R., Yang, J., Khosrovi, B., Robson, M., (2007). Hypochlorous acid as a potential wound care agent: Part 1. Stabilised hypochlorous acid: a component of the inorganic armamentarium of innate immunity. *Journal of burns and wounds*, 6, e5.

Wang, B., Zhang, W., Zhou, B., Hu, W., Hong, F., Chen, S. Y., (2011a). Method for preparing silver-loaded modified bacterial cellulose based complex moistened dressing for treating skin injury, wound, burn and scald wound. CN Patent 201110192110.9.

Wang, X., Sun, D. P., He, H.M., Yang, J. Z (2011b). Method for preparing antibacterial wound healing-promoting dressing. CN Patent 201010139908.2.

Watanabe, K., Tabuchi, M., Ishikawa, A., Takemura, H., Tsuchida, T., Morinaga, Y., Yoshinaga, F. (1998). *Bioscience Biotechnology and Biochemistry*, 62, 1290-1292.

Whitney, C., Brigham, E., Darke, H., Reid, G., Gidley, J. (1995). In vitro assembly of cellulose/xyloglucan networks: ultrastructural and molecular aspects. *Plant Journal*, 8, 491-504.

Wippermann, J., Schumann, D., Klemm, D., Kosmehl, H., Salehi-Gelani, S., Ahlers, T., (2009) Preliminary results of small Arterial substitute performed with a cylindrical biomaterial

composed of bacterial cellulose. *European journal of vascular and endovascular surgery* 37, 592-596.

Wong, C., Fear, L., Calhoont, D., Eichinger, H., Mayers, R., Benziman, M., Gelfand, H., Meade, H., Emerick, W., Bruner, R., Ben-Bassat, A., Tal, R. (1990). Genetic organization of the cellulose synthase operon in *Gluconacetobacter xylinum*. *Proceeding of National Academic of Sciences of U. S. A.*, 87, 8130-8134.

Wool, P., Sun, X. (2005). *Bio-based polymers and composites*. Elsevier, Academic press, Amsterdam.

Wu, C., Lai, S., Liao, H. (2002) Graft reaction of acrylic acid onto metallocene-based polyethylene-octene elastomer. *J Appl Polym Sci* 85, 14, 2905-2912.

Wu, C. (2005). A comparison of the structure, thermal properties, and biodegradability of polycaprolactone/chitosan and acrylic acid grafted polycaprolactone/chitosan. *Polymer*, 46, 147-155.

Wu, X., Torres, G., Vilaseca, F., Peijs, T. (2007). Influence of the processing conditions on the mechanical properties of chitin whiskers reinforced poly (caprolactone) nanocomposites. *Journal of Biobased Materials and Bioenergy*, 1, 341-350.

Wu, J., Zheng, Y., Song, W., Luan, J., Wen, X., Wu, Z., Chen, X., Wang, Q., Guo, S., (2014) In situ synthesis of silver nanoparticles/bacterial cellulose composites for slow released antimicrobial wound dressing. *Carbohydrate Polymer* 102, 762-771.

Wulf, D., Joris, K., Vandamme, J. (1996). Improved cellulose formation by an *Gluconacetobacter xylinum* mutant limited in (keto) gluconate synthesis. *Journal of Technology & Biotechnology*, 62, 1290-1292.

Xu, c., Inai, R., Kotaki, M., Ramakrishna, S. (2004), Aligned biodegradable nanofibrous structure, a potential scaffold for blood vessel engineering, *Biomaterials*, 25, 877-886.

Yamanaka, S., Watanabe, K., Kitamura, N., (1989). The structure and mechanical properties of sheets prepared from bacterial cellulose. *Journal of Material Science*, 24, 3141-3145.

Yamanaka, S., Ishihara, M., Sugiyama, J., (2000). Structural modification of bacterial cellulose. *Cellulose*, 7, 213-225.

Yang, J., Yu, J., Sun, D., Yang, X., (2011). Preparation of novel Ag/bacterial cellulose hybrid nanofibers for antimicrobial wound dressing. *Adv Mater Res* 152. 1771-1774.

Yano, H., Sugiyama, J., Nakagaito, A. N., Nogi, M., Hikita, M., Handa, K. (2005). Optically transparent composites reinforced with networks of bacterial nanofibres. *Advanced Materials*, 17, 153-155.

Yano, H., Nakatsubo, F., ABE, K. (2012), Optically transparent bio-based nanocomposites, Saci, Kyoto university, case number 121.

Yun, Y., Cho, J., Jin. (2010) Flow-induced liquid crystalline solutions prepared from aspect ratio-controlled bacterial cellulose nanowhiskers, *Molecular Crystals and Liquid Crystals*, 519, pp. 141–148.

Zaar, K. (1977). The biogenesis of cellulose by *Gluconacetobacter xylinum*. *Cytobiology*, 16, 1-15.

Zaar, K. (1979). Visualisation of pores (export sites) correlated with cellulose production in the envelope of the gram-negative bacterium *Gluconacetobacter xylinum*. *Journal of Cell Biology*, 80, 773-777.

Zaborowska, M., Bodin, A., Backdahl, H., Popp, J., Goldstein, A., Gatenholm, P., (2010) Microporous bacterial cellulose as a potential scaffold for bone regeneration. *Acta Biomaterials*, 6, 2540-2547.

Zhang, L., Webster, J., (2009) Nanotechnology and nanomaterials: Promises for improved tissue regeneration. *Nano Today*. 4. 66–80.

Zhao, H., Kwak, Z., Zhang, C., Brown, W., Arey, E. (2007), Studying cellulose fiber structure by SEM, XRD, NMR and acid hydrolysis, *Carbohydrate Polymers*, 68, pp. 235–241.

Zheng, Y.D., Wu, J., Gao, S., Ding, X., Cui, Q. Y., Yu, Y., (2012) Method for preparing collagen modified bacterial cellulose composite film. CN Patent 201110300494.1.

Zhong, Z., Sun, X., (2001) Properties of soy protein isolate/polycaprolactone blends compatibilized by methylene diphenyl diisocyanate. *Polymer*, 42 (16), 6961-6969.

Zhou, M., Yeung, P., & Yuen, M. (2002). Effect of NaOH mercerization on the crosslinking of ramie yarn using 1,2,3,4-butanetetracarboxylic acid. *Textile Research Journal*, 72 (6): 531-538.

Zhou, T., Chen, D., Jiu, J., Nge, T., Sugahara, T., Nagao, S., Koga, H., Nogi, M. (2013). Electrically conductive bacterial cellulose composite membranes produced by the incorporation of graphite nanoplatelets in pristine bacterial cellulose membranes. *Polymer Letters* 7(9), 756-766.

Zugenmaier, P. (2008). *Crystalline cellulose and derivatives: Characterization and structure*. Springer, New York.

Appendices

Appendix I

FTIR- Full List of Band Assignments

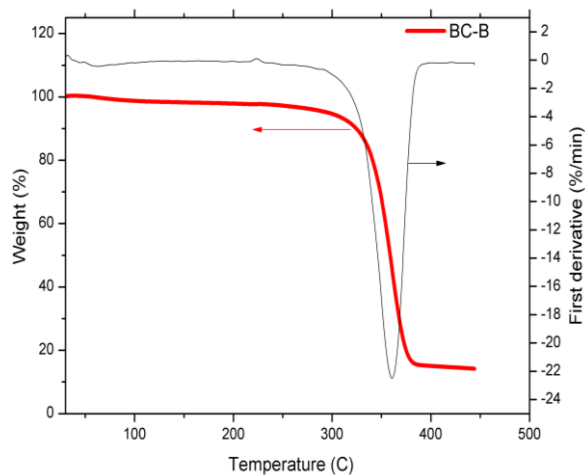
Wavenumber (cm-1)	Assignment	Reference
3352	stretching OH (hydrogen bonded) in CelluloseI	(Oh et al. 2005)
2892	Stretching CH in Cellulose II	(Oh et al. 2005)
1738-1709	C=O stretch in unconjugated ketons, carbonyls and in ester groups	(Schwanninger et al. 2004)
1431	bending CH2 (sym) at C-6 in Cellulose I	(Oh et al. 2005)
1426	symmetric-bending CH2	(Marta Kacurakova et al. 2002)
1362	symmetric-bending CH2 , wagging	(Marta Kacurakova et al. 2002)
1373-1376	bending C-H	
1336	C-OH in plane bending	Colom & Carrillo 2002)
1317	symmetric-bending CH2 , wagging	(Marta Kacurakova et al. 2002)
1319	bending CH2 (wagging) at C-6 -in Cellulose I	(Oh et al. 2005)
1282	bending C-H --> Cellulose I	(Oh et al. 2005)
1236	bending COH in plane at C-6 --> Cellulose I	(Oh et al. 2005)
1235	C-OH in plane bending	Colom & Carrillo 2002)
1202	bending COH in plane at C-6 / OH plane deformation	(Oh et al. 2005)(Schwanninger et al. 2004)
1162	stretching COC at beta-glucosidic linkage in Cellulose I	(Oh et al. 2005)
1160	asymmetric-stretching (C-O-C) --> glycosidic link, ring	(Marta Kacurakova et al. 2002)
1100	stretching (C-O),stretching (C-O) --> ring -->origin P	(Marta Kacurakova et al. 2002)
1111	ring asymmetric stretching- cel1-> 1111 , cel2--> 1007	collom, carrillo (2002)
1060	stretching (C-O),stretching (C-C) --> C-3_O-3	(Marta Kacurakova et al. 2002)

1055	C-O stretching , cell 1 and cel2	collom, carrillo (2002)
1030	stretching (C-O),stretching (C-C) --> C_6-H2_O-6	(Marta Kacurakova et al. 2002)
1032	stretching CO at C-6 --> Cellulose II	(Oh et al. 2005)
1000	stretching (C-O),stretching (C-C) --> C_6-H2_O-6 --> origin C	(Marta Kacurakova et al. 2002)
983	stretching CO at C-6 in Cellulose I	(Oh et al. 2005)
895	stretching (C-1-H) --> Beta-anomeric link--> origin C, XG COC in plane, symmetric stretching	(Marta Kacurakova et al. 2002) (Colom & Carrillo 2002)

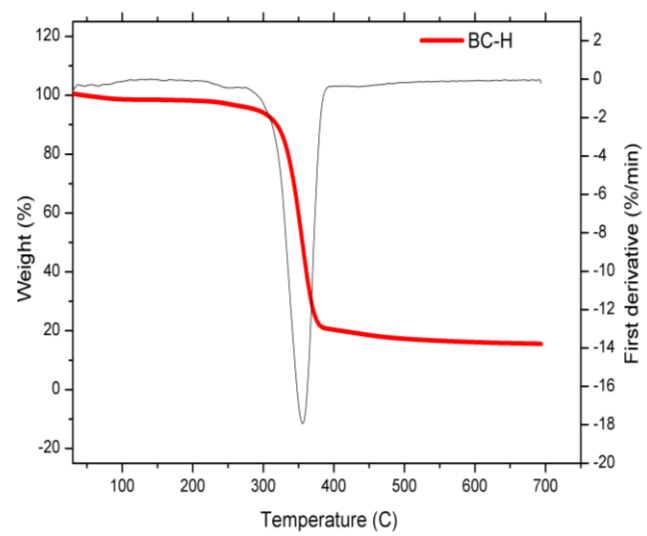
Appendix II

TG and DTG curves for samples B, E and H, respectively.

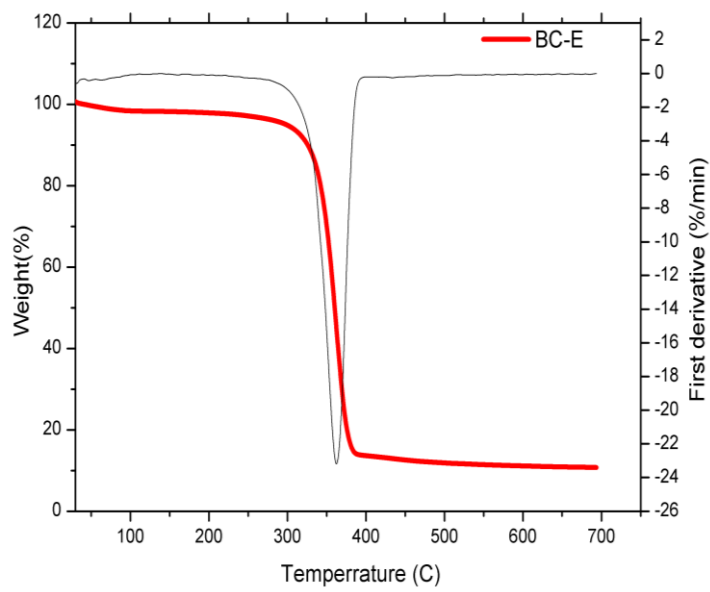
TG and DTG curves for BC-B (5%-10 hours).



TG and DTG curves for BC-H (9%-10 hours).



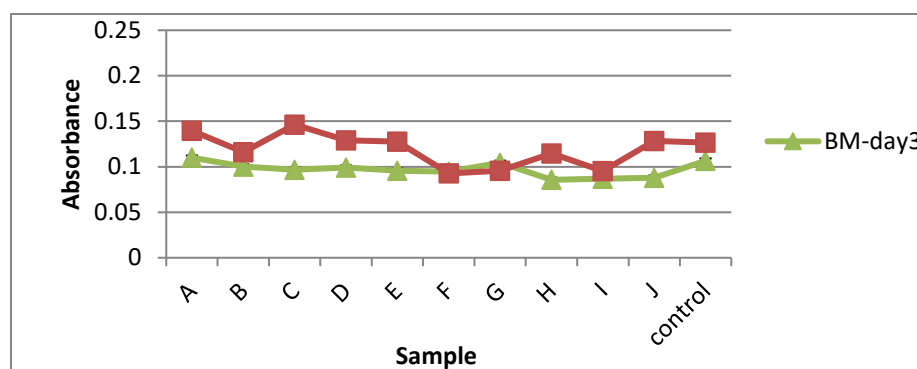
TG and DTG curves for BC-E (7%-10 hours).



Appendix III

MTT results of day 3

The MTT results for cell viability of dermal and bone marrow fibroblasts on and around scaffold are shown below:



Statistical analysis for MTT for surface modified bacterial cellulose

T Test	Bone Marrow day 6	Bone Marrow day 10	Dermal day 6	Dermal day 10
a-b	0.00001460	0.000156	0.24091	0.0284
a-c	0.00003535	0.023710	0.01132	0.0066
a-d	0.00000570	0.000051	0.00012	0.0047
a-e	0.00000972	0.012448	0.00060	0.1209
a-f	0.00057928	0.000878	0.00021	0.5000
a-g	0.00008016	0.058058	0.00027	0.0011
a-h	0.00003130	0.000000	0.00010	0.0003
a-i	0.00001263	0.172636	0.00003	0.0007
a-j	0.00028100	0.000005	0.00004	0.0124
a-control	0.00000291	0.000005	0.0000002	0.0000
b-c	0.00156279	0.002795	0.00375	0.3459
b-d	0.00000056	0.065889	0.00003	0.0011
b-e	0.00052529	0.000996	0.00034	0.1151

b-f	0.40124101	0.103076	0.00005	0.0212
b-g	0.01673587	0.000571	0.00006	0.0064
b-h	0.03338327	0.000005	0.00002	0.0026
b-i	0.00109606	0.000948	0.00001	0.0041
b-j	0.00374522	0.000106	0.00001	0.4208
b-control	0.00000038	0.000052	0.00000003	0.0000
c-d	0.00000348	0.000949	0.00003	0.0001
c-e	0.38382196	0.383822	0.00085	0.0334
c-f	0.00954103	0.012741	0.00007	0.0029
c-g	0.03696309	0.137288	0.00010	0.0039
c-h	0.00736030	0.000004	0.00002	0.0003
c-i	0.13728831	0.027520	0.00001	0.0020
c-j	0.00044919	0.003591	0.000003	0.1439
c-control	0.00000255	0.000025	0.00000001	0.0000
d-e	0.00000092	0.000304	0.07751	0.0017
d-f	0.00002544	0.017055	0.03524	0.0025
d-g	0.00000541	0.000193	0.01066	0.0002
d-h	0.00000168	0.000193	0.14393	0.0000
d-i	0.00000106	0.000470	0.00039	0.0001
d-j	0.00000421	0.000045	0.00375	0.0002
d-control	0.00388130	0.000065	0.000000013	0.0000
e-f	0.00806504	0.005723	0.40745	0.0963
e-g	0.03233845	0.143932	0.32166	0.0021
e-h	0.00402495	0.000001	0.03338	0.0005
e-i	0.14393207	0.025687	0.00065	0.0013
e-j	0.00019253	0.001801	0.00523	0.0775
e-control	0.00000067	0.000012	0.00000014	0.0000
f-g	0.07407407	0.002892	0.14393	0.0008
f-h	0.18695048	0.000008	0.01066	0.0001
f-i	0.01568787	0.002512	0.00019	0.0005
f-j	0.02568722	0.000393	0.00066	0.0057
f-control	0.00001734	0.000058	0.00000001	0.0000
g-h	0.13728831	0.000001	0.00402	0.3065
g-i	0.09450183	0.058058	0.00014	0.4450
g-j	0.00193142	0.004025	0.00034	0.0027
g-control	0.00000383	0.000010	0.00000002	0.0000
h-i	0.01065582	0.000007	0.00060	0.2209

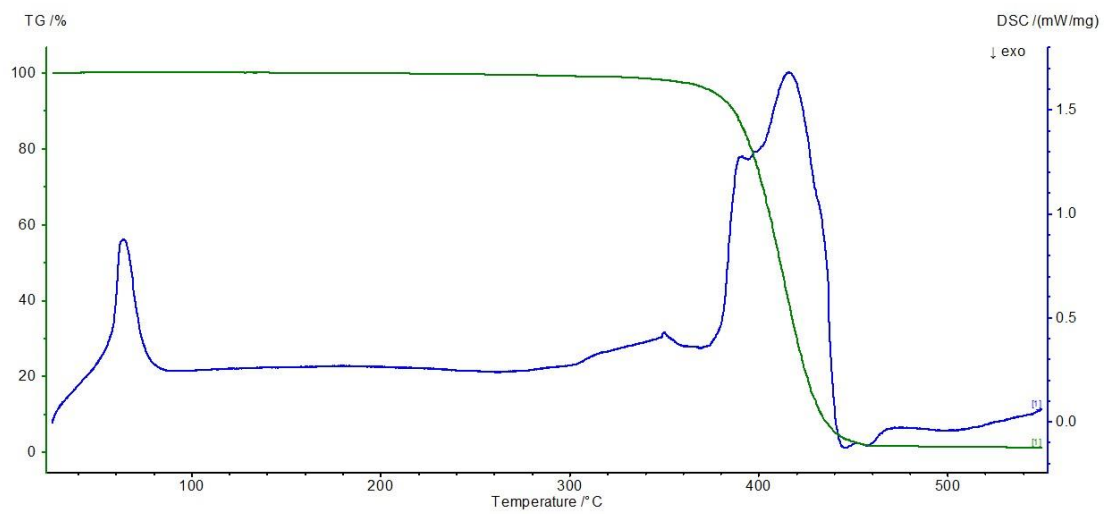
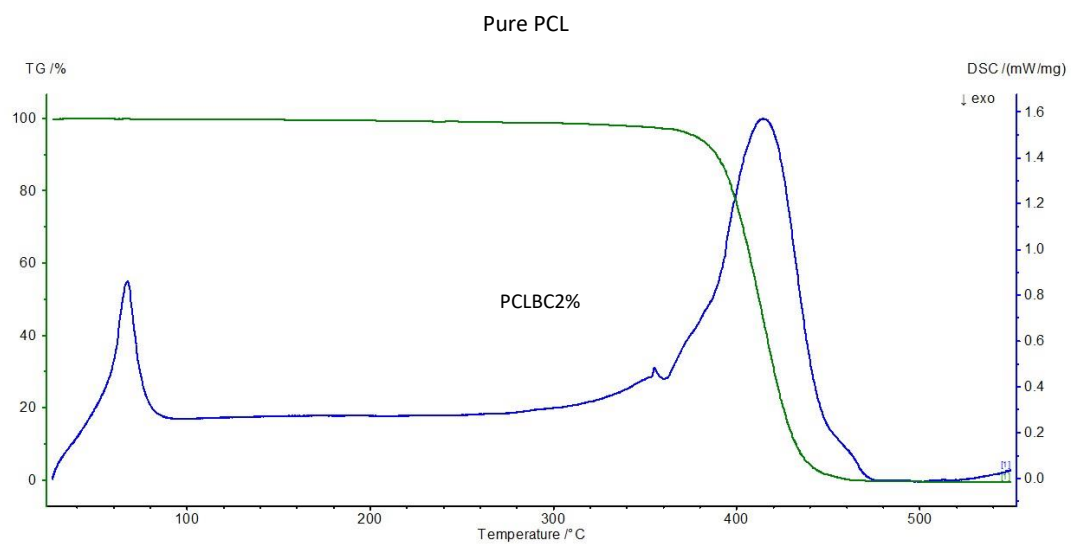
h-j	0.00180112	0.000001	0.01245	0.0002
h-control	0.00000117	0.000949	0.000000013	0.0000
i-j	0.00030409	0.186950	0.00128	0.0014
i-control	0.00000076	0.000027	0.00000003	0.0000
j-control	0.00000267	0.000006	0.000000004	0.0000

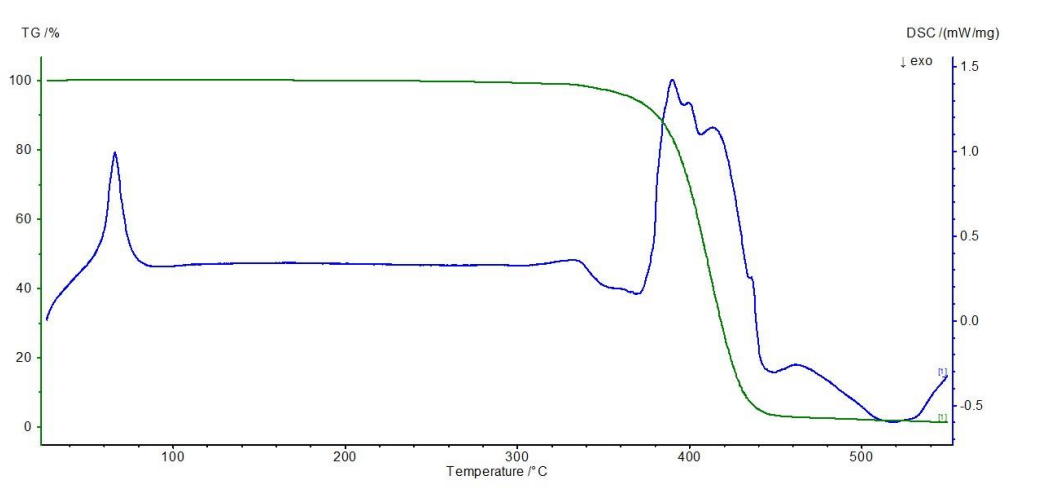
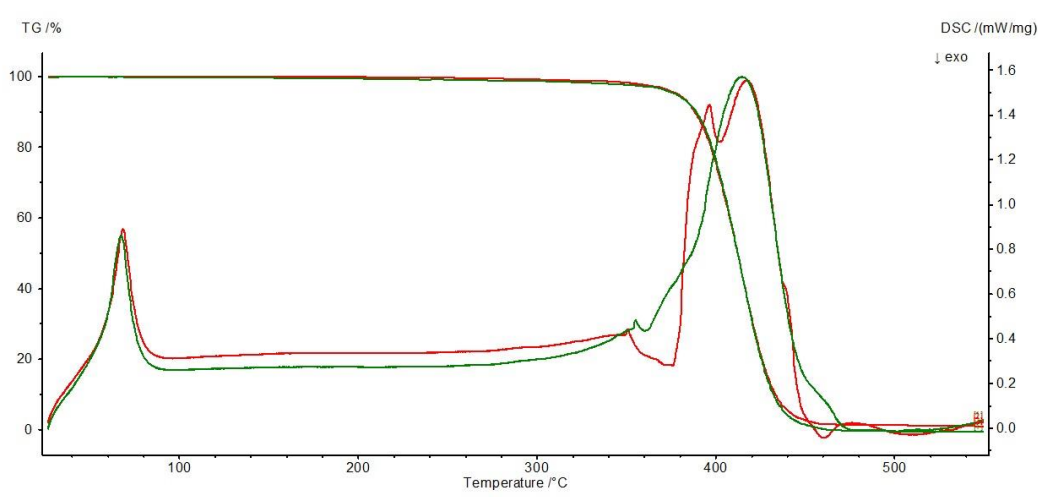
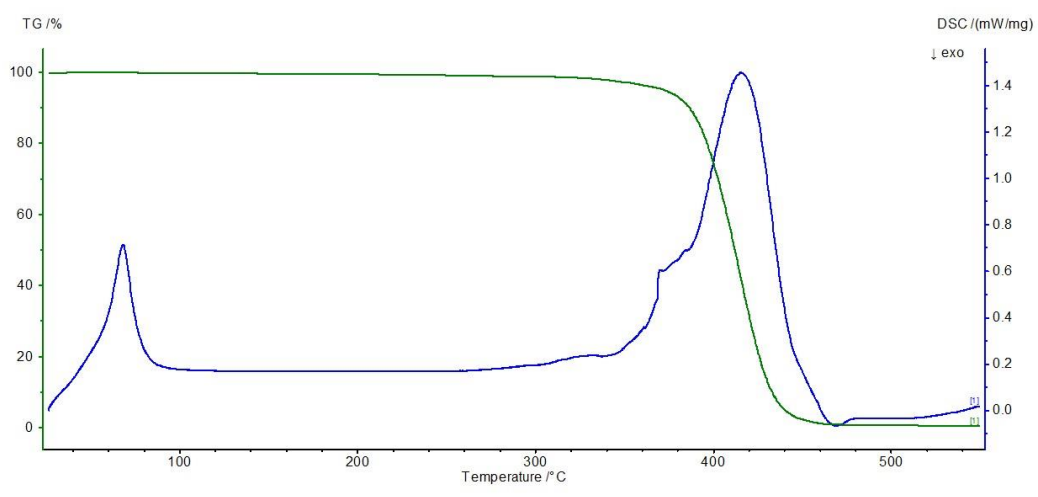
Appendix IV

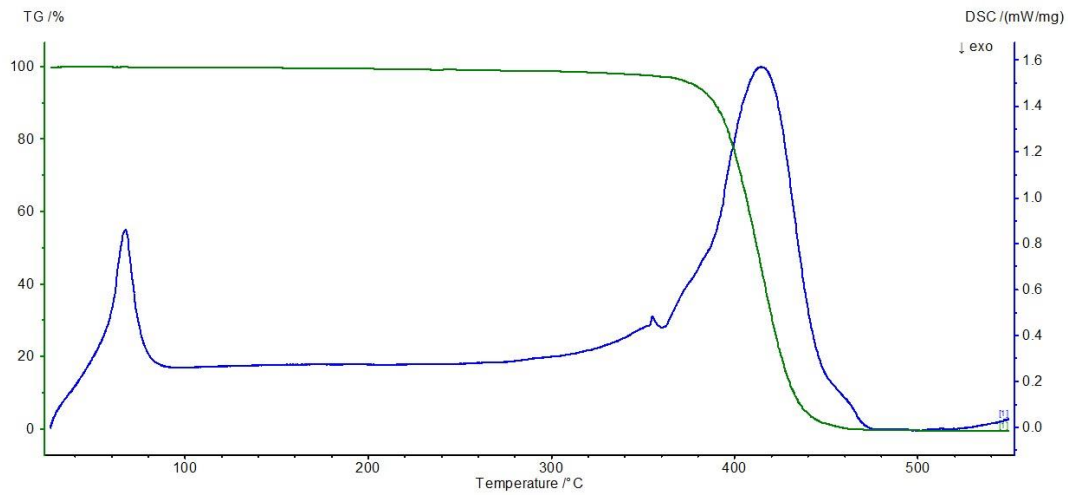
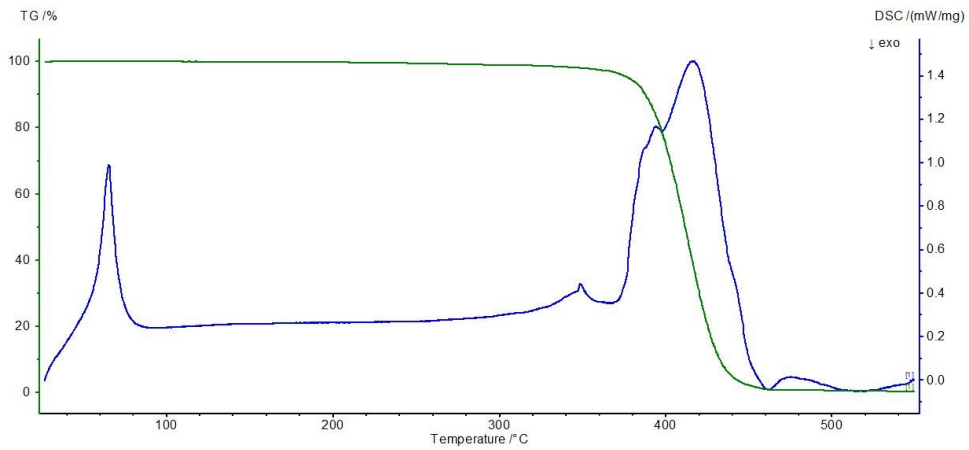
T-Test values for PCL-BC composites cell culture

T-Test	Bone Marrow 24 hours	Bone Marrow 48 hours	Dermal 24 hours	Dermal 48 hours
PCL-PCLBC2%	0.021	0.045	0.06336	0.0928
PCL-PCLBC4%	0.010	0.052	0.00039	0.0365
PCL-PCLBC6%	0.121	0.492	0.33336	0.0043
PCL-PCLBC8%	0.003	0.395	0.00003	0.0013
PCL-PCLBC10%	0.115	0.285	0.00005	0.0005
PCLBC2%-PCLBC4%	0.018	0.011	0.00330	0.2945
PCLBC2%-PCLBC6%	0.068	0.401	0.18482	0.0548
PCLBC2%-PCLBC8%	0.062	0.057	0.00170	0.0548
PCLBC2%-PCLBC10%	0.015	0.153	0.00101	0.0083
PCLBC4%-PCLBC6%	0.015	0.305	0.28988	0.0733
PCLBC4%-PCLBC8%	0.025	0.040	0.04970	0.1248
PCLBC4%-PCLBC10%	0.007	0.034	0.00620	0.0133
PCLBC6%-PCLBC8%	0.053	0.490	0.22024	0.1523
PCLBC6%-PCLBC10%	0.193	0.464	0.14732	0.1351
PCLBC8%-PCLBC10%	0.006	0.362	0.01504	0.0026

TGA curves for PCL and PCL-BC composites







Statistical analysis for PCL-BC mechanical testing.

Samples	T-test Young's Modulus	T-test Ultimate Tensile strength	T-test Yield Strength
PCL and BC2%	0.147	0.0146	0.262
PCL and BC4%	0.242	0.0003	0.410
PCL and BC6%	0.331	0.0002	0.326
PCL and BC8%	0.033	0.0005	0.060
PCL and BC10%	0.004	0.0001	0.299

2% and 4%	0.259	0.1574	0.250
2% and 6%	0.020	0.0225	0.416
2% and 8%	0.065	0.0021	0.476
2% and 10%	0.010	0.0002	0.182
4% and 6%	0.340	0.036	0.323
4% and 8%	0.017	0.001	0.198
4% and 10%	0.002	0.000	0.451
6% and 8%	0.010	0.040	0.352
6% and 10%	0.003	0.004	0.234
8% and 10%	0.069	0.017	0.074